UNIVERSIDADE DE LISBOA

INSTITUTO SUPERIOR TÉCNICO

Astrobiology analysis of icy biomes as a proxy for extra-terrestrial life in icy worlds

Lígia Patrícia Fonseca Coelho

Supervisor: Doctor Zita Carla Torrão Pinto Martins

Co-Supervisors: Doctor Rodrigo da Silva Costa

Doctor João Alfredo Vieira Canário

Thesis approved in public session to obtain the PhD Degree in Bioengineering

Jury final classification: Pass with Distinction

2022

UNIVERSIDADE DE LISBOA

INSTITUTO SUPERIOR TÉCNICO

Astrobiology analysis of icy biomes as a proxy for extra-terrestrial life in icy worlds

Lígia Patrícia Fonseca Coelho

Supervisor: Doctor Zita Carla Torrão Pinto Martins

Co-Supervisors: Doctor Rodrigo da Silva Costa

Doctor João Alfredo Vieira Canário

Thesis approved in public session to obtain the PhD Degree in Bioengineering

Jury final classification: Pass with Distinction

Jury:

Chairperson: Doctor Joaquim Manuel Sampaio Cabral, Instituto Superior Técnico, Universidade de Lisboa

Members of the Committee:

Doctor Warwick Farley Vincent, Faculté des sciences et de genie, Université Laval, Canada

Doctor Miguel Nobre Parreira Cacho Teixeira, Instituto Superior Técnico, Universidade de Lisboa

Doctor Lisa Kaltenegger, Carl Sagan Institute, Cornell University, EUA

Doctor Zita Carla Torrão Pinto Martins, Instituto Superior Técnico, Universidade de Lisboa

Doctor Bruno André Cunha de Vallêra Jacques Pedras, Instituto Superior Técnico, Universidade de Lisboa

Funding Institution – Fundação para a Ciência e Tecnologia

2022

All civilizations become either spacefaring or extinct.

Carl Saga

Resumo

Uma das questões que a astrobiologia pretende responder é se estamos sozinhos no universo. Alguns mundos gelados que orbitam Júpiter, Saturno, e outras estrelas, são locais de interesse para procurar vida extraterrestre. Missões espaciais *in-situ* são o derradeiro método que poderá fornecer uma resposta definitiva a esta questão, e várias missões a estes mundos estão planeadas acontecer nas próximas décadas. No entanto, ainda é necessário trabalho na Terra, com recurso a análogos planetários, para preparar estas missões. Análogos planetários são locais no nosso planeta que reproduzem características de ambientes extraterrestres. No inverno, a Baía de Hudson, no Canadá, é um análogo planetário para alguns mundos gelados. Foi realizado um estudo integrativo na costa da Baía de Hudson para determinar e relacionar a química e a microbiologia do seu gelo e água. Primeiro, foi concebido e testado um protocolo para o processamento de gelo após a colheita de amostras, e foi investigado a possível contaminação durante os processos de amostragem e processamento de gelo. Em sequência, a estrutura procariótica das amostras de gelo e água foi explorada, revelando uma assimetria íngreme entre estas comunidades e a sua relação com a salinidade. Os microrganismos de gelo revelaram produzir mais biopigmentos do que os microrganismos na água. Espectroscopia foi aplicada para explorar o conteúdo de biomoléculas fluorescentes. Moléculas húmicas, triptofano, e provavelmente ß-caroteno foram encontrados em amostras de gelo e água, variando ao longo do gradiente de salinidade, e dependendo do grau de degradação biológica. Clorofilas e carotenoides foram detetados em suspensões enriquecidas de microrganismos cultivados a partir das amostras, e os seus sinais refletiam-se de forma diferente dependendo da disponibilidade de água. Esta abordagem holística de análise astrobiológica do mesmo conjunto de amostras, que inova nas boas práticas de trabalho de campo para amostras de gelo polar, desvendou comunidades procarióticas do gelo e

da água da costa Baía de Hudson e suas assinaturas químicas, culminando no primeiro catálogo de bioassinaturas coloridas para procurar vida em mundos gelados.

Palavras-Chave: Baía de Hudson, bioassignaturas, biopigmentos, microbiologia polar, espectroscopia

Abstract

One of the questions astrobiology aims to answer is whether we are alone in the universe. Some icy worlds orbiting around Jupiter and Saturn as well as orbiting other stars are locations of interest to search for extra-terrestrial life. Space missions are the ultimate approach that may one day give us a definite answer and several space missions to these worlds will happen in the next decades. However, a great amount of work is needed on Earth, resorting to planetary field analogues, to prepare them. Planetary field analogues are places on our planet that reproduce some characteristics from extra-terrestrial environments. In the winter season, Hudson Bay in Canada is a planetary field analogue to some icy worlds. An integrative study of Hudson bay's coast was performed to determine, characterize, and relate the chemistry and microbiology of its ice and water, along a salinity gradient. As a first approach, a clean protocol for ice processing after sampling was designed and tested and ice sampling/processing contaminants were investigated and documented. Following, the prokaryotic structure of ice and water samples was explored revealing a steep asymmetry between the communities of ice and water and their relationship with salinity. Ice microorganisms were revealed to be more prone to produce biopigments than the microorganisms in water. Spectroscopy was applied to further explore the content of fluorescent biomolecules. Humic molecules, tryptophan, and likely ß-carotene were found in environmental samples of ice and water, varying along the salinity gradient, and depending on bio- and photodegradation. Chlorophylls and other carotenoids were detected in enriched suspensions of microorganisms cultivated from the samples, and their signals reflected differently depending on water availability. This holistic approach to astrobiology analysis of the same set of samples innovated in fieldwork good practices for polar ice samples, unraveled the prokaryotic communities from Hudson Bay coast's ice and water and their

chemical signatures, culminating in the first catalogue of colored biosignatures to search for life in icy worlds.

Key words: Hudson Bay, biosignatures, biopigments, polar microbiology, spectroscopy

Acknowledgments

Firstly, I want to express my gratitude to my supervisors, Professors Zita Martins, Rodrigo Costa, and João Canário for accepting me into their research groups, for their support, prompt inspiration, great knowledge, and guidance.

I am eternally thankful to the MIT-Portugal Program for trusting me with one of their PhD fellowships and introducing me to an ecosystem of highly driven and innovative people. This has always kept me motivated throughout all these years. A special thank you to the College on Polar and Extreme Environments (Polar2E) of the University of Lisbon for supporting me as a polar student and including my research within their framework.

I acknowledge Professor Joaquim Cabral, Director of the institute for Bioengineering and Biosciences (iBB), Professor Margarida Romão, co-coordinator of Chemistry for the Environment (Centro de Química Estrutural – CQE), and Professor Isabel Sá-Correia, Director of the Biological Sciences Research Group (BSRG), for the opportunity to develop my PhD work at the laboratories.

I acknowledge all the co-authors of the manuscripts presented in this dissertation for their scientific contributions, and the support provided.

I acknowledge Fundação para a Ciência e Tecnologia (FCT) for funding my PhD grant (PD/BD/139840/2018). I also acknowledge the projects of my supervisors and my host research centers (CQE and iBB) that have funded different parts of this research: projects UIDB/00100/2020 and UIDP/00100/2020 from CQE funded by FCT; Project UIDB/04565/2020 from iBB , funded by FCT; Project LA/P/0056/2020 from Institute of Molecular Sciences, funded by FCT; Project PERMAMERC funded by Portuguese Polar Program (PROPOLAR); and Project PTDC/FIS-AST/29932/2017, funded by Fundo Europeu de Desenvolvimento Regional (FEDER) funds through the COMPETE 2020 -

Operational Programme for Competitiveness and Internationalisation (POCI) and by Portuguese funds through FCT.

A sincere thank you to the Astrobiology and Cosmochemistry (TACG), MicroEcoEvo and Chem4Env research groups at Instituto Superior Técnico. It was a privilege to work in three different groups in my PhD and being welcomed so warmly by all of them. A especial mention to my amazing companions: Manuel Almeida, Tiago Ramalho, Joana Carneiro, Joana Couceiro, Catarina Miranda, Diogo Gonçalves, Francisco Calapez, Diogo Folhas, Sandra Godinho, Rúben Silva, Laurence Meunier, Matilde Marques, João Almeida, and Pedro Freitas. Thank you also to the senior collaborators who never hesitated to share valuable advice and support me: Doctors Rute Cesário, Tina Keller-Costa, Bruno Pedras, Carlos Monteiro, Sara Martinez, Nuno Borges, and Sean Jordan.

I would like to express my gratitude to the fieldwork crew Professor Alex Matveev, Doctor Martin Pilote, Professor Jérôme Comte, Martin Jusek, my supervisor Professor João Canário, Professor Warwick F. Vincent, and the Centre for Northern Studies (CEN) for the logistic support, the manager of the CEN research station Sidney Arruda, our local guide Frederick Audlarock, the community of Whapmagoostui-Kuujjuarapik and last, but not least, Marie-Amélie Blais with whom, in the middle of the deep cold subarctic winter, I formed a friendship connection which endured to sunnier days.

My sincere acknowledgement to the international research groups that hosted me during these three years: Connie Lovejoy's lab, Département de biologie (Université Laval – Canada), Warwick F. Vincent's lab, Département de biologie (Université Laval – Canada), CEN lab (Whapmagoostui-Kuujjuarapik), Glória Esquível's lab, Instituto Superior de Agronomia (ISA), and Jérôme Comte's lab (Institut National de la Recherche

Scientifique – Canada). A special mention to the Carl Sagan Institute (Cornell University -USA) for being my official international host. To Professors Lisa Kaltenegger, Stephen Zinder, William Philpot, and Stephen Winans – a heartfelt thank you for accommodating and training me, and for all your generosity in time to long science discussions. I grew immensely as an astrobiologist under your guidance.

A respectful and heartfelt thank you to Cecília Arraiano's lab in ITQB-Nova for hosting me at the beginning of this PhD, and for the continuous support through all these years. A special mention to Doctor Rute Matos, Professor Cecília Arraiano, and Doctors Sandra Viegas and Margarida Saramago - thank you for continuing to care about me, for the constant priceless career advice, and for making me feel at home.

To my international colleagues and friends: Claudia Pacelli, Jack Madden, Rebecca Payne, Jeremy Storming, Sofia Colombi, Micol De Simoni, Francesca Luoni, Eloise Pariset, Naser Burahman, Jake Turner, Zifan Lin, Gabriel Bonilla, and Thea Kozakis – thank you for making me feel at home.

A warm thank you to my family, especially my mother, brother, grandparents, stepdad, father, and Frederico Martins who have supported me unconditionally and taught me by example how to be the person I want to be, every day. A gigantic thank you to my closest friends: Joana Gonçalves, Inês Zêzere, Nuno Pinheiro, Rafael Marques, Marília Silva, Ana Rita Garizo, Rui Martins, Soraia Guerreiro, Marcelo Ramires, Inês Sousa, Sara Santos, Sara Marques, Inês Vilhalva, Mónica Botto e Rúben Almeida for being there every day and for your care and love. Rita Mendes, thank you also for motivating me into being my best self and being a great example of brilliance and resilience. Without you, this would have been impossible. My music mates from Orquestr'UP, thank you for reminding me every day that group work is the best type of work, and music makes us kinder humans. I hope you all know how devoted I am to all of you.

Table of Contents

List of acronyms

A - Adenine

ARIEL - Atmospheric Remote-sensing Infrared Exoplanet Large-survey

amu - atomic mass units

AVIRIS - Visible InfraRed Imaging Spectrometer

ASO - NASA Airborne Snow Observatory

ASW - Artificial Seawater

BRDF - Bidirectional Reflectance Distribution Function

C – Cytosine

CAS – Chemical Abstracts Service

CDA - Cosmic Dust Analyzer

CFU - Colony-forming Unit

Chl *a* – Chlorophyll *a*

Chl *b* – Chlorophyll *b*

CHNOPS – Carbon, Hydrogen, Nitrogen, Oxygen, Phosphorous, Sulfur

C-LIFE - Cold-Lightweight Imagers for Europa

COSPAR - The Committee of Space Research

DNA – Deoxyribonucleic Acid

cDOM – Colored Dissolved Organic Matter

DOM – Dissolved Organic Matter

fDOM – Fluorescent Dissolved Organic Matter

ELF - Enceladus Life Finder

ELM - Europa Luminescence Microscope

ELSAH - Enceladus Life Signatures and Habitability

ELSSIE - Europa Lander Stereo Spectral Imaging Experiment

ENA - European Nucleotide Archive

ENEX - Enceladus-Explorer

ESA – European Space Agency

Europa-UVS - Europa Ultraviolet Spectrograph

FL1 - Green fluorescence

G - Guanine

GCR - Galactic Cosmic Rays

GWR – Great Whale River

HabEx - Habitable Exoplanet Observatory

HMOC - High Mass Organic Cations

HPLC - High-Performance Liquid Chromatography

HST - Hubble Space Telescope

HZ – Habitable Zone

INMS - Ion and Neutral Mass Spectrometer

ISS – International Space Agency

JEM – Join Europa Mission

JUICE – JUpiter ICy moons Explorer

LED - Light-Emitting Diode

LIFE - Life Investigation For Enceladus

MAG - Cassini's Dual Technique Magnetometer

MAJIS - Moons And Jupiter Imaging

NASA – National Aeronautics and Space Administration

NCBI - National Center for Biotechnology Information

NIMS - Galileo Near-Infrared Mapping Spectrometer

PH - Phase-contrast

PCoA - Principal Coordinates Analysis

PERMANOVA - Permutational Analysis of Variance

PSU - Practical Salinity Units

QSU - Quinine Sulfate Units

ODO - Dissolved Oxygen

OTU - Operational Taxonomic Unit

R2A - Reasoner's 2A agar

RDP - Ribosomal Database Project

RNA – Ribonucleic Acid

SSC - Side-Scatter Signals

STIS - Space Telescope Imaging Spectrograph

T – Thymine

TAP - Tris-Acetate-Phosphate

TC-DNA - Total Community DNA

Trp - Tryptophan

Tyr - Tyrosine

U - Uracil

UVIS - Ultraviolet Imaging Spectrograph

UVS - Ultraviolet Spectrograph

VRE - Vegetation Red Edge

List of Figures

List of Tables

I INTRODUCTION

Publications:

Coelho, L.F. & Martins, Z. (2021). "The Geochemistry of Icy Moons." In *Encyclopedia of Geology, 2nd Edition, Elsevier, pp.* 207-216. https://doi.org/10.1016/B978-0-08-102908-4.00123-5

Coelho, L.F., Miranda, C., Gonçalves, D. & Martins, Z. (2022). "Habitability conditions in our solar system – the case for Mars and the icy moons." In *Habitable Worlds and Sustainable Life on Earth and Beyond*. Springer, Under review.

Astrobiology is the multidisciplinary science that aims to answer the following questions: “How did life begin and evolve on Earth?”, “What is the future of life on Earth and beyond?”, and “Is there life elsewhere in the Universe?”.

The search for life in the universe can focus on the detection of life elsewhere in the solar system, intersecting astrobiology with planetary science, or on the detection of life beyond the solar system, entering the fields of astrophysics and astronomy. The definition of life also plays an important role in this quest and scientists may look for signs of “life as we know it” (i.e., life on Earth is carbon-based and uses water) or alternative forms of life (e.g., using methane instead of water, or being silicon-based instead of carbon) (e.g., Stevenson *et al.*, 2015).

The search for life in the solar system is mainly based on the detection, and characterization of the three minimal requirements for habitability (liquid water, essential elements to life, and an energy source, see Cockell *et al.*, 2016), and organic molecules considered to be the building blocks of the basic unit of life – the cell - such as, among others, carboxylic acids, amino acids, nucleobases, and biological pigments (Chan *et al.*, 2012b; Martins *et al.*, 2013; Myrgorodska *et al.*, 2016; O’Malley-James *et al.*, 2018; Martins, 2020). Some of these chemical imprints of life may be called biosignatures. A biosignature is any measure or feature that can be interpreted as evidence of past or present life - (Europa Lander Mission, 2nd meeting, 2020). An important requirement when discussing biosignatures is that they cannot be produced in the absence of life, excluding many molecules within the chemical groups above-mentioned. For instance, there are amino acids that have abiotic origins, thus amino acids alone will not be considered evidence of life (Schwendner *et al.*, 2022). However, the chirality of amino acids may be used as a tool that helps to distinguish their origin, i.e., racemic mixtures of proteic amino acids have an abiotic origin, while an excess of L-proteic amino acids is

indicative of a biological origin. On another hand, other groups of molecules, such as biopigments, are known to be produced only by living organisms, thus being considered biosignatures (Baqué *et al.*, 2020).

The study of biosignatures on Earth is crucial to the success of future space missions designed mainly for their detection. Failure to properly identify what life looks like on our planet, the only example of life we have, will likely lead humankind to miss extra-terrestrial life signals, even if we are looking closely enough. The only bodies that are so far known to include the three minimal requirements for habitability are Mars and a few icy moons orbiting Jupiter and Saturn. The current knowledge of other planetary systems is still much limited due to the massive distance that separates us from the next star in the Milky Way. Nonetheless, it is already possible to determine when an exoplanet has conditions to sustain liquid water or not (Kaltenegger, 2017), and soon it will be also possible to know whether complex colorful biosignatures dominate their landscape (Kouveliotou *et al.*, 2014).

In this thesis, I will focus on "life as we know it". In this introductory chapter, I will describe the state-of-the-art on the identification of the three minimal requirements for habitability, the concept of habitability, how it applies to icy worlds, and how Earth can be used as a tool to prepare for the detection of extra-terrestrial life in icy environments.

I.1 The three pillars of habitability

The exact conditions for the origin of life remain unclear, yet the study of the Earth has allowed us to well-constrain the conditions needed for life to survive. Following those constraints, astrobiologists have proposed basic requirements for any environment to develop and carry life. Consequently, the habitability of a planet or moon does not refer to the presence of life *per se*, but instead to its capability to support life throughout all its

stages (Westall *et al.*, 2013). Often, the term "habitability" is used to target specific locations within the solar system (and beyond) in the so-called "habitable zones" (i.e., the orbits around a star within which the surface of a planetary body can retain liquid water), and on planets or moons outside this "habitable zone", which have the ideal conditions for extra-terrestrial life to develop (Hand *et al.*, 2020).

Variations to the definition of habitability occur when adding the factors related to life activity, where habitability means an environment with the necessary conditions for at least one known organism to be active. Here *active* refers to metabolically active as cell maintenance, growth, or reproduction (Cockell *et al.*, 2016). Habitability in this variation is necessarily defined by reference to specific organisms and their needs (Hall *et al.*, 1997; Aarts *et al.*, 2013). Since the search for extra-terrestrial life in our solar system is directed to microbial life detection, we must contemplate the minimal requirements for microorganisms on Earth (Farmer, 2018) – or as herein also referred to – the three pillars of habitability. Thus, as referred before briefly, the habitability of a planet or moon will rely on three conditions, if one considers "life as we know it" as using water and carbon, being able to survive, grow and reproduce. These requirements are liquid water availability (Westall *et al.*, 2018), specific chemical elements (carbon, hydrogen, nitrogen, oxygen, phosphorus, and sulfur - CHNOPS) (Cockell *et al.*, 2016; Martins, 2020), and an energy source (e.g., tidal heat, solar radiation, radioactive decay, or geochemical) (Nealson, 1997).

Life is, inherently, a chemical phenomenon, and thus subject to different forms of toxicity. Environment-induced toxicity is herein considered a habitability dimension alongside its three pillars of habitability (Cockell *et al.*, 2016). Many energy sources may cause undesired chemical reactivity - and thus biological toxicity -, such as solar radiation, Galactic Cosmic Rays (GCR), and other particles accelerated by the magnetosphere of

giant planets. Some extremophiles survive under ranging irradiation energies, intensities, and time periods (Merino *et al.*, 2019), and minerals shield biological building blocks from radiation-induced deterioration (dos Santos *et al.*, 2016; Laurent *et al.*, 2019; Ertem *et al.*, 2021). However, high-energy radiation remains an obstacle to the habitability of the surface of a planet or moon, (Nordheim *et al.*, 2018) and the integrity of biosignatures.

I.2 Icy worlds in the solar system

The unraveling of information about the outer solar system moons, especially the knowledge that some of them contain a significant amount of water ice, came centuries after their first observation. In the second half of the last century, modern telescopes and missions such as the Voyager 1 and 2 allowed: i) the description of the ice that covers some of the moons of Jupiter and Saturn (Dalton *et al.*, 2010); ii) the observation that some satellites show signs of recent geological activity (Lunine, 1990); iii) knowledge of episodes of exchange of material with their parent planet and with other close moons (Eviatar *et al.*, 1981); iv) the description of surface and atmospheric chemistry (Dalton *et al.*, 2010, and references therein); and most intriguing for astrobiologists, v) the possibility of liquid water in the subsurface of geologically active icy worlds (e.g. Squyres *et al*., 1983). At the turn of the century, the Galileo mission obtained significant evidence of liquid water underneath the ice crust of Europa, which seems to be in contact with the rocky core (Khurana *et al.*, 1998). The same was expected for Ganymede and later verified with aid of the Hubble Space Telescope (HST) (Saur *et al.*, 2015). In 2005, the Cassini-Huygens mission to study Saturn and its moons approached Enceladus and revealed what Voyager was not able to: cryovolcanic activity expelling what was suggested to be water vapor from its south pole (e.g. Porco *et al.*, 2006). Materials sampled by Cassini flybys through the Enceladus plumes are inferred to be directly

sourced from its interior ocean (Postberg *et al.*, 2011). The plausibility of an internal ocean of the moons Callisto, Mimas, and Dione is limited to a single line of evidence, and the interior oceans of Triton and Rhea are no more than a theoretical inference (McKinnon *et al.*, 2014; Neveu *et al.*, 2019).

Nonetheless, liquid water underneath the surface of these icy worlds has motivated discussions about the habitability of icy moons. Besides liquid water and a source of energy, life needs a supportive chemical composition to evolve. Geochemical processes, which can supply bioavailable nutrients, create reduction-oxidation (redox) potential, and provide catalyzing agents for polymerization reactions among other functions, are essential to support life on Earth and were fundamental for its origin. The presence of a rocky core in the icy moons of our solar system is therefore crucial for the existence of life-enabling geochemistry on these bodies (Vance *et al.*, 2007). Icy moons are modeled to have variations of silicate rocky cores. A recent model suggests that the cores of icy moons may also contain significant carbonaceous matter (Néri *et al.*, 2020). The interaction between the rocky core and the interior ocean is crucial for the occurrence of reactions known to sustain life. Through geochemical reactions (e.g., serpentinization), the core will potentially supply the ocean and the surface with CHNOPS. Thus, the astrobiology potential of the icy moons will depend on the chemistry of both the core and interior ocean. However, the existence of water/rocky core interactions is highly dependent on the level of differentiation and thermal evolution of these moons. Evidence suggests that both Enceladus and Europa have an active ocean/core interface, fueling geochemical processes such as hydrothermal activity (Glein *et al.*, 2020; Howell *et al.*, 2020).

I.3 Europa

While in Jupiter orbit, Galileo mission flybys brought a lot of attention to the Europa moon. Empirical observations of the ice shell, including limited crater counts, indicate a young and active surface (Carr *et al.*, 1998; Fischer *et al.*, 2015). However, it is what we know related to its interior that stimulates the curiosity and objectives of future missions to this moon. Gravitational and magnetic data from Galileo implicated that the geological model for Europa includes a globally-distributed interior ocean in contact with a silicate core, all under an ice shell with a thickness that is still under debate (e.g. Khurana *et al.*, 1998). If the chemical composition of the interior global ocean of Europa is adequate to sustain life is still an unanswered question. The moment of inertia and internal structure of this satellite implies the presence of a water/rock interface, which coupled with the internal heat generated from tidal stresses, creates an environment for reductive geochemical processes on the seafloor (Howell *et al.*, 2020). However, the chemical composition of the ocean also depends on material intrusions at hydrothermal vents, and the recycling of oxidative species from the highly irradiated surface via ice tectonics. Also, the ejection of material from Io onto the Europa surface may be subsequently incorporated into its interior through active regions, such as chaos terrains (Eviatar *et al.*, 1981; Dalton *et al.*, 2010). Thus, the ocean may engender a mixture of both endogenous and exogenous materials, just like the surface appears to.

Even though Europa receives a lot of exogenous material accelerated by the strong magnetosphere of Jupiter, this moon has a relatively smooth surface. However, there are significant observable surface irregularities such as craters, domes, and pits (lenticulae), dark streaks (lineae), and colorful mottled regions (yellow and brown) (Carr *et al.*, 1998). These differences are due to the distinct nature of the hemispheres, endogenous versus exogenous sourcing, and the chemistry of the material (Dalton *et al.*, 2010; Fischer *et al.*,

2015). Spectroscopy studies have found three chemically distinctive regions: the trailing hemisphere bullseye, the higher latitudes of the leading hemisphere, and the leading hemisphere chaos units (Fischer *et al.*, 2015). The spectra from higher latitudes of the leading hemisphere correspond well with water ice. The materials corresponding to the trailing hemisphere are interpreted as H_2SO_4 hydrate, mirabilite ($Na_2SO_4 \cdot 10H_2O$), hexahydrite ($MgSO_4 \cdot 6H_2O$), bloedite ($Na_2Mg(SO_4)_2 \cdot 4H_2O$), $MgSO_4$ brine, and water ice with grain sizes of 50, 75, 100, 250, and 1000 μm (Fischer *et al.*, 2015) **(Table I.1)**. The same results had been presented earlier using the Galileo Near-Infrared Mapping Spectrometer (NIMS) data (Dalton *et al.*, 2010, and references therein). Epsomite has also been predicted, although its origin is unclear (Brown *et al.*, 2013). The chemistry of the trailing hemisphere is most likely exogenous due to the implantation of materials from Io's volcanoes (Eviatar *et al.*, 1981).

Another effect of Jupiter's magnetosphere is the radiolysis of the ice on the surface of Europa. Thus, H_2SO_4 may be generated by radiolysis of water ice with implanted S and/or endogenic sulfurous salts brought up from the subsurface through volcanic events (Dalton *et al.*, 2010, and references therein). It has been suggested that $MgSO_4$ is also a product of surface radiolysis since observations of $MgSO_4$ were spatially coincident with sulfuric acid hydrates. However, outside contamination should still be considered, at least for sulfur, since observations using the Keck telescope showed that $MgSO_4$ is present on the side that is facing the highly active Io (Brown *et al.*, 2013). Indeed, the presence of SO_2 in the trailing hemisphere of Europa is also consistent with the in fall of sulfur from the Io plasma torus (Dalton *et al*., 2010 and references therein; Eviatar *et al*., 1981). Nevertheless, sulfur is considered an important geochemical biomarker for future missions to the icy moons, which will likely investigate S isotopes in sufficient detail to detect potential S biomarkers (Chela-Flores, 2017).

Distinctively, the leading hemisphere chaos units appear composed mostly of endogenous material. The chaos terrain is thought to be a conduit between the surface of Europa and its subsurface ocean since both ejection of the interior ocean and subduction of outside materials may occur (Fischer *et al.*, 2015). The generation of interior/exterior chemical cycles is favorable due to this interaction, aligning with the heavy effect of radiation. Nevertheless, ocean materials are supposed to exist on the surface, and if the ocean is briny, then salts are the favorite candidates. Indeed, studies have given crucial indications that chaos region dark zones have compositions indicative of salts that may have been expelled from the subsurface. Most recently, a study using data from the Space Telescope Imaging Spectrograph (STIS) of the HST detected signatures of irradiated NaCl on the surface of Europa. The deepest absorption of NaCl resembles the yellow color of Tara Regio. Other absorption data were also associated with other chaos regions (Trumbo *et al.*, 2019b). The correlation of NaCl signatures with the chaos terrain in conjunction with Galileo magnetic data strongly suggests an interior briny ocean.

Table I.1 - Geochemical characteristics of Europa, including the inventory of their detected/predicted atmospheric, surface, and interior materials. Adapted from Coelho *et al.*, 2021, in *Encyclopedia of Geology*, 2nd Edition, Elsevier.

	Predicted interior structure	**Materials detected or predicted in the atmosphere**	**Materials detected or predicted at the surface**	**Materials predicted in the subsurface ocean**	**Evidence or prediction of recent surface activity**	**Likelihood of water-rock interactions**
Europa	Differentiated. Rocky core in contact with the subsurface ocean[(1)]	O_2[(2)], Na[(3)], K[(3)]	H_2O[(4)], H_2SO_4[(4)] hydrate, mirabilite[(4)], hexahydrite[(4)], bloedite[(4)], $MgSO_4$ brine[(4)], epsomite[(5)] SO_2[(3)], NaCl[(6)], CO_2[(7)], O_2[(7)], H_2O_2[(7)]	NaCl[(6)]	Tectonic events and cryovolcanism[(8)]	High[(9)]

(1)(Khurana *et al.*, 1998); **(2)**(Hall *et al.*, 1995); **(3)**(Dalton *et al.*, 2010); **(4)**(Fischer *et al.*, 2015); **(5)**(Brown *et al.*, 2013); **(6)**(Trumbo *et al.*, 2019b); **(7)**(Trumbo *et al.*, 2019a); **(8)**(Jia *et al.*, 2018); **(9)**(Vance *et al.*, 2007).

Hydrothermal circulation could justify a salt-rich ocean and thus the presence of salts on the surface of Europa **(Table I.1)**, especially on the active parts such as the chaos regions (Trumbo *et al.*, 2019b). The other species known or presumed to exist on the Europa surface are usually primary or secondary products of the radiation bombardment upon this moon, promoting an oxidative surface. Molecular oxygen, a radiolytic product of water ice, was detected by HST (Hall *et al.*, 1995). Some of the hydrogen products of water radiolysis escape due to the weak gravity of Europa, leaving an atmosphere rich in oxygen behind. Hydrogen peroxide was also identified as representing another by-product of surface radiolysis (Trumbo *et al.*, 2019a) **(Table I.1)**. However, there is no proof of whether H_2O_2 is transient or stable since radiation could also be destructive to H_2O_2. The presence of CO_2 (detected by NIMS) and O_2 in the leading hemisphere chaos regions may slow down the destruction of H_2O_2 by scavenging electrons created during the continued irradiation of the ice (Trumbo *et al.*, 2019a). The presence of H_2O_2 on the surface of Europa, especially in the chaos regions, may be of astrobiology importance since the habitability potential of Europa's ocean will likely depend on the presence of oxidants, such as H_2O_2, to counterbalance the reductive hydrothermal environment on the seafloor (Howell *et al.*, 2020). Consequently, understanding the real role of the radiolytic cycle of Europa may lead to vital answers regarding its geochemistry.

I.3.1 Habitability conditions of Europa

Millions of kilometers away from the "habitable zone" of our solar system we find Europa's subsurface ocean (Khurana *et al.*, 1998; Kivelson *et al.*, 2000, 2002). This characteristic granted worlds like Europa a new category called "ocean worlds" (Lunine, 2017). By the new definition, it is possible to tell that one of the main requisites to sustain "life as we know it" is available - liquid water.

Europa is modeled to have water-rock interactions based on its high rock content. This results in higher heat production (Vance *et al.*, 2016), which leads to another requisite: energy. Europa has been recently modeled to produce enough energy to have present-day volcanic activity at the seafloor (McCord *et al.*, 2001; Běhounková *et al.*, 2021). Water-rock interactions potentiate key geochemical reactions for the enrichment of the ocean in vital elements and are even possibly mediated by life itself (Vance *et al.*, 2007; Dodd *et al.*, 2017; Kitadai *et al.*, 2018). Hydrothermal events are also associated with the origin of life on Earth (Miller *et al.*, 1988), thus, life in Europa could be recent, and/or relatively evolved microbial life – a product of multiple life genesis and the natural path of evolution.

Potential energy sources vary from internal tidal friction and radioactive decay (Běhounková *et al.*, 2021) to surface photolysis and radiolysis (Carlson *et al.*, 1999). The surface of the Galilean moons is highly irradiated by Jupiter's magnetosphere (Nordheim *et al.*, 2018). This creates a highly oxidative surface and some studies have suggested that the interior ocean of these moons may be a reductive environment, creating a potential redox gradient (Vance *et al.*, 2016). With tectonic movements, a redox differential may be created in Europa's interior ocean, which is an energetic and chemical requirement for "life as we know it".

Besides the abundance of water ice (e.g. Clark, 1980), past missions have also revealed a fraction of other minor chemical components present on the surface of these moons such as SO_2, CO_2, and O_3 (Lane *et al.*, 1981; Noll *et al.*, 1996, 1997; McCord *et al.*, 1997, 1998). However, it is still difficult to distinguish between endogenous and exogenous materials (Brown *et al.*, 2013). Examples of the sources of exogenous materials are the volcanic products of the sister moon Io that escape to space (Alvarellos *et al.*, 2008) and galactic particles (Martins *et al.*, 2013; Nordheim *et al.*, 2018), all of

which are accelerated through Jupiter's magnetosphere. The source of endogenous materials may be the ice shell composition that will endure radiolytic events due to UV (penetration limited to the surface) or ionizing (penetration up to 1 meter of dept) radiation, as well as thermal processes (Nordheim *et al.*, 2018; Trumbo *et al.*, 2019a). Another possible endogenous source is the interior ocean through cryovolcanic and tectonic events, making the identification of these internal components a priority to determine habitability (Russell *et al.*, 2017). Given the thick ice shell that covers all the surface of these moons, failing to know which surface materials come from the interior will leave the chemistry of the interior oceans a complete mystery. The Galileo mission data demonstrated the existence of several hydrated salts on the surface of Europa (McCord *et al.*, 1999) with possible origin in the interior ocean. However, a radiolitic origin could not yet be discarded considering that these salts were not exclusive to the most active locations on Europa (Brown *et al.*, 2013). Years later, evidence of NaCl in the active surface of Europa was reported, a much stronger suggestion of an endogenous ocean source (Trumbo *et al.*, 2019b). There is some consensus that Europa's interior ocean must be briny which the evidence of the presence of NaCl in the chaos region came to reinforce.

I.4 Enceladus

Enceladus is one of the few ocean worlds with direct evidence of geological activity. Its libration amplitude and ice/rock ratio indicate a global ocean that is completely differentiated from the rocky core and the thick (~40 km) ice shell (Choblet *et al.*, 2017; Hemingway *et al.*, 2019). The surface of this moon is covered by a complex pattern of smooth, extremely bright ice, being the brightest planetary body in our solar system. Cassini characterized the atmosphere of Enceladus, which is composed primarily

of ionized water vapor, CO_2, CH_4, and other organic molecules **(Table I.2)** (Dalton *et al.*, 2010).

Table I.2 - Geochemical characteristics of Enceladus, including the inventory of their detected/predicted atmospheric, surface, and interior materials. Adapted from Coelho *et al.*, 2021, in *Encyclopedia of Geology*, 2nd Edition, Elsevier.

	Predicted interior structure	**Materials detected or predicted in the atmosphere**	**Materials detected or predicted at the surface**	**Materials predicted in the subsurface ocean**	**Evidence or prediction of recent surface activity**	**Likelihood of water-rock interactions**
Enceladus	Differentiated. Rocky core in contact with the subsurface ocean**(1)**	H_2O**(2)**, CO_2**(2)**, CH_4**(2)**, light organics**(2)**	H_2O**(3)**, CO_2**(3)**, NH_3**(3)**, light organics**(3)**	H_2**(4)**, NaCl, K**(5)**, HMOC**(6)**, N-bearing**(7)**, O-bearing**(7)**, aromatics**(7)**, SiO_2**(8)**, CO_2**(4)**, CO**(4)**, NH_3**(4)**, N_2**(4)**, CH_4**(4)**, H_2S**(4)**, ^{40}Ar**(4)**	Cryovolcanism**(9)**	High**(10, 1)**

(1)(Glein *et al.*, 2020)**; (2)**(Dalton *et al.*, 2010); **(3)(**Brown *et al.*, 2006); **(4)**(Waite *et al.*, 2017); **(5)**(Postberg *et al.*, 2011); **(6)**(Postberg *et al.*, 2018); **(7)**(Khawaja *et al.*, 2019); **(8)**(Hsu *et al.*, 2015); **(9)**(Porco *et al.*, 2006); **(10)**(Vance *et al.*, 2007).

Traces of CO_2 and NH_3 were also detected near the surface (Brown *et al.*, 2006). Enceladus also shows many surface cracks and ridges, especially in the south pole, and four of them are informally referred to as tiger stripes (Porco *et al.*, 2006). It is from these subparallel cracks that large plumes were detected by Cassini's Dual Technique Magnetometer (MAG) and Ultraviolet Imaging Spectrograph (UVIS). The plumes found by Cassini were ejecting icy particles, vapor, and organics from the south pole into space (e.g. Porco *et al.*, 2006). A satellite of Enceladus' size would normally be expected to completely freeze shortly after accretion/differentiation, but cryovolcanic episodes suggest a strong and continuous source of heat. Tidal friction is likely the biggest contributor to the internal heat engine of Enceladus (Choblet *et al.*, 2017; Hemingway *et al.*, 2019).

Given the low gravitational pull of this small moon, the plume emissions to the thin atmosphere of Enceladus effectively escape to space, ultimately migrating towards Saturn. Indeed, Enceladus is one of five moons that contributes particles to Saturn's E-ring (Postberg *et al.*, 2009). The Ion and Neutral Mass Spectrometer (INMS) and the Cosmic Dust Analyzer (CDA) were two instruments onboard Cassini used to analyze these particles. The plumes eject material both in the gas phase (e.g., water vapor) and solid phase (e.g., ice grains). Apart from the dominance of H_2O, measurements of the plume particles by the INMS indicated the presence of CH_4, N_2, CO, ^{40}Ar, and organic compounds ranging from C_2H_2 to C_6H_6 **(Table I.2)**. Also, CO_2, H_2, and NH_3 were detected; notably, the observation of NH_3 was yet another indicator of subsurface liquid water (Waite *et al.*, 2017, and references therein). The CDA data allowed for compositional profiling of the solid materials emitted from the plume with an approach of 21 km. Particle stratification occurs because the grain ejection velocity decreases with size. There were three distinct classes of ice particles (type I, II, and III) ejected from the plume and present in the E-ring (Postberg *et al.*, 2009). Type III grains are thought to be frozen ocean spray since they are rich in potassium and sodium salts, namely NaCl (Postberg *et al.*, 2011). Such type III grains are some of the best indicators of an interior ocean, and rock/water interactions, since the ice shell is expected to be almost salt-free. Bubbles of a volatile gas (CO_2, CH_4, or H_2) are thought to reach the water and burst, generating these salt-rich grains. Because they are big, type III grains are challenged to escape from Enceladus' gravity, thus, cryovolcanic active regions may be covered with Na-bearing plume particles (Postberg *et al.*, 2009). The observed Na concentrations in plume-derived materials, as sampled by the Cassini CDA, imply an overall salinity of 3–8 g/kg, and based on the observed abundance of CO_2 in plume-derived gas the estimated pH is 8.5-9 or 8.5-11 (Postberg *et al.*, 2009; Hsu *et al.*, 2015; Glein *et al.*, 2020).

The presence of salt-rich grains in the plume and E-ring supports the concept of a hot interior in the south pole of Enceladus (Choblet *et al.*, 2017). Connected to this finding is the observation of N in the plume, which allows inferring interior temperatures from 500 to 800 K through processes of thermal decomposition of NH_3. These are exceptional conditions for the formation of complex organic molecules (Matson *et al.*, 2007). Indeed, Cassini has detected organic material both in the vapor phase and solid ice grains (Postberg *et al.*, 2018, and references therein). Consequently, type II grains are described as salt-poor ice particles, often associated with organic molecules, indicative of water/rock interaction on the seafloor and contemporary geochemical processing.

The first organics discovered were low mass molecules (e.g., <50 atomic mass units, or amu), and recently it has been unraveled the presence of High Mass Organic Cations (HMOC) with masses above 200 amu (Postberg *et al.*, 2018). It is suggested in the same study that these molecules derive from larger parent macromolecules. Given the low salt content associated with these organic compounds, these particles were likely not generated directly from ocean spray. Rather, the more plausible possibility is that these molecules were in a solid phase when they are incorporated into the type II grains. The existence of an organic film on top of the seafloor is a favorite hypothesis. In such a scenario, gas bubbles burst disturbing the organic film and producing aerosol organic material; the organics become coated by water ice and rise through the vents (Postberg *et al.*, 2018). Through analogue experiments, Khawaja *et al.* (2019) described a spectral differentiation between the low mass organic materials of type II grains, separating N-bearing, O-bearing, and aromatic compounds. By comparison with INMS results, low-mass amines [particularly (di)methylamine and/or ethylamine] and carbonyls (with acetic acid and/or acetaldehyde most suitable) were considered the best candidates for the N- and O-bearing compounds, respectively (Khawaja *et al.*, 2019).

It is also important to mention type I grains which are the smallest of the types and almost purely water ice grains (Postberg *et al.*, 2009). In 2015, the INMS was able to detect and quantify H_2 in the Cassini E21 flyby and hydrothermal processes are likely its source, as similar processes occur on Earth (Waite *et al.*, 2017). Although the ice shell is very robust, the radiolysis of water ice by the magnetosphere of Saturn cannot produce enough H_2. Through hydrothermal processes, high yields of H_2 could be produced by pyrolysis of accreted CHON, or by aqueous oxidation of reduced minerals (e.g., Mg-Si-Fe-S-O-H system). Hydrothermal processes would be possible in Enceladus from the creation of fracture pathways and heat generation driven by, for instance, tidal dissipations. The high production of H_2 and its implication for hydrothermal processes could suggest the necessary geochemical conditions for the existence of methanogenesis in the ocean of Enceladus (Waite *et al.*, 2017). Thus, the detection of H_2 aligns with the previous detection of CH_4, representing strong evidence of water/rock interactions and serpentinization reactions, a hydrogen-producing geochemical process. A hydrothermal scenario would also align with the possible generation of N_2 by decomposition of NH_3, which would also indicate high temperatures inside Enceladus, at least in the south pole (Matson *et al.*, 2007).

The presence of nanometer-sized SiO_2 particles in the plume detected by CDA is also a strong indicator of ongoing hydrothermal activity at the level of the seafloor occurring at high temperatures (Hsu *et al.*, 2015). A homogenous rocky core model fails to support the origin of both H_2 and SiO_2. Thus, Glein *et al.* (2018) suggested that a multi-rock model for the core could reconcile the detected H_2 and SiO_2 in the plumes. In this scenario, ferrous-bearing serpentinized rocks in contact with hydrothermal fluids would produce the H_2, and quartz-bearing carbonates would produce Si. The presence of CO_2 in the ocean of Enceladus also fits in the heterogenous rocky core model. Carbonated rocks

do not favor the production of H_2 but support the production of SiO_2 (Glein *et al.*, 2020), implicating that carbonation is limited in the rocky core of Enceladus.

Complex systems, such as those found on Enceladus **(Figure I.1)**, reflect a geologically active world comparable to Earth, where geochemical gradients are essential to sustain life (Glein *et al.*, 2018). The Cassini mission was remarkable, allowing a deep understanding of the Saturnian icy moons, providing strong evidence for geochemical reactions at the seafloor, and suggesting that hydrothermal environments are highly analogous to the ones we have on Earth (Matson *et al.*, 2007). However, direct analysis of life precursors will require more sensitive mass spectrometry extending out to higher molecular weights, along with other organic analysis techniques such as gas chromatography.

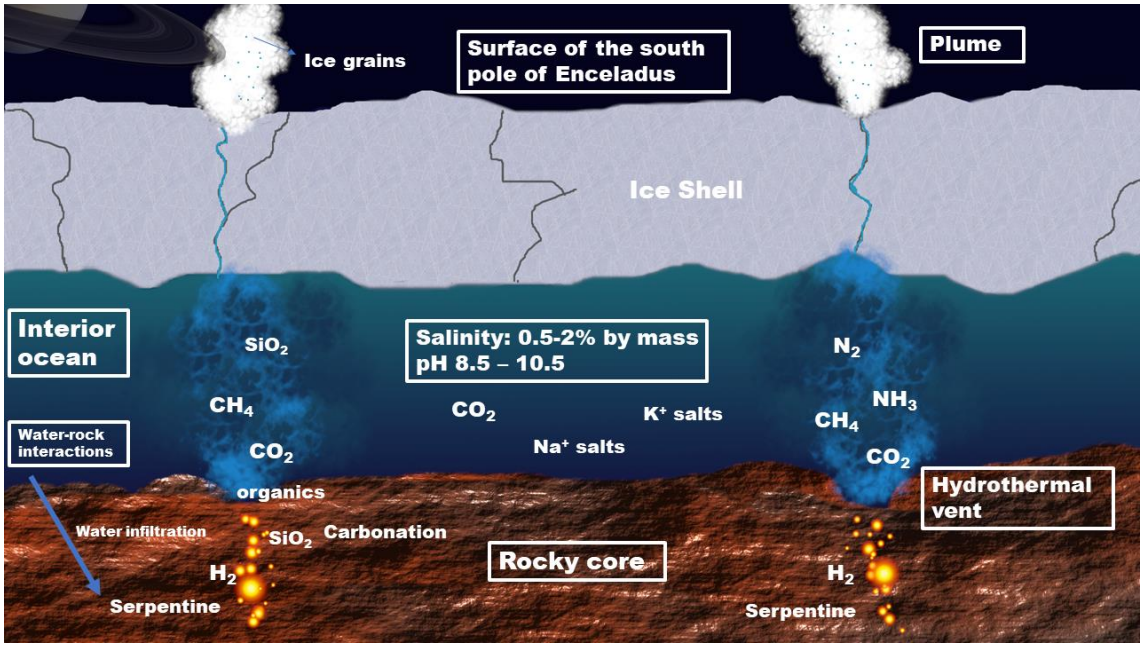

Figure I.1 - Model of the geochemistry of the subsurface of Enceladus considering a heterogeneous core (Glein and Waite, 2020). It takes into consideration the chemical signatures of the plumes detected by Cassini's INMS and CDA (Hsu *et al*., 2015; Khawaja *et al*., 2019; Postberg *et al.*, 2009, 2011, 2018; Waite *et al*., 2017). This illustration also includes the models for pH and salinity. For pH, both models (Postberg *et al*., 2018 model of pH 8.5–9; and Hsu *et al*., 2015 model of pH 8.5–10.5) are being considered. However, only the extremes are illustrated (Hsu *et al.*, 2015; Postberg *et al.*, 2009). For salinity, we used the salt concentration calculated by Postberg *et al.* (2011). This illustration is not to scale. From Coelho *et al*., 2021, in *Encyclopedia of Geology*, 2nd Edition, Elsevier.

I.4.1 Habitability conditions of Enceladus – A cryovolcanic moon

Enceladus is one of the smallest moons orbiting around Saturn. This moon is the most reflective body in the solar system due to the presence of crystalline water ice on the surface, becoming colder than expected (Brown *et al.*, 2006). Enceladus is one of the moons with the most direct proof of present cryovolcanic activity – images captured by the Cassini (Porco *et al.*, 2006). Enceladus had its plumes detected in the early 2000s, an unexpected event that changed the plans of the Cassini mission. It was not expected for such a small body to be able to sustain a global ocean, but tidal heating and possible hydrothermal activity **(Figure I.1)** make the oceans of Enceladus a potential reductive environment, and likely one of the most habitable (Waite *et al.*, 2017).

Due to the endogenic source of the eruptions, which were proved by the discovery of a high heated source in the south pole, these plumes represent a direct window to the subsurface ocean (Hsu *et al.*, 2015). The proximity to Saturn allows for the material of the plumes that escape the thin atmosphere of Enceladus to be captured by the rings of Saturn (Postberg *et al.*, 2009). If the ocean harbors life, fragments of it may be orbiting around Saturn for a long time, along with the salt grains that were already found by Cassini, making the E ring of Saturn an interesting target for future sampling missions (Judge, 2017).

Cassini was also able to sample the plume itself, however, due to the velocity of the material along with the velocity of the spacecraft, Cassini mostly detected organic fragments (Khawaja *et al.*, 2019). The plumes are concentrated in the south pole in structures informally called "tiger stripes" (Brown *et al.*, 2006), which are recent geological formations rich in ice grain depositions and thus crystallized water ice. From the CHNOPS **(Table I.2)** detected, carbon dioxide is the component, besides water, most firmly confirmed (Brown *et al.*, 2006; Waite *et al.*, 2006; Matson *et al.*, 2007), but

molecules such as light organics, hydrogen peroxide, methanol, ammonia hydrate, salts, and tholins are also inferred in previous analysis on data from the observations of Cassini's equipment (Newman *et al.*, 2007; Hodyss *et al.*, 2009; Waite *et al.*, 2009; Hendrix *et al.*, 2010; Postberg *et al.*, 2018). The origin of these molecules could be endogenic or due to radiolysis (Newman *et al.*, 2007) as the hydrogen peroxide also found on Europa's surface is suggested to be (Trumbo *et al.*, 2019a).

The Cassini mission expanded our catalogues of potentially habitable bodies, unraveling more than what was designed to. We now have more information about the habitability conditions of Enceladus than the notable Europa since the Galileo mission to the Jovian system preceded Cassini.

I.5 Icy worlds outside the solar system

The planets outside our solar system are called exoplanets and more than 5000 are currently known (https://exoplanets.nasa.gov/ in March 2022), a remarkable quantity considering the first exoplanets were only discovered less than 30 years ago (Mayor *et al.*, 1995). The definitions for "habitable" exoplanets are not comparable to the discussion of habitability in the solar system. It is not possible yet to know if there is liquid water, CHNOPS, or what energy sources Earth-like exoplanets might have. Instead, the concept of "Habitable Zone" (HZ) is used, and only a few dozen known exoplanets make the cut (e.g., Kaltenegger, 2017).

A planet is in the habitable zone of its star if, in theory, could sustain liquid water at its surface, if water is present. The calculations to model HZ planets use the amount of energy these worlds receive from their star to predict their temperature. The variables include the type of star, the size of the planet, and how distant it is from the star (Kopparapu *et al.*, 2013, 2014). The extension of the HZ can be more optimistic or more

conservative. The optimistic HZ considers the lower limits of habitability in planetary systems, as the regions that receive the same amount of energy Mars is predicted to have received 3.8 Gyr ago (also known as "early Mars - EM"), and as the upper limit of the energy Venus has received 1 Gyr ago (also known as "recent Venus - RV") (Kopparapu *et al.*, 2013). This model starts on the premise that Mars and Venus also sustained liquid oceans once in the above-mentioned periods. In the more conservative models of the HZ, the greenhouse effect (Kopparapu *et al.*, 2014; Ramirez *et al.*, 2018) is also considered a factor capable of drying oceans.

While searching for extra-terrestrial life in the solar system is restricted to microbial signatures, on exoplanets we can look for evolved life and even civilizations. However, the knowledge about exoplanets' composition is limited to their atmospheric chemical signatures. The reason for this is the limited observation capacity of current telescopes to only exoplanets in transit, - by the designated transit spectroscopy -, which does not allow for surface chemical characterization (Barstow *et al.*, 2015). Atmospheric biosignatures include pairs like O_2 and CH_4, or O_3 and CH_4 (Lederberg, 1965; Lovelock, 1965). In 1993, when Carl Sagan published the results on the Galileo fly-by of Earth (Sagan *et al.*, 1993), he found these signatures are combined with widely distributed surface pigments with a sharp reflection edge in the red part of the spectrum. Other studies have developed the concept of colors of life and added pigments to the list of biosignatures to search for in exoplanets (Seager *et al.*, 2005; Hegde *et al.*, 2015; Schwieterman *et al.*, 2015; Fujii *et al.*, 2018; O'Malley-James *et al.*, 2018).

The reflectance spectra of vegetation pigments were the first to be studied, having a characteristic feature at 700 nm – a feature widely named Vegetation Red Edge (VRE). However, not only plant life is responsible for coloring Earth. Microbial photosynthesis is abundant on Earth (O'Malley-James *et al.*, 2018), as well as non-photosynthetic

organisms, and both can produce colorful pigments with specific spectral features (Hegde *et al.*, 2015). These pigments are tools for biomass production and protection against several different conditions such as cold, dryness, radiation or even lack of resources.

The surface of exoplanets on the limits of the HZ may be cold, dry, and if around certain star types such as M stars, - the coolest and most abundant type of stars -, may also be heavily UV irradiated environments, due to magnetic phenomena (Stelzer *et al.*, 2013), making biopigments into very relevant biosignatures to search for in these worlds.

I.6 Future missions to the icy worlds in the solar system and beyond

Water/rock interactions on the seafloor of ocean worlds are likely major contributors to their ocean composition, and by extension influential factors for habitability potential. Missions such as Cassini-Huygens and Galileo may already have presented us with preliminary evidence of the geochemical evolution of active ocean worlds with the detection of N_2. Also, the ubiquitous presence of CO_2, frequent detection of CH_4, and the finding of H_2 in Enceladus plumes are key factors for the implication of hydrothermal activity at the level of the seafloor. However, pertinent questions regarding the geochemistry of ocean worlds remain unanswered: i) What is the complexity of the molecules dissolved in the interior oceans?; ii) Are there geological features that are produced by processes involving the dissolution or precipitation of solids?; iii) how thick is the ice shell?; And finally, iv) are there detectable biosignatures?. In the next decades, some, if not all, of the above questions will hopefully be answered by *in-situ* investigations.

I.6.1 Future Missions to the Galilean moons

JUpiter ICy moons Explorer (JUICE) from ESA will jumpstart this new era of life-detection missions to the Jovian icy moons in 2023 (Grasset *et al.*, 2013), and the Europa Clipper from NASA (Howell *et al.*, 2020) will follow in 2024 **(Figure I.2)**. The spacecraft JUICE will orbit Earth, more specifically three times between 2023 and 2026, creating opportunities to get relevant imaging information of life on our planet that can be used as a control for searching for life at a distance, as previously reported by Carl Sagan with the predecessor Galileo spacecraft (Sagan *et al.*, 1993). Europa Clipper will follow, focusing more on Europa, as both missions were designed in a complementary approach (Phillips *et al.*, 2014). Due to the great necessity of identifying and characterizing potential endogenous material emerging from the ocean, these missions have as a priority to describe the surface chemistry of these moons as well as look for signatures of life.

Since we will end this decade with much more information on the habitability of the Jovian moons given by these massive orbiters, the concept of the Europa Lander mission has been moving rapidly in the last couple of years (Hand *et al.*, 2021, 2022). Instrumentation pre-projects for the *in-situ* exploration on the surface of Europa have been presented publicly since 2019, including ELSSIE - Europa Lander Stereo Spectral Imaging Experiment (ELSSIE) (Murchie *et al.*, 2020). Since 2020, open virtual meetings called "Europa / Ocean Worlds Lander Virtual Meetings" have taken place. The objective of these meetings is to bring the scientific community together to speed up the process so the Europa Lander mission can be confirmed in time to occur soon after Europa Clipper, with a much more expressed purpose to detect life.

A Joint Europa Mission (JEM) has been proposed based on a possible future collaboration between ESA and NASA. This new mission concept aims to follow Europa Lander with a science payload for both an orbiter and a soft lander. The main objectives

of JEM are to understand and characterize the habitability of its potential biosphere and ultimately search for life (Blanc *et al.*, 2020).

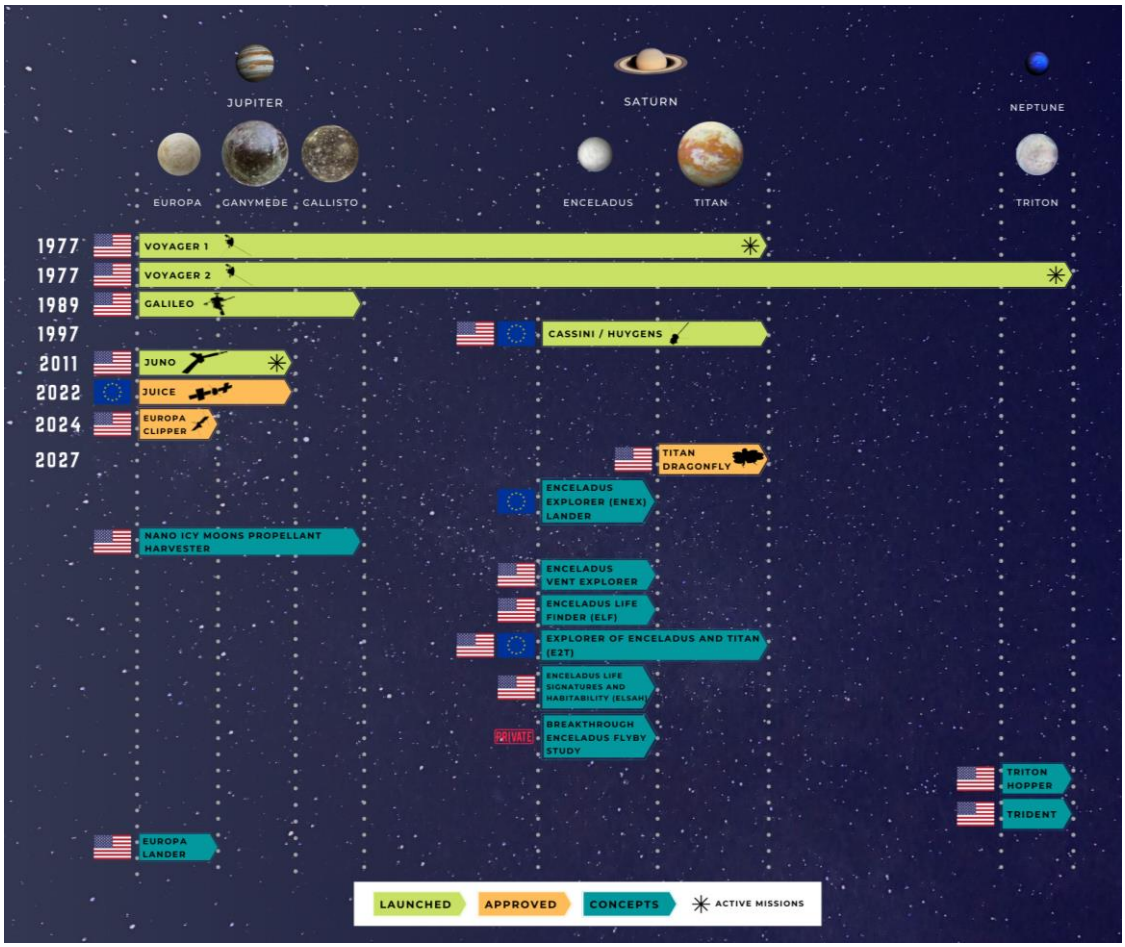

Figure I.2 - Illustrated diagram of some exploratory missions to the icy moons of our solar system. Launched missions (green) represent past missions to the outer solar system (and beyond, as of Voyager I and II) that reached the targeted icy moons. Approved missions (orange) represent missions to the icy moons that have been confirmed and will be launched before 2030. Mission concepts (blue) represent proposals for future missions to the outer solar system which has icy moons as the study target. Only icy moons with habitability potential were selected for this illustration. Icy moons were herein grouped by planetary systems (Jupiter, Saturn, and Neptune). Non-governmental space missions are represented with the symbol "Private". The symbol "*" represents missions that are still active in the present year (2022). This illustration is not to scale. From Coelho *et al*., 2022, under review in *Habitable Worlds and Sustainable Life on Earth and Beyond.* Springer.

I.6.2 Missions to Enceladus

Missions such as Enceladus Life Finder (ELF), which intended to analyze the plumes to search for habitability and would include high-resolution mass spectrometers, and the return mission Life Investigation For Enceladus (LIFE) have been proposed **(Figure I.2)**

but so far remain only concepts (Tsou *et al.*, 2012; Reh *et al.*, 2016). Yet, questions regarding the possible existence of geochemical gradients on the subsurface, and how accurately plume composition can inform us about ocean chemistry, remain unconstrained (Glein *et al.*, 2018).

New lander missions have been proposed to explore Enceladus: Enceladus-Explorer (ENEX) and Enceladus Orbilander (Eliseev *et al.*, 2014; MacKenzie *et al.*, 2021), an European and USA effort. Also, smaller missions only aiming to sample the active plumes in the south pole of Enceladus have been proposed, such as Enceladus Life Signatures and Habitability (ELSAH). The most recent NASA Decadal Survey for Planetary Science, released in April 2022, highlighted a mission to Enceladus as a top priority for the next decade (NASA, 2022).

I.6.3 Missions beyond the solar system

The James Webb Telescope has been launched at the end of 2021, holding promise in escalating drastically our knowledge of exoplanets chemistry (e.g., Mikal-Evans, 2021), at least in their atmospheres. The Atmospheric Remote-sensing Infrared Exoplanet Large-survey (ARIEL) mission from ESA is being developed to observe many transiting planets for statistical understanding, including Earth-size planets, and study their atmospheres. It is set to launch in 2029 (Tinetti *et al.*, 2018). However, future large space-based telescope concepts such as the Habitable Exoplanet Observatory (HabEx) (Mennesson *et al.*, 2016) and the Large UV/Optical/IR Surveyor (LUVOIR) (NASA, 2019) are within NASA's milestones for the next decades. Their design enables the possibility of doing more than transit-spectroscopy and being able to also look directly at surfaces, where signs of habitability, such as liquid water, or even signs of life, such as biopigments may be waiting to be discovered.

To increase the success of all these missions that will mark the next decades as a new era of spacial exploration, extensive work needs to be done on Earth. Otherwise, invaluable signs of life may be unnoticed, or false positives may become a real menace.

I.7 The Arctic water bodies as a planetary field analogue to icy worlds

A planetary field analogue is a location on Earth that mimics a characteristic, or multiple characteristics, of an extra-terrestrial environment (Martins *et al.*, 2017). These characteristics can be physical, geological, and/or chemical.

The Arctic Ocean is a small ocean with an ice shell that is present all year, covering almost completely the entire ocean in winter, influencing the access to light, the salinity gradient, and the communities of organisms (AMAP, 1998; Macdonald, 2000; Comeau *et al.*, 2011). Sea ice is a habitat for several forms of unicellular life (Christner *et al.*, 2000; Price, 2007; Bowman *et al.*, 2012; Martin *et al.*, 2017; Yergeau *et al.*, 2017; Pascoal *et al.*, 2021). As a habitat, sea ice can be challenging, presenting its native biota with a highly irradiated, reflective, dry, and shallow environment. It has been reported that polar pigment-producing microorganisms are better equipped to survive at the surface of ice due to their resistance to dryness, lack of resources, and photooxidation (Bonilla *et al.*, 2009; Lutz *et al.*, 2016; Vigneron *et al.*, 2018; Seel *et al.*, 2020). Their growth will increase the temperature in the ice and snow, decreasing ice-albedo (Maccario *et al.*, 2015) and thus shielding the rest of the community. Arctic sea ice is not an exception, and its colors are a phenomenon that can be seen from space (Lutz *et al.*, 2014, 2016; Williamson *et al.*, 2020). Icy exoplanets orbiting on the edge of the habitable zone of their star may also reflect different colors as a product of potential icy alien life, which may also be detectable from space.

The Arctic Ocean is structurally analogue to the briny global oceans of Europa and Enceladus (Kivelson *et al.*, 2000; Postberg *et al.*, 2009) given the ice shell covering the water. In the icy moons, the ice shell is always shielding the ocean, although the internal water masses are unlikely closed systems with no commutation with the surface (Russell *et al.*, 2017). One of the biggest questions regarding the ice shell of Europa and Enceladus relates to its thickness. Some models will approximate the ice length on hundreds of kilometers while others predict just a few meters (Billings *et al.*, 2005). It is also possible that both models are correct, and that thickness varies with location. In fact, the presence of subsurface liquid water lenses perched within the ice shell of both moons, closer to the surface, under Europa's chaos terrain and Enceladus's south pole have been reported (Schmidt *et al.*, 2011) and predicted (Walker *et al.*, 2015; Culberg *et al.*, 2022), respectively. These perched water bodies may communicate with the interior ocean through cryovolcanic or tectonic events (Soderlund *et al.*, 2020).

The lack of knowledge about the ice cover thickness of the icy moons is one of the limits astrobiologists face when aiming to replicate the icy moon's ocean physical conditions on Earth. Nevertheless, there is one condition we can all be certain of existing in these extra-terrestrial marine environments: the Arctic is a remarkable source of water/ice interactions and transitions.

I.7.1 Water/Ice dynamics and the case of Hudson Bay

The ice/water interface is a region of interest for the habitability of icy moons because it marks redox (reduced ocean *versus* oxidized surface) and energetic transitions. In fact, the freeze-out and water-ice interactions are thought to contribute to the formation of the highly active Chaos terrains of Europa (Schmidt *et al.*, 2011). On Earth, ice/water transition zones are known to expel chemicals when the water freezes, which will

accumulate in the interface water, and seed future microbial blooms and other communities, key to the trophic chain of the hydrosphere/cryosphere (Gosselin *et al.*, 1985).

Arctic aquatic systems have an interface water/ice dynamics with variable salinity concentration (Roff *et al.*, 1986; AMAP, 1998; Macdonald, 2000; Li *et al.*, 2007), replicating the internal briny oceans of Europa and Enceladus (Neveu *et al.*, 2017; Trumbo *et al.*, 2019b; Lobo *et al.*, 2021), as well as in the perched freshwater bodies closer to the surface (Schmidt *et al.*, 2011). The several water bodies composing the Arctic Ocean form singular marine subsystems surrounded by land and freshwater inputs (AMAP, 1998; Macdonald, 2000). Hudson Bay is one of these water masses.

The severe winters of Hudson Bay's subarctic regions will have more daylight hours than the up-north regions (Roff *et al.*, 1986; Ingram *et al.*, 1987; AMAP, 1998). Light, as elsewhere in the cold regions, is a critical factor in the growth regulation of the water and ice microbiomes at the bay. Microbes thriving in the underlying water of sea ice are supposed to be more adapted to lower light intensities in comparison with the ice microbes (Gosselin *et al.*, 1985). Ice and underlying water communicate creating a nutrition channel in between. Desalination and bacterial activity are examples of nutrient replenishment occurring in this junction. Thus, the biota from the ice/water interface, the salinity gradient, temperature, and light are likely the key environmental factors that control nutrient cycling in the Hudson Bay – making it a highly dynamic cold environment.

I.7.2 Hudson Bay – a planetary field analogue to Europa and Enceladus

Hudson Bay is covered with an ice shell of mostly first-year ice for most of the year, with periods of coverage decreasing in locations closer to land **(Figure I.3)**. In winter, the water temperature may vary from 0 to -2ºC, which is within the interval of the

interface water temperature of both Europa and Enceladus (-3.98 and 0ºC) (Melosh *et al.*, 2004; Glein *et al.*, 2015). The salinity of the interface water will be closer to 0% near the coast due to the influence of rivers surrounding the bay, while closer to the center and in deepness will be closer to 3%, being within the 0.5-4% (by mass) interval of Enceladus (Postberg *et al.*, 2009; Hsu *et al.*, 2015) and close to the 3% limit (by mass) predicted to Europa (Hand *et al.*, 2007).

Figure I.3 – Hudson Bay's coast in winter is completely ice-covered. The image was taken in February 2019 by Lígia F. Coelho at the shore of the Whapmagoostui-Kuujjuarapik communities.

The ice/water transition of Hudson Bay is analogue, physically, and chemically (see definitions in Martins *et al.*, 2017), to the ice/water interface environment found in Europa and Enceladus, in the ocean and the water bodies perched in ice.

I.7.3 Applications to future missions to the icy moons of studies on locations in the Arctic biome

The space applications of studies in polar ice include the fields of astrobiology (Garcia-Lopez *et al.*, 2017; Martin *et al.*, 2017; Martins *et al.*, 2017) and planetary protection (Onofri *et al.*, 2008; Kminek *et al.*, 2019).

First, the cryosphere is of great interest to astrobiology considering both fields of research regarding the origin of life and the search for extra-terrestrial life. Theories on the cold origin of life speculate that, in early times, the Earth could have been covered in snow – informally called "snowball Earth", where the first cells formed (Price, 2007). Icy extra-terrestrial environments, in the solar system and beyond, may combine some conditions similar to those of Earth's cryosphere: radiation exposure, dryness, and lack of resources. As referred to before, the ice microbiome survives and sometimes thrives under these conditions on Earth. Some of these microorganisms produce molecules with specific chemical signals (biosignatures) which may be detectable by optic equipment onboard space vehicles orbiting or landing on worlds in our solar system, or equipment attached to large telescopes, terrestrial-based or space-based, that search for life on exoplanets and exomoons. One type of molecule produced by ice microorganisms for, among others, self-preservation from inhospitable conditions is biopigments (Lemoine *et al.*, 2010; Seel *et al.*, 2020). These molecules are key biosignatures to search for in the solar system and beyond due to 1) being universal in the evolution of the tree or net of life, 2) being related with, among other functions, resistance to conditions found on extra-terrestrial icy environments, and 3) having specific optical identities and distinguishing spectroscopic properties, when considering absorbance, fluorescence emittance and reflectance (Baqué *et al.*, 2016, 2020).

Second, planetary protection is the field of study that aims to protect solar system environments from contamination, either forward (from Earth to other worlds) or reverse (from other planets back to Earth). The Committee of Space Research (COSPAR) and ESA's Planetary Protection Officer focus on planetary protection (Kminek *et al.*, 2017, 2019; Rettberg *et al.*, 2019). ESA's main effort is to prevent microorganisms from riding on missions to other planets and moons in our solar system, investing in curation facilities, and microbial monitoring of cleanrooms and launch facilities (Kminek *et al.*, 2019). The environment of each icy moon (e.g., Europa, Enceladus, Ganymede, and Callisto) is very different from one another, requiring different decontamination planning. NASA Response to Planetary Protection Independent Review Board Recommendations (2019) advised the study of mechanisms of contamination individually for each of these worlds (NASA, 2020). Indeed, on polar planetary field analogues, we can sample diverse model habitats. The cryosphere extremophiles are also relevant to planetary protection, including species resistant to cold, acid, alkaline, irradiated (UV or gamma radiation), and dry or shallow environments (Kminek *et al.*, 2019). The project LIFE, onboard the International Space Station, determined the effect of the space environment on extremophilic polar strains. These strains were subjected to vacuum 10−5 Pa, temperature variations from -20ºC to 20ºC, Mars atm. 600 Pa and monochromatic (254 nm, 71.4 $\mu W/cm^2$) and polychromatic (200–400 nm) UV irradiation (Onofri *et al.*, 2008). The results revealed that the most resistant strains to space radiation produced biopigments (Onofri *et al.*, 2018).

But lessons from Arctic ice studies are not limited to what we learn from their outputs. While drilling and sampling ice in previous Arctic and Antarctic campaigns, great sources of contamination were detected in the exterior layers of the ice cores coming from handling during sampling and during the posterior processing (Rogers *et al.*, 2004;

Christner *et al.*, 2005). Sampling in future lander missions to Europa and Enceladus, such as Europa Lander and Enceladus Orbilander, will also need to drill and remove ice to reach the underneath ocean. There is a critical lack of standardized processing and decontamination protocols for planetary field analogues specific to the planets and/or satellites in study **(Table IX.1)**. Thus, clean protocols to sample and examine Arctic ice serve as a testbed for future search-for-life space missions while improving the fieldwork practices in glacial environments that face the same concerns.

I.8 Aim of the study and thesis outline

Future missions to the icy worlds will have many forms, either distant observation from large telescopes, space vehicles orbiting around moons for many years while sampling their active plumes, lander vehicles equipped to reach the interior ocean, or even, more futuristically, return payloads. Although so different, all have one thing in common: they will need a great amount of data from Earth's cold habitats to be successful.

The first challenge, especially for missions in the solar system, will be planetary protection. The real risk of forward contamination is still unconstrained, and so ESA decided to euthanize the JUICE vehicle in Ganymede (a less habitable icy moon) (Grasset *et al.*, 2013), similarly to Cassini-Huygens, which was pushed into Saturn, in April 2017, after 20 years of exploration (Edgington *et al.*, 2016). However, this will not be a solution for lander or return missions. As a solution, the study of clean protocols for ice sampling, processing, and analysis in planetary field analogues is useful for future missions to the icy moons as well as for polar science in general, since polar biomes are also protected, and sometimes pristine environments, that allow us to visit Earth's past.

The second challenge, now for all mission types, is the unfamiliarity the scientific community still has about the microbial structure and chemical signatures of some planetary field analogues as is the case for Hudson Bay's cryosphere. Not only planetary field analogues are usually remote locations that require a lot of logistic capacity and preparation, but also the state-of-art techniques for cultivation – the standard for microbial identification - are still very limited with the current estimation of only roughly 1% of all microorganisms being culturable. One of many solutions is the use of high throughput sequencing techniques that allow for the mass identification of whole communities. DNA amplification is powerful in magnifying low-biomass habitats such as ice and thus coupled with sequencing techniques it is possible to characterize ice microbial communities.

The third and last challenge is the shortage of comprehensive catalogues of references for biosignatures that could be easily used as a tool to guide the search for extra-terrestrial life. Humanity is spending many resources on massive missions to explore the universe, which involves several different space agencies, yet it is still risking missing signals of extra-terrestrial life. The current databases that include some optical references for biosignatures are limited in terms of quantity and do not refer to any specific habitat, but specific organisms instead (Taniguchi *et al.*, 2021). The scientific community has a better chance of finding biosignatures linked unambiguously to types of extra-terrestrial environments, (e.g., ice *versus* hot environments) than to attempt to find the signals of particular life-forms, even if extra-terrestrial life evolved similarly to Earth's life. The solution is the creation of a reference database of biosignature spectra connected with a specific environment - ice in this case - since all missions above-mentioned in this section will use spectroscopy to observe and interact with cold extra-terrestrial surfaces.

In this thesis, a multidisciplinary and integrative study of ice and water samples from Hudson Bay's coast (a planetary field analogue to icy worlds) was performed. One of the main novelties is the connection between all approaches (chemistry, biology, and physics) in the same samples to lead to robust datasets. The present document is thus organized into five chapters:

Chapter I is a comprehensive literature review focused on the characterization of icy worlds and planetary field analogues of icy worlds. The applications to the preparation, execution, and success of future space missions to icy worlds are highlighted along with proposed solutions for some of the present-day challenges to space ventures.

Chapter II presents a new methodology to process and examine ice cores from planetary field analogues to the icy moons. It also includes an approach to monitoring microbial contamination and the identification of such contaminants. It highlights the relevance of such new protocols to future missions to the icy moons of Jupiter and Saturn.

Chapter III introduces the first characterization of the prokaryotic community structures in the ice and ice/water interface of Hudson Bay's coast in winter. It reveals sharp shifts in prokaryotic community composition between sea ice and interface water. While the sea ice community appears richer in marine bacteria, there is a larger dispersal of freshwater bacteria in the interface water underneath it, because of the extension of the river inputs to Hudson Bay in late winter. It also shows that pigmented bacteria are more prevalent in sea ice than in the water underneath.

Chapter IV is the spectroscopic characterization of fluorescent organic molecules from Hudson Bay's ice and water samples. It displays fluorescent biomolecules as crucial biosignatures and how their study effectively unravels trends in Hudson Bay's ecology.

Chapter V combines the knowledge from chapters II, III, and IV in a final research work with direct application in future missions to search for life in icy worlds. It delivers the first reference guide for the search for pigmented life in icy worlds. It comprises the study of the spectral signatures of 80 pigmented strains from the ice microbiome of Hudson Bay. It includes two sets of measurements referencing exoplanets with different levels of available liquid water.

II CONTAMINATION ANALYSIS OF ARCTIC ICE SAMPLES AS PLANETARY FIELD ANALOGUES OF ICY MOONS AND IMPLICATIONS FOR FUTURE LIFE-DETECTION MISSIONS

Publication:

Coelho, L.F.; Blais, M.A.; Matveev, A.; Keller-Costa, T.; Vincent, W.F.; Costa, R.; Martins, Z.; Canário, J. (2022). "Contamination analysis of Arctic ice samples as planetary field analogues and implications for future life-detection missions to Europa and Enceladus". *Scientific Reports*. Under review.

II.1 Summary

Missions to detect extra-terrestrial life are being designed to visit Europa and Enceladus in the next decades. The contact between the mission payload and the habitable subsurface of these satellites involves significant risk of forward microbial contamination. The standardization of protocols to decontaminate ice cores from planetary field analogues of icy moons, and monitor the contamination in downstream analysis, has a direct application for developing clean approaches crucial to life detection missions in these satellites. Here we developed a comprehensive protocol that can be used to monitor and minimize the microbiological contamination of Arctic ice cores in processing and downstream analysis. We used mechanical techniques to minimize bioburden from sampling in the exterior layers of ice cores, constructed artificial controls, and applied culture-dependent and culture-independent techniques, including 16S rRNA amplicon sequencing, to monitor contamination. We identified 13 bacterial contaminants, including a radioresistant species. This protocol decreases the contamination risk, provides quantitative and qualitative information about contamination agents, and allows validation of the results obtained. This study highlights the importance of decreasing and evaluating microbiological contamination in the processing of polar ice cores, including in their use as analogues of Europa and Enceladus.

II.2 Introduction

Europa and Enceladus are two icy moons from our solar system identified as ocean worlds due to the presence of a liquid ocean under their icy surface (Kivelson *et al.*, 2000; Postberg *et al.*, 2009). Europa has also secondary liquid water reservoirs, perched in the ice and closer to the active surface (Schmidt *et al.*, 2011). The water bodies present in these satellites are considered habitable environments (Chapter I, section 1). Several

concepts for future lander missions to these moons have been developed; e.g., Europa Lander, Enceladus Orbilander, and Joint Europa Mission (JEM) (Blanc *et al.*, 2020; MacKenzie *et al.*, 2021; Hand *et al.*, 2022). These missions will need to drill and sample a layer of ice (exact extension still undetermined) to eventually reach interface water.

COSPAR recommends that the study of methods of bioburden reduction for these missions should reflect the type of environments found on Europa or Enceladus, focusing on Earth organisms most likely to survive on these moons, such as cold and radiation tolerant organisms (Kminek *et al.*, 2017, 2019; Rettberg *et al.*, 2019). Environments on Earth that exhibit similar extreme conditions as planets and moons in our solar system are called planetary field analogues (Marlow *et al.*, 2008, 2011; Martins *et al.*, 2017). Both the Arctic and Antarctic offer locations that mimic environments present in the icy moons of Jupiter and Saturn (Martins *et al.*, 2017). These locations are populated by extremophiles - organisms adapted to survive these severe conditions such as extreme temperature and pH, dryness, oxidation, UV radiation, high pressure, and high salinity (Rothschild *et al.*, 2001; Merino *et al.*, 2019). Microbes from these habitats are viable despite hundreds to thousands of years in terrestrial glaciers and cryo-permafrost environments (Mackelprang *et al.*, 2017; Liu *et al.*, 2019), increasing the plausibility of finding putative life forms in similar habitats on those satellites. Polar extremophiles are also known to survive sterilization procedures for planetary protection (Crawford, 2005) and under space conditions onboard the International Space Station (ISS) (Onofri *et al.*, 2008).

The challenges of sampling, processing, and analyzing Arctic and Antarctic ice samples are the closest to those of future life-detection missions in these satellites (Christner *et al.*, 2005; Eigenbrode *et al.*, 2009). The constraints include difficulties in sampling, analysis of low biomass samples, and the need to minimize and monitor

potential sources (SCAR, 2017) of contamination from mesophilic environments on Earth, where microbes are ubiquitous and in high abundance.

When studying recent terrestrial ice, contamination is critical, and sources are mainly due to equipment such as ice corers, handling, and transportation (Rogers *et al.*, 2004; Christner *et al.*, 2005; Michaud *et al.*, 2020). In the context of planetary field analogues, we add more contamination sources such as snow, air, and soil microbes that are part of the atmospheric and soil microbiome but are not expected to be present in icy worlds with thin atmospheres and no regolith (Squyres *et al.*, 1983). Studies from the last 20 years of ice core research mention the use of sterile equipment in the field while drilling the ice cores **(Table IX.1)**. Codes of conduct and clean protocols to sample pristine subglacial lakes in Antarctica have also been created recently (SCAR, 2017; Michaud *et al.*, 2020), which represents a challenging and laudable effort by the scientific community to conserve these unique microbial ecosystems. However, the potential sources of contamination are not limited to the field. During manipulations of ice cores in the laboratory, microbial contaminants can be introduced from the laboratory air, equipment, materials, reagents, or even by humans during downstream analysis such as filtration, DNA extraction (the kitome), amplification, and sequencing, or during cultivation in a nutritive medium. These procedures will be robotized in lander space missions; however, they still represent more layers of contact between man-made equipment coming from Earth and extra-terrestrial samples. Sterilization methods used for equipment cannot be directly applied on ice samples (Eigenbrode *et al.*, 2009). Controlled heat, UV-C, and chemical disinfectants such as ethanol, benzethonium chloride, and sodium hypochlorite have been used directly in the exterior of ice samples being especially efficient in reducing active contaminants in cultivation work (Rogers *et al.*, 2004; Christner *et al.*, 2005; Kinasz, 2019). However, they are not adequate for life detection, molecular

methods of low-biomass ice samples, or the integrity of other microbial analyses. For example, ethanol is an effective disinfectant to decrease contamination for culture-dependent analysis, however, it does not destroy DNA molecules (Christner *et al.*, 2005). While excising the external layers of the ice cores has proved effective in removing most contaminating cells (Rogers *et al.*, 2004; Christner *et al.*, 2005; Zhong *et al.*, 2018; Kinasz, 2019), without compromising the interior native biota, no known protocol can completely prevent contamination, which leads us to the last possible resource for an ethical sampling and processing methodology: contamination monitoring through the use of background controls (Zhong *et al.*, 2018) that have proved to be very effective (Zhong *et al.*, 2018; Coelho *et al.*, 2022b). Culture-dependent and -independent analysis (Dancer *et al.*, 1997; Abyzov *et al.*, 2001; Sheridan *et al.*, 2003; Olsson-Francis *et al.*, 2010; Shivaji *et al.*, 2013; Xing *et al.*, 2016; Zhong *et al.*, 2018; Mitchell *et al.*, 2018; Regberg *et al.*, 2018; Shen *et al.*, 2018; Sherpa *et al.*, 2018; McCubbin *et al.*, 2019; Rettberg *et al.*, 2019) have been used in background controls and the planetary protection context. In past studies on ice cores, culture-dependent investigations appeared to instigate more care to prevent contaminants in comparison with culture-independent techniques **(Table IX.1).** This is likely because DNA contamination from the laboratory air or sterile material is commonly considered insignificant, due to its presumably low representation in comparison with the microbial load of the whole community present in the samples, which is now overcome by the increased sensitivity of polymerase chain reaction (PCR) and DNA sequencing techniques. The lack of standardized methodology adopted to decrease and monitor contaminations in ice core analysis, similar to what already exists in sampling (SCAR, 2017; Michaud *et al.*, 2020), remains a limiting issue for the scientific integrity of the acquired data in icy planetary field analogues, as well as for the design of proven and robust protocols for the future lander and return missions to icy

moons. As a result, the identity and function of microbial contaminants expected from ice core analysis remain a challenge in the field of planetary protection.

In this study, we propose a multidimensional approach to restrict and monitor the contamination inherent in the processing and analyzing ice samples, combining the most effective methods presented in the last 20 years of ice core studies **(Table IX.1)**. The decontamination methodology for the ice core surface was mechanical to decrease contaminants while preserving the natural biota. We constructed background controls **(Figure II.1)**: an artificial ice core made of sterile MiliQ water (Processing Control - PC) and a DNA extraction control sample (DNA-extraction Control - DC). We used both culture-dependent and -independent techniques, including 16S rRNA gene amplicon sequencing of metagenomic DNA samples, accessing several levels of visible and quantifiable microbial contamination.

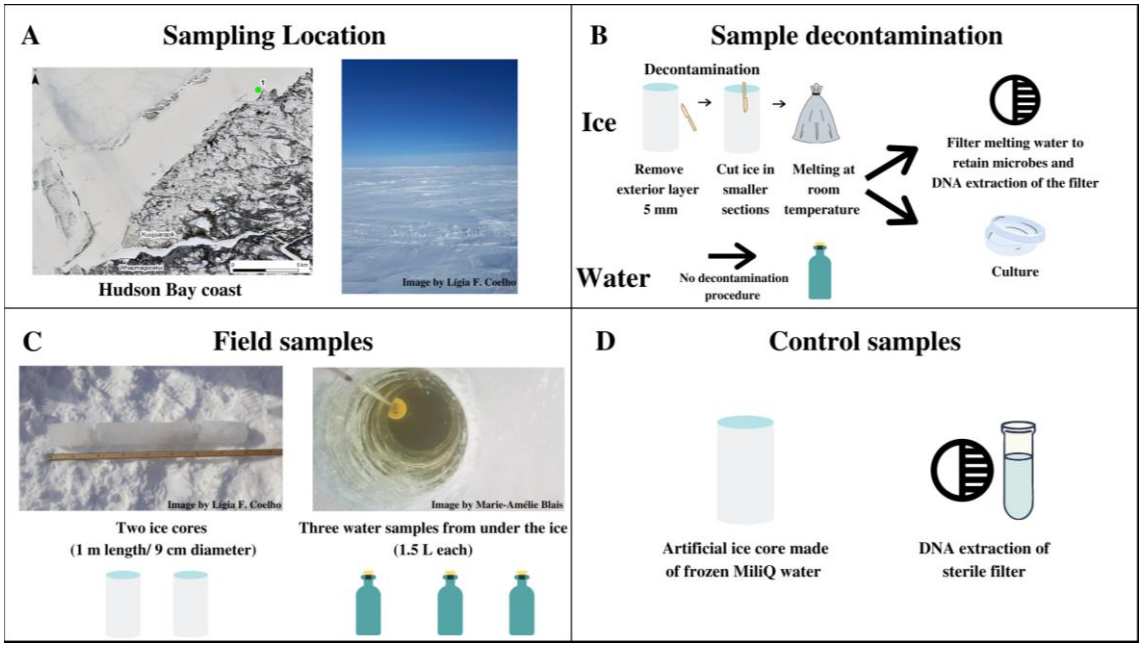

Figure II.1 - Sampling location on the east coast of Hudson Bay, Quebec, Canada, latitude 55.39°N; longitude 77.61°W (Map data © Sentinel-2); **(B)** Sampling decontamination procedure and following processing preceding culture-dependent and culture-independent analysis; **(C)** Description of environmental samples with respective replicates: ice cores (duplicate – Ice 1, Ice 2), and interface water (triplicate – Water 1, Water 2, Water 3); **(D)** Control samples: an artificial sterile ice core made in the laboratory referred as a processing control (PC), and a clean filter inside a clean microtube used as a control for downstream DNA analysis referred as DNA extraction control (DC). From Coelho *et al.*, 2022, under review in *Sci. Rep.*

We identified the contaminating microorganisms of the present study using an established ribosomal marker database to understand the astrobiology relevance of the contaminants. Such a decontamination protocol would be suitable for the design of life-detection experiments on planetary field analogues of Europa and Enceladus, targeting ice cores that may serve as a proxy for habitats of extra-terrestrial communities. Also, our protocol will serve as a testbed for procedures of decontamination of samples from future landing/return missions to the icy moons.

II.3 Materials and Methods

II.3.1 Sampling site and collection of ice and water

Sampling was performed in the southeast of Hudson Bay, a coastal point 12 km away (latitude 55.39°N; longitude 77.61°W) from the Indigenous communities of Whapmagoostui-Kuujjuarapik in Nunavik, northern Quebec, Canada **(Figure II.1)**. First-year sea ice formations are characterized by a one-meter-thick shell on top of Hudson Bay's water during winter, creating a highly dynamic freezing/melting cycle in the water-ice interface where nutrients and microbes accumulate (Legendre *et al.*, 1996). A river system (Great Whale River) is relatively close to influencing the surface bay waters with freshwater inputs (a typical phenomenon in Arctic aquatic systems) (Blais *et al.*, 2022). The ice and the interface water (water just beneath the ice) of the sampled point in Hudson Bay are considered analogues to the water-ice interface environment found in Europa and Enceladus (water bodies perched in ice) considering the low thickness of the first-year sea ice (1 m). Also, the salinity of the interface water was 1.05% by mass, being within the 0.5-4% interval of Enceladus and the interface water temperature was -0.4ºC which is within the interval of the interface water temperature of both satellites (-3.98ºC and

0ºC), either pondering perched liquid water reservoirs closer to the surface or even the internal ocean.

Samples were collected in late winter (Feb 27th, 2019) when ice, approximately 1-m thick, covered the bay. The snow cover (20 cm) was removed from the sampling site. An ice auger was used to drill a hole in the sea ice shell and the interface water was bottled right beneath the ice (1 L in triplicate) using a Kemmerer bottle with 2.2 L of volume **(Figure II.1)**. Ice cores were sampled in duplicate (50 cm apart and encompassing the interface water sampling site) using a Kovacs ice corer with 9 cm of diameter and 1 m of length. In total, five samples were collected: Ice 1, Ice 2, Water 1, Water 2, and Water 3, all from the same site. The ice cores were handled with gloves and placed inside sterile bags. The lowest temperature registered at the weather station of Whapmagoostui-Kuujjuarapik during sampling days was -28ºC, while the highest temperature reached was -11ºC at noon, with an almost constant wind flow of 21 km/h. The salinity and temperature data were collected on-site using YSI EXO2 multiparameter probe (YSI Inc. Ohio, USA), which was placed in the interface water after extracting the ice cores.

II.3.2 Design and construction of background controls

II.3.2.1 Construction of sterile artificial ice core – processing control (PC)

A sterile artificial ice core, called as "processing control" or "PC" was constructed from 1 L of sterile Milli-Q water **(Figure II.1)**, which was double filtered through a Millipore system (18.2 MΩ.cm, 25ºC) in the facilities of Centro de Química Estrutural (CQE), Instituto Superior Técnico (Portugal). The water was then doubled autoclaved at 121°C for 30 min and irradiated for 45 min using the UV germicide lamp present inside a class II Microbiological Safety Cabinet (Faster BH-EN 2004), in the facilities of Institute for Bioengineering and Biosciences (iBB), Instituto Superior Técnico, Portugal. The Milli-Q water was carefully transported to Centre d'Études Nordiques (CEN), a

research station located in Whapmagoostui-Kuujjuarapik, where it was solidified inside a sterile zipper bag placed in a cylinder shape container at -60ºC before the collection of the environmental ice cores used as a comparison in this study. This sterile artificial ice core (processing control) was later processed in parallel with the environmental ice cores and interface water samples as described below. This background control allowed the monitoring of contamination from the instruments and procedure used to cut and bag the ice and filter the ice meltwater (see below).

II.3.2.2 Design of DNA-extraction control (DC)

A clean filter, deposited in a clean microtube was also subjected to the same total-community DNA (TC-DNA) extraction protocol (see below) as the environmental samples and the processing control to assess possible contamination in downstream analysis. Even considering that only material with adequate sterility pre-treatment for molecular biology and specific for DNA analysis was used (DNA-, DNase- and PCR-inhibitors free plastics and reagents as well as filtered tips), it is important to evaluate possible contamination from the extraction materials and reagents used as well as the general environment of the laboratory (Lazarevic *et al.*, 2016). This blank DNA extraction is here called "DNA Extraction control" or "DC" **(Figure II.1)**.

II.3.3 Sample decontamination procedure and processing

Sample decontamination and processing took place in the laboratory facilities available at Centre d'Études Nordiques (CEN), using sterile equipment (autoclaved, irradiated, and/or washed with ethanol). The external layer (5 mm) of the ice cores was cut using an ice saw (pre-treated with ethanol) and then rinsed with autoclaved, irradiated, and doubled-filtered MiliQ water to reduce handling, air, and snow contamination as well as contamination from the sampling materials in the field. The remaining inner core was

rinsed with sterile MiliQ water and left melting at room temperature in sterile bags. Ice meltwater from environmental ice samples (1000 mL), ice meltwater from the processing control (500 mL) and interface water samples (500 mL) were filtered through 0.22 µm nitrocellulose filters (Millipore®, Sigma-Aldrich) using a vacuum pump **(Figure II.1)**. Before downstream analysis (DNA extraction, amplification, and sequencing), the filters remained frozen and were stored at -80ºC. Unfiltered ice meltwater and interface water were stored in sterile bottles and maintained at 4ºC until cultivation.

II.3.4 Total Community DNA extraction and quantification

TC-DNA extractions were performed on the filters of both the environmental samples (Ice1, Ice2, Water1, Water2, Water3) and the background controls (PC and DC) at iBB in Portugal. The TC-DNA extraction was carried out as described previously (Karimi *et al.*, 2017; Coelho *et al.*, 2022b). The bench was previously cleaned with both ethanol (70%) and HCl (0.1 M). Filters were cut into small pieces to ensure full submersion and improve the contact between the cells and the lysis buffer and enhance the probability of extracting low-abundance DNA (due to the nature of the ice samples). The Ultraclean Soil DNA Kit (MoBio Laboratories, Carlsbad, CA, USA) was used for DNA extraction, following the manufacturer's protocol, for offering vigorous membrane lysis, adequate for ice samples that typically house multiple sporulated microorganisms. Agarose gel electrophoresis procedures were used to examine the integrity of TC-DNA, not showing any DNA bands under UV radiation for either PC or DC. TC-DNA concentrations estimations were quantified using the Qubit 4 Fluorometer with the high-sensitivity dsDNA assay kit (Invitrogen, CA, USA) with a detection limit of 10 pg/µL.

II.3.5 DNA sequencing and processing

II.3.5.1 High-throughput sequencing of 16S rRNA genes and processing of sequencing data

The TC-DNA extracts were subjected to 16S rRNA gene-based high-throughput sequencing on an Illumina MiSeq platform at MR DNA following the company's protocol (www.mrdnalab.com, Shallowater, TX, USA) and using prokaryotic universal primers (for both bacterial and archaeal identification) 515F (5' -GTG YCA GCM GCC GCG GTAA-3') and 806RB (5'-GGA CTA CNV GGG TWT CTA AT-3') (Apprill *et al.*, 2015; Parada *et al.*, 2016). During sequencing, an average of around 300 bp (base-pairs) sequences were generated for all samples (Coelho *et al.*, 2022b). An average quantity of 23000, 21000, and 9000 paired-end sequences were generated per environmental interface water sample, background control sample, and environmental ice sample, respectively.

The 16S rRNA gene amplicon libraries generated in this study were processed within the framework of a previous microbial ecology study on the Hudson Bay coastal ice (Coelho *et al.*, 2022b, chapter III of this thesis) and deposited in the open-source online metagenomic repositorium European Nucleotide Archive (ENA) under the study accession number [PRJEB44116]. Briefly, raw sequences with less than 150 bp and with ambiguous base calls as well as chimeric sequences and singletons, were removed as described earlier (Keller-Costa *et al.*, 2017). Operational Taxonomic Units – (OTUs) were generated and defined by clustering at 3% divergence (97% similarity) with the UCLUST algorithm. A taxonomic classification of OTUs using the SINA sequence alignment tool (v1.2.11) of the SILVA database (https://www.arb-silva.de/aligner/) was performed. The OTUs displaying less than 70% identity were considered unclassified at the domain level and removed from the data, eukaryotes (3 OTUs), chloroplasts (147

OTUs), mitochondria (9 OTUs) reaching a total of 159 were also removed. The final analytical dataset comprised 2331 prokaryotic OTUs and 134230 sequence reads.

II.3.5.2 In-silico decontamination

In-silico decontamination procedures (Lazarevic *et al.*, 2016; Zhong *et al.*, 2018), consisted of the removal of all OTUs detected (through sequencing and data processing – see below) in the previously described background controls from the environmental samples. Different *in-silico* decontamination techniques may be applied such as the exclusion of OTUs whose relative abundance in background controls is above a given threshold; exclusion of OTUs with high relative abundance; exclusion of OTUs with higher relative abundance in background controls than in the environmental samples; or, more conservatively, remove all OTUs present in the background controls from the results of the environmental samples (Lazarevic *et al.*, 2016). Due to the application of this study in astrobiology and NASA recommendations on planetary protection, we assumed the most conservative approach of eliminating all OTUs also present in the background controls.

II.3.5.3 Analysis of taxonomic composition and beta-diversity

Stacked bar charts displaying the taxonomic composition were generated based on the relative abundance of prokaryotic taxa from phylum to genus ranks. Low abundance taxa (e.g., taxa below 0.5% of relative abundance) were merged into a single category called "Others" to improve the readability of the environmental samples which, as expected, were substantially more abundant than the background control samples. Venn diagrams were generated using the VennDiagram package in R to determine the number of OTUs specific to and shared by the environmental samples and the background control samples. The plots were created using R (v. 4.1.0) packages *phyloseq*, *plyr*, and *ggplot2*.

Non-rarefied data was used to prevent loss or ill-representation of low abundance OTUs, an important parameter for this study (McMurdie *et al.*, 2014). The taxonomic annotation of the OTUs present in the background controls (samples PC and DC) were further accessed using the Ribosomal Database Project (RDP) (Cole *et al.*, 2014) applying the tools "Classifier" for genus assignment and the tool "Sequence Match" to search for the closest type strain. Type strains were chosen because they are less likely to be poorly identified, giving us accurate information regarding the closest species found in the database. Taxonomic assignments by the RDP "Classifier" below the 70% confidence threshold were considered unclassified.

II.3.6 Sample cultivation in R2A medium and CFU counts

Culturing was performed at iBB (Portugal) after transporting (48 h) the environmental interface water and ice meltwater as well as the processing control samples, inside sterile bottles in a dark cooler at the average temperature of 4ºC. Interface water samples were serially diluted and cultured by spread-plating on 1:10 R2A agar medium, while 100 µL of both environmental ice meltwater and the processing control samples were directly spread on 1:10 R2A agar medium (Christner *et al.*, 2002). Water samples were cultured with R2A dissolved in sterile artificial seawater (ASW) and ice samples (environmental ice meltwater and processing control), were cultured with R2A dissolved in sterile MiliQ water. The two culture settings were designed due to: 1) the estuarine nature of the sampled environment, 2) the variable saline concentrations of ice, and 3) to widen putative possibilities of obtaining colonies from the processing control (a low-biomass sample) while still being able to compare the results with the environmental ice sampled. Spread plating was performed in triplicates (interface water) and duplicates (ice meltwater and processing control) per dilution. Plates were then incubated at 15°C, and

CFUs were counted every 5 days for 30 days. As a procedure control, clean plates were open during the culturing procedures, kept for 30 days, and no growth was registered.

II.4 Results and Discussion

II.4.1 Assessment of ice core contamination using cultivation-dependent and independent techniques

No colony forming units (CFUs) were registered on the processing control (PC) plates, during the 30 days of the experiment. The interface water samples had notable more culturable bacteria than the sea ice samples, an expected result since usually winter sea ice has relatively low biomass (Coelho *et al.*, 2022b). This suggests that the culture methodologies adopted were appropriate for the environmental samples used, validating the results of the processing control. The culture-independent cell counting method reported the presence of what could be prokaryotic cells in the PC **(Table II.1)**.

Table II.1 - Cultures results **(A)** and flow cytometry results **(B)** are presented in average colony-forming units (CFUs) and cells per mL, respectively, of water (interface water), melted environmental ice cores (ice meltwater), and processing control (PC). Environmental water culture results **(A)** and flow cytometry results **(B)** were partially adapted from Chapter III, Table III.1 (Coelho *et al*., 2022b) on the same ice cores. **(C)** DNA quantification (ng/µL) results on environmental water and ice and the processing control based on fluorescence (Qubit fluorometer). Values in the format of average±SD. From Coelho *et al*., 2022, under review in *Sci. Rep.*

A

Cultures (CFU mL^{-1})			
Days after culturing	Number of CFU/mL of water (x10^2)	Number of CFU/mL of ice meltwater (x10^2)	Processing control
5	400 ± 1.0	0.6 ± 0.02	0
10	30 ± 1.0	3 ± 0.1	0
15	50 ± 1.0	3 ± 0.7	0
20	20 ± 1.0	2 ± 0.4	0
25	30 ± 1.0	2 ± 0.6	0
30	10 ± 3.0	0	0
Total	500 ± 20	10 ± 2	0
*CFU- Colony-forming Unit			

B

Flow Cytometry (cells mL^{-1})		
Number of cells/mL of water (x10^4)	Number of cells/mL of ice meltwater (x10^4)	Processing control (x10^4)
36 ± 4.0	3.4 ± 1.0	0.3

C

DNA quantification (ng µL^{-1})						
Ice 1	Ice 2	Water 1	Water 2	Water 3	Processing control	DNA-extraction control
0.9 ± 0.1	0.4 ± 0.0	0.9 ± 0.1	1.1 ± 0.0	0.13 ± 0.1	DL*	DL*
DL – Below detection limit						

The whole prokaryotic biomass quantified in the control was only 0.8% of the total prokaryotic biomass quantified in interface water, and 8.8% of prokaryotic biomass quantified in ice. This shows how decontamination following the use of appropriate background controls is more crucial when studying ice than water since the magnitude of microbial contamination is expected to be higher for low-biomass samples. Although not culturable, these contaminating cells may still have their DNA undamaged and thus contaminate the downstream DNA analysis (DNA extraction, amplification, and sequencing).

The DNA quantification methodology used **(Table II.1)** accounted for DNA in all environmental samples (however in low quantities), but not in the background controls. These results suggest that flow cytometry results of the processing control were either an "artifact" or, that DNA in this sample was present in very low concentration and thus undetectable by standard fluorometric DNA quantification techniques (detection limit of 10 pg/µL). This is significant considering that following this protocol there will be less contaminating noise on DNA-quantification fluorometric techniques – a possible methodology to search for extra-terrestrial life in future missions.

II.4.2 Amplification and sequencing of 16S rRNA gene fragments detected prokaryotic contaminants in both background controls

Even though our control samples have presented undetectable DNA concentrations **(Table II.1)**, amplicon sequencing of the 16S rRNA gene revealed the presence of prokaryotic DNA in both the PC and the DC **(Figure II.2)**. The DNA sequences from the two controls were clustered in 13 OTUs based on 97% nucleotide similarity, which works as a proxy for prokaryotic species. Given their presence in the controls, we labeled them "contaminating OTUs". Seven of these OTUs were also present in the environmental

samples **(Figure II.2)**, although they represented only less than 0.6% of the total number OTUs identified **(Table II.2)**.

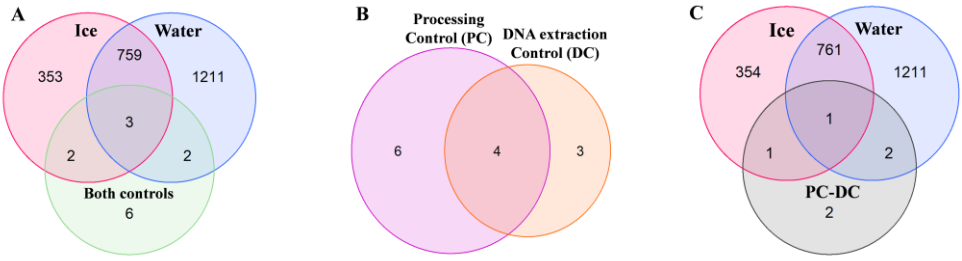

Figure II.2 - Specificity and sharedness of prokaryotic OTUs across environmental samples (interface water and ice) and controls. Venn diagrams display the number of **(A)** OTUs common and specific to environmental water, environmental ice, and both control samples, **(B)** OTUs common and specific to the processing control (PC) and the DNA extraction control (DC), and **(C)** OTUs common and specific to environmental interface water and ice samples comparing with PC-DC (contaminant OTUs exclusive from processing control PC). In diagrams (A) and (C) replicate samples within each sample type were pooled together. From Coelho *et al*., 2022, under review in *Sci. Rep*.

From these seven contaminating OTUs, two appeared only in sea ice samples, representing 0.2% **(Table II.2)** of the total number of sea ice OTUs; two were only in water samples, representing 0.1% of the total number of water OTUs **(Figure II.2)**; and three were present in both ice and water environmental samples.

While the PC had ten contaminating OTUs, the DC had seven **(Figure II.2)**. The PC was in direct contact with the same type of materials that were also used to process the environmental samples such as the ice saw, filtration system, sterile bags, and gloves, which could be the origin of its exclusive contaminating OTUs (six).

The DC contaminants could be from the extraction reagents, the laboratory environment, the personnel, the plastics as microtubes, and pipette tips (Lazarevic *et al.*, 2016), even though plastics were treated to be DNA-free by the company. Another possible source of contamination for the PC and the DC is the samples. Cross-contamination could occur during filtration (for PC), or DNA extraction (for PC and DC) (Lazarevic *et al.*, 2016; Zhong *et al.*, 2018), since both methodologies concentrate a great

quantity of biological material that will increase bioburden on the laboratory surfaces and air for a determined period. However, the small absolute quantity of contaminants detected in the samples discourages such conclusions.

Table II.2 - Relative abundance (%) of contaminating, prokaryotic OTUs in environmental ice (Ice 1, Ice 2), and interface water (Water 1, Water 2, Water 3). Values of the last column in the format of average±SD. From Coelho *et al*., 2022, under review in *Sci. Rep.*

OTU_ID	RDP classifier (>70%)	Ice 1	Ice 2	Water 1	Water 2	Water 3	Average±SD
OTU_4	*Stenotrophomonas*	0	0.02	0	0	0	0.004±0.01
OTU_5	*Corynebacterium*	0.07	0.09	0	0	0	0.03±0.03
OTU_19	*Pseudomonas*	0.09	0.04	0.004	0.009	0.02	0.03±0.03
OTU_22	*Sulfurospirillum*	0	0	0	0	0	0
OTU_25	*Acinetobacter*	0.03	0	0.06	0.20	0.2	0.1±0.09
OTU_36	*Asprobacter*	0	0	0	0	0.008	0.002±0.00
OTU_63	*Escherichia*/*Shigella*	0	0	0	0	0	0
OTU_70	*Chitinophagaceae* family	0	0	0	0	0	0
OTU_98	*Burkholderia*	0	0	0	0	0.008	0.002±0.00
OTU_103	*Sulfurimonas*	0	0	0	0	0	0
OTU_167	*Aridibacter*	0	0	0	0	0	0
OTU_209	*Acinetobacter*	0	0	0	0	0	0
OTU_1153	*Sulfurospirillum*	0.07	0.17	0.06	0.18	0.35	0.17±0.10
Total contamination abundance		0.25	0.32	0.12	0.40	0.61	0.3±0.2

Both controls share four of the 13 contaminants. To account only for processing contaminants, the OTUs of DC were *in-silico* subtracted from PC, remaining only exclusive contaminant OTUs from processing ("PC-DC"- **Figure II.2**). The results for only PC contaminants show that interface water maintained two shared OTUs with the control while ice now only just shared one contaminant OTU. One OTU remains ubiquitous in all samples. Predictably, interface water was much richer in biomass than ice **(Figure II.2)**, both native and contaminant **(Table II.2)** wherefore possible cross-contamination from interface water back to the controls, during processing, was more likely than from the sea ice.

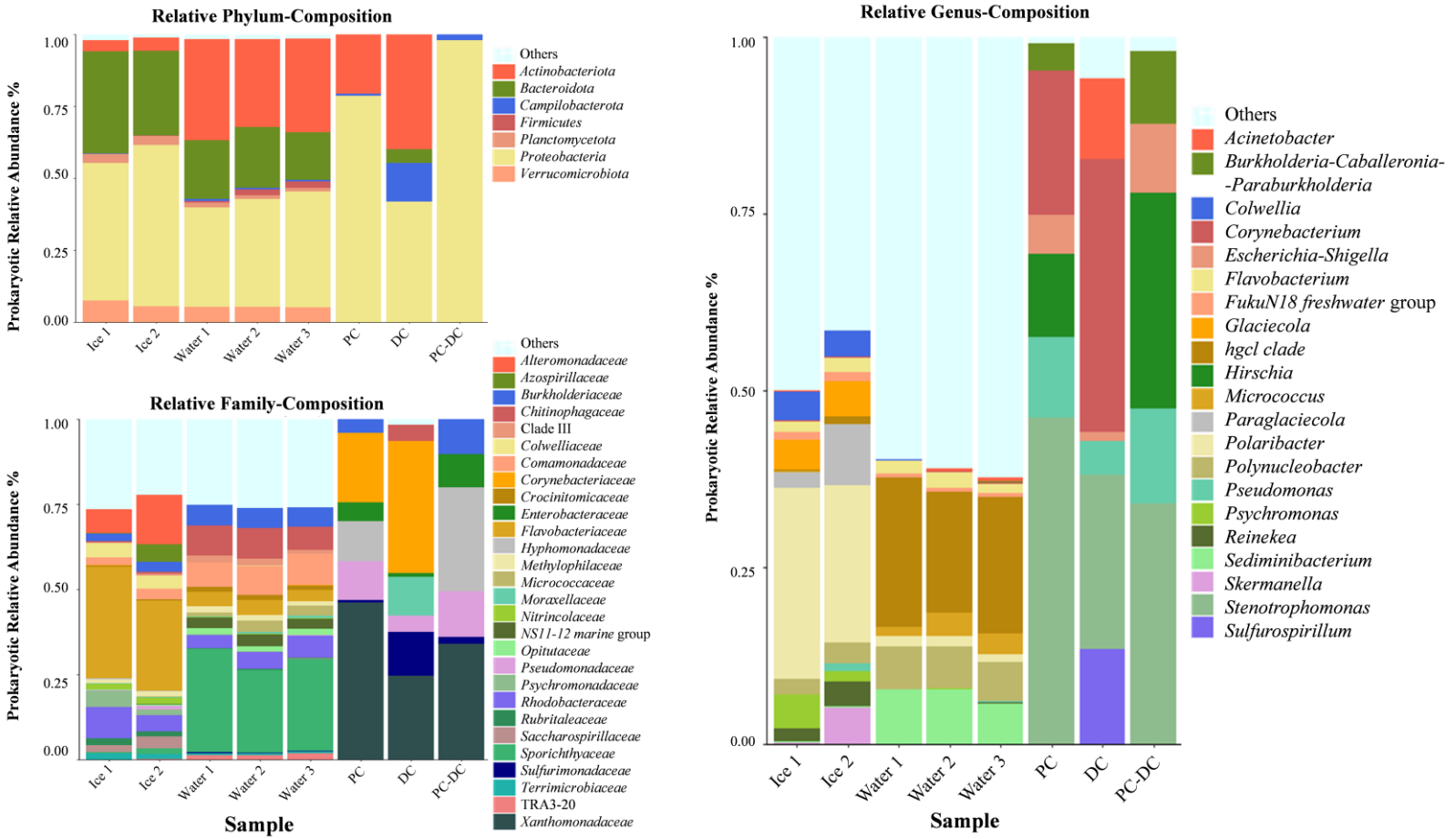

Figure II.3 - Taxonomic composition of prokaryotic communities in environmental samples (ice and interface water, including replicates) as well as controls (processing control -PC, DNA extraction control -DC, and contaminant OTUs exclusive from processing control -PC-DC), based on the relative abundance of OTUs of the non-rarefied dataset. For improved readability, taxa below 0.5% of relative abundance were joined under the category "Others". From Coelho *et al.*, 2022, under review in *Sci. Rep.*

II.4.3 Taxonomic profiles of background controls

While microbial contaminants represented a small group of just a few different prokaryotic identities (OTUs) and were very rare in environmental samples **(Table II.2),** the load of total contaminating DNA strands in controls was considerable **(Figure II.3)**. These results agree with the normal results of amplicon sequencing analysis to monitor reagent contamination which has been described to have taxon richness inversely correlating with the bacterial load (Salter *et al.*, 2014). Meaning that the contaminant community profile is usually distinguishable from the rich, and diverse environmental community, which we also see in our dataset **(Figure II.3)**.

The *in-silico* decontamination (exclusion of contaminants from environmental analysis outputs (Lazarevic *et al.*, 2016) **(Figure IX.1)** shows how evident some contaminants are (e.g., *Acinetobacter*) versus others less abundant which were grouped in "Others". Similar results were reported in past studies on decontamination methods for low biomass samples (Zhong *et al.*, 2018). The parallels between the taxonomic profiles of the environmental samples and controls stop at lower taxonomic ranks (order and genus) – **Figure II.3**. Some contaminating OTUs of the genera *Acinetobacter* and *Corynebacterium* were present, although not abundant, in the environmental samples (Ice 1, Ice 2, Water 2, and Water 3) – **Figure II.3**. In the controls, *Acinetobacter* was more abundant in the DC. Members from the *Acinetobacter* genus have been identified before as part of the kitome (i.e., contaminants from DNA extraction reagents) (Salter *et al.*, 2014), and as contaminants of the NASA Space Assembly Facility (Danko *et al.*, 2021; Wood *et al.*, 2021), where the last cleaning steps of space vehicles take place before launch. Finally, the *Acinetobacter* case shows how our method allows not only the

reduction, identification, and monitoring of likely contaminants but also a close trace of their possible origin.

Silva taxonomy (https://www.arb-silva.de/aligner/), as well as RDP database assignments, showed that OTUs were from the genera *Burkholderia-Caballeronia-Paraburkholderia*, *Acinetobacter*, *Escherichia-Shigella*, *Corynebacterium*, *Hirschia*, *Pseudomonas*, *Stenotrophomonas*, and *Sulfurospirillum* **(Table II.3)**. Previous studies reported *Corynebacterium*, *Burkholderia*, *Acinetobacter*, and *Pseudomonas* to be present in other background controls constructed from artificial sterile ice cores and DNA extraction blanks (Salter *et al.*, 2014; Zhong *et al.*, 2018), and another study report *Stenotrophomonas* and *Acinetobacter* to be able to grow after bioburden assays performed by ESA which include heat-shock treatment (Rettberg *et al.*, 2019).

Of the 13 contaminating OTUs, one was only identified at the family level (meaning that it may belong to an unknown genus), three were only identified at the genus level, eight were closely related to a type strain (>90% similarity), and one was identified at the species level with maximum confidence level from the software **(Table II.3)**. OTU 63 is closely related to human enterobacteria (*Shigella* spp.) and through this method, we were able to know that while this bacterium was present in the PC, it was not detected in any of the environmental samples. Processing ice samples demands much more human contact than DNA extraction, agreeing with this result. OTU 98 is a close match for *Burkholderia stabilis*, notably a known contaminant of class I medical devices including gloves (Wang *et al.*, 2015; Sommerstein *et al.*, 2017). This OTU was also mostly present in the PC.

Table II.3 - List of all OTUs retrieved in the processing control (PC) and DNA extraction control (DC). The OTU's abundance (number of reads) are presented from environmental ice meltwater (Ice 1, Ice 2), environmental interface water (Water 1, Water 2, Water 3), PC, DC, and PC-DC (removing PC shared OTUs with DC remaining only contaminant OTUs exclusive from PC). The OTUs are shown classified at the genus level based on the RDP classifier (OTUs with scores >70% confidence threshold were considered classified at the genus level). The closest type strain on RDP represents the closest type species at the RDP database and respective closeness score (a_b probability score). Note that OTU 209 was identified as species *Acinetobacter radioresistens*. From Coelho *et al*., 2022, under review in *Sci. Rep*.

OTU_ID	RDP classifier (>70%)	Closest RDP* type strain (Accession number)	a_b probabi-lity score	Number of reads in Ice 1	Number of reads in Ice 2	Number of reads in Water 1	Number of reads in Water 2	Number of reads in Water 3	Number of reads in Processing control (PC)	Number of reads in DNA extraction control (DC)	PC-DC
OTU_4	*Stenotrophomonas*	*Stenotrophomonas maltophilia* (T), ATCC 19867, AB021405	0.918	0	2	0	0	0	8506	6088	2418
OTU_5	*Corynebacterium*	*Corynebacterium tuberculostearicum* (T), CIP107291, AJ438050	0.966	5	10	0	0	0	3770	9522	0
OTU_19	*Pseudomonas*	*Pseudomonas proteolytica* (T), type strain: CMS 64, AJ537603	0.954	7	4	1	2	4	2122	1174	948
OTU_22	*Sulfurospirillum*	*Sulfurospirillum alkalitolerans* (T), HTRB-L1, GQ863490	0.742	0	0	0	0	0	0	3169	0
OTU_25	*Acinetobacter*	*Acinetobacter guillouiae* (T), DSM 590, X81659	0.962	2	0	14	46	57	0	2771	0
OTU_36	*Asprobacter*	*Asprobacter aquaticus* (T), DRW22-8, KF056993	0.947	0	0	0	0	2	2165	0	2165
OTU_63	*Escherichia/Shigella*	*Shigella sonnei* (T), type strain: CECT 4887, FR870445	0.977	0	0	0	0	0	1004	310	694
OTU_70	*Chitinophagaceae* family	*Ferruginibacter alkalilentus* (T), HU1-GD23, FJ177530	0.811	0	0	0	0	0	0	1170	0
OTU_98	*Burkholderia*	*Burkholderia stabilis* (T), LMG 14294, AF097533	0.954	0	0	0	0	2	728	0	728
OTU_103	*Sulfurimonas*	*Sulfurimonas denitrificans* (T), DSM 1251, CP000153	0.865	0	0	0	0	0	141	0	141
OTU_167	*Aridibacter*	*Aridibacter famidurans* (T), A22_HD_4H, KF245634	0.918	0	0	0	0	0	0	269	0
OTU_209	*Acinetobacter*	*Acinetobacter radioresistens* (T), DSM 6976, X81666	1.000	0	0	0	0	0	0	131	0
OTU_1153	*Sulfurospirillum*	*Sulfurospirillum alkalitolerans* (T), HTRB-L1, GQ863490	0.743	5	19	15	41	89	0	12	0

This result highlights how significant DNA contamination is when samples are handled by humans, even if properly equipped, and are then analyzed through sensitive DNA detection techniques.

OTU 1153 and OTU 25 were the most representing contaminants in the environmental samples, with approximately 0.1% of average relative abundance among all environmental samples (see **Table II.2**). The OTU 25, closely related to *Acinetobacter guillouiae,* was highly abundant in the DC (agreeing with **Figure II.3**). Some other OTUs present in **Table II.3** had low abundance (below detection limit) in the environmental samples while being detected in the DC.

Previous analyses of contaminants from DNA extraction reagents showed the presence of extremophilic strains such as members from the radioresistant genus *Deinococcus* (Salter *et al.*, 2014). A species exclusive from the DC, OTU 209, was a 100% match to *Acinetobacter radioresistens*. This bacterium is highly tolerant to gamma-ray radiation (Nishimura *et al.,* 1988), thus difficult to eliminate with radiation-based sterilization.

Overall, DC rather than PC was a more disruptive source of contamination, suggesting that DNA extraction protocols for life-detection analysis will always profit from the use of background controls. A recent study on the contaminants from NASA Spacecraft Assembly Facility has shown the significance of the kitome in the field of planetary protection. It has also demonstrated that bacteria of human origin prevail in the kitome while bacteria known to survive extreme conditions were more likely contaminants from the cleanroom environment (Wood *et al.,* 2021). Our data unravel a not so evident pattern suggesting that some bacteria from human origin were more prevailing in the processing control (which would be more relatable to the environment of the laboratory) instead of as a member of the kitome, while the DNA extraction kit was

a more likely source of the stress-resistant contaminating genus *Acinetobacter*. However, OTU 5, closely related to *Corynebacterium tuberculostearicum* type strain – part of the human skin microbiome, was found to prevail in the DC, likely being part of the kitome, agreeing with the previous NASA study (Wood *et al.*, 2021). These results highlight how relevant the disclosure and close monitoring of the communities present in controls, including the kitome, are for astrobiology analysis in planetary field analogues as well as future space missions.

II.5 Applications to future space missions to the icy moons

Space is inhospitable for (most) known biological systems when considering the combination of vacuum conditions, extreme temperatures, microgravity, and, the most deleterious, unfiltered solar and galactic radiation (Olsson-Francis *et al.*, 2010). Although it is considered unlikely that terrestrial microbes could survive multi-year cruises to the outer solar system, the fact is that there is no real statistical calculation of the risk of forward contamination, and thus it remains a concern for the exploration of icy worlds (Kminek *et al.*, 2019; Coustenis *et al.*, 2021). Only future analysis of the equipment from missions directed to collect and return with samples from celestial bodies, such as Hayabusa2 and OSIRIS-REX will allow assessment of such inferences (Regberg *et al.*, 2019; Chan *et al.*, 2020; Martins *et al.*, 2020).

II.5.1 Relevance of the contaminants found in this work to planetary protection

Out of the 13 bacterial entities found in the controls analyzed, 12 were related to known extremophile species, and one was identified at the species level: *Acinetobacter radioresistens*, a gamma-ray resistant bacterium (Nishimura *et al.*, 1988). Radiation is the most challenging condition for contaminants, so limiting that even putative extra-

terrestrial radiation-adapted life on the surface of icy moons is unlikely. Terrestrial microorganisms capable of surviving high-energy irradiation would be especially important as planetary protection agents to screen for.

The other 12 contaminants were not identified at the species level but are all related to organisms that thrive in environments with conditions close to the limits of growth and survival. The species *Sulfurospirillum alkalitolerans*, *Ferruginibacter alkalilentus*, *Sulfurimonas denitrificans*, *Pseudomonas proteolytica*, and *Aridibacter famidurans* are known to be tolerant to cold temperatures, high or low pH, dryness, and high-energy radiation environments (UV and gamma-ray), resuming the general microbial features that COSPAR and NASA flagged for future lander missions to Europa and Enceladus (Kminek *et al.*, 2017; Rettberg *et al.*, 2019; NASA, 2020). However functional genomics using full metagenome sequencing of DNA will be needed in future studies to assess the extremophilic potential of ice contaminants in planetary field analogues since these communities are dominated by uncultured microorganisms.

Members of *Aridibacter famidurans* can survive without liquid water and nutrients for long periods (Huber *et al.*, 2014), and these abilities are linked to increased radiation resistance. *Sulfurospirillum alkalitolerans* and *Ferruginibacter alkalilentus* are species resistant to high pH environments and *Sulfurimonas denitrificans* are reported as a species from deep-sea vents. Enceladus is modeled to have alkaline waters (pH between 8.5 and 10.5) and to have extensive hydrothermal activity at the ocean floors (Vance *et al.*, 2007; Hsu *et al.*, 2015; Postberg *et al.*, 2018).

A previous study has flagged a psychrophilic (cold-resistant) biofilm-producer, *Psychromonas antarcticus*, as relevant for forward contamination risk to the icy moons (Rettberg *et al.*, 2019). Biofilms are biotic structures that allow microorganisms to be additional resistant to external pressures. In this study, we can reinforce the risk of strains

such as these based on our data from planetary analogues. We found a similar microorganism in our contamination list, closely related to *Pseudomonas proteolytica*, which is a psychrophilic strain also originally isolated from biofilms in Antarctica (Reddy *et al.*, 2004). This species is a concern for planetary protection because it can virtually survive for many years trapped in ice (Reddy *et al.*, 2004) and biofilm formation increases its resistance to the effects of space (Kminek *et al.*, 2018; Mosca *et al.*, 2021).

If microbial life on these icy moons evolved along similar paths to microorganisms on Earth, bacteria such as these are a double concern to future missions, given that, besides the risk of disturbing Europa's putative ecosystem, they could also contaminate any extra-terrestrial signals of life with misleading signatures.

II.5.2 Relevance to future missions to explore icy moons

The NASA Procedural Requirements (NPR) defines forward contamination in ocean worlds as "the introduction of a single viable terrestrial microorganism into a liquid-water environment". COSPAR considers the risk of forward contamination in spacecraft missions more significant in the case of Europa and Enceladus and advises reducing the probability of contamination to less than $1x10^{-4}$ (Kminek *et al.*, 2019). NASA Response to Planetary Protection Independent Review Board Recommendations (2019) advised the study of mechanisms of contamination individually for each icy moon (NASA, 2020), with more concern for Europa and Enceladus (Kminek *et al.*, 2019). The environment of each icy moon is very different from one another (Coelho *et al.*, 2021) requiring different decontamination planning. Thus, there is an emerging need for well-established decontamination and background control-design protocols with years of proven data. The development of tools, such as the presented in this study, to monitor contamination in

samples from icy terrestrial analogues will serve as a testbed for future search-for-life space missions and simultaneously improve fieldwork practices in icy environments.

Astrobiologists and microbial ecologists working with ice from planetary field analogues to icy moons should continue to share their contaminant identifications with the community. This has been established regarding Mars-related research (Regberg *et al.*, 2018; McCubbin *et al.*, 2019; Bell *et al.*, 2021; Spry *et al.*, 2021) and we recommend based on our findings that this practice should extend to icy moons as well. This way, the contaminating sources, and recurrent microbial contaminants, if existing, of ice samples collected in the planetary field analogues to icy moons will be unraveled during the next years. With these data, future comparative analysis between ice contaminations and NASA's cleanroom contaminating metagenome will be possible, in time for life-detection space missions landing on these habitable satellites.

Drilling the thick ice shell of Europa and Enceladus surface, as conceived in Europa Lander, Enceladus Orbilander Mission, and JEM (Blanc *et al.*, 2020; Hand *et al.*, 2021; MacKenzie *et al.*, 2021), will require core recovery strategies analogous to those used in terrestrial studies, although substantially more complicated logistically. Decontamination techniques using UV-C and chemical disinfectants are suggested by the Task Group on the Forward Contamination of Europa (Kminek *et al.*, 2019) to sterilize hardware before the spacecraft launch to Europa. However, these agents are unsuitable to be used on the external layers of ice cores since they would change the putative extra-terrestrial community's abundance and diversity profiles (Rogers *et al.*, 2004; Kinasz, 2019). Our results show how mechanical removal of external ice core layers is effective in reducing bioburden and not aggressive to the natural biota. We recommend that the design of ice corers for future missions should incorporate a mechanism to remove or degrade the external layer of the ice cores mechanically or through the application of heat.

The processing and downstream analysis for these missions is based on the ones used in planetary field analogues (Kuhn *et al.*, 2014; Goordial *et al.*, 2017). For instance, Enceladus Orbilander Mission is designed to use Nanopore sequencing innovation to detect life, a small device able to sequence long strands of DNA and RNA in real-time, identifying long polymeric strands of nucleic acids if present (MacKenzie *et al.*, 2021). More data using lab-on-chip approaches like Nanopore sequencing technology [accepted as adequate for space missions (Rezzonico, 2014)] are needed for the preparation of missions and thus it is also our recommendation that future applications of the present protocol also use long-strand sequencing using lab-on-a-chip approaches. Nevertheless, the identification of contaminants based on amplicon techniques is still useful in this field (Kminek *et al.*, 2019). Our microbial monitoring success relied heavily on the power of PCR to detect contaminants in the controls. The increased sensitivity of this technique has been used to closely explore total communities, including the polar "rare biosphere" (Pascoal *et al.*, 2021), and has been applied to the analysis of ice samples in planetary field analogues to the icy moons (Miteva *et al.*, 2004; D'Elia *et al.*, 2008; Shtarkman *et al.*, 2013; Hatam *et al.*, 2014a; Yergeau *et al.*, 2017; Itcus *et al.*, 2018; Kayani *et al.*, 2018), as well as planetary protection investigations (Crawford, 2005). Thus, while long-strand sequencing will be necessary to characterize extra-terrestrial DNA, amplicon sequence remains as preferential to monitoring forward DNA contaminations. In a future analysis of planetary field analogues to prepare for space missions we recommend including replication in the design of the experiment to decrease PCR bias as well as to allow for a deeper assessment of the origin of contaminations. We also strongly reinforce the need for new research on functional metagenomics for characterizing the physiological potential of microbial contaminants.

Returning samples have been described as a fundamental part of future landing missions in Europa and Enceladus (Sherwood, 2016; Neveu *et al.*, 2020). In fact, Icy Moon Sample Return Mission is considered an "inspirator" by ESA to bring Europe's space ambitions to the next level (ESA's Intermediate Ministerial Meeting 2021). However, a planetary protection concern regarding return missions is that extra-terrestrial life may contaminate Earth (backward contamination). Thus, future return missions fall into the V category (COSPAR planetary protection policy 2017) (Kminek *et al.*, 2017), which is restricted in cases of Europa and Enceladus. The contamination controls for such missions need to avoid "false positive" indications in life-detection, the protocol for biohazards during cruise, landing, and after it is returned. "False positive" contamination could lead to unnecessarily increased rigor in the requirements for all later Europa or Enceladus missions and prevent the distribution of the sample from containment and their further study. A pre-condition for such missions is that a program of life detection and biohazard testing, or a proven sterilization process, shall be commenced for the controlled distribution of any portion of the sample. Currently, Europe does not have a laboratory prepared to receive and analyze return extra-terrestrial samples (Smith *et al.*, 2021). Thus, as recommended, new research based on the bulk use of standardized decontamination protocols in planetary field analogues to the icy moons is a key necessity to formulate curational procedures for such future laboratories to guarantee the maximum efficiency and safety of future extra-terrestrial life-detection missions.

II.6 Conclusions

Landing missions to Europa and Enceladus are at least two decades away. However, implementing clean sampling strategies for extra-terrestrial life detection experiments, based on verifiable and standardized control methods used in planetary field analogues

will take a long time. We recommend that the community does not only rely on the effects of the natural radiation environment of these moons for decontamination and incorporate the degradation of the external layers of ice cores contacting with man-made equipment in the mission's design. We recommend microbial contamination monitoring on strategic checkpoints during these missions. Our results suggest that the most appropriate techniques to search for forward contaminants on extra-terrestrial ice cores may not be the same considered appropriate to search for extra-terrestrial life and that the incorporation of both methodologies in future missions should be considered. Finally, we encourage the scientific community working on planetary field analogues to keep sharing their contaminants. Searching for a "core" contaminating microbiome of ice sampling and processing procedures from planetary field analogues will also take years of consistent research and public deposition of data, culminating in comparative studies. This represents an additional technological barrier to an already difficult mission. In fact, space missions require massive resources, since the best methods are needed to unambiguously convince the scientific community of the prospective discovery of the century – finding extra-terrestrial life. However, contamination of an extra-terrestrial world with terrestrial biota would have a severe impact with unquantifiable long-term costs, especially if this contamination is not immediately detected and monitored.

III STRUCTURAL SHIFTS IN SEA ICE PROKARYOTIC COMMUNITIES ACROSS A SALINITY GRADIENT IN THE SUBARCTIC

Publication:

Coelho, L. F.; Couceiro, J. F.; Keller-Costa, T.; Valente, S. M.; Ramalho, T. P.; Carneiro, J.; Comte, J.; Blais, M.A.; Vincent, W.F.; Martins, Z.; Canário, J. & Costa, R. (2022). "Structural shifts in sea ice prokaryotic communities across a salinity gradient in the subarctic". *Science of The Total Environment*, 827, 154286.

https://doi.org/10.1016/j.scitotenv.2022.154286

III.1 Summary

Current knowledge of the processes that shape prokaryotic community assembly in sea ice across polar ecosystems is scarce.

Here, we coupled culture-dependent (bacterial isolation on R2A medium) and culture-independent (high-throughput 16S rRNA gene sequencing) approaches to provide the first comprehensive assessment of prokaryotic communities in the late winter ice and its underlying water along a natural salinity gradient in coastal Hudson Bay, an iconic cryo-environment that marks the ecological transition between Canadian subarctic and Arctic biomes.

We found that prokaryotic community assembly processes in the ice were less selective at low salinity since typical freshwater taxa such as *Frankiales*, *Burkholderiales*, and *Chitinophagales* dominated both the ice and its underlying water. In contrast, there were sharp shifts in community structure between the ice and underlying water samples at sites with higher salinity, with the orders *Alteromonadales* and *Flavobacteriales* dominating the ice, while the abovementioned freshwater taxa dominated the underlying water communities. Moreover, primary producers including *Cyanobium* (*Cyanobacteria*, *Synechococcales*) may play a role in shaping the ice communities and were accompanied by known *Planctomycetes* and *Verrucomicrobiae* taxa. Culture-dependent analyses showed that the ice contained pigment-producing psychrotolerant or psychrophilic bacteria from the phyla *Proteobacteria*, *Actinobacteriota*, and *Bacteroidota*, likely favored by the combination of low temperatures and the seasonal increase in sunlight. Our findings suggest that salinity, photosynthesis and dissolved organic matter are the main drivers of prokaryotic community structure in the late winter ice of coastal Hudson Bay, the ecosystem with the fastest sea ice loss rate in the Canadian North.

III.2 Introduction

The Arctic Ocean and its marginal seas constitute an estuary-like biome that is strongly influenced by large inputs of freshwater from numerous inflowing rivers (Macdonald, 2000). Among these seas, Hudson Bay (Canadian subarctic/Low Arctic) is a semi-enclosed marine ecosystem that has been the subject of several research programs over the past decades. However, studies of its winter ice ecology are limited and mostly associated with an oceanographic project in the 1990s (summarized in Nozais *et al.*, 2021). The cold waters of Hudson Bay, partially influenced by cold air from the Arctic Ocean basin, push the 10°C isotherm southward. Thus, the winters in this region can be as cold as in the high Arctic (AMAP, 1998), a phenomenon called the "Hudson Bay effect". Sea ice covers the bay for at least nine months of the year and provides a vast cryo-habitat for microbial colonization and growth. The salinity gradient in Hudson Bay has been shown to shape the structure of zooplankton and phytoplankton assemblages (Archambault *et al.*, 2010; Jacquemot *et al.*, 2021), and is known to drive bacterioplankton composition and activity elsewhere in the Arctic basin (Garneau *et al.*, 2006). A similar response is expected from the native prokaryotic community as salinity is a well-known driver of prokaryote biogeography (Lozupone *et al.*, 2007). Yet the prokaryotic community structure of sea ice in Hudson Bay and its relationship to salinity has not been explored thus far.

One of the major freshwater inputs to Hudson Bay is the Great Whale River, on the southeastern side of the bay at latitude 55.3°N, and the location of the Indigenous communities of Whapmagoostui (Cree First Nation) and Kuujjuarapik (Inuit). The river mouth lies at the transition between the subarctic and Arctic (Bhiry *et al.*, 2011), in the coastal forest-tundra zone (ecozone: Taiga Shield; ecoregion: Southern Ungava Peninsula). Over the last decades, studies in this region have revealed the widespread

geophysical influence of the Great Whale River on the eastern coastal waters of Hudson Bay (Ingram *et al.*, 1987; Li *et al.*, 2007). Although river discharges are significantly higher during summer, the plume expansion across the surface waters of the bay can be four times greater when it is ice-covered, and the sea ice is therefore associated with freshwater-influenced salinity gradients over large distances.

Although Hudson Bay winters are severe in terms of temperature, the Low Arctic latitudes of this region mean that there are more daylight hours than further north, and sea ice in the bay can experience prolonged bright irradiance between March and September (CEN, 2020). Light is likely to be a critical factor in the regulation of sea ice microbiomes, and the psychrophilic and psychrotolerant organisms that grow in this environment, particularly near the upper surface, must therefore contend with photooxidative stress. Pigment-producing microorganisms are better equipped to survive at the surface of ice due to their photooxidative resistance, and their surface growth can decrease ice-albedo while shielding the microbial communities beneath (Maccario *et al.*, 2015). At the lower ice surface, solutes and microbes may be exchanged through microchannels with the underlying water (Gosselin *et al.*, 1985), and materials including dissolved organic matter, nutrients, and cells incorporated into the ice via ice accretion processes (Imbeau *et al.*, 2021).

Hudson Bay has the fastest rate of sea ice loss of all sectors in the Canadian North (Bhiry *et al.*, 2011), and its coastal ice microbiomes are therefore likely vulnerable to ongoing climate change, being a good model for subarctic ice melt. Yet despite recent progress enabled by the advent of next-generation sequencing technologies (Yergeau *et al.*, 2017), for most polar ecosystems we still lack accurate and comprehensive documentation of the abundance, diversity, and structure of prokaryotic communities that thrive in sea ice. This knowledge is fundamental to improving our understanding of the

microorganisms and microbial-mediated processes that shape ecosystem functioning in the Arctic and cold biomes at large.

The main goal of this study was to provide the first description and analysis of the late winter sea ice prokaryotic communities of the Canadian subarctic, as irradiance increases, and ice starts to melt. We used a combination of culture-dependent approaches (custom methodology to isolate cold-adapted bacteria in the laboratory) and culture-independent methods (high-throughput 16S rRNA gene sequencing) to 1) determine bacterial community structure in ice along a steep salinity gradient at Hudson Bay's southeast coast in winter, near the Great Whale River system; 2) evaluate whether shifts in community structure exist between the sea ice cover (hereafter referred to as "ice") and the interface water, which is water immediately underneath the ice (hereafter referred to as "water"), along the salinity gradient; 3) identify the key organisms underlying any such shifts in community structure, and 4) evaluate ecological relationships through the analysis of abundance distributions of bacterial taxa in the ice and water and their relationship with biological and environmental parameters. We hypothesized that the structure of the coastal sea ice microbiome is shaped not only by cold temperatures and physical constraints typical of this habitat but also by salinity and relevant biological processes taking place at the underlying, interface water such as photosynthesis. Moreover, we anticipated that the degree of distinctiveness between ice and water prokaryotic community structure was likely to increase at higher salinity sites farther from the river mouth.

III.3 Materials and Methods

III.3.1 Sampling and processing of ice and water

Sampling was performed on the southeast coast of Hudson Bay near Whapmagoostui-Kuujjuarapik in Nunavik, northern Quebec, Canada, an estuarine ecosystem influenced by the Great Whale River. Samples of ice and the water beneath the ice were collected in winter (February 27th and 28th 2019) when ice approximately 1-m thick covered the bay.

Ice cores (in duplicate) of 1-m length and 9 cm in diameter and water beneath the ice (1 L in triplicate) were collected from three different locations (sites 1, 2, and 3). One ice core and one water sample were further collected at the intersection with the river (site 4) **(Figure III.1)**. Replicate sampling at site 4 was not possible due to technical restrictions. The geographic location of sites 1 to 4 corresponds to a decreasing gradient in water salinity along the coast, with site 4 representing the location with the lowest salinity due to its proximity to the river **(Figure III.1)**. In total, 17 samples were collected belonging to 8 distinct sample groups: 1I, 1W, 2I, 2W, 3I, 3W, 4I, and 4W (numbers represent the sites, with "I" meaning ice and "W" meaning water samples). Sites 1, 2, and 3 were sampled on Feb 27th, 2019, and site 4 on Feb 28th, 2019. The mean temperature difference between the two sampling days was 3ºC. The lowest temperature registered at the weather station of Kuujjuarapik during sampling days was -28ºC, while the highest temperature reached was -11ºC at noon, with an almost constant wind flow of 21 km/h.

Sample processing took place in the laboratory facilities available at the Centre d'études Nordiques (CEN) research station located in Whapmagoostui-Kuujjuarapik. The external layer (5 mm) of each ice core was cut using a sterile ice saw and then the same ice cores were left to melt at room temperature in sterile bags, following established ice core decontamination and sampling protocols (Christner *et al.*, 2005). Ice water (1000

mL) and water (500 mL) samples were filtered through 0.22 µm nitrocellulose filters (Millipore®, Sigma-Aldrich) using a vacuum pump. The filters were immediately frozen and stored at −80°C until DNA extraction (see below). For flow cytometry estimates of cell abundance (see below), 5 mL of each ice water and water sample were fixed with glutaraldehyde to a final concentration of 2% (v/v) and then stored at -80ºC. The rest of the ice/water samples were stored separately in sterile glass bottles, which were maintained at approximately 4ºC, for the future cultivation of aerobic, heterotrophic bacteria.

Metadata was collected on-site using a multiparameter water quality sonde (YSI model EXO2®), which was placed in the water after extracting the ice cores. The data collected comprised temperature (°C), salinity (Practical Salinity Units - PSU) calculated automatically from the measured conductivity, dissolved oxygen (ODO) through optical detection, fluorescent dissolved organic matter (fDOM, in quinine sulfate units - QSU), as well as both chlorophyll *a* (µg/L) and cyanobacterial fluorescence BGA-PC (phycocyanins in µg/L) through fluorescence detection. Snow depth (cm) on top of the ice surface was also measured on-site.

III.3.2 Flow cytometry estimates of prokaryotic abundance

Samples were transported in coolers to INRS - Institut National de la Recherche Scientifique (Quebec City, Canada) where flow cytometry was conducted. Prokaryotes were enumerated with FACScalibur flow cytometer (BD, Mississauga, ON, Canada) as described previously (Comte *et al.*, 2016). In brief, cells in samples previously fixed with glutaraldehyde were stained by adding 20 µL of 50X SYBR Green I (Life Technologies, Thermo Fisher Scientific, Waltham, MA, USA) to 500 µL of sample followed by 10 min incubation in the dark. Discrimination of prokaryotic cells was achieved based on green fluorescence (FL1) and side-scatter signals (SSC), with excitation at 488 nm, using

yellow-green spheres with 1 µm of diameter (Polysciences Inc., Warrington, PA, USA) as an internal size standard. CellQuest Pro software was used to analyze the data. Flow cytometry counts are displayed as averages in cell number/mL ± standard deviation for each sample group. Significant differences in flow cytometry counts were assessed by One Way ANOVA using PAST software (Hammer *et al.*, 2001) v.4.02.

III.3.3 Total Community DNA extraction and high-throughput sequencing of 16S rRNA genes

Total Community DNA (TC-DNA) extractions were performed on the filters of ice water (1000 mL) and water samples (500 mL) at the Institute for Bioengineering and Biosciences (iBB) in Portugal. A sample processing control (C1) made of frozen MilliQ water was added to the experiment. This MilliQ "ice core" was processed and filtered in the same way as the remaining samples (ice and water, see Chapter II). The filter of the MilliQ water sample (C1) and a new, clean filter (C2 - DNA extraction control) were then subjected to the same TC-DNA extraction protocol. The filters were cut into small pieces to ensure full submersion and improve the contact between the cells and lysing buffer. TC-DNA extraction was carried out as described previously (Karimi *et al.*, 2017) using the Ultraclean Soil DNA Kit (MoBio Laboratories, Carlsbad, CA, USA) on the filter pieces of each sample according to the manufacturer's protocol. TC-DNA yields and integrity were examined under UV light after standard agarose gel electrophoresis procedures. TC-DNA concentrations were thereafter estimated using the Qubit 4 Fluorometer with the high-sensitivity dsDNA assay kit (Invitrogen, CA, USA), and stored at −80°C until further analysis.

TC-DNA extracts were subjected to 16S rRNA gene-based high-throughput sequencing on an Illumina MiSeq platform at MR DNA (www.mrdnalab.com, Shallowater, TX, USA). First, the V4 hypervariable region (*E. coli* positions 515–806) of

the 16S rRNA gene was amplified at MR DNA in a 30-cycle PCR using the primers 515F (5' -GTG YCA GCM GCC GCG GTAA-3') (Caporaso *et al.*, 2011) and 806RB (5'-GGA CTA CNV GGG TWT CTA AT-3') (Apprill *et al.*, 2015) using barcodes on the forward primer. The HotStarTaq Plus Master Mix Kit (Qiagen, USA) was employed to prepare the reactions under the following conditions: 95°C for 5 min, followed by 30-35 cycles of 95°C for 30 sec, 53°C for 40 sec and 72°C for 1 min, after which a final elongation step at 72°C for 10 min was performed. After amplification, samples were multiplexed using unique dual indices, then pooled together, and later purified using calibrated Ampure XP beads. The purified PCR products were then used to prepare the Illumina DNA library. During sequencing, an average of 20000 paired-end sequences of around 300 bp were generated per sample. Controls were subjected to the same extraction and sequencing process.

III.3.4 Processing and analysis of amplicon sequencing data

The 16S rRNA gene amplicon libraries generated in this study were processed and analyzed following previously established methodologies (Keller-Costa *et al.*, 2017). Briefly, sequence reads obtained from all 17 samples were first processed using MR DNA's custom data analysis pipeline. Raw sequences with less than 150 bp and with ambiguous base calls were removed. Subsequent "denoising" of the data consisted of removing chimeric sequences and singletons using UCHIME (Edgar *et al.*, 2011). OTUs were generated and defined by clustering at 3% divergence (97% similarity) with the USEARCH algorithm (Edgar, 2010). In total, quality-filtering and clustering procedures returned 5352 OTUs and 572404 reads across the data, which were used in downstream analyses.

Taxonomic assignment of OTUs was then performed using the SINA sequence alignment tool (v1.2.11) of the SILVA database v.138 (https://www.arb-

silva.de/aligner/). OTUs displaying less than 70% identity with valid taxa (2292 OTUs) were regarded as unclassified at the domain level and removed from the data. OTUs identified as singletons that were not removed in previous processing (4 OTUs), eukaryotes (4 OTUs), chloroplasts (169 OTUs), mitochondria (14 OTUs), or detected in the sample processing (C1) and DNA extraction (C2) controls (30 OTUs) were subsequently filtered out, reaching a total of 221 removed OTUs. The final analytical dataset comprised 2839 prokaryotic OTUs (12 archaeal and 2827 bacterial OTUs) and 353648 reads (median of 22398 reads per sample). Data analyses, described in detail below, comprised (i) estimates of prokaryotic (OTU) richness and diversity per sample and sample groups, (ii) taxonomic profiling of each sample from phylum to genus levels, (iii) determination of specific and common OTUs among sample groups using Venn diagrams and (iv) prokaryotic community ordination based on OTU profiles. While size-rarefied sequence libraries were used in alpha diversity analyses (i), both rarefied and non-rarefied (full) data were employed in analyses (ii) to (iv). Analyses of non-rarefied sequence libraries benefited from the relatively even sequence depths obtained for most samples examined in this study **(Figure IX.2)** and involved data transformation (specified below) to account for such differences while preventing read counts from relatively low abundance OTUs to be lost or ill-represented due to rarefaction (McMurdie *et al.*, 2014). Given that the analyses performed with both rarefied and non-rarefied data were overall congruent, we here present the results obtained with the non-rarefied dataset while the complementary analyses performed for the rarefied dataset are presented as supplementary material to this article.

III.3.5 Alpha-diversity analyses: OTU richness and diversity

To determine alpha-diversity metrics for each sample and compare these metrics among sample groups, sequence libraries were size-normalized by rarefying the data

using the rarefy_even_depth function from the *phyloseq* R (4.0.2) package (McMurdie *et al.*, 2013). The rarefied library size was 7634 reads corresponding to the lowest number of reads detected in a sample. Observed and estimated (Chao1 index) OTU richness, and OTU diversity metrics (Shannon-Wiener index) were thereafter computed in R using the estimate_richness function from the *phyloseq* package. Moreover, to portray the extent to which OTU richness in each sample increases as a function of sequence depth, rarefaction curves were plotted in R using the rarecurve function of the vegan package (Oksanen *et al.*, 2020).

The Kruskal-Wallis test was performed to test for significant differences in alpha diversity measures between sample groups. A Post Hoc Dunn's test was performed thereafter to reveal whether pairwise differences among sample groups were significant. Both analyses were done using PAST software v.4.02. Additionally, alpha diversity measures of water and ice samples from the four sampling sites were respectively pooled together and tested for significant differences with the Mann-Whitney U-test, using the wilcox.test function from the stats package implemented in R.

III.3.6 Analysis of taxonomic composition

To display the taxonomic composition of each sample, stacked bar charts were plotted based on the relative abundance of prokaryotic taxa from phylum to genus levels, for both rarefied and non-rarefied (full) data. To improve the readability of the graphs, low abundance taxa (e.g., taxa below 1% of relative abundance for the order plot and 0.5% for the genus plot) were merged into a single category called "Others". The plots were created using R packages *phyloseq*, *plyr*, and *ggplot2*.

III.3.7 Beta-diversity analyses

Venn diagrams were generated using the VennDiagram package in R to determine the number and proportion of OTUs specific to and shared by ice and water samples

within each site and across all sites along the salinity gradient. Venn diagrams were first built using both non-rarefied and rarefied datasets in an exploratory-oriented approach to reveal whether the total OTU richness observed in ice was contained in water and vice-versa.

To identify shifts in prokaryotic community structure between the ice and water and along the salinity gradient, a multivariate analysis of OTU profiles was carried out. To this end, the non-rarefied data were adjusted by Hellinger transformation (square root of OTU relative abundances), after which a Bray-Curtis similarity matrix was calculated from the OTU *versus* sample table using the phyloseq package for R. Additionally, we also produced a Bray-Curtis similarity matrix from the rarefied OTU table (all sequence libraries rarefied at 7634 reads per sample). The resulting Bray-Curtis similarity matrices (from both rarefied and non-rarefied data) were then used to ordinate the samples via Principal Coordinates Analysis (PCoA) according to their OTU profiles using the R packages phyloseq and ggplot2. A Similarity Percentages (SIMPER) test was carried out (PAST v.4.02) to rank the OTUs contributing the most to community dissimilarities among sample groups, from which the top 15 most differentiating OTUs were plotted as 'species data' in the respective PCoA graphs. Additionally, quantitative variables measured in water samples at each site **(Table IX.2)** were as well portrayed as vectors in custom ordination biplots using PAST v.4.02 to explore relationships between quantitative biological/environmental parameters and prokaryotic community structures across sites.

To ascertain whether there was a significant difference between the sample groups, a Permutational Analysis of Variance (PERMANOVA) was performed in PAST v.4.02. This test was conducted using the Bray-Curtis distance matrix of the Hellinger-

transformed data with all samples and 999 permutations. Pairwise differences were assessed by performing the PERMANOVA Post Hoc test in PAST v.4.02.

We also examined the extent of variation (dispersion around Bray-Curtis similarity means) in taxonomic (OTU) profiles within groups of samples using the betadisper function from the vegan package (v.2.4-2) of R (Oksanen *et al.*, 2020). With betadisper, we tested whether community dispersion among ice samples was larger than that of the water communities along the salinity gradient (sites 1 to 4). In addition, we evaluated whether community dispersion among water and ice samples from one single site was higher than dispersions observed for (i) ice samples only along the salinity gradient, and (ii) water samples only along the salinity gradient.

III.3.8 Cultivation, isolation, and identification of aerobic, heterotrophic bacteria

The following steps were conducted at iBB in Portugal, immediately after transportation of ice and water samples (within a cooler at an average external temperature of 4^{o}C, 48 h) to the laboratory.

All samples were diluted and cultured by spread-plating on 1:10 R2A agar medium (Christner *et al.*, 2002) prepared with sterile artificial seawater (ASW). While 10^{-2} to 10^{-4} serial dilutions were used to process water samples, 10^{-1} dilutions were plated for ice samples. Spread-plating was performed in triplicates (water) and duplicates (ice) per dilution. Plates were then incubated at 15^{o}C, and bacterial colonies were counted every 5 days for 30 days. The negative control plates were blank by the end of the incubation period. Counts of aerobic, heterotrophic bacteria were expressed as averages of colony-forming units (CFUs)/mL ± standard deviation for each sample group. Significant differences in CFU counts were assessed by One Way ANOVA using PAST software v.4.02.

Site 4 is exposed to a higher freshwater inflow due to its proximity to the GWR **(Figure III.1)**. Therefore, we also included a salt-free cultivation procedure under the same conditions to widen the diversity of bacterial cultures examined in this study. For this additional treatment, water samples from site 4 and ice samples from all sites were cultured by spread-plating on 1:10 R2A agar medium prepared with sterile MilliQ water following the procedures described above.

A total of 109 and 66 colonies deriving from the first (R2A prepared with ASW) and second (R2A prepared with MilliQ water) cultivation attempt were obtained, respectively, representing all different colors and morphotypes observed at each site and sample type (ice or water), and were streaked until purity on R2A agar medium. Thereafter, pure isolates were freshly grown in R2A broth and glycerol stocks prepared and stored at –80ºC.

Genomic DNA was extracted from a fresh liquid culture of each isolate using the Wizard Genomic DNA Purification Kit (Promega, Madison, USA) according to the manufacturer's instructions. For taxonomic identification of all isolates, genomic DNA samples were subjected to 16S rRNA gene amplification by PCR using the universal primers 27F-1492R and then purified using Sephadex G-50 as described previously (Esteves *et al.*, 2013). Amplicons were then subjected to Sanger sequencing at STAB VIDA, Lda. (Caparica, Portugal) using the forward primer 27F (5'- AGA GTT TGA TCM TGG CTC AG – 3'). 16S rRNA gene sequences were trimmed and edited with the Sequence Scanner Software version v1.0 (Applied Biosystems, Foster, CA, USA) resulting in high-quality sequences of 670-1100 bp. Taxonomic assignment of bacterial isolates to the genus level was performed using the classifier tool of the Ribosomal Database Project (RDP, release 11) (Wang *et al.*, 2007; Cole *et al.*, 2014). Closest type strains to all sequence queries were determined using the RDP sequence match tool

(http://rdp.cme.msu.edu/seqmatch) and closest sequence hits in public databases were determined using nucleotide BLAST (BLASTN tool from NCBI).

III.3.9 Cultivation-dependent and -independent data integration

To compare the taxonomic profiles obtained from cultivation-dependent and independent methods, we adopted standardized taxon names for all 16S rRNA gene sequences (SILVA database v.138 nomenclature) and identified the common genera in both datasets. To determine the total number of OTUs present in the library of isolates, we first aligned the 16S rRNA gene sequences of all 175 isolates using the ClustalW algorithm in MEGA software (v.10.2.4). The aligned sequences were then subjected to OTU picking at a 97% similarity threshold using Mothur (Mothur v1.44.3, http://www.mothur.org) with the nearest neighbor clustering method. Bacterial OTU richness and taxonomic composition at the genus level from cultivation-dependent and -independent data were thereafter examined and contrasted.

III.4 Results

III.4.1 Environmental parameters

Water salinity ranged from 0.6 PSU (prevailing freshwater environment) to 10.54 PSU (brackish environment) from study sites 4 to 1, located the closest and furthest away from the mouth of the river, respectively **(Figure III.1)**. Values for temperature, fDOM, snow cover, chlorophyll *a* fluorescence, and phycocyanin fluorescence (as a measure of cyanobacterial biomass) displayed considerable variation among sites **(Table IX.2)**. Noticeably, the highest values recorded for the latter two parameters, which can be considered indicators of photosynthetic biomass and activity, coincided with the lowest measure obtained for snow depth at site 3 **(Table IX.2)**.

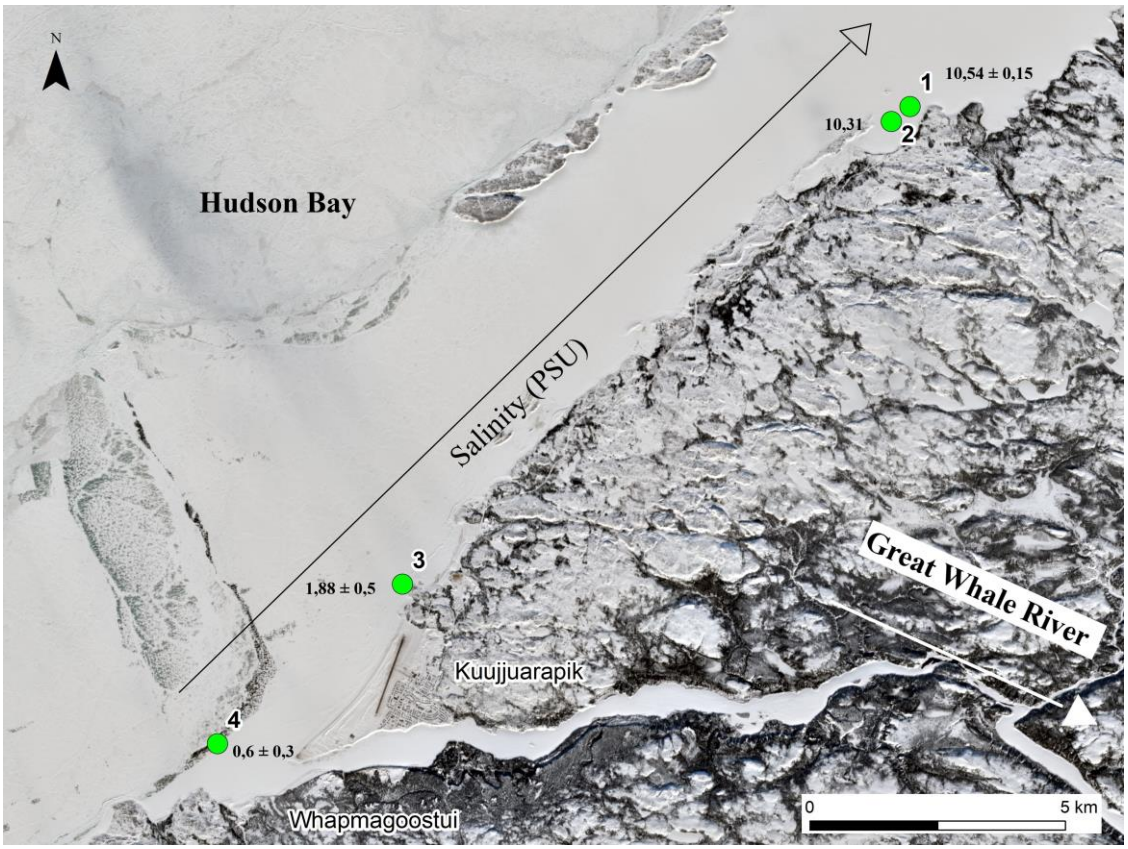

Figure III.1 - Location of sampling stations on the east coast of Hudson Bay (Whapmagoostui-Kuujjuarapik, Quebec, Canada). Map data © Sentinel-2. Salinity data (PSU) were taken on-site during water sampling using The YSI EXO2®. Values of salinity in the format of average±SD for sites 1, 3 and 4. From Coelho *et al.*, 2022, in *STOTEN*.

III.4.2 Counts of prokaryotic cells and bacterial colony-forming units

Total counts of prokaryotic cells by flow cytometry in ice from the four different sites ranged from 3.4 to 8.9x10^4 cells/mL with increased abundance at site 3 **(Table III.1)**. In the water, total prokaryotic cell counts ranged from 3.1 to 5.4x10^5 cells/mL with the highest abundance at site 4, most proximate to the river **(Table III.1)**. Counts of culturable, aerobic, heterotrophic bacteria in the water were considerably higher than those of the ice samples, eventually representing up to 35% of the total prokaryotic counts estimated by flow cytometry, while CFU estimates of culturable bacteria in ice samples varied from 0.1 to 0.18% of the total cell counts estimated by flow cytometry **(Table III.1)**.

Table III.1 - Counts of total prokaryotic cells (assessed by flow cytometry) and bacterial colony forming units (CFU) in sea ice and water[1]. Counts are in the format of average±SD. From Coelho *et al*., 2022, in *STOTEN*.

Site	Sea ice			Interface water		
	Cell counts (cells ml^{-1})	CFU counts (cells ml^{-1})	CFU/Total counts (%)	Cell counts (cells ml^{-1})	CFU counts (cells ml^{-1})	CFU/Total counts (%)
Site 1	$(3.4\pm1.0) \times 10^4$	$(4.4\pm1.1) \times 10^1$	0.13	$(3.6\pm0.4) \times 10^5$	$(9.0\pm3.5) \times 10^4$	24.8
Site 2	$(3.2\pm0.8) \times 10^4$	$(1.8\pm0.6) \times 10^1$	0.05	$(3.1\pm0.4) \times 10^5$	$(1.1\pm0.5) \times 10^5$	34.9
Site 3	$(8.9\pm5) \times 10^4$	$(1.6\pm0.1) \times 10^2$	0.18	$(3.2\pm1.0) \times 10^5$	$(6.9\pm1.9) \times 10^4$	21.5
Site 4	$(5.6\pm0.4) \times 10^4$	2.0×10^1	0.04	$(5.4\pm0.2) \times 10^5$	$(1.3\pm0.01) \times 10^5$	23.0

1 Counts were performed on 1:10 R2A culture medium prepared with sterile artificial seawater.

III.4.3 Cultivation-independent analyses of prokaryotic community structure

III.4.3.1 Alpha diversity measures

Alpha diversity was assessed for sequence libraries rarefied at 7634 reads per sample **(Figure IX.2)**. Significant differences ($P<0.05$) in observed OTU richness were detected between water and ice samples for sites 1 to 3, where replicate sampling was possible **(Figure III.2)**.

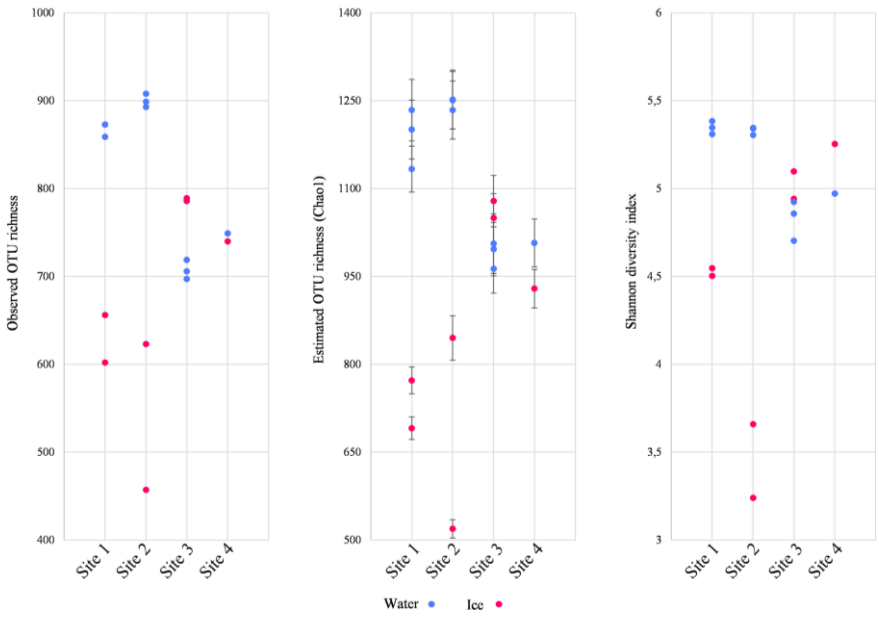

Figure III.2 - Alpha diversity measures of prokaryotic communities in ice and water. Metrics were estimated based on 16S rRNA gene amplicon-derived OTUs (97% similarity) detected in even-depth, rarefied sequence libraries (7634 seqs per sample). Observed and Chao1 estimated OTU richness per sample are shown on the "A" and "B" panels, respectively. OTU diversity per sample estimated with the Shannon (C) diversity index is shown on the right panel. Red-colored symbols are used to label ice samples. Blue-colored symbols are used to label water samples. From Coelho *et al*., 2022, in *STOTEN*.

Intriguingly, while higher OTU richness was recorded for water than ice samples from sites 1 and 2, at site 3 this trend was reversed, with higher richness observed for ice than water samples **(Figure III.2)**. The highest cell counts **(Table III.1)** across all ice samples analyzed in this study were recorded for samples from site 3, suggesting that this site hosts the densest, richest, and likely more active ice-associated prokaryotic communities across the salinity gradient investigated here. At site 4 (lower salinity), OTU richness values from ice and water samples were similar, converging at about 750 OTUs per sample **(Figure III.2)**. The observed OTU richness values in water and ice samples diverged more from one another in sites with higher salinity (sites 1 and 2), where the highest (850-900 OTUs per water sample) and lowest (c. 450-650 OTUs per ice sample) measures were documented across the dataset **(Figure III.2)**. In general, the observed richness measures were congruent among replicates of the same sample group, except for ice replicate samples from sites 1 and 2, particularly the latter, in which a much larger extent of variability was observed. Overall, the trends for observed OTU richness were followed by those of estimated OTU richness (Chao1) and OTU diversity (Shannon-Wiener index, **Figure III.2**).

Estimated OTU richness (Chao1) was usually larger than the respective, observed OTU richness measures, especially among all water samples **(Figure III.2)**. This trend suggests that additional OTU richness/diversity would be captured for most samples if sequencing depths higher than the rarefaction threshold were used, as evidenced by rarefaction curves created for each sample using non-rarefied data **(Figure IX.2)**.

III.4.3.2 Taxonomic composition

From 2839 prokaryotic OTUs classified at the domain level using the SILVA database, only 12 OTUs (669 reads – 0.2%) were from *Archaea*, while the remaining

2827 OTUs (352979 reads – 99.8%) belonged to *Bacteria*. Archaeal OTUs were classified into 8 distinct genera, whereas bacterial OTUs were classified into 652 genera. The *Archaea* community composition differed between the ice and water and changed along the salinity gradient. *Archaea* OTUs belonged to the phyla *Crenarchaeota*, *Thermoplasmatota* (Marine group II order), *Halobacterota*, *Nanoarchaeota*, and *Euryarchaeota*, whereby most archaeal reads (>93%) were detected in water samples from the higher salinity sites 1 and 2.

Although all archaeal phyla represented less than 1% relative abundance in all samples, notably *Crenarchaeota* was the 5th most abundant phylum in water samples from site 2, represented by the genera *Candidatus* Nitrosopumilus, *Halobacterium*, AR15, and *Methanobacterium*.

The most abundant bacterial phyla detected in this study were *Proteobacteria* (38% of the total reads analyzed), *Bacteroidota* (26%), and *Actinobacteria* (23%), which collectively shared dominance of all prokaryotic communities in water and ice samples across the gradient, followed by smaller proportions of *Verrucomicrobia* (8%), *Planctomycetota* (3%), *Cyanobacteria* (1%), and several other low abundance (<1%) phyla **(Figure IX.3)**. The *Proteobacteria* phylum was essentially represented by the classes *Gammaproteobacteria* (29%) and *Alphaproteobacteria* (9%) **(Figure IX.3)**. Clear differences in taxonomic composition between ice and water communities could already be depicted at high taxonomic levels (phylum) and were pronounced at sites 1 and 2 where salinity is higher **(Figure IX.3)**. At these sites, the phylum *Bacteroidota* was more abundant than *Actinobacteriota* in ice samples, whereas the opposite was observed in water samples.

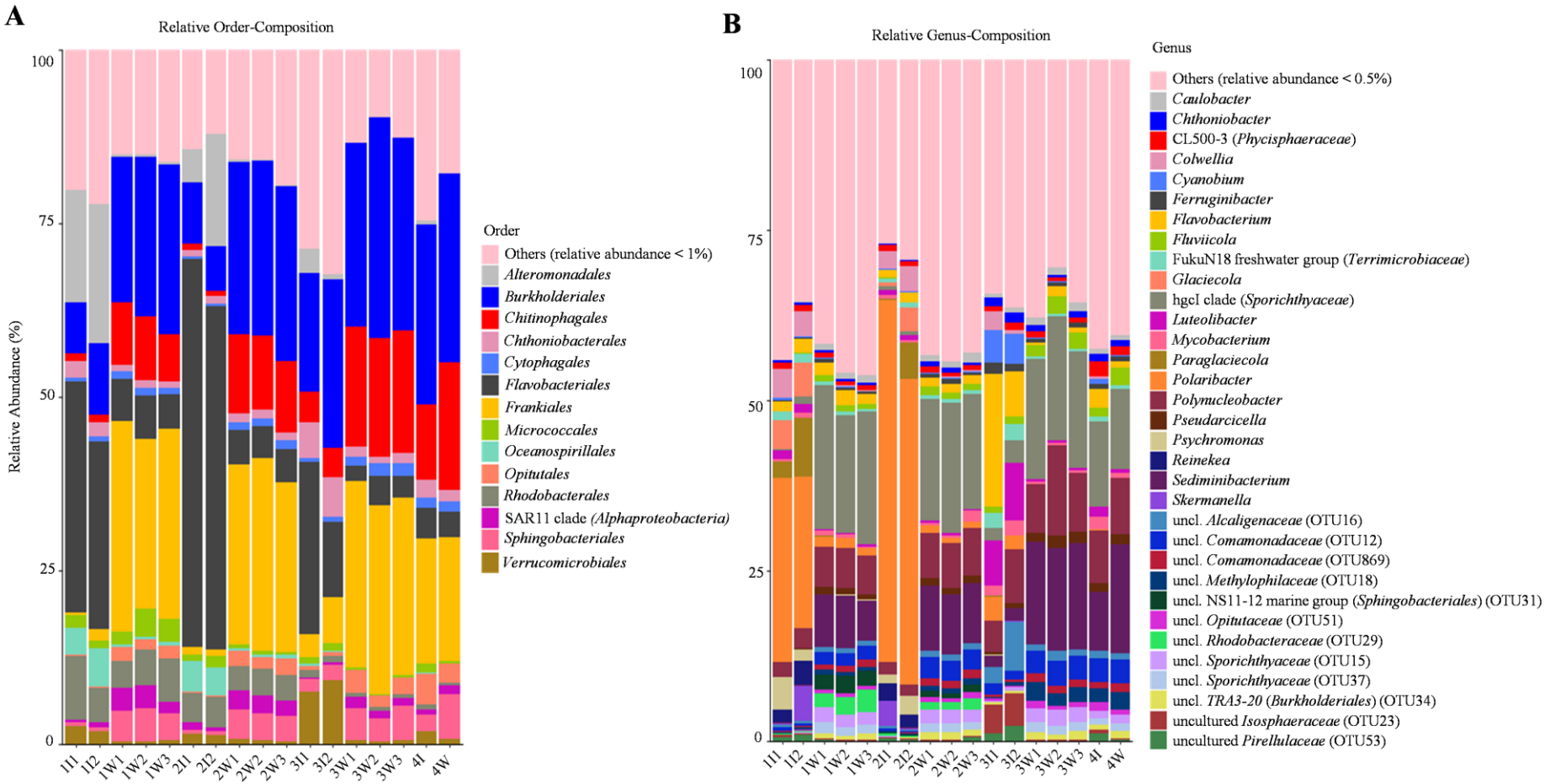

Figure III.3 - Taxonomic composition of prokaryotic communities in ice and water. Order-level prokaryotic community composition based on the relative abundance of OTUs of the non-rarefied dataset. For improved readability, orders below 1% relative abundance across the entire dataset were joined under the category "Others" (A). Genus-level prokaryotic community composition based on the relative abundance of OTUs of the non-rarefied dataset. For improved readability, genera below 0.5% relative abundance were joined under the category "Others" (B). Diverse genera possessing low relative abundances (pink-labeled bars) are an integral part of both ice and water microbiomes. From Coelho *et al*., 2022, in *STOTEN*.

A notable increase in *Cyanobacteria, Planctomycetes,* and *Verrucomicrobia* relative abundance was furthermore observed in ice samples from site 3 in comparison with the corresponding water samples. Prokaryotic community composition of ice and water samples at site 4 (lower salinity) was similar at all taxonomic levels (**Figure III.3** and **Figure IX.3**). Genera such as *Sediminibacterium, Polynucleobacter,* hgcl and TRA3-20 clades, and unclassified genera from the *Comamonadaceae* and *Methylophilaceae* families were shared by both sample categories at site 4 in relatively similar proportions **(Figure III.3)**.

Differences in community composition among ice and water samples became even more evident at lower taxonomic levels as salinity increased **(Figure III.3)**. The order *Frankiales* dominated all water samples but were only abundant in ice at site 4. The relative abundance of the orders *Chitinophagales* and *Burkholderiales* increased in water samples from sites 3 and 4, closer to the river. Orders such as *Alteromonadales, Flavobacteriales, Verrucomicrobiales,* and *Oceanospirillales* were more abundant in ice than in water samples **(Figure III.3)**. At sites 1 and 2, particularly, an overall high abundance of the psychrophilic genera *Polaribacter*, *Psychromonas*, *Paraglaciecola*, *Colwellia,* and *Reinekea* was observed **(Figure III.3)**. Abundance distributions of *Flavobacteriales* genera can serve as markers for the ice/water community shift at higher salinity sites. For instance, while *Polaribacter* decreased in abundance in ice from sites 1 and 2 (higher salinity) to sites 3 and 4 (lower salinity) the opposite occurred for *Flavobacterium* and *Fluviicola*. The genus *Cyanobium*, particularly several OTUs tentatively affiliated with *Cyanobium gracile* strain PCC-6307, originally isolated from a freshwater lake (Gerloff *et al.*, 1950), was the main contributor to the enrichment in *Cyanobacteria* proportions observed in ice samples from site 3 **(Figure III.3)**.

Finally, we found a high diversity of low-abundance genera across all ice and water samples (marked as "Others" in **Figure III.3**) strengthening the emerging evidence of a highly complex rare prokaryotic biosphere in the Arctic (Pascoal *et al.*, 2021). As in another study on an Arctic estuarine dataset (Kellogg *et al.*, 2019), we ran a subset of analyses of the taxonomic composition using rarefied OTU tables **(Figure IX.4)** and found no significant difference in results or conclusions when comparing to the non-rarefied data.

III.4.3.3 Specificity and sharedness of prokaryotic OTUs

Venn diagram assessments revealed that only 14% of the OTUs detected in ice were shared among ice samples from all sites 1 to 4, whereas 36% of the OTUs detected in water were common to all sites **(Figure III.4)**. These shared OTUs were found to represent 20% and 60% of the total number of reads included in both analyses, respectively. Noticeably, all OTUs from ice samples were contained within the pool of OTUs detected in the water, which was expected since this ice originates from the underlying water. About 20% of the total OTUs detected in this study were absent in ice samples, possibly reflecting an important transition in microbiome structure that occurs when the water freezes **(Figure III.4)**. However, this pool of OTUs represented 1.5% of the total number of reads in the dataset.

At higher salinity sites (sites 1 and 2), many OTUs were unique for water **(Figure III.4)**, and fewer OTUs were shared between the respective ice and water samples than at lower salinity sites (sites 3 and 4), where ice and water shared the majority of OTUs **(Figure IX.4)**. Ice samples from site 3 had the highest percentage of unique OTUs (approximately 18%) when compared with ice samples from the other sites **(Figure III.4)**. This was in line with the observation that the highest richness measures and a distinct community composition characterized the ice communities from site 3 (**Figure**

III.2 and **Figure III.3**), where the highest abundance in *Cyanobacteria*, *Planctomycetes*, and *Verrucomicrobiae* was registered.

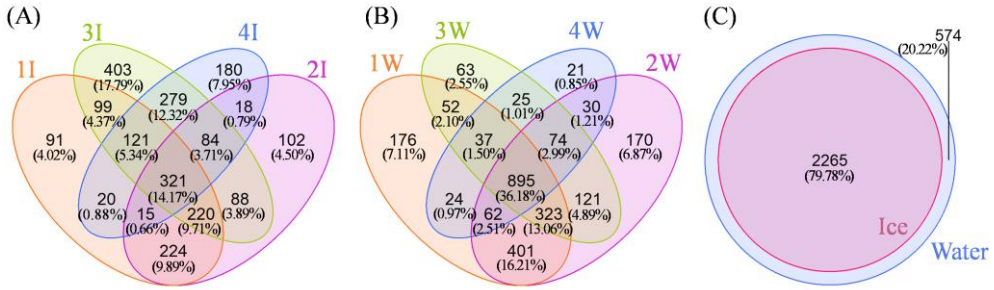

Figure III.4 - Specificity and sharedness of prokaryotic OTUs of the non-rarefied dataset across ice and water samples. Venn diagrams display the number and proportion (in brackets) of (A) OTUs common and specific to ice samples along the salinity gradient, (B) OTUs common and specific to water samples along the salinity gradient, and (C) OTUs from all ice and water samples, whereby samples of sites 1 to 4 were pooled per biotope (ice *versus* water). In diagrams (A) and (B) replicate samples within each location were pooled. Note that the prokaryotic richness found in ice is contained within water. From Coelho *et al*., 2022, in *STOTEN*.

Overall, the major trends depicted above were maintained in Venn diagrams of the rarefied dataset **(Figure IX.5)**, yet with a somewhat smaller proportion of "core" OTUs shared by all sample groups in analyses (A), (B), and (C). Noticeably, analyses of both non-rarefied and rarefied data congruently revealed that all the prokaryotic richness observed in ice was contained within the water communities (**Figure III.4** and **Figure IX.5**).

III.4.3.4 Prokaryotic community ordination

Principal Coordinates Analysis (PCoA) performed on all samples revealed a sharp separation of ice and water OTU profiles, with water samples clustering closer together **(Figure III.5)**. The spatial distribution of the ice-associated communities was overall more variable than that observed for water communities **(Figure III.5)**, an outcome that strengthens previous observations made on water/ice microbial communities in the Arctic marine environment (Yergeau *et al.*, 2017).

Betadisper analysis **(Table IX.3)** showed that the community dispersion in each site becomes smaller as we move from sites 1 and 2 to site 4, validating a larger difference between ice and water communities in habitats more distant from the river. In fact, community dispersion within sites 1 and 2 (water and ice included in each site) proved to be larger than community dispersion observed for ice samples (only) and water samples (only) along the gradient **(Table IX.3)**. These results are congruent with the largest difference in alpha diversity measures between ice and water **(Figure III.2)** and the closest proximity of sites 1 and 2 **(Figure III.1)**. Samples from sites 1 and 2 were proximate to one another in the ordination space, which means that OTU composition within each biotope was consistent with geographical proximity.

Prokaryotic communities in ice seemed to respond more to the unique environmental/biological features of each site than those from water **(Figure III.5)**. First, there was a clear diagonal division along both axes responding to the different salinity levels (sites 1 and 2 *versus* sites 3 and 4). Further, ice and water samples from site 4 were located near to one another in the ordination space **(Figure III.5)** indicating that community similarities between ice and water increased with proximity to the river, corroborating the trends observed for OTU richness **(Figure III.2)** and taxonomic composition **(Figure III.3)**. The genera *Psychromonas, Reinekea*, *Paraglaciecola*, *Glaciecola*, and *Polaribacter* (OTU 9) were proximate to ice samples from sites 1 and 2, illustrating the higher relative abundance of these groups in ice from both sites, and distant from water samples.

The measurements of chlorophyll *a* fluorescence, cyanobacterial biomass (phycocyanin fluorescence), and dissolved oxygen (ODO) in water decreased with increasing salinity, and these parameters were found to reflect the separation of water communities of sites 1 and 2 from those of sites 3 and 4 along coordinate 1 **(Figure III.5)**.

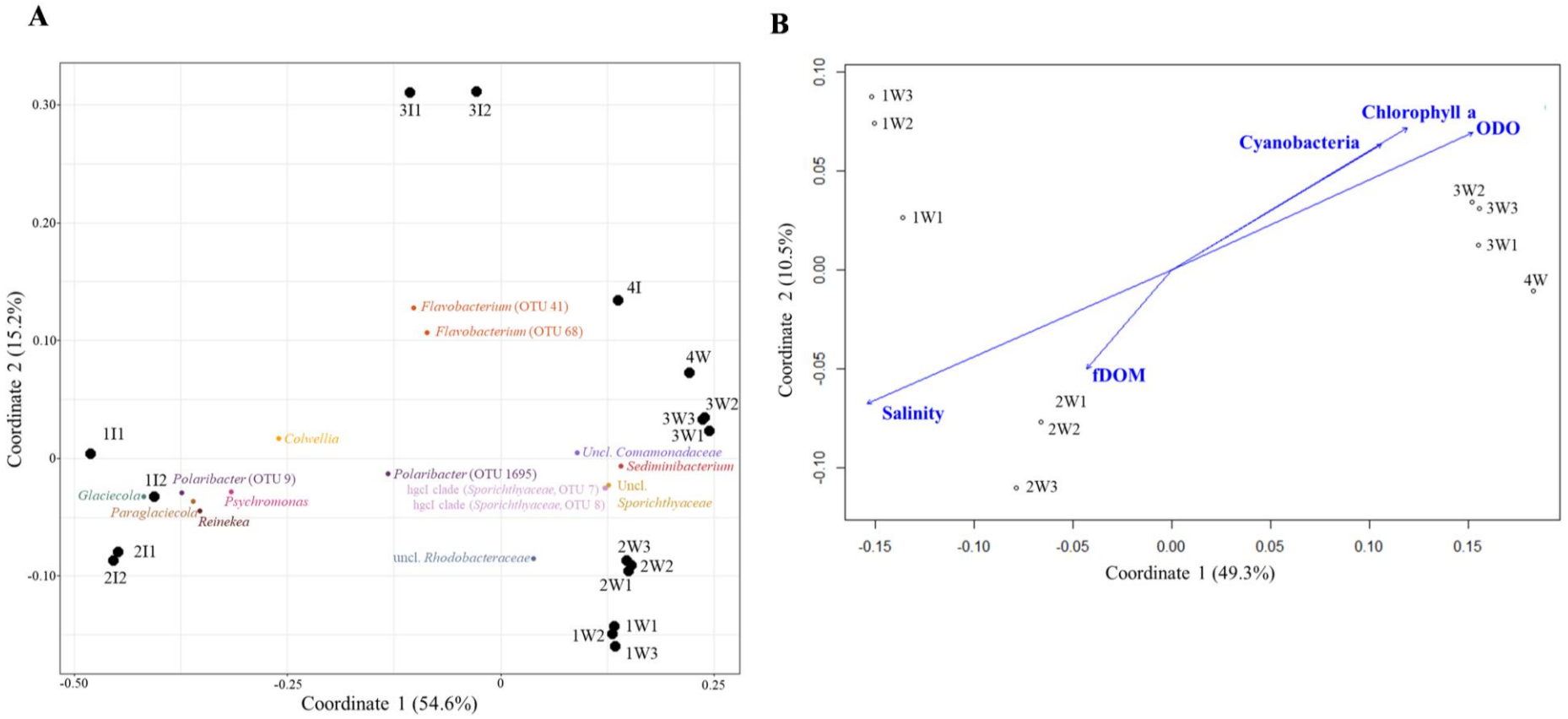

Figure III.5 - Ordination of ice and water prokaryotic communities. Community ordination in (A) and (B) was performed based on a Bray-Curtis similarity matrix calculated from Hellinger-transformed OTU abundance profiles. (A) Principal Coordinates Analysis of all prokaryotic communities. Samples are represented by black dots. The 15 most dominant phylotypes (OTUs) of the entire dataset are plotted in color, and their position in the ordination diagram represents relative abundance data recorded for each OTU across all samples. The closer a phylotype is to any given sample, the higher its relative abundance in that sample. (B) Principal Coordinates Analysis of prokaryotic communities in water samples in relation to quantitative variables measured for each site. Blue arrows indicate the average values of the quantitative variables salinity, fluorescent dissolved organic matter (fDOM), cyanobacterial fluorescence (phycocyanins fluorescence), Chlorophyll *a*, and dissolved oxygen (ODO). Percentages in each axis title correspond to the amount of variance explained by that coordinate. From Coelho *et al.*, 2022, in *STOTEN*.

In agreement, sites 3 and 4 displayed higher abundances of *Cyanobacteria* (especially in ice – **Figure III.3**) as well as *Planctomycetes* and *Verrucomicrobiae*. Sites 3 and 4 also displayed higher fluorescence values of phycocyanin and chlorophyll *a* in the water **(Table IX.2)**. Site 3 was the habitat with the highest photosynthetic biomass indicators **(Figure III.3** and **Figure III.5**). Snow depth was lowest at site 3 **(Table IX.2)** and may have played a role in this trend through its effects on UV attenuation. The highest fDOM measures were observed for samples from site 2, while the lowest fDOM measures were recorded for sites 3 and 4.

III.4.4 Community structure based on culture-dependent methods

We were able to cultivate a small portion of the bacterial communities from ice and water when compared with the richness present in the culture-independent dataset (652 genera in the *Bacteria* domain). Two isolates were classified at the species level, 169 isolates at the genus level, and four isolates only at the family level. Nonetheless, the culturable bacterial richness uncovered in this study encompassed a large variety of genera (N=34), including three potentially novel genera from different families, and phylotypes represented by 41 OTUs defined at 97% sequence similarity, among a collection of 175 isolates.

Of the 29 phyla detected by the culture-independent analysis, four were cultured **(Figure III.6)**: *Proteobacteria* (72%), *Actinobacteria* (16%), *Bacteroidota* (9%), and *Firmicutes* (3%), being the former three phyla also the most dominant in the culture-independent data **(Figure III.3)**. Overall, the taxonomy profiles of the culturable communities in ice and water samples along the salinity gradient differed sharply from those retrieved via culture-independent analysis, with the disparity between the two datasets increasing at lower taxonomic levels.

At the phylum level, there was an increase in the relative abundance of *Firmicutes* and *Bacteroidota* in the culturable community from ice in comparison with water samples, in agreement with the culture-independent results. For example, the genus *Bacillus* was only present in the ice samples **(Figure III.6)** cultivated on R2A with ASW **(Figure IX.6)**. Further, from the 31 formally described genera identified from the isolate's 16S rRNA gene sequences **(Figure III.6)**, only 18 were detected in the cultivation-independent dataset. The isolates belonging to the remaining cultivated genera were often closely related to extremophilic strains.

Isolates from the genus *Marinomonas* (*Oceanospirillales*) were retrieved from water samples on R2A with ASW **(Figure IX.6)** and detected at site 1 by both culture-dependent and -independent assessments. Also agreeing with the culture-independent analysis, a few representatives of the *Xanthomonadales* and *Alteromonadales* orders, such as *Stenotrophomonas* and *Shewanella*, respectively, were found in ice samples cultivated on R2A with ASW (**Figure III.6** and **Figure IX.6**).

Conversely, *Alphaproteobacteria* isolates (23%) could be retrieved from almost all samples from all sites. Although members of the SAR11 clade were found in all samples using culture-independent analyses **(Figure III.3)**, they were not among our cultivated strains, and would not be expected to be, given the culture conditions used in this study. Instead, alphaproteobacterial orders previously described in association with Arctic freshwater or Arctic sea ice in the summer (Bottos *et al.*, 2008; Ortega-Retuerta *et al.*, 2013) such as *Caulobacterales* (10%), *Sphingomonadales* (8%), *Rhodobacterales* (1%), and *Rhizobiales* (1%), were cultivated in this study from both R2A with ASW and R2A with MilliQ water. These orders were also detected in the cultivation-independent dataset.

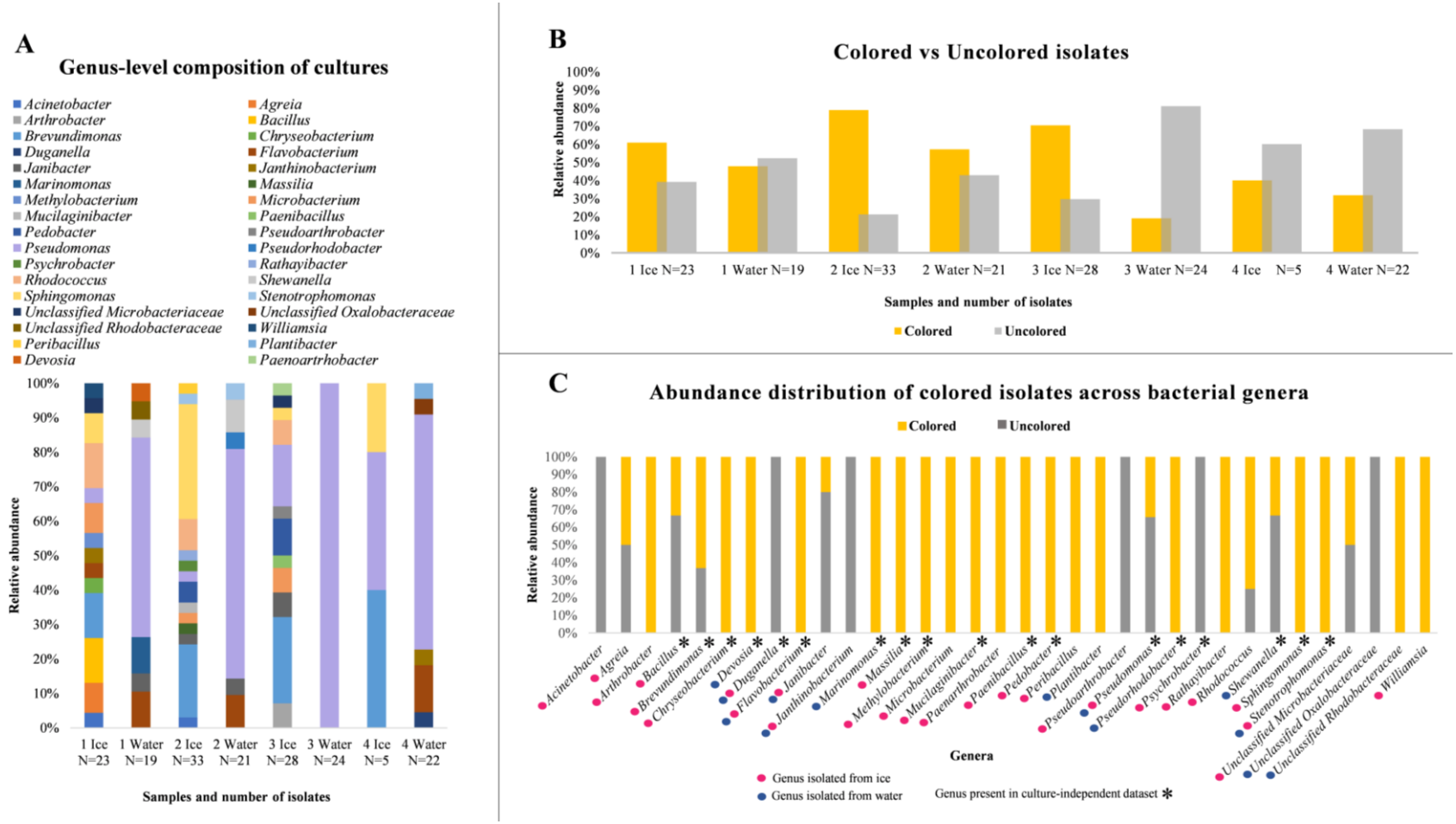

Figure III.6 - (A) Relative abundance of bacterial genera cultivated from ice and water from all sampling sites. (B) Relative abundance of colored (yellow, pink, salmon, orange, violet) and uncolored (translucent, white, cream, grey) isolates retrieved from ice and water at sampling sites 1 to 4. "N" represents the number of isolates from each sample. (C) Percentage of colored *versus* uncolored colonies within genera isolated from all sampling sites. Red dots refer to genera isolated from ice and blue dots refer to genera isolated from water. Genera found in both water and ice have dots of both colors. Genera found in both culture-dependent and -independent datasets are represented with an asterisk. From Coelho *et al*., 2022, in *STOTEN*.

A higher relative abundance of pigmented bacteria was isolated from the ice than from the water **(Figure III.6)**, on both R2A media **(Figure IX.7)**. These cultures showed observable pink, yellow, orange, and violet pigments, and most genera that were only represented by colored colonies were isolated exclusively from ice **(Figure III.6)**. As expected, the two R2A media chosen to cover this estuarine system differ in the relative abundance of some groups, especially at the genus level. Seven genera were isolated using both media: *Pseudomonas*, *Brevundimonas*, *Rhodococcus*, *Microbacterium*, *Flavobacterium*, *Janibacter*, and *Sphingomonas*. Of the remaining 27 genera, 13 were cultivated on R2A with ASW and 14 on R2A with MilliQ water. Generally, the class *Gammaproteobacteria* was the most dominant in water, as 93% of the isolates retrieved from water samples were mostly *Pseudomonas* strains closely related to cold environment species such as *P. antarctica* and *P. psychrophila* **(Figure III.6)**. At site 4 (lowest salinity) only two genera, *Pseudomonas* and *Brevundimonas*, were cultured on R2A with ASW, while eight genera were obtained from R2A with MilliQ water, including *Macrobacterium*, *Arthrobacter*, and *Plantibacter* (all belonging to *Actinobacteriota*) as well as *Janthinobacterium* and *Duganella* (*Betaproteobacteria*). These results agree with the higher input of freshwater at site 4.

III.5 Discussion

The ice prokaryotic communities examined in this study are part of the broad spectrum of Arctic marine microbiomes, which contrast in many respects with the microbial communities of the Southern Ocean (Brinkmeyer *et al.*, 2003; Ghiglione *et al.*, 2012; Yergeau *et al.*, 2017). This distinctiveness between the poles in part is related to the strong impact of terrestrial environments on the Arctic Ocean ecosystem, and this is

especially the case for subarctic Hudson Bay with its numerous inputs from rivers that flow through well-vegetated catchments.

III.5.1 Differences between sea ice and interface water prokaryotic communities increase with salinity

The differences in alpha and beta diversity between ice and water at sites 1 and 2, particularly, were more pronounced than the differences observed within each biotope - ice or water - along the salinity gradient, and this is evident in all analyses performed. Congruent with the notion that prokaryotic community structures of ice and water are more divergent from one another at higher salinity sites, the extent of OTU sharedness between ice and water decreased from 88% in site 4 to less than 50% in sites 1 and 2.

The ice from sites 1 and 2 showed a greater prominence of genera usually associated with the marine environment (e.g., *Polaribacter*, *Paraglaciecola*, *Colwellia*, *Reinekea*, and *Glaciecola*) unlike the water from the same sites, or the water samples in general, which were dominated by genera usually associated with freshwater environments influencing Arctic marine systems (e.g. *Sediminibacterium* and the hgcl clade) and which are known to play an important role in the nutrient cycles (Llirós *et al.*, 2014; Adyasari *et al.*, 2020; Mohapatra *et al.*, 2020). Two hypotheses may explain this phenomenon: 1) the freshwater groups were negatively selected in ice upon freezing at the higher salinity sites, and/or 2) the freshwater groups we found in the ice-covered waters were not as dominant during the open-water season at ice formation (e.g., higher dispersion of the river plume during winter). Freezing alone did not appear to be negatively selecting against the freshwater groups since they were abundant in ice from site 4. However, osmotic stress could still be a cause for de-selection since ice brine channels would be expected to decrease from site 1 to site 4.

The fact that the bay surface is less influenced by freshwater before ice formation at the end of the open-water season in comparison with the ice-covered season (winter) may support the second hypothesis. The river plume size in Hudson Bay is more vertically localized and spatially extensive under the ice than in open waters (Ingram *et al.*, 1987) as a result of protection from wind-induced mixing. When the bay is ice-covered, the water from the river spreads out as a thin layer over the denser seawater and covers hundreds of kilometers of the bay surface (Ingram *et al.*, 1987). The shifts in prokaryotic community structures of ice *versus* water presented in this study are consistent with this pattern. For example, *Oceanospirillales,* commonly found in the marine Canadian Arctic (Ortega-Retuerta *et al.*, 2013), as well as *Flavobacteriales,* were more prevalent in ice at higher salinity sites but not in the water. In fact, the genus *Polaribacter* in the order *Flavobacteriales* is one of the most abundant genera in the Arctic Ocean and occurs in annual ice, brackish waters, and saline environments (Comeau *et al.*, 2011; Bowman *et al.*, 2012; Hatam *et al.*, 2014; Yergeau *et al.,* 2017). Also, the marine/brackish genera found almost exclusively in ice from sites 1 and 2 were from the order *Alteromonadales*: *Paraglaciecola, Psychromonas, Glaciecola, Shewanella, Marinobacter, and Colwellia*. The latter is a typical genus from cold environments that can maintain metabolic activity down to -20ºC (Methé *et al.*, 2005; Junge *et al.*, 2006).

Hudson Bay is an adjacent sea to the Arctic Ocean where SAR11 clade phylotypes abound (Bano *et al.*, 2002; Alonso-Sáez *et al.*, 2008; Comeau *et al.*, 2011; Ghiglione *et al.*, 2012). Our data show that this group is likely de-selected during ice formation in Hudson Bay, consistent with previous findings on the distribution of the SAR11 clade in ice versus water in the high Arctic (Hatam *et al.*, 2014). Despite such a clear-cut response to the emergence of novel microniches (that is, ice) in cold biomes, the diversity of SAR11 clade phylotypes in the Arctic is still not well known. Of our 38 SAR11 clade

OTUs, only 3 could be classified at the genus level (Subgroup 1a). This subgroup (*Pelagibacteraceae*) has been previously associated with cold waters, freshwater conditions, UV exposure, low nutrient availability, and algal blooms (Kraemer *et al.*, 2020). It has been suggested that the Arctic Ocean houses endemic SAR11 clade ecotypes due to its relative isolation from other oceans and the long seasonal presence of ice overlying its freshwater-influenced water column (Kraemer *et al.,* 2020). It is possible that the unique waters of Hudson Bay harbor endemic SAR11 ecotypes, whose physiology and ecological roles have yet to be unveiled.

Salinity gradients are well-known determinants of the structure and function of microbial communities (Lozupone *et al.*, 2007; Beier *et al.*, 2011). Steep salinity gradients (from 0 up to >30 PSU) reflecting freshwater-marine transitions perpendicular to Hudson Bay's coast appear to act as a dispersal barrier for microbial eukaryotes in summer (Jacquemot *et al.*, 2021; Blais *et al.*, 2022). Our study, in contrast, examined prokaryotic community assembly in both ice and water within a brackish salinity range (from 0.6 to 10.5 PSU) along the coastline, and the results suggest that first-year sea ice, particularly at sites farther away from freshwater inputs, houses prokaryotic taxa, such as the *Oceanospirillales* and *Flavobacteriales* phylotypes mentioned above, that may be more dominant in water during summer. Future studies must shed light on this hypothesis.

III.5.2 Potential influence of phytoplankton and dissolved organic matter on the prokaryotic community structure

We also observed shifts in the structure of prokaryotic communities of both ice and water according to measures of fDOM and phytoplankton fluorescence that were made *in-situ* across the salinity gradient. The potential phytoplankton effect was most conspicuous on the ice samples of site 3, which had the highest bacterial richness and most distinct taxonomic composition among ice samples from all sites. *Cyanobacteria*

contributed 5% of the total reads in both ice samples from this site, similar to the abundance found in other coastal environments of the Arctic Ocean, especially those subject to inputs from rivers, which are well known to be prime Arctic environments for picocyanobacteria (Waleron *et al.*, 2007; Bowman *et al.*, 2012; Vincent *et al.*, 2012). Consistent with this notion, several OTUs belonging to the genus *Cyanobium* (order *Synechococcales*), considered to be the most abundant picocyanobacterial group in fresh and brackish waters worldwide (Albrecht *et al.*, 2017), were collectively responsible for the enrichment in *Cyanobacteria* proportions in ice samples from site 3. This result supports the higher abundance of *Cyanobacteria* previously reported in Hudson Bay (Legendre *et al.*, 1999). *Verrucomicrobiae* and *Planctomycetes* were also abundant in ice from site 3 **(Figure IX.3)**, and in studies elsewhere, these have been linked to the presence of photoautotrophs (Pizzetti *et al.*, 2011; Dedysh *et al.*, 2019). Subarctic *Planctomycetes* are not well characterized (Pizzetti *et al.*, 2011), and in our dataset, most OTUs corresponded to unknown or uncultured genera, while *Verrucomicrobiae* is recognized as abundant in the Arctic Ocean and has been previously identified on Arctic ice shelves (Bottos *et al.*, 2008) and in sea ice (Bowman *et al.*, 2012; Comeau *et al.*, 2011).

Chlorophyll *a* and phycocyanin fluorescence values were also higher in the water from site 3. We suggest that snow depth being lower in site 3 **(Table IX.2)** along with the river influence, contributed to the increase in photoautotrophs in this site. Snow also plays an important role in the abiotic regulation of ice microbiomes due to the reflection and filtering of visible light and UV radiation (Perovich, 2002), contributing to the light protection of heterotrophs while the autotrophs struggle to harvest enough light for photosynthesis. The sustained presence of heterotrophs would enrich the ice with trace elements that may facilitate autotrophic growth in spring and after ice-out (Riedel *et al.*, 2008). Similarly, Imbeau *et al*. (2021) found that northern lake ice retained high

concentrations of bacterial fatty acids, and they postulated that the release of these materials into the water at ice-out would stimulate planktonic microbial activities (Imbeau *et al.*, 2021).

Although we recorded a low abundance of cyanobacterial fluorescence and chlorophyll *a* in ice from sites 1 and 2, *Glaciecola* and *Paraglaciecola* - groups known to be associated with algal aggregates (Rapp *et al.*, 2018) - were abundant in ice samples from these sites. Past studies have also shown that the recruitment of bacteria into ice is primarily facilitated through their attachment to microalgae or particles (Brinkmeyer *et al.*, 2003). Notably, fDOM measures in water were higher at sites 1 and 2. The DOM in the Arctic ice and water environments is usually directly correlated with the presence of algae. In fact, the water communities from sites 1 and 2 were rich in saprophytic taxa such as *Burkholderiales* which depend on the carbon inputs available during the summer algal blooms typical of the high Arctic (Kirchman *et al.*, 2010; Ghiglione *et al.*, 2012; Llirós *et al.*, 2014; Yergeau *et al.*, 2017). Although some light is available in winter at these subarctic latitudes, the day length is short and available light is attenuated strongly by the snow and ice. Decaying algal populations may have contributed to the higher fDOM coupled with diminished abundance in chlorophyll *a* in sites 1 and 2. However, additional measurements would be needed to assess the relative abundance of microalgal taxa in these sites, for example by 18S rRNA gene sequencing. Possibly, higher fDOM values could also indicate lower DOM turnover rates, related to reduced bacterial growth and metabolic activity in the microbial loop. Overall, our results indicate that the structure of prokaryotic communities in ice and the underlying water at the Hudson Bay coast shifts significantly across a salinity gradient largely determined by freshwater inputs and that such shifts correlate with changes in ecosystem-level abiotic and biotic parameters such as dissolved oxygen, phytoplankton (higher levels of chlorophyll *a* and producers such as

Cyanobacteria in sites closer to freshwater) and fDOM (higher at sites distant from the freshwater input).

III.5.3 Cultivation-dependent and -independent analyses indicate the importance of pigmented bacteria in ice

Sea ice has been considered a selective agent favoring a seed bank of psychrophilic bacteria that would ultimately dominate Arctic coastal waters (Junge *et al.*, 2002; Connelly *et al.*, 2006). Cell and CFU counts obtained in this study fall within the range reported previously for prokaryotic abundance in Arctic ice and seawater (Maccario *et al.*, 2015), agreeing with the general estuarine description of Arctic marine environments. Our results are also consistent with some of the previous reports on the "culturability" of polar ice bacteria, estimated to be lower than 1% using solid media (Helmke *et al.*, 1995; Christner *et al.*, 2002). However, it is difficult to establish a reference value for the expected ice "culturability" within the literature since the selective pressures present in the ice habitats will depend on the ice origin, age, and sampling season. Therefore, finding an optimal cultivation method that supports all conditions is challenging. In this study, we used standard methodology (R2A medium prepared with either ASW or MilliQ water) to generate baseline data on culturable, heterotrophic bacteria from Hudson Bay. In future studies, it would be useful to extend this work by applying novel culture media with salt concentrations that mimic those of the salinity gradient along the coast, which would likely expand the diversity of bacteria that can be cultivated from this ecosystem.

We found evidence, based on both cultivation-dependent and independent analyses, that ice may be a selective force favoring the prevalence of pigmented bacteria in this environment. Colored bacterial colonies were more often detected in the ice than in water samples, suggesting that pigmentation within this diverse group of culturable bacteria is likely to underpin their success and viability in ice. Likewise, our culture-independent

approach revealed that many other typically pigmented bacterial genera such as *Polaribacter* (Gonzalez *et al.*, 2008), *Ferruginibacter* (Lim *et al.*, 2009), *Chthoniobacter* (Sangwan *et al.*, 2004), *Colwellia* (Deming *et al.*, 1988), *Fluviicola* (Dahal *et al.*, 2018) and *Luteolibacter* (Jiang *et al.*, 2012) were enriched in the ice samples. In contrast, *Brevundimonas*, an alphaproteobacterial genus previously detected on Arctic ice shelves (Bottos *et al.*, 2008) and composed of mostly pigmented bacteria, was abundant and exclusively cultured from ice, while only detected at low relative abundance in the cultivation-independent dataset. The prevalence of *Brevundimonas* observed among the cultures, and of *Polaribacter* and several other pigmented genera in the culture-independent results, is consistent with the view that ice microbial communities are enriched in pigmented species (Brown *et al.*, 2001).

Ice microorganisms are exposed to photooxidative stress, while microbes thriving in the water column are likely to be adapted to a lower solar radiation regime (Gosselin *et al.*, 1985). The most common mechanism against photooxidative stress is the production of carotenoid pigments, resulting in orange, pink, or yellow coloration, that quench photochemically produced reactive oxygen species (Vincent *et al*., 1993b). Similar results have been reported in previous studies of modern ice cores, regardless of geographical origin (Christner *et al.*, 2002). Biopigments are also reported to act as a response to nutrient depletion and dryness, all conditions present in the cryosphere (Lemoine *et al.*, 2010; Seel *et al.*, 2020). In Arctic lakes, pigmented, heterotrophic bacteria have been reported to participate in solar energy capture, behaving as mixotrophs and enhancing the pathways of carbon flow, and some prokaryotic pigments may provide protection of the whole community against harsh environmental conditions (Vigneron *et al.*, 2018). Our results raise the possibility of this phenomenon also occurring in surface ice and other light-exposed polar surfaces. Given the presence of several orange-to-red pigmented

bacteria among our cultures, including members of the phylum *Bacteroidetes* such as the genera *Flavobacterium*, *Chryseobacterium,* and *Mucilaginibacter*, it is reasonable to argue that carotenoids constitute a prevailing pigment type within our culture collection. Future, spectroscopy-based pigment characterization will shed more light on the identity and concentration of pigments found among the bacterial taxa isolated in this study.

As observed for the genus *Brevundimonas* in ice, the genus *Pseudomonas* was likewise almost rare (<1%) in the culture-independent data, but dominated the culturable community, particularly in the water samples. The *Pseudomonas* isolates were most closely related to species usually observed in cold environments. Isolate 4W1V, for example, was closely related to *Pseudomonas yamanorum*, a psychrotolerant bacterium first isolated from subantarctic habitats (Arnau *et al.*, 2015). Moreover, some of the Gram-positive isolates were closely related to typical ice-thriving species such as *Arthrobacter agilis* (Christner *et al.*, 2002) and *Bacillus* spp. One of these isolates, *Bacillus* sp. 1I18W was closely related to *Bacillus safensis*, a species highly resistant to the cold and high energy radiation, including in space-borne experiments (Coil *et al.*, 2016).

III.6 Conclusions

Our observations of the sea ice-water interface at the Hudson Bay coast show that there can be striking patterns in prokaryotic community structure that are related to environmental gradients. There were strong differences between ice and water communities, especially in regions with higher salinity. Sea ice more distant from the shore was dominated by marine phylotypes, while all water environments, as well as ice closer to the river mouth, were dominated by freshwater taxa. Salinity creates a pronounced vertical ecological stratification between ice and water and is one of the key drivers shaping the ice microbiome through the cold but sunlit winter at this subarctic

latitude. Our complementary insights into prokaryotic community structure by culture-dependent and -independent analyses show that sea ice may host higher proportions of pigmented bacteria than the sub-ice waters, potentially resulting from the increased solar radiation exposure in the ice. We further show that besides salinity, DOM and phytoplankton (as measured by fluorescence proxies) appear to influence the composition of prokaryotic communities in the ice. The ongoing study of these microbial communities inhabiting subarctic ice and the interface water that lies close to freezing will allow an improved understanding of the short- and long-term effects of ice melting in a rapidly changing climate.

IV CHARACTERIZATION OF THE FLUORESCENT ORGANIC MOLECULES IN THE ARCTIC ICE AND WATER AS A PROXY FOR LIFE-DETECTION IN EUROPA AND ENCELADUS

Manuscript in preparation

IV.1 Summary

Future missions to Europa and Enceladus will have spectroscopic equipment on board to characterize the surface of these moons and search for biosignatures. Reference data, from planetary field analogues to these satellites are required for the success of these missions to tailor new equipment and create reference databases. Hudson bay's coast is an ice-covered marine environment in winter, analogue to the water-ice interactions on Europa and Enceladus, also considering water bodies perched in the ice shell and close to the surface. Here fluorescent organic molecules from Hudson bay's ice and interface water were detected and characterized in our laboratory, using *in-situ* proxy measurements and pure compounds as reference. Tryptophan, humic-like molecules, and likely carotenoids are fluorescent organic molecules present in samples of ice and water from three locations that follow a salinity gradient due to increased proximity to a river. These molecules are more resilient to time, biodegradation, light, and ice melting than chlorophylls. Our spectroscopy results unmask the same trends observed previously through microbiology analysis, showing that the ice's organic content varies with the relative distance to the river while water's organic content is less disturbed by freshwater inputs. Finally, biological degradation is a factor when comparing freshly-melted-ice with old-melted-ice, likely due to the resilience of extremophilic life to the cold temperatures of storage.

IV.2 Introduction

Some models of Europa and Enceladus predict the existence of communication between different water bodies in the subsurface, which will likely incur a salinity gradient (Schmidt *et al.*, 2011; Walker *et al.*, 2015; Culberg *et al.*, 2022). First, the ocean in Enceladus is modeled to be very similar to Earth's oceans (Affholder *et al.*, 2021; Lobo

et al., 2021), and thus the establishment of "life as we know it" as a model when designing life-detection missions is a plausible assumption. Second, the ice brine channels and perched water bodies constitute liquid water reservoirs much closer to the surface, and thus much easier to sample (Hendrix *et al.*, 2019). These freshwater water bodies are analogue to lakes, and putative communication channels with flowing water are analogue to rivers, and these complex hydrological structures could in fact explain the difficulty in constraining the ice shell thickness (Billings *et al.*, 2005). The possibility of liquid water near the subsurface and the likely presence of plumes allow speculation regarding whether there might be detectable biosignatures. These biosignatures may include fluorescent molecules such as biopigments and humic-like substances. Identifying the chemical make-up of planetary field analogues of icy worlds is essential to prepare for future missions to these extra-terrestrial environments (Foing *et al.*, 2011; Kotler *et al.*, 2011; Chan *et al.*, 2012a; Martins *et al.*, 2017; Martins, 2020). Hudson bay is an ice-covered aquatic system during winter, with multiple inputs of freshwater from the surrounding rivers, and as such, it contains colored dissolved organic matter (cDOM) distributed along coastal margins (Coble *et al.*, 2014). Part of this colored dissolved organic matter is fluorescent. Reported fluorescent components of aquatic organic matter include proteins, tyrosine (Tyr), tryptophan (Trp), biopigments, lignin phenols, humic substances, and hydrocarbons (Coble *et al.*, 2014). Aquatic cDOM can be either autochthonous when referring to organic matter which originated in that location (e.g., microbial production), or allochthonous if referring to organic matter transported from the surrounding land (vegetation and/or soil) (Coble *et al.*, 2014). Fluorescence organic matter from an aquatic environment is a mixture of compounds, some of which have overlapping excitation and emission spectra, being thus challenging to characterize. The position of maximum fluorescence across environments is variable, shifting along both

excitation and emission axes in response to chemistry and the matrix effects, in this case, water contents (Coble *et al.*, 2014). Organic matter's fluorescence is one of the most common life signatures of aquatic systems, being part of fDOM content, and is characterized by three main peaks: C (terrestrial humic-like/soil and vegetation), M (marine humic-like/microorganisms), and T (tryptophan-like) (Coble *et al.*, 2014). In fact, the three aromatic amino acids - tryptophan, tyrosine, and phenylalanine - fluoresce in the lower UV region when measured in pure form (Cory *et al.*, 2005), with tryptophan absorption maximum registered at 280 nm and emission maximum at 340-360 nm (λ_{ex} = 275-280 nm) (Du *et al.*, 1998; Dixon *et al.*, 2005). Components of peak C emit at 420-470 nm when at λ_{ex} = 320-365 nm. The emission maximum occurs at 450 nm varying in the width of the peak depending on the sample. Components of peak M emit at 370-420 nm when at λ_{ex} = 290-310 nm. Peak width is not constant but rather is dependent on the relative amounts of fluorophores comprising the mixture in the sample (Coble *et al.*, 2014).

Biopigments are fluorescent organic molecules produced by various types of organisms for different purposes, such as biomass production and protection against photooxidation, lack of resources, and dryness (Bonilla *et al.*, 2009; Seel *et al.*, 2020). The distinct chemistry and optical properties of biopigments grant them a status of importance as targets in the search for signs of life (Wolstencroft *et al.*, 2002; Seager *et al.*, 2005; Baqué *et al.*, 2020). Previous results from studies in Arctic water bodies have shown that the production of photoprotective biopigments is correlated with UV-penetration, and inversely correlated with temperature and colored dissolved organic matter (Bonilla *et al.*, 2009; Przytulska *et al.*, 2016; Coelho *et al.*, 2022b - Chapter III). Chlorophyll *a* and chlorophyll *b* are green pigments virtually universal in all oxygenic photosynthetic organisms. Chlorophylls are porphyrins that act in the conversion of light

into chemical energy by taking part in the light absorption and electron transfer in the photosynthetic reaction center (Grossman *et al.*, 1995). Chlorophyll's absorption spectral features are usually characterized by two regions: the Soret or B band, which is the most intense peak and appears in the near UV region, and the Q band, which is weaker and occurs in the visible region. The Soret band can also be accompanied by an N-band of lower intensity (Hasegawa *et al.*, 1998; Sundholm, 1999; Ustin *et al.*, 2009). In pure chloroform, the absorption maximum of chlorophylls Q bands is previously reported to be 670 nm and 659 nm, for *a* and *b* respectively. The absorption maximum of the Soret bands is 432 nm and 460 nm, respectively (Wellburn, 1994; De Boni *et al.*, 2010). The Stokes shift is the difference of wavelength between positions of the band maxima of the absorption and emission spectra (Albani, 2004). The Stokes shift of chlorophylls specifically in the region of the Q band (Szalay *et al.*, 1974) is very narrow, being preferable to use the maximum of the Soret band as excitation wavelength or even lower wavelengths. The fluorescence emission maximum has been reported to be 674 nm and 669 nm, respectively (Fiedor *et al.*, 2003; Oktavia *et al.*, 2021).

Phycobiliproteins are molecules produced by cyanobacteria and algae that act as primary light-harvesting photosynthetic pigments, along with chlorophylls. Phycocyanins are blue phycobiliproteins that have phycocyanobilin as the chromophore. Due to being water-soluble, phycocyanins are present in the interior of cyanobacteria cells (Eriksen, 2008). In an aqueous solution, the absorbance maximum of phycocyanins from *Spirulina* (both crude and purified) is reported to be 620 nm, with a shoulder at 650 nm, and the emission maximum has been reported to be 658 nm when λ_{ex} = 580 nm (Böcker *et al.*, 2020), while some fluorescence variability occurs depending on the subtype of phycocyanin and organism. The Stokes shift of phycocyanins' spectral signatures is thus,

also, very narrow (<38 nm) (Glazer *et al.*, 1983; Eriksen, 2008), sometimes being necessary to choose a wavelength for λ_{ex} lower than the absorption maximum.

Carotenoids are a broad family of hydrophobic molecules (>750 compounds), found in all the kingdoms of life (Armstrong, 1997; Yabuzaki, 2017). Their structure is characterized by a long polyene chain with the conjugated double bond system (Fraser *et al.*, 2004) responsible for their light absorption in the spectral region of 300–550 nm. Carotenes are a sub-group of carotenoids characterized by the absence of oxygen in their structure (e.g., β-carotene) (Manning, 2022). Carotenoids are highly resilient to oxidation, which will not easily affect the chromophore. What alters the absorption spectral features of carotenoids is the type of the solvent, which may be challenging to select due to their hydrophobic nature (Zang *et al.*, 1997; Popova, 2017). In pure chloroform, the absorption maximum of ß-carotene is previously reported to be 479 nm with a shoulder at 490 nm and emission between 539-541 nm when λ_{ex} = 420 nm (Van Riel *et al.*, 1983; Wellburn, 1994).

Upcoming orbit missions will focus on collecting absorption spectral features of Europa's surface to identify its chemistry. NASA's Europa Clipper and ESA's JUICE spacecraft will be equipped with ultraviolet spectrographs, Europa Ultraviolet Spectrograph (Europa-UVS) and Ultraviolet Spectrograph (UVS), respectively, with a spectral range of 55-210 nm, which is too low to be able to detect complex organic molecules and thus will only search for simple molecules (e.g., H_2, O_2, OH, CO_2, CH_4 or C_2H_6). ESA's JUICE mission will also take on board the spectrometer MAJIS - Moons And Jupiter Imaging Spectrometer with a spectral range from 500-5500 nm, which would be virtually able to detect some biopigments (namely the Q-band of chlorophylls and phycocyanins).

The future mission Europa Lander is conceptualized to use fluorescence-based technology to detect biomolecules (Hand *et al.*, 2021). These fluorescence detectors include Cold-Lightweight Imagers for Europa (C-LIFE), which incorporates a light-emitting diode (LED) flashlight able to identify biogenic material through fluorescence, and Europa Luminescence Microscope (ELM), a luminescence microscope complemented with a fluorescence spectrometer that will perform excitation of native fluorescence, using UV-Vis for characterization of sample organic content (Hand *et al.*, 2022). This last equipment could theoretically detect all organic molecules mentioned so far in this chapter. Finally, a lab-on-a-chip approach for fluorescence detection is currently being developed for both future Europa and Enceladus Landers. Enceladus Organic Analyzer (EOA) and the Microfabricated Organic Analyzer for Biosignatures (MOAB) are fluorescence detection-based microfluidic instruments designed for targeted *in-situ* analysis of potential biosignature compounds at the ppb levels and include the detection of amino acids, and carboxylic acids (Golozar *et al.*, 2020).

To prepare for these missions more data using remote sensing applications, photochemistry, and photobiology techniques to characterize organic molecules from analogue environments is needed. The use of airborne and space-based imaging spectrometers to detect and map photosynthetic pigments is already implemented (Sagan *et al.*, 1993; Serrano *et al.*, 2002; Carey *et al.*, 2018). However, advances in algorithm development are still necessary before pigment concentrations can be routinely retrieved from space to search for biosignatures in extra-terrestrial environments, or even to monitor Earth's changes. This will require that different instruments are used in environments with different fluorescent biomolecules to catalogue their signatures and characterize the noise. New methods to identify and quantify individual fluorescent biomolecules in the presence of overlapping absorption features would provide a major

advance in understanding their biological functions, quantifying net carbon exchange, and preparing future orbit and lander missions to the icy moons of the solar system.

IV.3 Materials and Methods

IV.3.1 Reagents and solutions

All reagents and compounds used in the present work were commercially available and used without further purification. Chlorophyll *a* (CAS:479-61-8), chlorophyll *b* (CAS:519-62-0), and humic acids (CAS:1415-93-6) were bought from Sigma-Aldrich. ß-carotene (CAS:7235-40-7) and phycocyanins from *Spirulina* were bought from TCI chemicals. The purchased chlorophylls and ß-carotene were ACS grade (≥95%). Humic acids and phycocyanins were technical grade. Spectrophotometric grade chloroform (99.8%) was bought from Sigma-Aldrich, and water was obtained from a Millipore system Milli-Q (18.2 MΩ.cm, 25ºC). For stock solutions, chlorophyll *a*, chlorophyll *b*, and ß-carotene were dissolved in chloroform to a concentration of 10^{-4} M (10^{-1} g/L, 10^{-1} g/L, and $7x10^{-2}$ g/L, respectively). Phycocyanins were dissolved in water to a final concentration of $6x10^{-2}$ g/L (no molecular weight information was available). Humic acids were dissolved in water to a final concentration of $9x10^{-5}$ M ($2x10^{-2}$ g/L), not dissolving completely, in agreement with previous protocols (Penru *et al.*, 2012). Chlorophylls and ß-carotene were further diluted, in chloroform, into a final concentration of 10^{-5} M ($9x10^{-3}$ g/L and $5x10^{-3}$ g/L, respectively). This final step was taken considering the molar absorption coefficient (ϵ) of these molecules (Strain *et al.*, 1963; Bennett *et al.*, 1986), a variable of Beer-Lambert's Law, that translates into the amount of light absorbed by the substance for a specific wavelength and directly correlates with the concentration of the absorbing species.

IV.3.2 Samples

Sampling was performed on the southeast coast of Hudson Bay near Whapmagoostui-Kuujjuarapik in Nunavik, northern Quebec, Canada, an estuarine ecosystem greatly influenced by river systems (Blais *et al.*, 2022; Coelho *et al.*, 2022b - Chapter III). Samples of ice and the water beneath the ice were collected in winter (February 27th and 28th 2019) when ice approximately 1-m thick covered the bay, according to Chapter III (Coelho *et al.*, 2022b). Briefly, ice cores of 1-m length and 9 cm in diameter, and water beneath the ice (1 L) were collected from three different locations - sites 1 (55.39°; -77.61°), 3 (55.30°; -77.76°), and 4 (55.27°; -77.81°). The geographic location of sites 1 to 4 corresponds to a decreasing gradient in water salinity along the coast, with site 4 representing the location with the lowest salinity due to its proximity to the river (**Figure IV.1**). In total, 6 distinct sample groups were collected: 1I, 1W, 3I, 3W, 4I, and 4W (numbers represent the sites, with "I" meaning ice, and "W" meaning water samples).

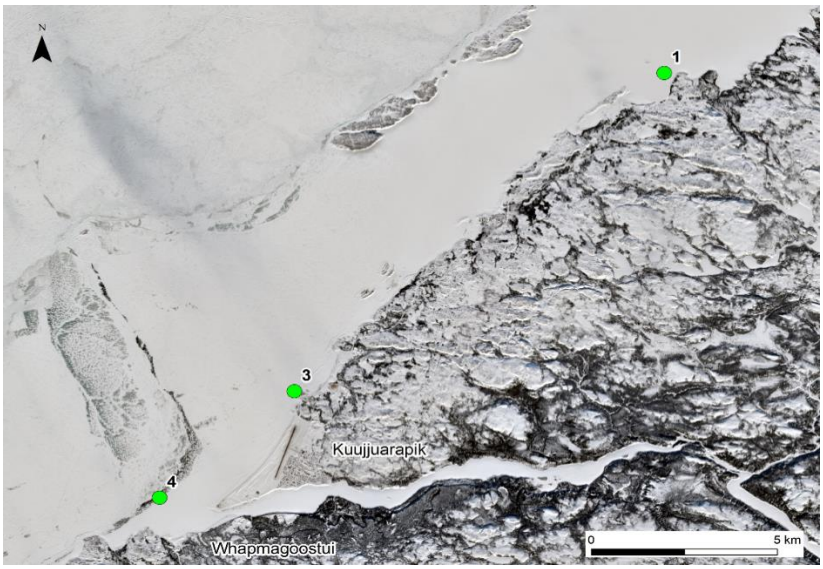

Figure IV.1 - Location of sampling stations on the east coast of Hudson Bay (Whapmagoostui-Kuujjuarapik, Quebec, Canada). Map data © Sentinel-2. Adapted from Figure III.1.

Sample processing took place in the laboratory facilities available at the Centre d'études Nordiques (CEN) research station located in Whapmagoostui-Kuujjuarapik. Ice

samples were decontaminated following the method in Chapter II, Section 5. Ice water (100 mL) for samples 1 and 3 and water (100 mL) from all samples were stored separately in sterile glass bottles, which were shipped to Portugal and maintained at approximately 4ºC until spectroscopic measurements were performed. Ice melted water was named thereafter "old-melted-ice". Ice samples for site 1 and site 4 were shipped to Portugal, where they were maintained in freezing conditions, and were only melted before measurements and named afterward as "freshly-melted-ice". Metadata was collected on-site using a multiparameter water quality probe (YSI model EXO2®), which was placed in the water after extracting the ice cores. The data collected comprised fDOM in quinine sulfate units (QSU), chlorophyll *a* (µg/L), and cyanobacterial fluorescence BGA-PC (phycocyanins in µg/L) through fluorescent detection. Snow depth (cm) on top of the ice surface was also measured on-site.

IV.3.3 Instruments and measurements

IV.3.3.1 Absorption

The electronic absorption of the standard solutions and samples was recorded at room temperature in quartz cuvettes (12.5 × 12.5 × 45 mm), with an optical path length of 1.0 cm. The absorption spectra were recorded between 300 and 800 nm for chlorophylls and ß-carotene, and between 250 and 800 nm for humic acids and phycocyanins, using a Jasco V-660 UV–VIS spectrophotometer (as used in Baraket *et al.*, 2020). As a blank, chloroform was used for measurements of chlorophylls and ß-carotene, while water was used for measurements of phycocyanins and humic acids.

IV.3.3.2 Fluorescence (steady-state emission spectra)

Fluorescence analyses were performed for standard solutions and samples with a Fluorolog FL-1040 Horiba Jobin Yvon spectrofluorimeter (as used in Baraket *et al.*,

2020). Standard solutions and samples were measured in quartz cuvettes (12.5 × 12.5 × 45 mm), at room temperature. Fluorescence analyses in the UV-VIS region were performed using the S1 detector, where excitation wavelengths varied between 250 nm and 650 nm, and the acquisition between 280 nm and 800 nm. In cases where emission was observed, the respective excitation spectra were also collected. Excitation and emission slits varied according to the characteristics of each sample.

IV.4 Results and Discussion

IV.4.1 *In-situ* measurements

There is an inverse relation between snow depth (cm) and the concentration of photosynthetic pigments **(Table IV.1)**. Less snow cover signifies more access to light photons, a requirement for photosynthesis.

Table IV.1 - *In-situ* measurements of snow depth (cm), chlorophylls (µg/L), phycocyanins – BGA-PC (µg/L) and fDOM (QSU) in the water of sampling sites 1, 3, and 4. A more complete format of this table is available in the appendix – Table IX.2.

Sampling site	Snow depth (cm)	Chlorophylls (µg/L)	BGA-PC (µg/L)	fDOM (QSU)
1	20	0.86	1.49	35.9
3	10	1.40	2.129	30.1
4	37	0.92	1.44	41.5

More photosynthetic activity will increase the autotrophic biomass, and thus the number of pigments. Indeed, the results of the amplicon sequencing of the 16 rRNA gene (Coelho *et al.*, 2022b) show that cyanobacteria, producers of chlorophylls and phycocyanins, were more abundant in site 3 in contrast with the other studied sites. The predicted quantity of fDOM is lower on site 3 and higher on site 4. The probe's sensitivity to fDOM detection may be more tailored to detect more humic-like molecules (Peak C) instead of microbial molecules (Peak M), and thus it will detect less fDOM when

photosynthetic organic matter appears to be increased (site 3) and more fDOM where the river influence is more pronounced (site 4). In this case, sensitive spectroscopic equipment, such as the ones used in laboratories, is needed to confirm this hypothesis.

IV.4.2 Characterization of spectral features of pure fluorescent organic molecules

Chlorophylls characterization through UV-Vis spectroscopy shows the two expected absorption spectral features of chlorophylls – the Soret band and Q band (**Figure IV.2**). Our measurements of chlorophyll *a* in chloroform recorded an absorption maximum of the Q band at 667 nm and for the Soret band at 434 nm with other smaller peaks at 335, 380, and 415 nm.

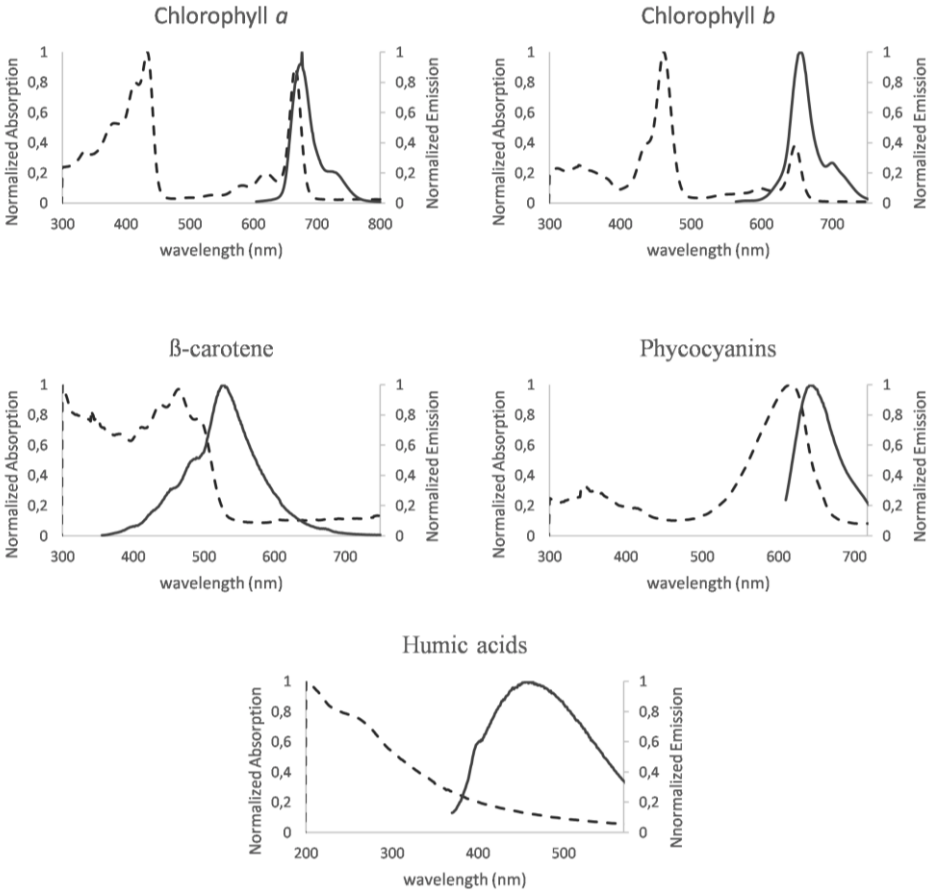

Figure IV.2 - Normalized absorption (dashed line) and emission (solid line) spectra of chlorophyll *a* [10^{-5} M; $9x10^{-3}$ g/L], chlorophyll *b* [10^{-5} M; $9x10^{-3}$ g/L], ß-carotene [10^{-5} M; $5x10^{-3}$ g/L], phycocyanins [$6x10^{-2}$ g/L] and humic acids [$9x10^{-5}$ M; $2x10^{-2}$ g/L]. Chlorophylls and ß-carotene were solubilized in chloroform and phycocyanins and humic acids in water. λ_{exc} = 380 nm for chlorophyll *a*, λ_{exc} = 350 nm for chlorophyll *b* and humic acids, λ_{exc} = 336 nm for ß-carotene and λ_{exc} = 590 nm for phycocyanins. Entrace and exit slits width: 5 nm.

Chlorophyll *b* in chloroform recorded absorption maximum of Q band at 650 nm and of Soret band at 460 nm with two smaller peaks at 600 and 350 nm (**Figure IV.2**). Fluorescence emission of chlorophyll *a* shows a signature peak at 680 nm, with a shoulder at 740 nm when excited at 380 nm, and chlorophyll *b* emits fluorescence at 660 nm, with a shoulder at 700 nm when excited at 350 nm. These values approximate what is reported in the literature (Hasegawa *et al.*, 1998; Sundholm, 1999; Fiedor *et al.*, 2003; Ustin *et al.*, 2009; Oktavia *et al.*, 2021). ß-carotene in chloroform recorded the maximum absorption at 468 nm, and smaller peaks at 336, 412, 440, and 496 nm (**Figure IV.2**), similarly to previously reported values (Popova, 2017). Also, as expected, emits fluorescence at 530 nm with shoulders at 427, 455, and 484 nm when excited at 336 nm (Van Riel *et al.*, 1983; Wellburn, 1994). Phycocyanins recorded maximum absorption at 617 nm, and emission at 647 nm when excited at 590 nm (**Figure IV.2**), which are values close to the previously reported for both pure and crude phycocyanins (Böcker *et al.*, 2020). The excitation wavelength of 617 nm was tried first but, due to the modest Stokes shift, it only captured half of the emission peak, and thus a marginally lower excitation wavelength had to be applied instead. Humic acids recorded a continuous absorption band with a small peak at 267 nm. Excitation at 350 nm showed one of the best quality emission peaks between 370 and 580 nm, with an emission maximum at 460-482 nm, with a less accentuated curve, likely due to its heterogeneity. These values agree with the known fDOM references for peaks C and M (Coble *et al.*, 2014) which are possibly overlapped.

IV.4.3 Spectral characterization of environmental samples

The first spectral signature investigated was proteins, which usually register an absorption maximum between 275-280 nm, and emit between 303-340 nm. Old-melted-ice samples from sites 1 and 3 showed very similar absorption signatures with no clear

peaks at 280 nm **(Figure IV.3)**. However, defined emission features were attained at λ_{exc} = 280 nm. In the water, only 3W had a clear absorption feature at 278 nm.

Ice absorption features had clear differences from water. First, water absorption values reach a minimum at lower wavelengths than ice. Ice samples recorded maximum emission peaks between 325-340 nm, suggesting the presence of tryptophan.

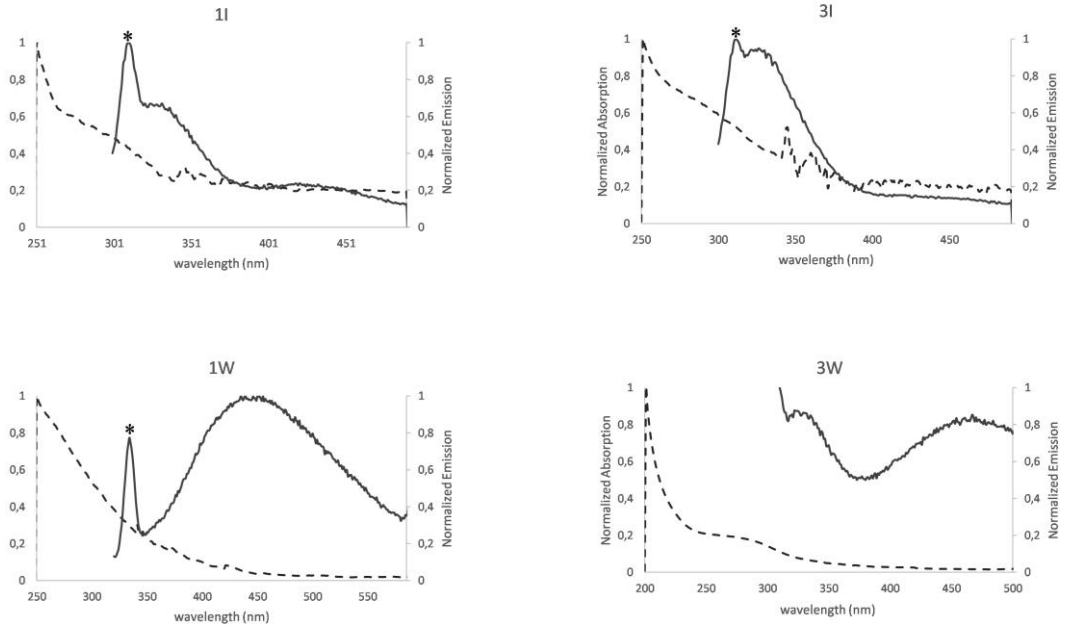

Figure IV.3 - Normalized absorption (dashed line) and emission (solid line) spectra of old-melted-ice samples (1I and 3I) and water samples (1W and 3W). λ_{exc} = 280 nm for 1I and 3I, λ_{exc} = 300 nm for 1W and λ_{exc} = 278 nm for 3W. * Asterisk denotes a peak resulting from solvent Raman scattering. Entrace and exit slits width: 5 nm.

While the fluorescent signature that appeared in ice with a peak at 325-340 nm was not visible in the water from site 1, it was faintly present in water from site 3, which would be an expected result if this signature is indeed tryptophan. This site registered the highest concentration of photosynthetic pigments *in-situ* **(Table IV.1)** and the highest microbial density in samples from this location as shown in chapter III (Coelho *et al.*, 2022b). Roles of tryptophan in photosynthesis including its use in the biosynthesis of chlorophylls have been described (Vavilin *et al.*, 1999; Gondek *et al.*, 2021).

A second signature appears however in 3W, which also seems to be present in 1W with a peak maximum between 430-465 nm, and covering the whole region between 400-500 nm for 3W and 350-550 for 1W, which suggests the presence of both fDOM known peaks C and M in both water samples, and possibly some residual overlapping features of ß-carotene (or other carotenoid-like) in 1W.

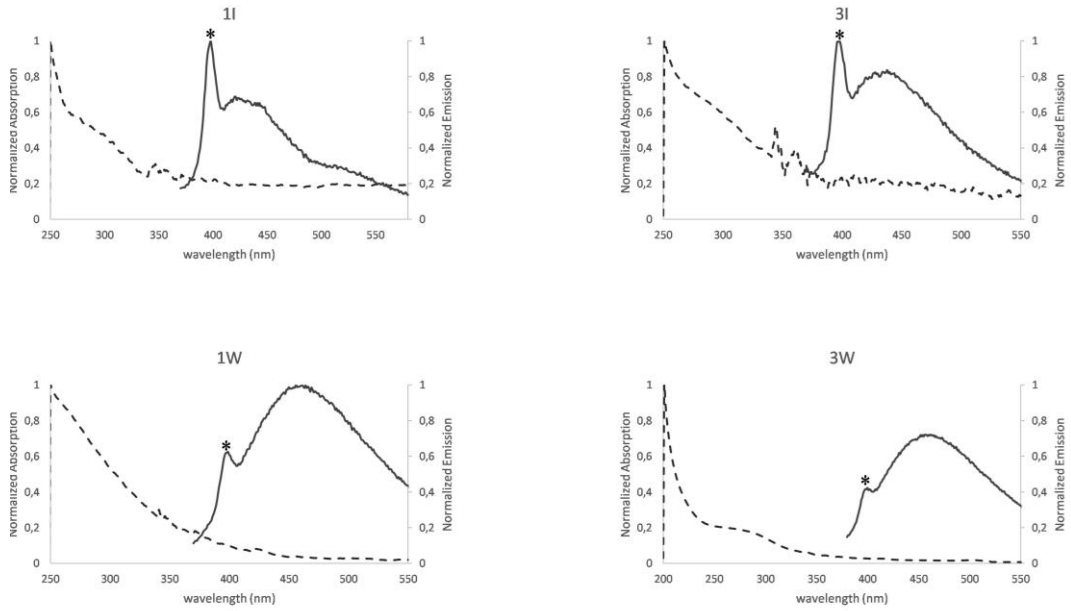

Figure IV.4 - Normalized absorption (dashed line) and emission (solid line) spectra of old-melted-ice samples (1I and 3I) and water samples (1W and 3W). λ_{exc} = 350 nm. * Asterisk denotes a peak resulting from solvent Raman scattering. Entrace and exit slits width: 5 nm.

Further investigation was performed to detect peaks C and M which were previously hinted in water samples in **Figure IV.3**, although not quite in the known optimum excitation wavelength between 300-350 nm. Thus, in this second analysis **(Figure IV.4)** all samples were excited at 350 nm, the optimum λ_{exc} = 350 of peak C. The results are what appear to be the same signature in water from sites 1 and 3 in **Figure IV.3** - a peak covering the region between 400-550 nm (now interrupted earlier by the Raman feature – i.e., inelastic scattering of the incoming light from the solvent, this case, the matrix), suggestive of the presence of peaks C and M, and again possibly ß-carotene overlapping.

The maximum of the peaks is a broad curve instead of a narrow peak and differs slightly between ice and water and not as much along the salinity gradient (site 1 higher salinity, site 3 lower salinity), with water samples having an emission maximum between 450-470 nm (closer to peak C) and ice samples between 422 and 446 nm (closer to peak M).

While the presence of several chlorophylls in Hudson Bay is demonstrated by the *in-situ* data **(Table IV.1)**, further investigation on higher wavelengths to investigate the detection of chlorophylls through spectroscopy did not produce any results, suggesting biological and/or photodegradation.

IV.4.4 Spectral differences between old and freshly melted ice samples

Freshly-melted-ice samples have a different absorption and emission signature from old-melted-ice **(Figure IV.5)**. First, absorption spectra recorded the steepest peak at approximately 280 nm - a more distinct absorption peak T (tryptophan), and second, absorbance values reached zero around 400 nm.

The emission signature is also more defined in freshly-melted-ice than in old-melted-ice samples when excited at 280 nm, although both recorded a maximum emission between 310-352 nm. In both results the resemblance with pure tryptophan, in phosphate buffer, is significant. Though, the emission maximum has a slight shift to the right, of 10-20 nm, when the melted water is fresh recording a maximum at 342-352 nm, making the spectral feature almost identical to pure tryptophan. The fresher the ice, the clearer the tryptophan signature, either in absorption or emission spectra. In fact, there is an earlier interruption by Raman peaks in old-melted-ice samples.

Raman features are matrix-dependent and although the matrix of both samples is the same (ice melted water), the time between melting the ice and measurements apparently affected the matrix.

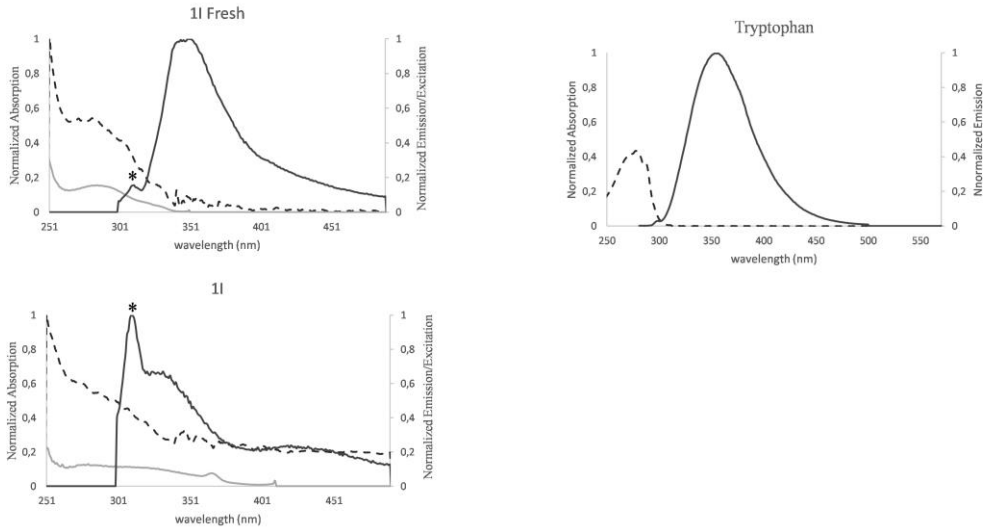

Figure IV.5 - Normalized absorption (dashed lines), excitation (solid grey line), and emission (solid black line) spectra of ice samples from site 1. Tryptophan spectra (solubilized in phosphate buffer, 0.1 M) added on the right, for comparison, source: PhotochemCAD™ (Du *et al.*, 1998; Dixon *et al.*, 2005). "Fresh" means measurements were taken right after melting (freshly-melted-ice). λ_{exc} = 280 nm * Asterisk denotes a peak resulting from solvent Raman scattering. Entrace and exit slits width: 5 nm.

A reason may be the fact that during ice formation some microbial cycles will freeze and some of the excreted molecules – as tryptophan may be - will be preserved.

Also, UV light is not an especially penetrative type of radiation form, and thus, not being particularly efficient in unmasking molecular content inside cells, especially the ones in less exposed microbial layers. Thus, an increase in tryptophan in fresh ice results may be linked with cell lysis and freedom of internal molecules, such as amino acids and proteins, to the exterior. In contrast, old-melted-ice was stored at 4ºC and the microorganisms that could resume their activity after ice-melting had a new opportunity of proliferating and recreating a new version of their ecosystem, now dominated by the survivors. This would result in the recycling of the excreted proteins and amino acids which would not be in the matrix but instead internalized in the cells and thus less available to interact with light – as spectroscopy techniques require.

Old-melted-ice showed a second distinct peak between 370-480 nm, the peaks C and M signatures. The freshly-melted-ice (1I Fresh) did not show such a definite peak,

which could either be a result of the absence of detectable organic matter or be a result of concentration bias, which we are not constraining. Future analysis with concentration gradients should be performed.

IV.4.5 Spectral characterization of samples from the transition between marine and terrestrial ecosystems

Freshly-melted-ice from site 4 **(Figure IV.6)** recorded a different absorption and emission pattern than freshly-melted-ice from site 1 **(Figure IV.5)**. In ice from site 4, there was still some marginal absorption signal at wavelengths higher than 400 nm while on freshly-melted-ice from site 1 almost no signal was visible after 400 nm.

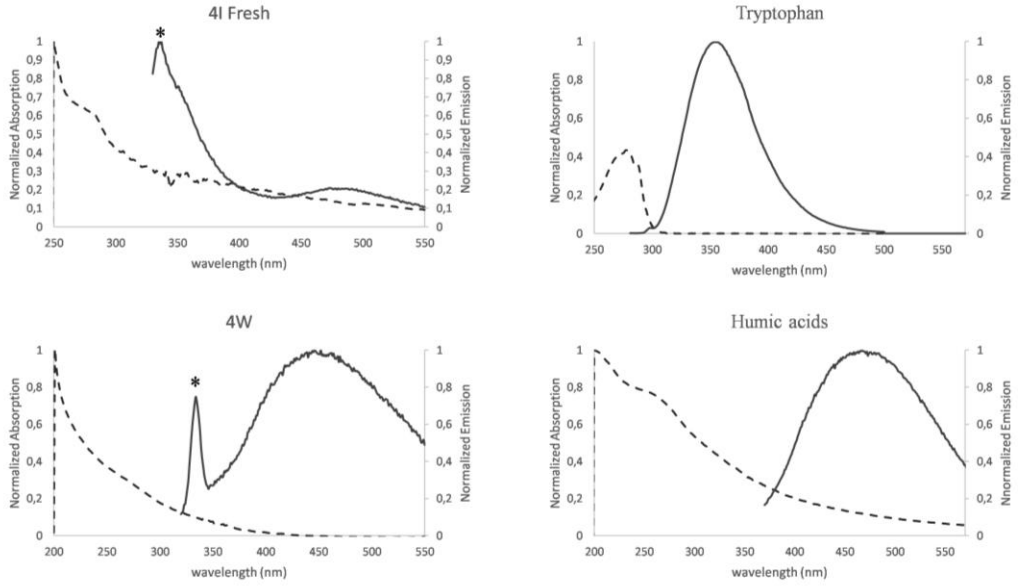

Figure IV.6 - Normalized absorption (dashed line) and emission (solid line) spectra of (upper left) freshly-melted-ice samples from site 4 (4I) located at the Great Whale River mouth, (down left) from the water underneath (4W), (upper right) tryptophan (solubilized in phosphate buffer, 0.1 M) from PhotochemCAD™ (Du *et al.*, 1998; Dixon *et al.*, 2005) and (down right) humic acids (partially solubilized in water). Fresh means measurements were taken right after melting. λ_{exc} = 300 nm for 4I, 4W and humic acids, and λ_{exc} = 280 nm for tryptophan. * Asterisk denotes a peak resulting from solvent Raman scattering. Entrace and exit slits width: 5 nm.

The spectra of 4I, similarly to old-melted-ice, also include what seems to be an interrupted tryptophan signature (the Raman feature also occurred when applied the optimal λ_{exc} = 280 nm – data not shown). Tryptophan, also known as autochthonous DOM

in aquatic systems, is thus present in ice from all sites (1, 3, and 4), which suggests that sun exposure, salinity, and proximity to the river inputs are not relevant factors to the conservation of this fluorescent amino acid in the ice cover of Hudson Bay.

A faint emission signature of what might be organic matter, with a possible overlay of ß-carotene or another carotenoid-like molecule was recorded on ice **(Figure IV.6)**. While the presence of carotenoids is demonstrated by the microbiology characterization in Chapter III, more specifically, the cultivation results (Coelho *et al.*, 2022b), spectroscopy results do not appear to be clear on their detection. This is similar to the failure of UV-Vis spectroscopy and fluorescence spectroscopy analysis in detecting chlorophylls that it is above reported, which may be attributed to degradation, the same could have happened to carotenoids, at least in water and old-melted-ice.

In the natural environment, biodegradation and photodegradation can happen simultaneously (Hansen *et al.*, 2016). Pigments are labile molecules, especially porphyrin-based pigments such as chlorophylls. Carotenoids can endure more photooxidative exposure than chlorophylls, not easily losing their ability to emit fluorescence – shifting instead the transmitted wavelength – changing colors visibly. In water and old-melted-ice, surviving microbes had a long time to adapt to the new ecosystem of the sampling bottle. While the temperature of 4ºC would not prevent the growth of some of the present groups, the lack of radiation in the storage room could attenuate their expression of biopigments, since their use is light-dependent, and these molecules are very expensive for a biological system to produce. In fact, the production of microbial carotenoids has been proved to follow positively the radiation incidence in cold waters (Roos *et al.*, 1998; Bonilla *et al.*, 2009 and references therein). Thus, it is plausible that freshly-melted-ice will have a more distinct carotenoid signature since the pigments were conserved until analysis - being the closest copy of the Hudson Bay's coast

natural cryosphere. The presence of the putative carotenoids signature in fresh-melted-ice from site 4 and apparent absence in fresh-melted-ice from site 1 could be related to the location with most snow cover *in-situ*, enabling some extra photopreservation before sampling, or it could be related to the closeness to the river. The question remains if the putative carotenoids thay appeart to be present are more autochthonous or allochthonous (e.g., from microorganisms or plants).

Water from site 4 however, likewise the other analyzed water samples, shows a very similar emission peak to the humic acids' emission signature, which englobes peaks C and M, although with a marginal shift to longer wavelengths of 30 nm likely due to the complexity of the environmental matrix.

It would be expected that Hudson Bay has more autochthonous DOM while the river plume has more allochthonous DOM (e.g., type C humic acids). Chapter III shows how the ice seems to be more related to the marine microbiome while the water underneath is dominated by microbial groups usually associated with freshwater environments (Coelho *et al.*, 2022b). The spectroscopy results agree with the previous microbiology results since the humic-like organic matter was present in all water samples regardless of proximity to the river, while water shows no definite tryptophan signature. This is likely due to how extensive the Great Whale River plume is when Hudson Bay is ice-covered (Ingram *et al.*, 1987).

IV.4.6 Applications to life-detection space missions to the icy moons

Tryptophan, and maybe phenylalanine and tyrosine, appear to be logical candidates for biosignatures to look for in the near subsurface ice of Europa and Enceladus, especially the ice surrounding the perched water bodies closer to the surface. However, future studies constraining fundamentally the link between tryptophan and photosynthesis

would be important for the definition of new biosignatures since tryptophan is more resilient than biopigments.

Humic molecules are a natural byproduct of Earth ecosystems, however usually associated with macroscopic forms of life. The putative life of Europa and Enceladus is more likely to be microscopic. The oceans from the icy moons are modeled to be global and to have contact with a hot seafloor with possible hydrothermal activity and geochemical reactions. Chapter I described how extensive the expected chemical flow generated between the rocky core and the seafloor of the icy moons is, including the leaching of the core materials into the interior ocean. Such a massive water body, if habited, could be the home of several different ecosystems (e.g., hotter closer to the seafloor and colder in transition with ice) enclosed in a unique subsurface where biomass recycling would be inevitable. And if Europan and Enceledan putative life is made of carbon, then substances like dark humic molecules could be the product of degradation of extra-terrestrial small water-based life-forms. Also, photoexposure can mask the DOM source signal by making algae-derived DOM resemble that of soil-derived DOM (Hansen *et al.*, 2016).

Pigments are one of the priorities biosignatures to search for when searching for life in the solar system (Baqué *et al.*, 2020) and beyond (Coelho *et al.*, 2022a, see Chapter V). In Europa and Enceladus, putative analogous molecules to biopigments could shield microorganisms in water bodies closer to the surface against radiation (Russell *et al.*, 2017; Nordheim *et al.*, 2018). In habitable exoplanets, extra-terrestrial pigments could cover whole planets. Thus, it is important to extend the present work to include experimental designs using UV-Vis spectroscopy and fluorescence spectroscopy at different time points to learn more about the pigments signatures in analogue environments to the icy worlds as well as their different degradation patterns. It is also

important to use different analytic methodologies such as High-performance liquid Chromatography (HPLC) which are widely used by scientists and thus have a robust data record available. It is important to complement studies such as these with microbiology analysis to link the signatures with the present microorganisms and better define which signatures are autochthonous and allochthonous. Finally, enriched suspensions with pigmented microbes isolated from planetary field analogues to icy worlds should be measured to build a catalogue of spectral signatures tailored to icy environments to search for life in icy exoplanets – which may have a great part of their surface landscape covered with biopigments-like molecules.

IV.5 Conclusions

The spectral characterization of the fDOM of Hudson Bay, a planetary field analogue to the water-ice interactions on Europa and Enceladus, supports future missions to these two locations with reference data, crucial for the design and preparation of the spectroscopic equipment on board, as well as for the interpretation of future results. Tryptophan, humic-like molecules, and likely carotenoids were detected, through UV-Vis spectroscopy and fluorescence spectroscopy, in ice and water samples from Hudson Bay. While water samples showed clear signatures of humic substances, ice revealed tryptophan features, agreeing with microbiology results present in the previous chapters. The feature of tryptophan was more distinctive in freshly-melted-ice as opposed to old-melted-ice. In contrast, the humic acids signature was less pronounced in freshly-melted-ice, likely a result of biodegradation from the cold-adapted bacteria that re-populated old-melted-ice samples in the cold temperatures of storage. Overall, our preliminary results suggest that humic acids, carotenoids, and tryptophan are spectral signatures more resilient over time to biodegradation, solar radiation, and ice melting, when compared to

chlorophylls. Future missions to the icy moons of our solar system should thus include spectroscopic equipment covering the UV to the visible spectrum. Finally, the next steps of planetary field analogue studies aiming for the preparation of future missions to the icy worlds should include *in-situ* spectral characterizations, degradation assays, and reference databases of these molecules.

V COLOR CATALOGUE OF LIFE IN ICE: SURFACE BIOSIGNATURES ON ICY WORLDS

Publication:

Coelho, L. F.; Madden, J.; Kaltenegger, L.; Zinder, S.; Philpot, W.; Esquível, M. G.; Costa, R.; Canário, J.; Vincent, W.F. & Martins, Z. (2022). "Color Catalogue of Life in Ice: Surface Biosignatures on Icy Worlds". *Astrobiology*, 22(3).

https://doi.org/10.1089/ast.2021.0008

V.1 Summary

With thousands of discovered planets orbiting other stars and new missions that will explore our solar system, the search for life in the universe has entered a new era. However, a reference database to enable our search for life on the surface of icy exoplanets and exomoons using records from Earth's icy biota is missing. Therefore, we developed a spectra catalogue of life in ice to facilitate the search for extra-terrestrial signs of life. We measured the reflection spectra of 80 microorganisms - with a wide range of pigments - isolated from ice and water. We show that carotenoid signatures are wide-ranged and indisputable signs of life. Our measurements allow identifying such surface life on icy extra-terrestrial environments in preparation for observations with the upcoming ground- and space-based telescopes. Dried samples reveal even higher reflectance, suggesting that signatures of surface biota could be more intense on exoplanets and -moons that are drier than Earth, or on environments like Titan where potential life forms may use a different solvent.

Our spectral library covers the visible to near-infrared and is available online. It provides a guide for the search for surface life on icy worlds based on biota from Earth's icy environments.

V.2 Introduction

More than 5000 planets orbiting other stars have been detected to date (exoplanets.nasa.gov, March 2022), with dozens of Earth-sized planets orbiting in the temperate zone of their stars (Kane *et al.*, 2016; Berger *et al.*, 2018) that would allow for liquid water on the surface of an Earth-like planet. Upcoming ground-based Extremely Large Telescopes (ELTs), as well as the recently launched James Webb Space Telescope, can search for signs of life on extrasolar planets (Ben-Ami *et al.*, 2018; Serindag *et al.*,

2019). However, the detection of a planet in the temperate zone does not guarantee its habitability (Kaltenegger, 2017). Detailed characterization requires observations of the planet's or moon's spectrum to assess its atmosphere and surface properties. In addition to atmospheric biosignatures pairs like O_2 and CH_4 or O_3 and CH_4 (Lederberg, 1965; Lovelock, 1965), several studies explored whether surface features could indicate life in the spectrum of an exoplanet (Seager *et al.*, 2005; Schwieterman *et al.*, 2015; O'Malley-James *et al.*, 2018, 2019). Future large space-based telescope designs such as the Large Ultraviolet Optical Infrared Surveyor (LUVOIR) (e.g. Kouveliotou *et al.*, 2014) and the Habitable Exoplanet Observatory (HabEx) (e.g., Mennesson *et al.*, 2016) are being formulated to explore biosignatures in the atmosphere and on the surface of exoplanets.

Biological pigments dominate many diverse landscapes on Earth and are present in a wide range of organisms (Hegde *et al.*, 2013, 2015; Schwieterman *et al.*, 2015). Pigments of microbes present in green algae blooms, pink "watermelon" snow, red saltern crystallizer ponds, and heterogeneous microbial mats are signs of life on Earth's surface that can be detected from orbiting satellites (Oren *et al.*, 2001; Lutz *et al.*, 2016; Williamson *et al.*, 2020) as well as space-missions like the Galileo Probe (Sagan *et al.*, 1993). Biological pigments on the surface of the Earth could have indicated life for up to 2 billion years (O'Malley-James *et al.*, 2018, 2019). Pigmented organisms have unique reflectance signatures to search for on exoplanets orbiting other stars (Hegde *et al.*, 2015; Kaltenegger, 2017; Fujii *et al.*, 2018). A previous color catalogue of life by some of the authors of this study (Hedge *et al.* published in 2015) established a database of reflectivity spectra for a diverse set of 137 biota from different environments as it would be seen on an exoplanet (Hegde *et al.*, 2015). However, the database did not include any biota from frozen environments.

A great abundance of pigmented microbes found in the highly diverse ice microbial community (Vincent *et al.*, 1993a; Vincent *et al.*, 2004) - isolated from the Arctic and Antarctic, which include locations that are icy planetary field analogues (Martins *et al.*, 2017) - suggests that icy worlds orbiting other stars as well as icy moons in low radiation environments in the solar system may provide promising targets for the search for life. Life may have even started on Earth in ice - the so-called "cold origin of life" hypothesis (Price, 2007).

Ice is widely considered an extreme habitat for life. Besides extreme dryness and low temperatures, radiation can be excessive in this environment. Ice acts as a selective agent against organisms that are not efficient in photooxidative protection (Lemoine *et al.*, 2010). Hence, pigmented organisms have been reported to be dominant in the microbiota of icy environments (Cottrell *et al.*, 2009; Marizcurrena *et al.*, 2019).

Most of these pigments have a role in photosynthesis (e.g. chlorophylls and carotenoids). Photosynthetic pigments absorb and channel part of the incoming light as usable energy for organisms. Photosynthesis turns inorganic carbon into biomass using light as the energy source and molecules such as e.g. H_2, H_2S, Fe^{2+}, or H_2O, as electron donors. Photosynthetic pigments become oxidized while capturing light photons, and redirect their energy (Bassham *et al.*, 1960; Cohen *et al.*, 1986).

While chlorophylls are virtually universal among oxygenic photoautotrophs (Lubitz *et al.*, 2019), carotenoids are widespread among the three domains of life, including non-photosynthetic organisms (e.g. heterotrophs) (Yabuzaki, 2017). Due to their hydrophobic nature, they are immersed in biological membranes, playing a role in the modulation of membrane fluidity to survive under low temperature conditions (Seel *et al.*, 2020). Carotenoids also behave as light-absorbing chromophores playing important roles in photooxidative protection (Mathews *et al.*, 1959). Radiation is deleterious to

biomolecules, such as DNA and proteins, and creates reactive oxygen species (ROS) which are major oxidative stress agents. Carotenoids quench photosensitizers and singlet oxygen consequently becoming oxidized and dissipating excess energy and oxidative power, protecting other sensitive molecules. Their color depends on chemical modifications of the original molecule determined by the number of conjugated double bonds within the hydrocarbon backbone (Armstrong, 1997). As a result of oxidation upon radiation stress, carotenoids change the color of organisms turning them yellow, orange, pink, or ultimately red (Latowski *et al.*, 2011). Thus, the presence of carotenoids in icy biota is a strategy of adaptation to the extremely cold temperatures and high radiation - analogues to conditions of extra-terrestrial icy environments (Dieser *et al.*, 2010).

A reference database of biota in icy environments on Earth is a critical tool to enable our search for life on the surface of icy exoplanets and -moons. Thus, we created such a reference catalogue for life in ice by measuring the reflection spectra of 80 colorful microorganisms, isolated from ice and water below the ice, collected in the Canadian subarctic, to identify potential signs of life on icy worlds.

The ice and water come from the mildly briny Hudson Bay and the Great Whale River (freshwater) that floods into the bay. The isolated microorganisms used in this study were previously identified and include 77 bacteria, 1 yeast (all heterotrophs), and 2 algae (photosynthetic). Our database provides a crucial tool to detect and identify potential signatures of life on icy planets and moons orbiting other stars.

V.3 Materials and Methods

We collected the 80 microorganisms from ice and water at Kuujjuarapik, Canadian subarctic, in collaboration with Université Laval during the winter of 2019. The microorganisms belong to the Culture Collection of psychrotolerant and psychrophilic

subarctic strains of the University of Lisbon, Portugal (78 isolates from Instituto Superior Técnico and 2 isolates from Instituto Superior de Agronomia). From the 80 microorganisms, 66 were isolated from the Hudson Bay (salinity approx. 1%) and 14 from the Great Whale River (freshwater). No particular pigment was dominating the landscape on those sampling days, allowing for less challenging cultivation of a more diverse group of pigmented microorganisms afterward. They arrived at Zinder lab on solid media and were stored at 4ºC before transfer and growth. All hemispherical reflectance measurements were performed at Philpot's lab at the School for Civil and Environmental Engineering at Cornell University. Both labs are part of the interdisciplinary Carl Sagan Institute at Cornell.

V.3.1 Sample preparation

We grew bacteria and fungi in Reasoner's 2A broth (R2A) and microalgae in Tris-Acetate-Phosphate (TAP) liquid media at 18-20ºC. The heterotrophic cultures were grown aerobically up to a stationary phase, except for phototrophic cultures which were grown under 16-hours light/8-hours dark cycles, using white light. All cultures were grown at room temperature. Depending on the isolate, the time required for growth varied from about 24 hours to 1 week. All procedures during the culturing process occurred under sterile conditions. Pure sample cultures were transferred to 50 mL Falcon centrifuge tubes until filtration.

V.3.2 Spectrometer system

We used an ASD FieldSpec 4 Spectrometer, which covered the wavelength range from 350-2500 nm at intervals of 1 nm, and an ASD integrating sphere to measure the reflectance of our samples, as described in Hegde *et al*. (Hegde *et al.*, 2015). Bidirectional reflectance measurements at a single viewing angle often result in a poor approximation

of the albedo, especially if, for given biomass, the sample has a high bidirectional reflectance distribution function (BRDF) anisotropy (Kriebel, 1978; Hegde *et al.*, 2015). For exoplanets, remote observations will be disk-integrated, and hence disk-integrated reflectance measurements that use hemispherical geometry are needed for more realistic surface albedo modeling of Earth-like exoplanets.

V.3.3 Sample measurements

We deposited cultures on a 25 mm plain white mixed cellulose ester filter (0.45 μm) using a 10 mL syringe and a filtration system as described previously (Hegde *et al.*, 2015). Cells were homogeneously layered when deposited onto the filter substrate (Hegde *et al.*, 2015), and the saturation limit was reached at about 20 mL of cell suspension for most cultures. The sample was then used to acquire high-resolution hemispherical reflectance measurements using the spectrometer system described before. The same sample was measured at 2 different times: immediately after being deposited on the filter (fresh) and after 1 week (dry). Translucent cultures were measured as biological control. Unused filters, filters with only culture media, and filters with only water were measured as experimental controls.

V.3.4 Microscopy

The micrographs were obtained by analyzing 2 μL of fresh cell suspension of each sample fixed on agar slides through a Nikon Eclipse E600 microscope. Micrographs of cells were taken under a bright field with phase-contrast (PH) microscopy at 400× magnification for all samples and 1000x (using immersion oil) for all bacteria.

V.4 Results

The 80 pigmented microorganisms were previously isolated from ice and water below the ice, collected the Canadian subarctic, and identified using rRNA gene-based taxonomic affiliation: 77 isolates are bacteria belonging to the phyla *Proteobacteria*, *Actinobacteria*, *Firmicutes,* and *Bacteroidetes*. Three are eukaryotes: fungi from the division *Basidiomycota* and microalgae from the phylum *Chlorophyta*.

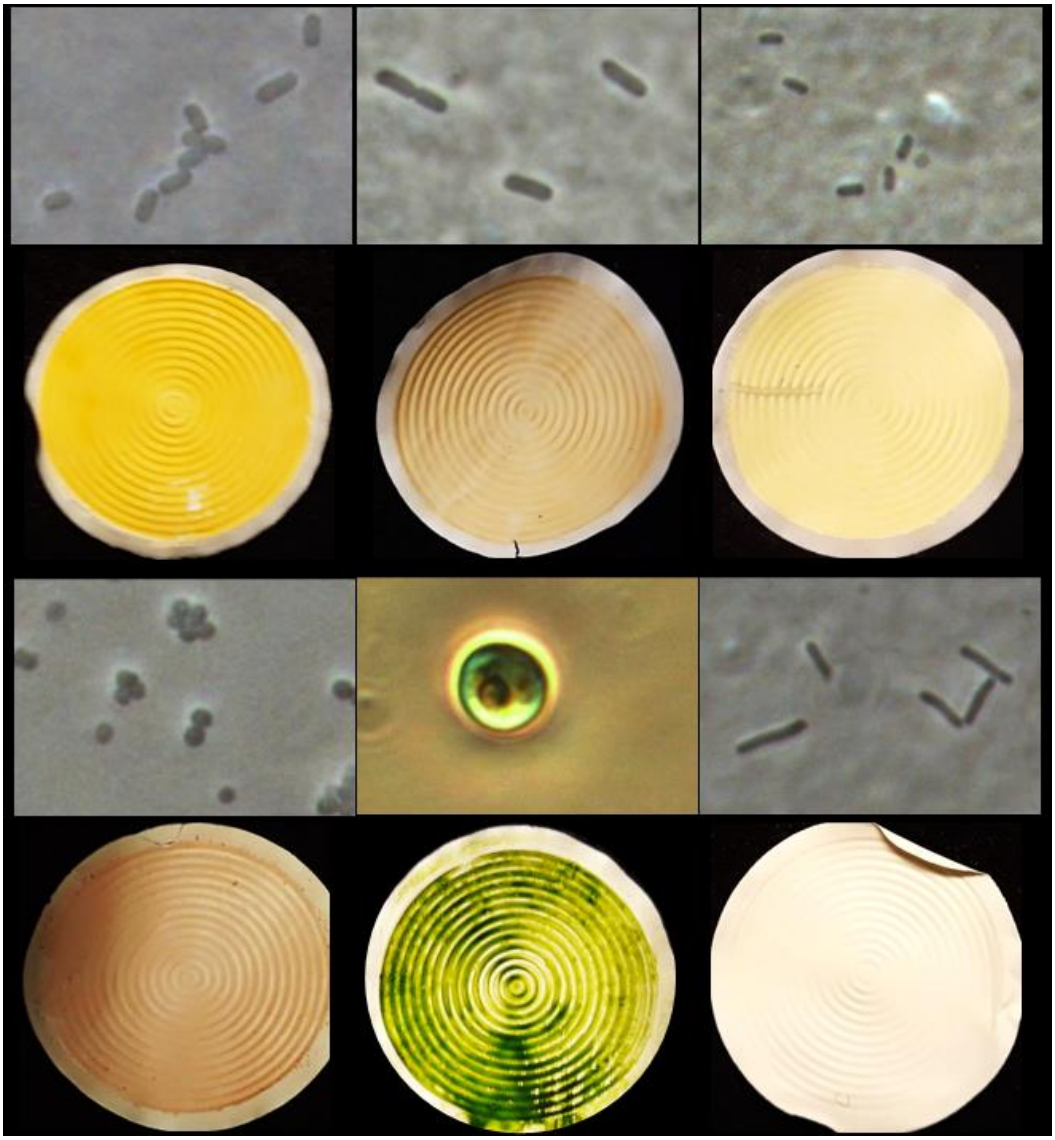

Figure V.1 - Six samples of psychrotolerant microorganisms of the 80 diverse microorganisms collected from Arctic ice cores: isolates from (top left to right) *Sphingomonas* sp. (bright and dark orange), *Microbacterium* sp. (yellow), (bottom left to right) *Arthrobacter* sp. (pink), *Chlorophyta* algae (green) and *Bacillus* sp.(white). From Coelho *et al*., 2022, in *Astrobiology*.

Figure V.1 shows an example of the diversity in color among six samples from the 80 isolates: *Sphingomonas* sp. (bright and dark orange), *Microbacterium* sp. (yellow), *Arthrobacter* sp. (pink), *Chlorophyta* algae (green), and *Bacillus* sp. (white), along with their photomicrographs.

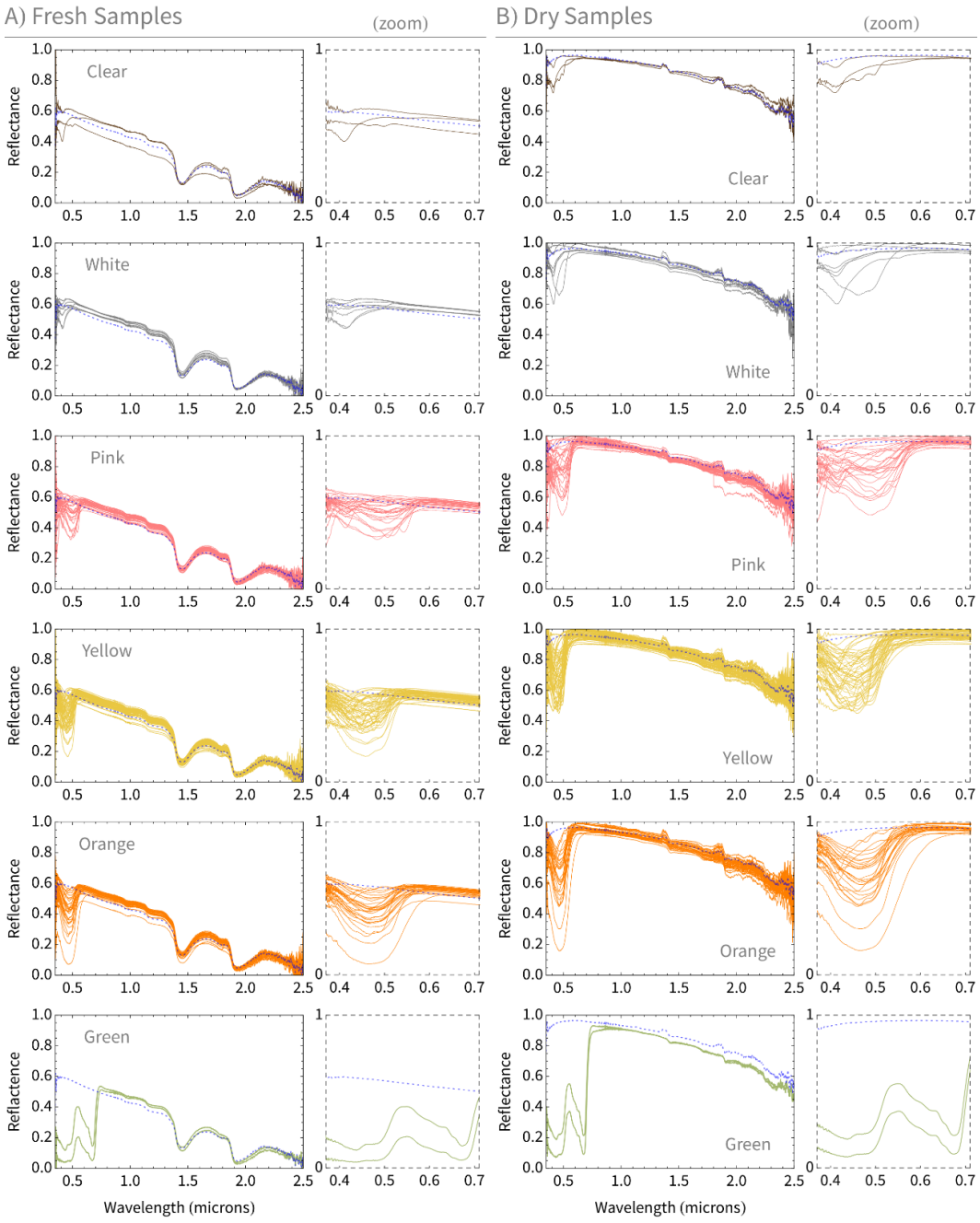

Figure V.2 - Spectra of all 80 samples grouped by color: orange (N=20), pink (N=15), yellow (N=33), white (N=8), green (N=2), and clear (translucent) (N=2). N denotes the number of samples per color. Column 2A shows fresh organisms and 2B dry organisms. Dry samples provide a stronger reflection. The colors of pigments show the strongest reflection between 0.35–1 µm, water absorption at 1.5 and 2 µm. Columns "(zoom)" represent a version of the figures on the left on the wavelength range of 0.35-0.7 µm. The blue dotted line represents the control (the reflection of the culture medium only). From Coelho *et al*., 2022, in *Astrobiology*.

Figure V.2 shows the diversity in color signatures of pigmented biota isolated from an icy environment on Earth: we group different organisms by their colors - yellow, orange, pink, green, or white. Unpigmented translucent organisms (clear) act as a biological control for uncolored pigments/unpigmented biota in our measurements. The colors of the pigments have the strongest influence on the reflectance spectra in the wavelength range between 0.35–0.7 μm (see the "zoom" panels in **Figure V.2**). The blue dotted line in each graph shows the experimental control spectra i.e. a filter containing only culture media. Fresh samples are shown in **Figure V.2A** and dry samples in **Figure V.2B**. The reflection spectra of the collected biota changed with water content: **Figure V.2** (left) shows the reflection spectra shortly after depositing the fresh organisms on the filter representing a hydrated sample (fresh). **Figure V.2** shows the dry reflection spectra after one week of deposition of the organisms on the filter (dry). Fresh samples showed a weaker reflection than dry samples. Indeed, strong water absorption features can be seen around 1.5 and 2.0 μm in the fresh sample reflection spectra in **Figure V.2**. Fresh samples correspond to life on a planet like the Earth, with available liquid water. Dry samples provided a stronger reflection of the pigment for all samples, because the water, which reduces the reflectance, had been evaporated. The red edge peaks at a slightly higher wavelength for some dry samples than it does for fresh ones: For carotenoids, this agrees with a known strategy to endure oxidation (Vítek *et al.*, 2017). Translucent samples (clear) showed a similar reflection spectrum to the experimental control (only culture media) for both fresh and dry samples.

Related organisms (same taxa) can have very different colors and thus different corresponding reflection spectra (see **Figure V.2**). Moreover, yellow, orange, and red carotenoids are produced by a wide range of organisms: photosynthetic and non-photosynthetic bacteria as well as eukaryotes such as algae, fungi, and plants (Armstrong,

1997). Although specific colors can be abundant in specific phyla, they are not exclusive of any phylum or genus as discussed below (see **Figure V.3**).

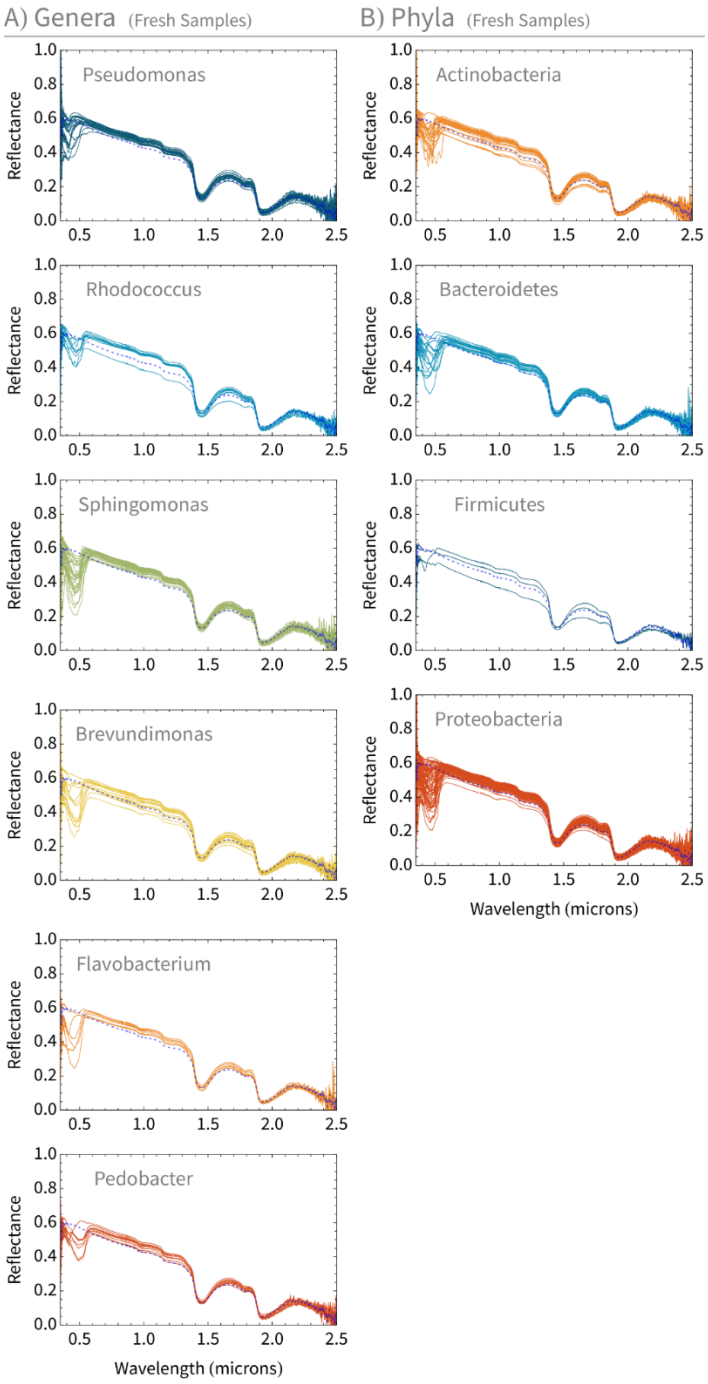

Figure V.3 - Spectra of non-photosynthetic samples separated by genus (3A) and phylum (3B). Colors do not relate to any specific taxon. Blue dotted line represents the control (reflection of the culture medium only). From Coelho *et al*., 2022, in *Astrobiology*.

The collection of ice microorganisms shows neither color relation between heterotrophic (non-photosynthetic) organisms from the same phylum nor a relation

between their genus and specific color signatures. For example, *Brevundimonas* and *Sphingomonas*, both *Alphaproteobacteria*, have very different spectra. *Pedobacter* and *Rhodococcus*, from the *Bacteroidetes* and *Actinobacteria* respectively, are more uniform, likely because of the few representative isolates of these genera in our database **Figure V.3**. Almost all these genera share the same colors. These are expected results from colors given by the presence of carotenoids. These traits are not produced as primary metabolites and may even be passed through lateral transfer events between unrelated organisms as will be discussed later. The spectral features of carotenoid pigments are broad indisputable signs of life, but they cannot be associated with a specific organism.

V.5 Discussion

V.5.1 Carotenoids as potential biosignatures in icy extra-terrestrial environments

We find no relation between the phylum of the tested heterotrophic organisms and their color signature as shown in **Figure V.3** (see also discussion in Hegde *et al.*, 2015). Carotenoids are widespread pigments among the three domains of life, and their color is highly dependent on interactions with the ecosystem. It has been suggested that the evolutionary path of microbial carotenoids appears to be more web-like instead of tree-like due to the occurrence of extensive lateral gene transfer, gene loss, and gene duplication events (Klassen, 2010). Lateral gene transfer can occur between individuals of different taxa, which means that the gene - or gene cluster underlying pigment biosynthesis - will not exclusively be passed through its hereditary line (vertically) but will instead be lineage-unspecific and feature in unrelated places of the evolutionary tree (being more relatable with a web). Carotenoids are signatures of life not limited to a small taxonomic group of organisms or specific populations of both photosynthetic and non-photosynthetic groups.

These molecules cover different physiological roles in the overall adaptation of all types of cells to conditions found in extremely cold environments, such as low temperature, radiation, photooxidation, lack of resources, and dryness. The functions of carotenoids include energy dissipation, antimicrobial activities, and regulation of membrane fluidity (Lemoine *et al.*, 2010; Seel *et al.*, 2020). These physiological functions would be useful for life beyond Earth as well. Carotenoids dominate some of Earth's landscapes like salty red lakes. Pink and red carotenoids present in lakes and snow have been detected by astronauts on the International Space Station (ISS) (https://eol.jsc.nasa.gov/), spectrometers flying at high altitudes, such as Airborne Visible InfraRed Imaging Spectrometer (AVIRIS) (Painter *et al.*, 2001; Serrano *et al.*, 2002; Dalton *et al.*, 2009), and NASA Airborne Snow Observatory (ASO) (Carey *et al.*, 2018).

Future large space-based telescopes designs like HabEx (e.g. Mennesson *et al*., 2016) and LUVOIR (e.g. Kouveliotou *et al*., 2014) could search for blooms of microbial pigments on exoplanets to detect carotenoids.

V.5.2 Dry samples reflect stronger: Implications for searching for life

Dried samples show more intense colors and a higher reflectance overall than fresh samples in our studies, indicating that water absorption reduces the reflectivity of pigments. In our study, fresh samples **(Figure V.2)** have higher water content than dry samples, which are dried for one week, **(Figure V.2)**; Water evaporates while the pigments remain on the filter. The water absorption features also decrease for dry samples, shown in **Figure V.2** at about 1.5, and 2.0 μm with a slight dependence on the specific pigment (Dalton *et al.*, 2003; Hegde *et al.*, 2015; Ball, 2017). A recent study using Raman spectroscopy on carotenoids also shows higher pigment signal intensities on dried cells (Baqué *et al.*, 2020), consistent with our results. This increase in reflectance of dried cells is likely due to the change in the relative index of refraction at the water-

cell interface as the cell dries. The relative index of refraction at the water-cell interface is relatively small and would tend to enhance the absorption into the cell. When the water evaporates, the higher relative index of refraction would lead to increased reflectance at the surface (and less absorption). A similar phenomenon has been described for sand particles as the water evaporated (Tian *et al.*, 2018). This is the reason why a geologist will wet the surface of a rock to better see the mineral colors. With water on the surface more light penetrates, is partially absorbed, and the light reflected from the interior (still at the surface) is richer in color (Lekner *et al.*, 1988).

The type of pigment determines the chemical relationship with water; for example, carotenoids are hydrophobic and chlorophylls are partially hydrophobic. Thus, the influence of water on the reflectivity of the pigment depends on the type of cell, organism, and pigment. Fresh samples are representative of life on Earth, where liquid water is readily available for most biota. However, our results show that dry samples would make the detection of pigment-biosignatures easier. Icy worlds would provide such dry environments.

The samples used in this study are not expected to have an abundance of liquid water available in their natural environment in the Arctic. This is expected to help the organisms adapt to the high photooxidative stress they are subjected to being in ice. Thus, dry microbial cells tend to be more resilient to high radiation environments, making them interesting targets to search for in dryer and highly irradiated planets (Billi *et al.*, 2019). The closest potentially habitable worlds outside our solar system orbit a different kind of star than our Sun, smaller red dwarf stars. Such stars can flare frequently, bombarding their planets with biologically damaging high-energy UV radiation, placing planetary atmospheres at risk of erosion and bringing the habitability of these worlds into question (e.g. discussion in Scalo *et al*., 2007; Tarter *et al*., 2007; Segura *et al*., 2010; Shields *et*

al., 2016; Kaltenegger, 2017; A. *et al.*, 2019). However, the surface UV flux of these worlds is unknown. Models of the surface UV environment for the four closest potentially habitable exoplanets: *Proxima-b, TRAPPIST-1e, Ross-128b,* and *LHS-1140b* assuming different atmospheric compositions, from Earth-analogue to eroded and anoxic atmospheres, show that surface UV radiation remains below early Earth levels, even during flares (O'Malley-James *et al.*, 2019). But even high UV radiation on the surface of rocky exoplanets circling active M stars may not limit extra-terrestrial life evolution if carotenoid-like pigments are developed for photooxidative protection.

In addition, while liquid water is widely considered the "matrix of life" (Ball, 2017), discussions on other solvents such as methane are becoming more pertinent, informing ideas on the evolution of alternative non-water-based "weird life" (Stevenson *et al.*, 2015). We speculate that on other planets biota could use similar pigments to the ones used on Earth, independent of the solvent. For dry planets and planets with solvents other than water, biopigments could provide stronger signatures than on worlds with abundant water, like Earth.

V.5.3 Our solar system and the search for life

The search for life in our solar system focuses on a dry planet - Mars - as well as three cold moons - Titan, Enceladus, and Europa: can the color catalogue for biota in ice also be used for the search for life closer to home?

The idea that the building blocks of life (dos Santos *et al.*, 2016; Laurent *et al.*, 2019) or even dried cells may be preserved (Bryce *et al.*, 2015; Baqué *et al.*, 2016) can be expanded to currently dry planets like Mars (Baqué *et al.*, 2020). For example, one of our samples - *Bacillus safensis* – has also been isolated from the spacecraft Mars Odyssey Orbiter (Satomi *et al.*, 2006) and could have survived the extreme radiation environment in space. The same bacterium has also been described in a study as growing better on the

ISS than on Earth (Coil *et al.*, 2016). This type of bacterium forms spores, which are inactive dried latent cell forms with increased resistance to almost any type of stress. Thus, the dry samples of our color catalogue of life in ice can provide insights into what spectral features missions to Mars could look for.

Earth is the only known place with surface blooms of microbial pigments. A key issue when considering the search for biological pigments in our solar system is the radiation environment. All biological pigments presented in this article are found in icy environments on Earth, which are sheltered by Earth's atmosphere and magnetic field. Biological pigments disintegrate rapidly in high radiation environments. For example, UVA radiation causes a significant drop in productivity of ice algae communities (McMinn *et al.*, 1999). Thus, finding biological pigments on the surface of cold moons without an atmosphere, especially in strong radiation environments like Europa is unlikely. Nevertheless, searching for building blocks of life (Martins *et al.*, 2013; d'Ischia *et al.*, 2021) and signatures of traces of biological pigments on the icy near-subsurface (Nordheim *et al.*, 2018) and in ice particles in jets of geysers could provide an alternative way to search for life on icy moons. The high success of Earth-orbiting spectrometers on detecting microbial pigments (Painter *et al.*, 2001; Serrano *et al.*, 2002; Dalton *et al.*, 2009; Carey *et al.*, 2018) serves as inspiration for high-resolution imaging spectrometers exploring the icy moons in the solar system, such as Mapping Imaging Spectrometer for Europa (MISE) that will fly on the NASA Europa Clipper in late 2024 to explore the potential signatures of extremophiles implanted in the ice surface (Carey *et al.*, 2018), as well as Europa Lander Stereo Spectral Imaging Experiment (ELSSIE) (Murchie *et al.*, 2020). Antarctic microbes forming complex communities have also been successfully identified from their carotenoid-like pigmentation by low-altitude unmanned aerial

vehicles carrying spectrometers on Earth (Levy *et al.*, 2020), which are a similar concept to future small missions such as Titan's Dragonfly.

V.6 Conclusions

The unequivocal proof of the existence of extra-terrestrial life is one of the most thought-provoking events humanity could experience. To enable the search for life on the surface of icy exoplanets and -moons we developed the first catalogue of microbial life in ice. We measured the reflection for a diverse range of pigmented microorganisms isolated from the subarctic - an analogue for those extra-terrestrial environments. Similar biota could become the dominant life form on icy worlds orbiting other stars. Life might have even originated in such icy environments.

Here, we present the first database of surface reflection for biota from icy environments to provide a tool for upcoming space- and ground-based telescopes that will search for life in the cosmos. While our color catalogue of life in ice has been developed as a guide to search for life on icy planets and moons orbiting other stars, it also holds the key to expanding the search for life in the solar system.

For the first time in human history, we have the tools to search for life in the universe. Icy environments on Earth show a surprisingly wide diversity of life and might have even provided the environment for life to originate. The color catalogue of life on Earth's subarctic will serve as the guide to search for surface life on icy worlds to find out whether we are alone in the cosmos.

VI GENERAL DISCUSSION AND FUTURE PERSPECTIVES

VI.1 General discussion

One of the conclusions of the present thesis is that an integrative approach to astrobiology studies in samples from planetary field analogues can produce relevant data for different space-related fields. Connecting chemistry, physics, and biology to the same samples allows for a holistic perspective on the connection between analogues and extra-terrestrial environments.

First, as shown in chapter II, the use of standardized methodology to process analogue ice and water samples to icy moons' environments is significant to future studies on similar polar locations, for both astrobiology and ecology. The contaminations found were also relevant to planetary protection studies. There are two main concerns about landing missions to Europa and Enceladus. First, the terrestrial biological contamination (forward contamination) may create reasonable doubt against proof of extra-terrestrial life, invalidating valuable results from expensive missions that take decades to prepare and creating unnecessary restrictions for future missions (Raulin *et al.*, 2010; Chan *et al.*, 2020; Martins *et al.*, 2020). Second, and even direr, is that the pristine environment of these habitable moons is irreversibly changed with the introduction of Earth's biota (Raulin *et al.*, 2010; McCoy *et al.*, 2021). On polar planetary field analogues, we can sample diverse model habitats yet more analysis to define standardized sampling, processing, and decontamination protocols specific for the planets and/or satellites in study are needed.

Second, planetary field analogues provide us with complex environmental samples with diverse and adapted microbial communities which facilitate a close observation of real biotic-biotic and biotic-abiotic relationships under extreme conditions, as shown in chapter III.

Third, the integrative study of ice and water samples from planetary field analogues allows the connection between chemical characterization and biology (chapters III, IV, and V) – an essential relationship to determine and catalogue biosignatures. In the last decades, information regarding the chemistry of the icy moons (those in the outer reaches of the solar system) has been collected and our understanding furthered due to modern telescopes and the success of space missions such as Voyager, Galileo, and Cassini-Huygens. Some work has been done on connecting the atmospheric, surface, and interior chemistry of the icy moons to predict which geochemistry processes could be responsible for the origin of organic molecules tentatively detected to date. Future missions to the icy moons, such as JUICE from ESA and Europa Clipper and Europa Lander from NASA, will be focused on solving their geochemical mysteries and searching for biosignatures. Observation missions from future space-based large telescopes such as LUVOIR and HabEx will be searching for habitability signatures and will have the capacity to detect sharp and characteristic biosignatures such as biological pigments. All these missions need comprehensive reference catalogues to be used as tools so that humanity does not miss signs of life. In this work, we were able to characterize fluorescent biosignatures from a planetary field analogue of icy worlds through absorption, emission, and reflectance spectroscopy. Spectral data unraveled ecological trends and the presence of humic-like molecules, tryptophan, and likely carotenoids in ice and water samples from Hudson Bay. Afterward, the spectral signatures from pigmented microorganisms isolated from Hudson Bay's ice and water were measured, registered, and interpreted to produce the first-ever catalogue of colorful signatures linked to life on ice, and more catalogues such as this will hopefully follow.

VI.2 Future perspectives

Due to the multidisciplinary character of this thesis, each chapter has different future perspectives and the data produced so far justifies this branching in future studies.

VI.2.1 Further investigation following chapter II

Further improvement of fieldwork practices in polar environments is necessary for the success of work on planetary field analogues to the icy moons. These locations serve as a testbed for future search-for-life space missions and thus it is necessary to incorporate, as well as possible, in analogue studies the constraints of sampling on extra-terrestrial environments and the measures that will be necessary to avoid contamination. Furthermore, the next studies on clean processing practices for ice samples will need to integrate functional genomics and new technology such as lab-on-a-chip approaches.

Cleanrooms in research facilities, industry, and space agencies are full of extremophiles, which resist the robust sterilization techniques applied to achieve "microbial-free" environments (Regberg *et al.*, 2018). The biological mechanisms of resistance include, among others, the production and action of biopigments, which reinforce the importance of their study (Cox *et al.*, 2005; Methé *et al.*, 2005; Dieser *et al.*, 2010; Seel *et al.*, 2020). Strains like these could contaminate the space vehicles assigned to missions to the icy moons. As observed in this study, and in agreement with previous concepts (Lazarevic *et al.*, 2016), contaminations can be high in microbial load, maybe even forming biofilms. A considerable abundant load of extremophiles in space vehicles may be enough for at least one viable organism to be able to land on these satellites which would represent forward-contamination by NPR definitions. Thus, the creation of a contaminants database by the astrobiology community working with ice field analogues and cleanroom curations (from space stations and industry) would allow for more

accurate planetary protection protocols in time for lander life-detection missions in habitable extra-terrestrial environments.

VI.2.2 Further investigation following chapter III

The unraveling of Hudson Bay microbial ecology boomed in the last few years, after decades of hiatus - with the published study of chapter III representing the first identification of the prokaryotic community native to its ice shell. Future seasonal studies describing the microbial function through transcriptomics, including also microeukaryotes, are important to corroborate some of our findings. It is also important that future studies in the Arctic with space applications are extended to other analogue samples. Other Arctic habitats (e.g., recent, or ancient land ice, glacier ice at high depths) also have astrobiology interest depending on the sub-type of the extra-terrestrial environment intended to mimic or the aim of the study. For instance, studying ancient ice could be of interest to the "origin of life" field of study since it holds clues about the microbiome of earlier periods preserved in deep layers of ice, while land ice and methane-rich lakes could be relevant for Titan.

VI.2.3 Further investigation following chapter IV

One of the outputs of this thesis was the understanding of how challenging it is to characterize fluorescent organic signatures in icy environments. It is difficult to measure these biosignatures because their low concentration in icy environments coupled with their complexity is a test to fieldwork spectrographs while their labile nature condemns any attempt for an accurate measurement after transportation back to the laboratory. Thus, portable spectroscopic equipment with increased sensitivity should be introduced massively to the study of icy planetary field analogues, as well as rigorous studies on fluorescent biosignatures' degradation. Adding, tests with different concentrations and using artificial matrixes as blank should be attempted. Likewise, comparison with

measurements on the same samples from other established techniques, with years of data recording, such as HPLC, followed by microbiology analysis, would be groundbreaking in linking decades of biology and chemistry knowledge in the quest for space exploration.

VI.2.4 Further investigation following chapter V

Chapter V is an example of a ready-to-use tool for observation missions searching for biosignatures in exoplanets – and was a direct product of astrobiology studies in planetary field analogues. Catalogues of biosignatures designating biomes – habited ecosystems – of Earth instead of specific organisms are paramount so humanity does not miss on priceless, bright, and colorful signals of extra-terrestrial life in the next decades. Similar catalogues should be built using different selections of organisms that characterize other biomes that are analogue to extra-terrestrial environments – and that are still missing.

VI.2.5 General remarks on the future perspectives for the exploration of icy worlds

The essence and prevalence of the phenomenon of life remain largely unconstrained, continuing to be a challenge to future astrobiology work. According to extant models of habitability, the solar system itself includes many possible living habitats. The field of astrobiology can benefit from improvements in present habitability models and further modeling of the conditions on the described planetary bodies. The latter modulatory effort is largely informed by *in-situ* studies. Thus, space missions are the only approach to ultimately produce unchallenged proof of active or past life beyond Earth.

Although Mars has had many such exploratory missions, icy moons are terrains yet to be charted. JUICE and Europa's Clipper will be launched in the upcoming years but also mission concepts for the search-for-life on icy moons, such as Enceladus Orbilander Mission from NASA and future missions within the Voyage 2050 program from ESA are

on the horizon (Favata *et al.*, 2021; NASA, 2022). Enceladus Orbilander Mission aims to analyze the ice and water of Enceladus to search for biosignatures or even life forms (MacKenzie *et al.*, 2021).

However, future perspectives are not limited to these already extensively mentioned missions. The answers may lay elsewhere and so an extension of the focus to other planetary bodies is also crucial. Triton is the largest satellite of Neptune and, so far, it is one of the few icy moons (other includes, e.g., Enceladus) with clear-cut evidence for recent volcanism on the surface (Lunine, 1990). Voyager 2 images showed dark materials coming from its surface vents. Thus, there is increasing interest in Triton, which was already a compelling astrobiology target due to the possibility of an internal ocean given its internal heat, and observations of recent surface activity. Indeed, it has been suggested that Triton's interior ocean may have organic molecules very similar to Earth's early hydrothermal systems (Shock *et al.*, 1993). Since we have clear proof of active plumes on both Enceladus and Triton, less expensive fly-by missions, with less contamination risk and as well as less conundrum regarding ice-drilling would be a reasonable investment to sample the materials coming directly from the subsurface. Hopefully, studies like the present work inspire funding and research efforts towards the exploration of the icy moons of Jupiter or Saturn, but also of transneptunian bodies such as Triton or even Pluto.

Ultimately, the discovery of extra-terrestrial life would be one of the most remarkable marks of humankind's legacy. The quest to resolve the uncertainty humans have regarding the uniqueness of biological life in the universe should unite scientific efforts.

VII PUBLICATIONS AND COMMUNICATIONS

VII.1 Scientific publications

VII.1.1 Peer-reviewed publications

VII.1.1.1 Published:

Coelho, L. F.; Madden, J.; Kaltenegger, L.; Zinder, S.; Philpot, W.; Esquível, M. G.; Costa, R.; Canário, J.; Vincent, W.F. & Martins, Z. (2022). "Color Catalogue of Life in Ice: Surface Biosignatures on Icy Worlds". *Astrobiology*, 22(3). https://doi.org/10.1089/ast.2021.0008 (Selected for the journal's Cover).

Coelho, L. F.; Couceiro, J. F.; Keller-Costa, T.; Valente, S. M.; Ramalho, T. P.; Carneiro, J.; Comte, J.; Blais, M.A.; Vincent, W.F.; Martins, Z.; Canário, J. & Costa, R. (2022). "Structural shifts in sea ice prokaryotic communities across a salinity gradient in the subarctic". *Science of The Total Environment*, 827, 154286. https://doi.org/10.1016/j.scitotenv.2022.154286

VII.1.1.2 Submitted:

Coelho, L.F.; Blais, MA.; Matveev, A.; Keller-Costa, T.; Vincent, W.F.; Costa, R.; Martins Z.; Canário, J. (2022). "Contamination analysis of Arctic ice samples as planetary field analogues and implications for future life-detection missions to Europa and Enceladus". *Scientific Reports*, submitted.

VII.1.2 Book Chapters

VII.1.2.1 Published:

Coelho, L.F. & Martins, Z. (2021). "The Geochemistry of Icy Moons". In *Encyclopedia of Geology*, 2nd Edition, Elsevier, pp 207-216. https://doi.org/10.1016/B978-0-08-102908-4.00123-5

VII.1.2.2 Submitted:

Coelho, L.F.; Miranda, C.; Gonçalves, D Martins, Z. (2022). "Habitability conditions in our solar system – the case for Mars and the icy moons". In *Habitable Worlds and Sustainable Life on Earth and Beyond*, Springer, submitted

VII.2 Oral presentations and Posters

VII.2.1 Oral presentations

Coelho, L.F.; Almeida, M.,; Stroming J. (July, 2020). "Effect of Microgravity on Microbial Chlorophyll". Ciência 2020. Oral presentation.

Coelho, L. F.; Madden, J.; Kaltenegger, L.; Zinder, S.; Philpot, W.; Esquível, M. G.; Costa, R.; Canário, J.; Vincent, W.F. & Martins, Z. (May, 2022). "Color Catalogue of Life in Ice: Surface Biosignatures on Icy Worlds". AbSciCon 2022. Oral Presentation.

Coelho, L. F.; Madden, J.; Kaltenegger, L.; Zinder, S.; Philpot, W.; Esquível, M. G.; Costa, R.; Canário, J.; Vincent, W.F. & Martins, Z. (scheduled for July, 2022). "Color

Catalogue of Life in Ice: Surface Biosignatures on Icy Worlds". COSPAR 2022. Oral presentation.

VII.2.2 Posters

Coelho, L.F.; Canário, J.; Costa, R.: Martins Z. (October, 2018). "Astrobiology study of icy biomes as a proxy for extra-terrestrial life in the icy moons of Jupiter and Saturn". MIT Portugal annual conference. Poster.

Coelho, L.F., Couceiro, J.F.; Keller-Costa, T. Martinez, S.; Ramalho, T.P.; Carneiro, J., Comte, J.; Blais, M.A.; Vincent, W.F.; Martins Z.; Costa, R.: Canário, J.; (July, 2019). "Field work in the Canadian subarctic - a terrestrial analogue of the icy moons of Jupiter and Saturn". Ciência 2019. Poster.

Coelho, L.F., Couceiro, J.F.; Keller-Costa, T. Martinez, S.; Ramalho, T.P.; Carneiro, J., Comte, J.; Blais, M.A.; Vincent, W.F.; Martins Z.; Costa, R.: Canário, J.; (2020). "Field work in the Canadian subarctic - a terrestrial analogue of the icy moons of Jupiter and Saturn". CQE open days. Poster.

Coelho, L.F., Couceiro, J.F.; Keller-Costa, T. Martinez, S.; Ramalho, T.P.; Carneiro, J., Comte, J.; Blais, MA.; Vincent, W.F.; Martins Z.; Canário, J.; Costa, R. (June, 2021). "Structural shifts revealed for ice prokaryotes across a salinity gradient in the subarctic". World Microbe Forum. Poster.

VIII REFERENCES

Aarts, G., Fieberg, J., Brasseur, S., et al. (2013) ‘Quantifying the effect of habitat availability on species distributions’, *Journal of Animal Ecology*, 82(6), pp. 1135–1145. doi: 10.1111/1365-2656.12061.

Abyzov, S. S., Mitskevich, I. N., Poglazova, M. N., et al. (2001) ‘Microflora in the basal strata at Antarctic ice core above the Vostok lake’, *Advances in Space Research*, 28(4), pp. 701–706. doi: 10.1016/S0273-1177(01)00318-0.

Adyasari, D., Hassenrück, C., Montiel, D., et al. (2020) ‘Microbial community composition across a coastal hydrological system affected by submarine groundwater discharge (SGD)’, *PLOS ONE*, 15(6), p. e0235235. doi: 10.1371/journal.pone.0235235.

Affholder, A., Guyot, F., Sauterey, B., et al. (2021) ‘Bayesian analysis of Enceladus’s plume data to assess methanogenesis’, *Nature Astronomy*, 5(8), pp. 805–814. doi: 10.1038/s41550-021-01372-6.

Albani, J. R. (2004) ‘Chapter 2 - Fluorescence: Principles and Observables’, *Structure and Dynamics of Macromolecules: Absorption and Fluorescence Studies*. Elsevier. pp. 55-98. doi: 10.1016/B978-0-444-51449-3.X5000-X.

Albrecht, M., Pröschold, T. and Schumann, R. (2017) ‘Identification of cyanobacteria in a eutrophic coastal lagoon on the southern baltic coast’, *Frontiers in Microbiology*, 8(MAY), p. 923. doi: 10.3389/fmicb.2017.00923.

Alonso-Sáez, L., Sánchez, O., Gasol, J. M., et al. (2008) ‘Winter-to-summer changes in the composition and single-cell activity of near-surface Arctic prokaryotes’, *Environmental Microbiology*, 10(9), pp. 2444–2454. doi: 10.1111/j.1462-2920.2008.01674.x.

Alvarellos, J. L., Zahnle, K. J., Dobrovolskis, A. R., et al. (2008) ‘Transfer of mass from Io to Europa and beyond due to cometary impacts’, *Icarus*, 194(2), pp. 636–646. doi: 10.1016/j.icarus.2007.09.025.

AMAP (1998) ‘Chapter 2: Physical/geographical characteristics of the arctic’, *AMAP Assessment Report: Arctic Pollution Issues.*

Apprill, A., McNally, S., Parsons, R., et al. (2015) ‘Minor revision to V4 region SSU rRNA 806R gene primer greatly increases detection of SAR11 bacterioplankton’, *Aquatic Microbial Ecology*, 75(2), pp. 129–137. doi: 10.3354/ame01753.

Archambault, P., Snelgrove, P. V. R., Fisher, J. A. D., et al. (2010) ‘From sea to sea: Canada’s three oceans of biodiversity’, *PLOS ONE*, 5(8), p. e12182. doi: 10.1371/journal.pone.0012182.

Armstrong, G. A. (1997) ‘Genetics of eubacterial carotenoid biosynthesis: a colorful tale’, *Annual Review of Microbiology*, 51(1), pp. 629–659. doi: 10.1146/annurev.micro.51.1.629.

Arnau, V. G., Sánchez, L. A. and Delgado, O. D. (2015) ‘*Pseudomonas yamanorum* sp. nov., a psychrotolerant bacterium isolated from a subantarctic environment’, *International Journal of Systematic and Evolutionary Microbiology*, 65(Pt_2), pp. 424–431. doi: 10.1099/ijs.0.065201-0.

Ball, P. (2017) ‘Water is an active matrix of life for cell and molecular biology’, *Proceedings of the National Academy of Sciences*, 114(51), pp. 13327–13335. doi: 10.1073/pnas.1703781114.

Bano, N. and Hollibaugh, J. T. (2002) ‘Phylogenetic composition of bacterioplankton assemblages from the arctic ocean’, *Applied and Environmental Microbiology*, 68(2), pp. 505–518. doi: 10.1128/AEM.68.2.505-518.2002.

Baqué, M., Verseux, C., Böttger, U., et al. (2016) ‘Preservation of biomarkers from cyanobacteria mixed with Mars -like regolith under simulated Martian atmosphere and UV flux’, *Origins of Life and Evolution of Biospheres*, 46, pp. 289–310. doi: 10.1007/s11084-015-9467-9.

Baqué, M., Napoli, A., Claudia, F., et al. (2020) ‘Carotenoid Raman signatures are better preserved in dried cells of the desert *Cyanobacterium chroococcidiopsis* than in hydrated counterparts after high-dose gamma irradiation’, *Life*, 10(6), p. 83. doi: 10.3390/life10060083.

Baraket, F., Pedras, B., Torres, É., et al. (2020) ‘Novel phenoxazine-benzonitrile and phenothiazine-benzonitrile donor-acceptor molecules with thermally activated delayed fluorescence (TADF)’, *Dyes and Pigments*, 175(108114). doi: 10.1016/J.DYEPIG.2019.108114.

Barstow, J. K., Aigrain, S., Irwin, P. G. J., et al. (2015) ‘Transit spectroscopy with James Webb Space Telescope: systematics, starspots and stitching’, *MNRAS*, 448(3), pp. 2546–2561. doi: 10.1093/mnras/stv186.

Bassham, J. A. and Calvin, M. (1960) ‘The path of carbon in photosynthesis’, *in Die CO_2-Assimilation / The Assimilation of Carbon Dioxide*. Berlin, Heidelberg: Springer Berlin Heidelberg, pp. 884–922. doi: 10.1007/978-3-642-94798-8_30.

Běhounková, M., Tobie, G., Choblet, G., et al. (2021) ‘Tidally induced magmatic pulses on the oceanic floor of Jupiter’s moon Europa’, *Geophysical Research Letters*. Blackwell Publishing Ltd, p. e2020GL090077. doi: 10.1029/2020GL090077.

Beier, S., Jones, C. M., Mohit, V., et al. (2011) ‘Global phylogeography of chitinase genes in aquatic metagenomes’, *Applied and Environmental Microbiology*, 77(3), pp. 1101–1106. doi: 10.1128/AEM.01481-10.

Bell, M. S., Regberg, A., Rucker, M., et al. (2021) ‘Tool to assess forward contamination from the human microbiome and protect returned samples.’, *43rd COSPAR Scientific Assembly*. Held 28 January-4 February, 43, p. 166. *(Accessed: 17 August 2021).*

Ben-Ami, S., López-Morales, M., Garcia-Mejia, J., et al. (2018) ‘High-resolution spectroscopy using fabry–perot interferometer arrays: an application to searches for O2 in exoplanetary atmospheres’, *The Astrophysical Journal*, 861(2), p. 79. doi: 10.3847/1538-4357/aac835.

Bennett, W. E., Maas, J. L., Sweeney, S. A., et al. (1986) ‘Phototoxicity in aquatic organisms: the protecting effect of beta-carotene’, *Chemosphere*, 15(6), pp. 781–786. doi: 10.1016/0045-6535(86)90045-7.

Berger, T. A., Huber, D., Gaidos, E., et al. (2018) ‘Revised radii of Kepler stars and planets using Gaia data release 2’, *The Astrophysical Journal*, 866(2), p. 99. doi: 10.3847/1538-4357/aada83.

Bhiry, N., Delwaide, A., Allard, M., et al. (2011) ‘Environmental change in the Great Whale River region, Hudson Bay: five decades of multidisciplinary research by Centre d’études Nordiques (CEN)’, *Écoscience*, 18(3), pp. 182–203. doi: 10.2980/18-3-3469.

Billi, D., Verseux, C., Fagliarone, C., et al. (2019) ‘A desert *Cyanobacterium* under simulated Mars-like conditions in low Earth orbit: implications for the habitability of Mars’, *Astrobiology*, 19(2), pp. 158–169. doi: 10.1089/ast.2017.1807.

Billings, S. E. and Kattenhorn, S. A. (2005) ‘The great thickness debate: ice shell thickness models for Europa and comparisons with estimates based on flexure at ridges’, *Icarus*, 177(2), pp. 397–412. doi: 10.1016/J.ICARUS.2005.03.013.

Blais, M.-A., Matveev, A., Lovejoy, C., et al. (2022) ‘Size-fractionated microbiome structure in subarctic rivers and a coastal plume across DOC and salinity gradients’, *Frontiers in Microbiology*, 12(760282), p. 4022. doi: 10.3389/fmicb.2021.760282.

Blanc, M., Prieto-Ballesteros, O., André, N., et al. (2020) ‘Joint Europa Mission (JEM): a multi-scale study of Europa to characterize its habitability and search for extant life’, *Planetary and Space Science*, 193(104960). doi: 10.1016/j.pss.2020.104960.

Böcker, L., Hostettler, T., Diener, M., et al. (2020) ‘Time-temperature-resolved functional and structural changes of phycocyanin extracted from Arthrospira platensis/Spirulina’, *Food Chemistry*, 316(126374). doi: 10.1016/J.FOODCHEM.2020.126374.

De Boni, L., Correa, D. S. and Mendonça, C. R. (2010) ‘Nonlinear optical absorption of organic molecules for applications in optical devices’, in *Advances in Lasers and Electro Optics*. *InTech*, 2100327. doi: 10.5772/8641.

Bonilla, S., Rautio, M. and Vincent, W. F. (2009) ‘Phytoplankton and phytobenthos pigment strategies: implications for algal survival in the changing Arctic’, *Polar Biology*, 32(9), pp. 1293–1303. doi: 10.1007/S00300-009-0626-1.

Bottos, E. M., Vincent, W. F., Greer, C. W., et al. (2008) ‘Prokaryotic diversity of Arctic ice shelf microbial mats’, *Environmental Microbiology*, 10(4), pp. 950–966. doi: 10.1111/j.1462-2920.2007.01516.x.

Bowman, J. S., Rasmussen, S., Blom, N., et al. (2012) ‘Microbial community structure of Arctic multiyear sea ice and surface seawater by 454 sequencing of the 16S RNA gene’, *The ISME Journal*, 6(1), pp. 11–20. doi: 10.1038/ismej.2011.76.

Brinkmeyer, R., Knittel, K., Ju, J., et al. (2003) ‘Diversity and structure of bacterial communities in Arctic versus Antarctic pack ice’, *Applied and Environmental Microbiology*, 69(11), pp. 6610–6619. doi: 10.1128/AEM.69.11.6610.

Brown, M. E. and Hand, K. P. (2013) ‘Salts and radiation products on the surface of Europa’, *The Astronomical Journal*, 145(4), pp. 1–7. doi: 10.1088/0004-6256/145/4/110.

Brown, M. V. and Bowman, J. P. (2001) ‘A molecular phylogenetic survey of sea-ice microbial communities (SIMCO)’, *FEMS Microbiology Ecology*, 35(3), pp. 267–275. doi: 10.1111/j.1574-6941.2001.tb00812.x.

Brown, R. H., Clark, R. N., Buratti, B. J., et al. (2006) ‘Composition and physical properties of Enceladus’ surface’, *Science*, 311(5766), pp. 1425–1428. doi: 10.1126/science.1121031.

Bryce, C. C., Horneck, G., Rabbow, E., et al. (2015) ‘Impact shocked rocks as protective habitats on an anoxic early Earth’, *International Journal of Astrobiology*, 14(1), pp. 115–122. doi: 10.1017/S1473550414000123.

Caporaso, J. G., Lauber, C. L., Walters, W. A., et al. (2011) 'Global patterns of 16S rRNA diversity at a depth of millions of sequences per sample', *Proceedings of the National Academy of Sciences*, 108(127470), pp. 4516–4522. doi: 10.1073/PNAS.1000080107.

Carey, E., Bormann, K. J., Skiles, S. M., et al. (2018) 'NASA Airborne Snow Observatory: analysis of snow algae in the Sierra Nevada snowpack', *AGUFM, 2018*, pp. C13E-1191.

Carlson, R. W., Johnson, R. E. and Anderson, M. S. (1999) 'Sulfuric acid on Europa and the radiolytic sulfur cycle', *Science*, 286(5437), pp. 97–99. doi: 10.1126/science.286.5437.97.

Carr, M. H., Belton, M. J. S., Chapman, C. R., et al. (1998) 'Evidence for a subsurface ocean on Europa', *Nature*, 391(6665), pp. 363–365. doi: 10.1038/34857.

CEN (2020) 'Climate station data from Whapmagoostui-Kuujjuarapik region in Nunavik, Quebec, Canada, v. 1.5 (1987-2019)', D4. doi: 10.5885/45057SL-EADE4434146946A7.

Chan, H. S., Martins, Z. and Sephton, M. A. (2012a) 'Fluorescence spectroscopy for the detection of life in the Salten Skov Mars regolith analogue', *Planetary and Space Science*, 68(1), pp. 42–47. doi: 10.1016/j.pss.2011.06.004.

Chan, H. S., Martins, Z. and Sephton, M. A. (2012b) 'Spectrofluorometric analysis of amino acid mixtures: implications for future space missions', *Planetary and Space Science*, 60(1), pp. 336–341. doi: 10.1016/j.pss.2011.10.011.

Chan, Q. H. S., Stroud, R., Martins, Z., et al. (2020) 'Concerns of organic contamination for sample return space missions', *Space Science Reviews*, 216(4), p. 56. doi: 10.1007/s11214-020-00678-7.

Chela-Flores, J. (2017) 'Instrumentation for testing whether the icy moons of the gas and ice giants are inhabited', *Astrobiology*, 17(10), pp. 958–961. doi: 10.1089/ast.2016.1621.

Choblet, G., Tobie, G., Sotin, C., et al. (2017) 'Powering prolonged hydrothermal activity inside Enceladus', *Nature Astronomy*, 1(12), pp. 841–847. doi: 10.1038/s41550-017-0289-8.

Christner, B. C., Mosley-Thompson, E., Thompson, L. G., et al. (2000) 'Recovery and identification of viable bacteria immured in glacial ice', *Icarus*, 144(2), pp. 479–485. doi: 10.1006/icar.1999.6288.

Christner, B. C., Mosley-Thompson, E., Thompson, L. G., et al. (2002) 'Isolation and identification of bacteria from ancient and modern ice cores', in *The Patagonian Icefields. Springer, Boston, MA*, pp. 9–15. doi: 10.1007/978-1-4615-0645-4_2.

Christner, B. C., Mikucki, J. A., Foreman, C. M., et al. (2005) 'Glacial ice cores: A model system for developing extra-terrestrial decontamination protocols', *Icarus*, 174(2), pp. 572–584. doi: 10.1016/j.icarus.2004.10.027.

Clark, R. N. (1980) 'Ganymede, Europa, Callisto, and Saturn's rings: compositional analysis from reflectance spectroscopy', *Icarus*, 44(2), pp. 388–409. doi: 10.1016/0019-1035(80)90033-0.

Coble, P. G., Spencer, R. G. M., Baker, A., et al. (2014) 'Aquatic organic matter fluorescence', *Aquatic Organic Matter Fluorescence*, pp. 75–122. doi: 10.1017/CBO9781139045452.006.

Cockell, C. S., Bush, T., Bryce, C., et al. (2016) 'Habitability: a review', *Astrobiology*, 16(1), pp. 89–117. doi: 10.1089/ast.2015.1295.

Coelho, L. F., Madden, J., Kaltenegger, L., et al. (2022a) ‘Color catalogue of life in ice: surface biosignatures on icy worlds’, *Astrobiology*, 22(3), pp. 313–321. doi: 10.1089/ast.2021.0008.

Coelho, L. F., Couceiro, J., Keller-Costa, T., et al. (2022b) ‘Structural shifts in sea ice prokaryotic communities across a salinity gradient in the subarctic’, *Science of The Total Environment*, 827, 154286. doi: 10.1016/J.SCITOTENV.2022.154286.

Coelho, L. F. and Martins, Z. (2021) ‘The geochemistry of icy moons’, in *Encyclopedia of Geology. Elsevier*, pp. 207–216. doi: 10.1016/B978-0-08-102908-4.00123-5.

Cohen, Y., Jørgensen, B. B., Revsbech, N. P., et al. (1986) ‘Adaptation to hydrogen sulfide of oxygenic and anoxygenic photosynthesis among cyanobacteria’, *Applied and Environmental Microbiology*, 51(2), pp. 398–407. doi: 10.1128/aem.51.2.398-407.1986.

Coil, D. A., Neches, R. Y., Lang, J. M., et al. (2016) ‘Growth of 48 built environment bacterial isolates on board the International Space Station (ISS)’, *PeerJ*, 4(e1842). doi: 10.7717/peerj.1842.

Cole, J. R., Wang, Q., Fish, J. A., et al. (2014) ‘Ribosomal Database Project: data and tools for high throughput rRNA analysis’, *Nucleic Acids Research*, 42(D1), pp. D633–D642. doi: 10.1093/nar/gkt1244.

Comeau, A. M., Li, W. K. W., Tremblay, J.-É., et al. (2011) ‘Arctic ocean microbial community structure before and after the 2007 record sea ice minimum’, *PLOS ONE*, 6(11), p. e27492. doi: 10.1371/journal.pone.0027492.

Comte, J., Lovejoy, C., Crevecoeur, S., et al. (2016) ‘Co-occurrence patterns in aquatic bacterial communities across changing permafrost landscapes’, *Biogeosciences*, 13(1), pp. 175–190. doi: 10.5194/bg-13-175-2016.

Connelly, T. L., Tilburg, C. M. and Yager, P. L. (2006) ‘Evidence for psychrophiles outnumbering psychrotolerant marine bacteria in the springtime coastal Arctic’, *Limnology and Oceanography*, 51(2), pp. 1205–1210. doi: 10.4319/lo.2006.51.2.1205.

Cory, R. M. and McKnight, D. M. (2005) ‘Fluorescence spectroscopy reveals ubiquitous presence of oxidized and reduced quinones in dissolved organic matter’, *Environmental Science and Technology*, 39(21), pp. 8142–8149. doi: 10.1021/ES0506962.

Cottrell, M. T. and Kirchman, D. L. (2009) ‘Photoheterotrophic microbes in the arctic ocean in summer and winter’, *Applied and Environmental Microbiology*, 75(15), pp. 4958–4966. doi: 10.1128/AEM.00117-09.

Coustenis, A., Hedman, N. and Kminek, G. (2021) ‘The COSPAR panel on planetary protection: recent activities’, in *43rd COSPAR Scientific Assembly*, p. 43E2232C. (Accessed: 10 February 2022).

Cox, M. M. and Battista, J. R. (2005) ‘*Deinococcus radiodurans* — the consummate survivor’, *Nature Reviews Microbiology*, 3(11), pp. 882–892. doi: 10.1038/nrmicro1264.

Crawford, R. L. (2005) ‘Microbial diversity and its relationship to planetary protection’, *Applied and Environmental Microbiology*, 71(8), pp. 4163–4168. doi: 10.1128/AEM.71.8.4163-4168.2005.

Culberg, R., Schroeder, D. M. and Steinbrügge, G. (2022) ‘Double ridge formation over shallow water sills on Jupiter’s moon Europa’, *Nature Communications*, 13(1), pp. 1–10. doi: 10.1038/s41467-022-29458-3.

D'Elia, T., Veerapaneni, R. and Rogers, S. O. (2008) 'Isolation of microbes from lake Vostok accretion ice', *Applied and Environmental Microbiology*, 74(15), pp. 4962–4965. doi: 10.1128/AEM.02501-07.

d'Ischia, M., Manini, P., Martins, Z., et al. (2021) 'Insoluble organic matter in chondrites: Archetypal melanin-like PAH-based multifunctionality at the origin of life?', *Physics of Life Reviews*, 37, pp. 65–93. doi: 10.1016/J.PLREV.2021.03.002.

Dahal, R. H. and Kim, J. (2018) '*Fluviicola kyonggii* sp. nov., a bacterium isolated from forest soil and emended description of the genus *Fluviicola*', *International Journal of Systematic and Evolutionary Microbiology*, 68(6), pp. 1885–1889. doi: 10.1099/IJSEM.0.002759.

Dalton, J. B., Mogul, R., Kagawa, H. K., et al. (2003) 'Near-infrared detection of potential evidence for microscopic organisms on Europa', *Astrobiology*, 3(3), pp. 505–529. doi: 10.1089/153110703322610618.

Dalton, J. B., Palmer-Moloney, L. J., Rogoff, D., et al. (2009) 'Remote monitoring of hypersaline environments in', *International Journal of Remote Sensing*, 30(11), pp. 2933–2949. doi: 10.1080/01431160802558642.

Dalton, J. B., Cruikshank, D. P., Stephan, K., et al. (2010) 'Chemical composition of icy satellite surfaces', *Space Science Reviews*, 153, pp. 113–154. doi: 10.1007/s11214-010-9665-8.

Dancer, S. J., Shears, P. and Platt, D. J. (1997) 'Isolation and characterization of coliforms from glacial ice and water in Canada's High Arctic', *Journal of Applied Microbiology*, 82(5), pp. 597–609. doi: 10.1111/j.1365-2672.1997.tb03590.x.

Danko, D. C., Sierra, M. A., Benardini, J. N., et al. (2021) 'A comprehensive metagenomics framework to characterize organisms relevant for planetary protection', *Microbiome*, 9(1), p. 82. doi: 10.1186/s40168-021-01020-1.

Dedysh, S. N. and Ivanova, A. A. (2019) '*Planctomycetes* in boreal and subarctic wetlands: diversity patterns and potential ecological functions.', *FEMS microbiology ecology*, 95(2), p. fiy227. doi: 10.1093/femsec/fiy227.

Deming, J. W., Somers, L. K., Straube, W. L., et al. (1988) 'Isolation of an obligately barophilic bacterium and description of a new genus, *Colwellia* gen. nov.', *Systematic and Applied Microbiology*, 10(2), pp. 152–160. doi: 10.1016/S0723-2020(88)80030-4.

Dieser, M., Greenwood, M. and Foreman, C. M. (2010) 'Carotenoid pigmentation in antarctic heterotrophic bacteria as a strategy to withstand environmental stresses', *Arctic, Antarctic, and Alpine Research*, 42(4), pp. 396–405. doi: 10.1657/1938-4246-42.4.396.

Dixon, J. M., Taniguchi, M. and Lindsey, J. S. (2005) 'PhotochemCAD 2: a refined program with accompanying spectral databases for photochemical calculations', *Photochemistry and photobiology*, 81(1), pp. 212-213. doi: 10.1562/2004-11-06-TSN-361.

Dodd, M. S., Papineau, D., Grenne, T., et al. (2017) 'Evidence for early life in Earth's oldest hydrothermal vent precipitates', *Nature*, 543(7643), pp. 60–64. doi: 10.1038/nature21377.

Du, H., Fuh, R. C. A., Li, J., et al. (1998) 'PhotochemCAD: a computer-aided design and research tool in photochemistry', *Photochemistry and Photobiology*, 68(2), pp. 141–142. doi: 10.1111/J.1751-1097.1998.TB02480.X.

Edgar, R. C. (2010) ‘Search and clustering orders of magnitude faster than BLAST’, *Bioinformatics*, 26(19), pp. 2460–2461. doi: 10.1093/bioinformatics/btq461.

Edgar, R. C., Haas, B. J., Clemente, J. C., et al. (2011) ‘UCHIME improves sensitivity and speed of chimera detection’, *Bioinformatics*, 27(16), pp. 2194–2200. doi: 10.1093/bioinformatics/btr381.

Edgington, S. G. and Spilker, L. J. (2016) ‘Cassini’s grand finale’, *Nature Geoscience*, 9(7), pp. 472–473. doi: 10.1038/ngeo2753.

Eigenbrode, J., Benning, L. G., Maule, J., et al. (2009) ‘A field-based cleaning protocol for sampling devices used in life-detection studies’, *Astrobiology*, 9(5), pp. 455–465. doi: 10.1089/ast.2008.0275.

Eliseev, D., Heinen, D., Helbing, K., et al. (2014) ‘Acoustic in-ice positioning in the Enceladus Explorer project’, *Annals of Glaciology*, 55(68), pp. 253–259. doi: 10.3189/2014AoG68A035.

Eriksen, N. T. (2008) ‘Production of phycocyanin - a pigment with applications in biology, biotechnology, foods and medicine’, *Applied Microbiology and Biotechnology*, 80(1), pp. 1–14. doi: 10.1007/S00253-008-1542-Y.

Ertem, G., Glavin, D. P., Volpe, R. P., et al. (2021) ‘Evidence for the protection of N-heterocycles from gamma radiation by Mars analogue minerals’, *Icarus*, 368(114540). doi: 10.1016/J.ICARUS.2021.114540.

Esteves, A. I. S., Hardoim, C. C. P., Xavier, J. R., et al. (2013) ‘Molecular richness and biotechnological potential of bacteria cultured from *Irciniidae* sponges in the north-east Atlantic’, *FEMS Microbiology Ecology*, 85(3), pp. 519–536. doi: 10.1111/1574-6941.12140.

Eviatar, A., Siscoe, G. L., Johnson, T. V., et al. (1981) ‘Effects of Io ejecta on Europa’, *Icarus*, 47(1), pp. 75–83. doi: 10.1016/0019-1035(81)90092-0.

Farmer, J. D. (2018) ‘Habitability as a tool in astrobiological exploration’, in *From Habitability to Life on Mars. Elsevier*, pp. 1–12. doi: 10.1016/B978-0-12-809935-3.00002-5.

Favata, F., Hasinger, G., Tacconi, L. J., et al. (2021) ‘Introducing the Voyage 2050 White Papers, contributions from the science community to ESA’s long-term plan for the Scientific Programme’, *Experimental Astronomy*, 51(3), pp. 551–558. doi: 10.1007/S10686-021-09746-4.

Fiedor, L., Stąsiek, M., Myśliwa-Kurdziel, B., et al. (2003) ‘Phytol as one of the determinants of chlorophyll interactions in solution’, *Photosynthesis research*, 78(1), pp. 47–57. doi: 10.1023/A:1026042005536.

Fischer, P. D., Brown, M. E. and Hand, K. P. (2015) ‘Spatially resolved spectroscopy of Europa: the distinct spectrum of large-scale chaos’, *Astronomical Journal*, 150(5), p. 164. doi: 10.1088/0004-6256/150/5/164.

Foing, B. H., Stoker, C., Zavaleta, J., et al. (2011) ‘Field astrobiology research in Moon–Mars analogue environments: instruments and methods’, *International Journal of Astrobiology*, 10(3), pp. 141–160. doi: 10.1017/S1473550411000036.

Fraser, P. D. and Bramley, P. M. (2004) ‘The biosynthesis and nutritional uses of carotenoids’, *Progress in Lipid Research*, 43(3), pp. 228–265. doi: 10.1016/J.PLIPRES.2003.10.002.

Fujii, Y., Angerhausen, D., Deitrick, R., et al. (2018) ‘Exoplanet biosignatures: observational prospects’, *Astrobiology*, 18(6), pp. 739–778. doi: 10.1089/ast.2017.1733.

Garcia-Lopez, E. and Cid, C. (2017) ‘Glaciers and ice sheets as analog environments of potentially habitable icy worlds’, *Frontiers in Microbiology*, 8(JUL), pp. 1–13. doi: 10.3389/fmicb.2017.01407.

Garneau, M., Vincent, W., Alonso-Sáez, L., et al. (2006) ‘Prokaryotic community structure and heterotrophic production in a river-influenced coastal arctic ecosystem’, *Aquatic Microbial Ecology*, 42(1), pp. 27–40. doi: 10.3354/ame042027.

Gerloff, G. C., Fitzgerald, G. P. and Skoog, F. (1950) ‘The isolation, purification, and culture of blue-green algae’, *American Journal of Botany*, 37(3), p. 216. doi: 10.2307/2437904.

Ghiglione, J.-F., Galand, P. E., Pommier, T., et al. (2012) ‘Pole-to-pole biogeography of surface and deep marine bacterial communities’, *Proceedings of the National Academy of Sciences*, 109(43), pp. 17633–17638. doi: 10.1073/pnas.1208160109.

Glazer, A. N. and Stryer, L. (1983) ‘Fluorescent tandem phycobiliprotein conjugates. Emission wavelength shifting by energy transfer’, *Biophysical journal*, 43(3), pp. 383–386. doi: 10.1016/S0006-3495(83)84361-6.

Glein, C. R., Baross, J. A. and Waite, J. H. (2015) ‘The pH of Enceladus’ ocean’, *Geochimica et Cosmochimica Acta*, 162, pp. 202–219. doi: 10.1016/j.gca.2015.04.017.

Glein, C. R., Postberg, F. and Vance, S. D. (2018) ‘The geochemistry of Enceladus: composition and controls’, in *Enceladus and the Icy Moons of Saturn. The University of Arizona Press*, pp. 1–32. doi: 10.2458/azu_uapress_9780816537075-ch003.

Glein, C. R. and Waite, J. H. (2020) ‘The carbonate geochemistry of Enceladus’ ocean’, *Geophysical Research Letters*, 47(3), p. e2019GL085885. doi: 10.1029/2019GL085885.

Golozar, M., Casto, L. D., Kim, J., et al. (2020) ‘Maturation of automated microfluidic organic analyzers for highly sensitive and selective detection of biosignatures in the solar system’, in *51st Lunar and Planetary Science Conference*.

Gondek, K. and Mierzwa-Hersztek, M. (2021) ‘Effect of soil-applied L-tryptophan on the amount of biomass and nitrogen and sulfur utilization by maize’, *Agronomy*, 11(12), p. 2582. doi: 10.3390/AGRONOMY11122582.

Gonzalez, J. M., Fernandez-Gomez, B., Fernandez-Guerra, A., et al. (2008) ‘Genome analysis of the proteorhodopsin-containing marine bacterium *Polaribacter* sp. MED152 (*Flavobacteria*)’, *Proceedings of the National Academy of Sciences*, 105(25), pp. 8724–8729. doi: 10.1073/pnas.0712027105.

Goordial, J., Altshuler, I., Hindson, K., et al. (2017) ‘In situ field sequencing and life detection in remote (79°26′N) Canadian High Arctic permafrost ice wedge microbial communities’, *Frontiers in Microbiology*, 8(DEC), p. 2594. doi: 10.3389/fmicb.2017.02594.

Gosselin, M., Legendre, L., Demers, S., et al. (1985) ‘Responses of sea-ice microalgae to climatic and fortnightly tidal energy inputs (Manitounuk Sound, Hudson Bay)’, Canadian *Journal of Fisheries and Aquatic Sciences*, 42(5), pp. 999–1006. doi: 10.1139/f85-125.

Grasset, O., Dougherty, M. K., Coustenis, A., et al. (2013) ‘JUpiter ICy moons Explorer (JUICE): An ESA mission to orbit Ganymede and to characterise the Jupiter system’, *Planetary and Space Science*, 78, pp. 1–21. doi: 10.1016/j.pss.2012.12.002.

Grossman, A. R., Bhaya, D., Apt, K. E., et al. (1995) 'Light-harvesting complexes in oxygenic photosynthesis: diversity, control, and evolution', *Annual Review of Genetics*, 29(1), pp. 231–288. doi: 10.1146/annurev.ge.29.120195.001311.

Hall, D. T., Strobel, D. F., Feldman, P. D., et al. (1995) 'Detection of an oxygen atmosphere on Jupiter's moon Europa', *Nature*, 373(6516), pp. 677–679. doi: 10.1038/373677a0.

Hall, L. S., Krausman, P. R. and Morrison, M. L. (1997) The habitat concept and a plea for standard terminology. *Wildlife Society Bulletin.*

Hammer, D. A. T., Ryan, P. D., Hammer, Ø., et al. (2001) 'Past: paleontological statistics software package for education and data analysis', *Palaeontologia Electronica*, 4(1), p. 178. (Accessed: 10 September 2021).

Hand, K., Murray, A. E., Garvin, J. B., et al. (2021) 'Science of the Europa Lander mission concept', *Bulletin of the AAS*, 53(4). doi: 10.3847/25c2cfeb.ad4ae39e.

Hand, K. P., Sotin, C., Hayes, A., et al. (2020) 'On the habitability and future exploration of ocean worlds', *Space Science Reviews*, 216(5), p. 95. doi: 10.1007/s11214-020-00713-7.

Hand, K. P., Phillips, C. B., Murray, A., et al. (2022) 'Science goals and mission architecture of the Europa Lander mission concept', *The Planetary Science Journal*, 3(1), p. 22. doi: 10.3847/PSJ/AC4493.

Hand, K. P. and Chyba, C. F. (2007) 'Empirical constraints on the salinity of the Europan ocean and implications for a thin ice shell', *Icarus*, 189(2), pp. 424–438. doi: 10.1016/j.icarus.2007.02.002.

Hansen, A. M., Kraus, T. E. C., Pellerin, B. A., et al. (2016) 'Optical properties of dissolved organic matter (DOM): effects of biological and photolytic degradation', *Limnology and Oceanography*, 61(3), pp. 1015–1032. doi: 10.1002/LNO.10270.

Hasegawa, J., Ozeki, Y., Ohkawa, K., et al. (1998) 'Theoretical study of the excited states of chlorin, bacteriochlorin, pheophytin *a*, and chlorophyll *a* by the SAC/SAC−CI method', *Journal of Physical Chemistry* B, 102(7), pp. 1320–1326. doi: 10.1021/JP972894O.

Hatam, I., Charchuk, R., Lange, B., et al. (2014a) 'Distinct bacterial assemblages reside at different depths in Arctic multiyear sea ice', *FEMS Microbiology Ecology*, 90(1), pp. 115–125. doi: 10.1111/1574-6941.12377.

Hegde, S., Paulino-Lima, I. G., Kent, R., et al. (2015) 'Surface biosignatures of exo-Earths: remote detection of extra-terrestrial life', *Proceedings of the National Academy of Sciences*, 112(13), pp. 3886–3891. doi: 10.1073/pnas.1421237112.

Hegde, S. and Kaltenegger, L. (2013) 'Colors of extreme exo-Earth environments', *Astrobiology*, 13(1), pp. 47–56. doi: 10.1089/ast.2012.0849.

Helmke, E. and Weyland, H. (1995) 'Bacteria in sea ice and underlying water of the eastern Weddell Sea in midwinter', *Marine Ecology Progress Series*, 117, pp. 269–287. doi: 10.3354/meps117269.

Hemingway, D. J. and Mittal, T. (2019) 'Enceladus's ice shell structure as a window on internal heat production', *Icarus*, 332, pp. 111–131. doi: 10.1016/j.icarus.2019.03.011.

Hendrix, A. R., Hurford, T. A., Barge, L. M., et al. (2019) 'The NASA roadmap to ocean worlds', *Astrobiology*, 19(1), pp. 1–27. doi: 10.1089/ast.2018.1955.

Hendrix, A. R., Hansen, C. J. and Holsclaw, G. M. (2010) 'The ultraviolet reflectance of Enceladus: implications for surface composition', *Icarus*, 206(2), pp. 608–617. doi: 10.1016/j.icarus.2009.11.007.

Hodyss, R., Parkinson, C. D., Johnson, P. V., et al. (2009) 'Methanol on Enceladus', *Geophysical Research Letters*, 36(17), p. L17103. doi: 10.1029/2009GL039336.

Howell, S. M. and Pappalardo, R. T. (2020) 'NASA's Europa Clipper—a mission to a potentially habitable ocean world', *Nature Communications*, 11(1), p. 1311. doi: 10.1038/s41467-020-15160-9.

Hsu, H.-W., Postberg, F., Sekine, Y., et al. (2015) 'Ongoing hydrothermal activities within Enceladus', *Nature*, 519(7542), pp. 207–210. doi: 10.1038/nature14262.

Huber, K. J., Wüst, P. K., Rohde, M., et al. (2014) '*Aridibacter famidurans* gen. nov., sp. nov. and *Aridibacter kavangonensis* sp. nov., two novel members of subdivision 4 of the *Acidobacteria* isolated from semiarid savannah soil', *International Journal of Systematic and Evolutionary Microbiology*, 64(Pt_6), pp. 1866–1875. doi: 10.1099/ijs.0.060236-0.

Imbeau, E., Vincent, W. F., Wauthy, M., et al. (2021) 'Hidden stores of organic matter in northern lake ice: selective retention of terrestrial particles, phytoplankton and labile carbon', *Journal of Geophysical Research: Biogeosciences*, 126(8), p. e2020JG006233. doi: 10.1029/2020JG006233.

Ingram, R. G. and Larouche, P. (1987) 'Variability of an under-ice river plume in Hudson Bay', *Journal of Geophysical Research*, 92(C9), p. 9541. doi: 10.1029/JC092iC09p09541.

Itcus, C., Pascu, M. D., Lavin, P., et al. (2018) 'Bacterial and archaeal community structures in perennial cave ice', *Scientific Reports*, 8(1), p. 15671. doi: 10.1038/s41598-018-34106-2.

Jacquemot, L., Kalenitchenko, D., Matthes, L. C., et al. (2021) 'Protist communities along freshwater–marine transition zones in Hudson Bay (Canada)', *Elementa: Science of the Anthropocene*, 9(1), pp. 1–21. doi: 10.1525/elementa.2021.00111.

Jia, X., Kivelson, M. G., Khurana, K. K., et al. (2018) 'Evidence of a plume on Europa from Galileo magnetic and plasma wave signatures', *Nature Astronomy*, 2(6), pp. 459–464. doi: 10.1038/s41550-018-0450-z.

Jiang, F., Li, Wenjuan, Xiao, M., et al. (2012) '*Luteolibacter luojiensis* sp. nov., isolated from Arctic tundra soil, and emended description of the genus *Luteolibacter*', *International Journal of Systematic and Evolutionary Microbiology*, 62(9), pp. 2259–2263. doi: 10.1099/IJS.0.037309-0.

Judge, P. (2017) 'A novel strategy to seek biosignatures at Enceladus and Europa', *Astrobiology*, 17(9), pp. 852–861. doi: 10.1089/ast.2017.1667.

Junge, K., Imhoff, F., Staley, T., et al. (2002) 'Phylogenetic diversity of numerically important arctic sea-ice bacteria cultured at subzero temperature', *Microbial Ecology*, 43(3), pp. 315–328. doi: 10.1007/s00248-001-1026-4.

Junge, K., Eicken, H., Swanson, B. D., et al. (2006) 'Bacterial incorporation of leucine into protein down to -20 degrees C with evidence for potential activity in sub-eutectic saline ice formations.', *Cryobiology*, 52(3), pp. 417–429. doi: 10.1016/j.cryobiol.2006.03.002.

Kaltenegger, L. (2017) ‘How to characterize habitable worlds and signs of life’, *Annual Review of Astronomy and Astrophysics*, 55(1), pp. 433–485. doi: 10.1146/annurev-astro-082214-122238.

Kane, S. R., Hill, M. L., Kasting, J. F., et al. (2016) ‘A catalog of kepler habitable zone exoplanet candidates’, *The Astrophysical Journal*, 830(1), p. 1. doi: 10.3847/0004-637X/830/1/1.

Karimi, E., Ramos, M., Gonçalves, J. M. S., et al. (2017) ‘Comparative metagenomics reveals the distinctive adaptive features of the *Spongia officinalis* endosymbiotic consortium’, *Frontiers in Microbiology*, 8(DEC), p. 2499. doi: 10.3389/fmicb.2017.02499.

Kayani, M. ur R., Doyle, S. M., Sangwan, N., et al. (2018) ‘Metagenomic analysis of basal ice from an Alaskan glacier’, *Microbiome*, 6(1), p.123. doi: 10.1186/s40168-018-0505-5.

Keller-Costa, T., Eriksson, D., Gonçalves, J. M. S., et al. (2017) ‘The gorgonian coral *Eunicella labiata* hosts a distinct prokaryotic consortium amenable to cultivation’, *FEMS Microbiology Ecology*, 93(12), pp. 1–14. doi: 10.1093/femsec/fix143.

Kellogg, C. T. E., McClelland, J. W., Dunton, K. H., et al. (2019) ‘Strong seasonality in arctic estuarine microbial food webs’, *Frontiers in Microbiology*, 10(2628). doi: 10.3389/fmicb.2019.02628.

Khawaja, N., Postberg, F., Hillier, J., et al. (2019) ‘Low-mass nitrogen-, oxygen-bearing, and aromatic compounds in Enceladean ice grains’, *Monthly Notices of the Royal Astronomical Society*, 489(4), pp. 5231–5243. doi: 10.1093/mnras/stz2280.

Khurana, K. K., Kivelson, M. G., Stevenson, D. J., et al. (1998) ‘Induced magnetic fields as evidence for subsurface oceans in Europa and Callisto’, *Nature*, 395(6704), pp. 777–780. doi: 10.1038/27394.

Kinasz, C. T. (2019) ‘Desenvolvimento de metodologias para descontaminação de testemunhos de gelo para análises de ecologia microbiana e astrobiologia’, *PhD Thesis, Universidade Federal de Santa Catarina, Brazil*. (Accessed: 13 August 2021).

Kirchman, D. L., Cottrell, M. T. and Lovejoy, C. (2010) ‘The structure of bacterial communities in the western Arctic Ocean as revealed by pyrosequencing of 16S rRNA genes’, *Environmental Microbiology*, 12(5), pp. 1132–1143. doi: 10.1111/j.1462-2920.2010.02154.x.

Kitadai, N. and Maruyama, S. (2018) ‘Origins of building blocks of life: a review’, *Geoscience Frontiers*, 9(4), pp. 1117–1153. doi: 10.1016/j.gsf.2017.07.007.

Kivelson, M., Khurana, K., Russell, C., et al. (2000) ‘Galileo magnetometer measurements: a stronger case for a subsurface ocean at Europa’, *Science*, 289(5483), pp. 1340–1343. doi: 10.1126/science.289.5483.1340.

Kivelson, M. G., Khurana, K. K. and Volwerk, M. (2002) ‘The permanent and inductive magnetic moments of Ganymede’, *Icarus*, 157(2), pp. 507–522. doi: 10.1006/icar.2002.6834.

Klassen, J. L. (2010) ‘Phylogenetic and evolutionary patterns in microbial carotenoid biosynthesis are revealed by comparative genomics’, *PLOS ONE*, 5(6), p. e11257. doi: 10.1371/journal.pone.0011257.

Kminek, G., Conley, C., Hipkin, V., et al. (2017) COSPAR’s Planetary Protection Policy.

Kminek, G., Clark, B., Conley, C., et al. (2018) 'Report of the COSPAR workshop on refining planetary protection requirements for human missions', *in 2nd COSPAR Workshop on Refining Planetary Protection Requirements for Human Missions.*

Kminek, G., Rettberg, P., Moissl-Eichinger, C., et al. (2019) 'The international planetary protection handbook', Space Research Today, 205, pp. e1–e120. doi: 10.1016/j.srt.2019.09.001.

Kopparapu, R., Ramirez, R., Kasting, J. F., et al. (2013) 'Habitable zones around main-sequence stars: new estimates', *Astrophysical Journal*, 765(2). doi: 10.1088/0004-637X/765/2/131.

Kopparapu, R., Ramirez, R. M., SchottelKotte, J., et al. (2014) 'Habitable zones around main-sequence stars: dependence on planetary mass', *Astrophysical Journal Letters*, 787(2), p. L29. doi: 10.1088/2041-8205/787/2/L29.

Kotler, J. M., Quinn, R. C., Foing, B. H., et al. (2011) 'Analysis of mineral matrices of planetary soil analogues from the Utah Desert', *International Journal of Astrobiology*, 10(3), pp. 221–229. doi: 10.1017/S1473550411000103.

Kouveliotou, C., Agol, E., Batalha, N., et al. (2014) 'Enduring Quests-Daring Visions (NASA Astrophysics in the Next Three Decades)'. (Accessed: 8 July 2021).

Kraemer, S., Ramachandran, A., Colatriano, D., et al. (2020) 'Diversity and biogeography of SAR11 bacteria from the Arctic Ocean', *ISME Journal*, 14(1), pp. 79–90. doi: 10.1038/s41396-019-0499-4.

Kriebel, K. T. (1978) 'Measured spectral bidirectional reflection properties of four vegetated surfaces', *Applied Optics*, 17(2), p. 253. doi: 10.1364/ao.17.000253.

Kuhn, E., Ichimura, A. S., Peng, V., et al. (2014) 'Brine assemblages of ultrasmall microbial cells within the ice cover of Lake Vida, Antarctica', *Applied and Environmental Microbiology*, 80(12), pp. 3687–3698. doi: 10.1128/AEM.00276-14.

Lane, A. L., Nelson, R. M. and Matson, D. L. (1981) 'Evidence for sulphur implantation in Europa's UV absorption band', *Nature*, 292(5818), pp. 38–39. doi: 10.1038/292038a0.

Latowski, D., Kuczyńska, P. and Strzałka, K. (2011) 'Xanthophyll cycle – a mechanism protecting plants against oxidative stress', *Redox Report*, 16(2), pp. 78–90. doi: 10.1179/174329211X13020951739938.

Laurent, B., Cousins, C. R., Pereira, M. F. C., et al. (2019) 'Effects of UV-organic interaction and Martian conditions on the survivability of organics', *Icarus*, 323, pp. 33–39. doi: 10.1016/j.icarus.2019.01.020.

Lazarevic, V., Gaïa, N., Girard, M., et al. (2016) 'Decontamination of 16S rRNA gene amplicon sequence datasets based on bacterial load assessment by qPCR', BMC *Microbiology*, 16(1), p. 73. doi: 10.1186/s12866-016-0689-4.

Lederberg, J. (1965) 'Signs of life: criterion-system of exobiology', *Nature*, 207(4992), pp. 9–13. doi: 10.1038/207009a0.

Legendre, L., Robineau, B., Gosselin, M., et al. (1996) 'Impact of freshwater on a subarctic coastal ecosystem under seasonal sea ice (southeastern Hudson Bay, Canada) II. Production and export of microalgae', *Journal of Marine Systems*, 7(2–4), pp. 233–250. doi: 10.1016/0924-7963(95)00007-0.

Legendre, L., Robineau, B. and Leblanc, B. (1999) 'Single-celled cyanobacteria in the first-year sea ice and ice-covered waters of the Northern Hemisphere', in *Bulletin de l'Institut océanographique, Monaco Special*, 19, pp. 169-174.

Lekner, J. and Dorf, M. C. (1988) 'Why some things are darker when wet', *Applied Optics*, 27(7), pp. 1278–1280. doi: 10.1364/AO.27.001278.

Lemoine, Y. and Schoefs, B. (2010) 'Secondary ketocarotenoid astaxanthin biosynthesis in algae: a multifunctional response to stress', *Photosynthesis Research*, 106, pp. 155–177. doi: 10.1007/s11120-010-9583-3.

Levy, J., Craig Cary, S., Joy, K., et al. (2020) 'Detection and community-level identification of microbial mats in the McMurdo Dry Valleys using drone-based hyperspectral reflectance imaging', *Antarctic Science*, 32(5), pp. 367–381. doi: 10.1017/S0954102020000243.

Li, S. S. and Ingram, R. G. (2007) 'Isopycnal deepening of an under-ice river plume in coastal waters: field observations and modeling', *Journal of Geophysical Research*, 112(C7), p. C07010. doi: 10.1029/2006JC003883.

Lim, J. H., Baek, S. H. and Lee, S. T. (2009) '*Ferruginibacter alkalilentus* gen. nov., sp. nov. and *ferruginibacter lapsinanis* sp. nov., novel members of the family "*Chitinophagaceae*" in the phylum *Bacteroidetes*, isolated from freshwater sediment', *International Journal of Systematic and Evolutionary Microbiology*, 59(10), pp. 2394–2399. doi: 10.1099/IJS.0.009480-0.

Liu, Y., Priscu, J. C., Yao, T., et al. (2019) 'Culturable bacteria isolated from seven high-altitude ice cores on the Tibetan Plateau', *Journal of Glaciology*, 65(249), pp. 29–38. doi: 10.1017/jog.2018.86.

Llirós, M., Inceoğlu, Ö., García-Armisen, T., et al. (2014) 'Bacterial community composition in three freshwater reservoirs of different alkalinity and trophic status', *PLOS ONE*, 9(12), p. e116145. doi: 10.1371/journal.pone.0116145.

Lobo, A. H., Thompson, A. F., Vance, S. D., et al. (2021) 'A pole-to-equator ocean overturning circulation on Enceladus', *Nature Geoscience*, 14(4), pp. 185–189. doi: 10.1038/s41561-021-00706-3.

Lovelock, J. E. (1965) 'A physical basis for life detection experiments', *Nature*, 207(4997), pp. 568–570. doi: 10.1038/207568a0.

Lozupone, C. A. and Knight, R. (2007) 'Global patterns in bacterial diversity', *Proceedings of the National Academy of Sciences*, 104(27), pp. 11436–11440. doi: 10.1073/PNAS.0611525104.

Lubitz, W., Chrysina, M. and Cox, N. (2019) 'Water oxidation in photosystem II', *Photosynthesis Research. Springer Netherlands*, pp. 105–125. doi: 10.1007/s11120-019-00648-3.

Lunine, J. I. (1990) 'Voyager at Triton', *Science*, 250(4979), pp. 386–386. doi: 10.1126/science.250.4979.386.

Lunine, J. I. (2017) 'Ocean worlds exploration', *Acta Astronautica*, 131(September 2016), pp. 123–130. doi: 10.1016/j.actaastro.2016.11.017.

Lutz, S., Anesio, A. M., Jorge Villar, S. E., et al. (2014) 'Variations of algal communities cause darkening of a Greenland glacier', *FEMS Microbiology Ecology*, 89(2), pp. 402–414. doi: 10.1111/1574-6941.12351.

Lutz, S., Anesio, A. M., Raiswell, R., et al. (2016) ‘The biogeography of red snow microbiomes and their role in melting Arctic glaciers’, *Nature Communications*, 7(1), pp. 1–9. doi: 10.1038/ncomms11968.

Maccario, L., Sanguino, L., Vogel, T. M., et al. (2015) ‘Snow and ice ecosystems: not so extreme’, *Research in Microbiology*, 166(10), pp. 782–795. doi: 10.1016/j.resmic.2015.09.002.

Macdonald, R. W. (2000) ‘Arctic estuaries and ice: a positive—negative estuarine couple’, in *The Freshwater Budget of the Arctic Ocean. Dordrecht. Springer Netherlands*, pp. 383–407. doi: 10.1007/978-94-011-4132-1_17.

Mackelprang, R., Burkert, A., Haw, M., et al. (2017) ‘Microbial survival strategies in ancient permafrost: insights from metagenomics’, *The ISME Journal*, 11(10), pp. 2305–2318. doi: 10.1038/ismej.2017.93.

MacKenzie, S. M., Neveu, M., Davila, A. F., et al. (2021) ‘The Enceladus Orbilander Mission concept: balancing return and resources in the search for life’, *The Planetary Science Journal*, 2(2), p. 77. doi: 10.3847/PSJ/ABE4DA.

Manning, S. R. (2022) ‘Microalgal lipids: biochemistry and biotechnology’, *Current Opinion in Biotechnology*, 74, pp. 1–7. doi: 10.1016/J.COPBIO.2021.10.018.

Marizcurrena, J. J., Cerdá, M. F., Alem, D., et al. (2019) ‘Living with pigments: the colour palette of Antarctic life’, in. *The Ecological Role of Micro-organisms in the Antarctic Environment. Springer*, pp. 65–82. doi: 10.1007/978-3-030-02786-5_4.

Marlow, J. J., Martins, Z. and Sephton, M. A. (2008) ‘Mars on Earth: soil analogues for future Mars missions’, *Astronomy and Geophysics*, 49(2), pp. 20-23. doi: 10.1111/J.1468-4004.2008.49220.x.

Marlow, J. J., Martins, Z. and Sephton, M. A. (2011) ‘Organic host analogues and the search for life on Mars’, *International Journal of Astrobiology*, 10(1), pp. 31–44. doi: 10.1017/S1473550410000303.

Martin, A. and McMinn, A. (2017) ‘Sea ice, extremophiles and life on extra-terrestrial ocean worlds’, *International Journal of Astrobiology*, 17(1), pp. 1–16. doi: 10.1017/S1473550416000483.

Martins, Z., Price, M. C., Goldman, N., et al. (2013) ‘Shock synthesis of amino acids from impacting cometary and icy planet surface analogues’, *Nature Geoscience*, 6(12), pp. 1045–1049. doi: 10.1038/ngeo1930.

Martins, Z., Cottin, H., Kotler, J. M., et al. (2017) ‘Earth as a tool for astrobiology—a European perspective’, *Space Science Reviews*, 209(1–4), pp. 43–81. doi: 10.1007/s11214-017-0369-1.

Martins, Z. (2020) ‘Detection of organic matter and biosignatures in space missions’, *Current Issues in Molecular Biology*, 38(1), pp. 53–74. doi: 10.21775/cimb.038.053.

Martins, Z., Chan, Q. H. S., Bonal, L., et al. (2020) ‘Organic matter in the solar system—implications for future on-site and sample return missions’, *Space Science Reviews*, 216(4), pp. 1–23. doi: 10.1007/S11214-020-00679-6.

Mathews, M. M. and Sistrom, W. R. (1959) ‘Function of carotenoid pigments in non-photosynthetic bacteria’, *Nature*, 184(4702), pp. 1892–1893. doi: 10.1038/1841892a0.

Matson, D. L., Castillo, J. C., Lunine, J., et al. (2007) 'Enceladus' plume: compositional evidence for a hot interior', *Icarus*, 187(2), pp. 569–573. doi: 10.1016/j.icarus.2006.10.016.

Mayor, M. and Queloz, D. (1995) 'A Jupiter-mass companion to a solar-type star', *Nature*, 378(6555), pp. 355–359. doi: 10.1038/378355a0.

McCord, T. B., Carlson, R. W., Smythe, W. D., et al. (1997) 'Organics and other molecules in the surfaces of Callisto and Ganymede', *Science*, 278(5336), pp. 271–275. doi: 10.1126/science.278.5336.271.

McCord, T. B., Hansen, G. B., Clark, R. N., et al. (1998) 'Non-water-ice constituents in the surface material of the icy Galilean satellites from the Galileo near-infrared mapping spectrometer investigation', *Journal of Geophysical Research: Planets*, 103(E4), pp. 8603–8626. doi: 10.1029/98JE00788.

McCord, T. B., Hansen, G. B., Matson, D. L., et al. (1999) 'Hydrated salt minerals on Europa's surface from the Galileo near-infrared mapping spectrometer (NIMS) investigation', *Journal of Geophysical Research E: Planets*, 104(E5), pp. 11827–11851. doi: 10.1029/1999JE900005.

McCord, T. B., Hansen, G. B. and Hibbitts, C. A. (2001) 'Hydrated salt minerals on Ganymede's surface: evidence of an ocean below', *Science*, 292(5521), pp. 1523–1525. doi: 10.1126/science.1059916.

McCoy, K. J., DiNicola, M., Everline, C., et al. (2021) 'Europa Clipper planetary protection probabilistic risk assessment summary', *Planetary and Space Science*, 196, p. 105139. doi: 10.1016/J.PSS.2020.105139.

McCubbin, F. M., Herd, C. D. K., Yada, T., et al. (2019) 'Advanced curation of astromaterials for planetary science', *Space Science Reviews*, 215(8), p. 48. doi: 10.1007/s11214-019-0615-9.

McKinnon, W. B. and Kirk, R. L. (2014) 'Triton', in *Encyclopedia of the Solar System. Elsevier*, pp. 861–881. doi: 10.1016/B978-0-12-415845-0.00040-2.

McMinn, A., Ashworth, C. and Ryan, K. (1999) 'Growth and productivity of Antarctic sea ice algae under PAR and UV irradiances', *Botanica Marina*, 42(4), pp. 401–407. doi: 10.1515/BOT.1999.046.

McMurdie, P. J. and Holmes, S. (2013) 'phyloseq: An R package for reproducible interactive analysis and graphics of microbiome census data', *PLOS ONE*, 8(4), p. e61217. doi: 10.1371/journal.pone.0061217.

McMurdie, P. J. and Holmes, S. (2014) 'Waste not, want not: why rarefying microbiome data is inadmissible', *PLOS Computational Biology*, 10(4), p. e1003531. doi: 10.1371/journal.pcbi.1003531.

Melosh, H. J., Ekholm, A. G., Showman, A. P., et al. (2004) 'The temperature of Europa's subsurface water ocean', *Icarus*, 168(2), pp. 498–502. doi: 10.1016/J.ICARUS.2003.11.026.

Mennesson, B., Gaudi, S., Seager, S., et al. (2016) 'The habitable exoplanet (HabEx) imaging mission: preliminary science drivers and technical requirements', *Space Telescopes and Instrumentation 2016: Optical, Infrared, and Millimeter Wave*, 9904, p. 99040L. doi: 10.1117/12.2240457.

Merino, N., Aronson, H. S., Bojanova, D. P., et al. (2019) ‘Living at the extremes: extremophiles and the limits of life in a planetary context’, *Frontiers in Microbiology*, 10(MAR), p. 780. doi: 10.3389/fmicb.2019.00780.

Methé, B. A., Nelson, K. E., Deming, J. W., et al. (2005) ‘The psychrophilic lifestyle as revealed by the genome sequence of *Colwellia psychrerythraea* 34H through genomic and proteomic analyses’, *Proceedings of the National Academy of Sciences of the United States of America*, 102(31), pp. 10913–10918. doi: 10.1073/pnas.0504766102.

Michaud, A. B., Vick-Majors, T. J., Achberger, A. M., et al. (2020) ‘Environmentally clean access to Antarctic subglacial aquatic environments’, *Antarctic Science*, 32(5), pp. 329–340. doi: 10.1017/S0954102020000231.

Mikal-Evans, T. (2021) ‘Detecting the proposed CH_4–CO_2 biosignature pair with the James Webb Space Telescope: TRAPPIST-1e and the effect of cloud/haze’, *Monthly Notices of the Royal Astronomical Society*, 510(1), pp. 980–991. doi: 10.1093/MNRAS/STAB3383.

Miller, S. L. and Bada, J. L. (1988) ‘Submarine hot springs and the origin of life’, *Nature*, 334(6183), pp. 609–611. doi: 10.1038/334609a0.

Mitchell, A. L., Scheremetjew, M., Denise, H., et al. (2018) ‘EBI Metagenomics in 2017: Enriching the analysis of microbial communities, from sequence reads to assemblies’, *Nucleic Acids Research*, 46(D1), pp. D726–D735. doi: 10.1093/nar/gkx967.

Miteva, V. I., Sheridan, P. P. and Brenchley, J. E. (2004) ‘Phylogenetic and physiological diversity of microorganisms isolated from a deep Greenland glacier ice core’, *American Society for Microbiology*, 70(1), pp. 202–213. doi: 10.1128/AEM.

Mohapatra, M., Behera, P., Kim, J. Y., et al. (2020) ‘Seasonal and spatial dynamics of bacterioplankton communities in a brackish water coastal lagoon’, *Science of The Total Environment*, 705, 134729. doi: 10.1016/j.scitotenv.2019.134729.

Mosca, C., Fagliarone, C., Napoli, A., et al. (2021) ‘Revival of anhydrobiotic cyanobacterium biofilms exposed to space vacuum and prolonged dryness: implications for future missions beyond low Earth orbit’, *Astrobiology*, 21(5), pp. 541–550. doi: 10.1089/ast.2020.2359.

Murchie, S. L., Boldt, J., Ehlmann, B. L., et al. (2020) ‘Europa Lander Stereo Spectral Imaging Experiment (ELSSIE)’, *American Geophysical Union, Fall Meeting 2020*, abstract #P044-0009, 2020, pp. P044-0009. (Accessed: 4 June 2021).

Myrgorodska, I., Meinert, C., Martins, Z., et al. (2016) ‘Quantitative enantioseparation of amino acids by comprehensive two-dimensional gas chromatography applied to non-terrestrial samples’, *Journal of Chromatography A*, 1433, pp. 131–136. doi: 10.1016/j.chroma.2016.01.014.

NASA (2019) ‘The LUVOIR Mission Concept Study Final Report’. doi: 10.48550/arxiv.1912.06219.

NASA (2020) *Assessment of the Report of NASA’s Planetary Protection Independent Review Board. Washington, D.C.: National Academies Press*. doi: 10.17226/25773.

NASA (2022) ‘Origins, Worlds, and Life: A Decadal Strategy for Planetary Science and Astrobiology 2023-2032’, *Planetary Science and Astrobiology Decadal Survey*. doi: 10.17226/26522.

Nealson, K. H. (1997) ‘The limits of life on Earth and searching for life on Mars’, *Journal of Geophysical Research: Planets*, 102(E10), pp. 23675–23686. doi: 10.1029/97JE01996.

Néri, A., Guyot, F., Reynard, B., et al. (2020) ‘A carbonaceous chondrite and cometary origin for icy moons of Jupiter and Saturn’, *Earth and Planetary Science Letters*, 530, pp. 1–10. doi: 10.1016/j.epsl.2019.115920.

Neveu, M., Anbar, A. D., Davila, A. F., et al. (2020) ‘Returning samples from Enceladus for life detection’, *Frontiers in Astronomy and Space Sciences*, 7, p. 26. doi: 10.3389/fspas.2020.00026.

Neveu, M., Desch, S. J. and Castillo-Rogez, J. C. (2017) ‘Aqueous geochemistry in icy world interiors: Equilibrium fluid, rock, and gas compositions, and fate of antifreezes and radionuclides’, *Geochimica et Cosmochimica Acta*, 212, pp. 324–371. doi: 10.1016/j.gca.2017.06.023.

Neveu, M. and Rhoden, A. R. (2019) ‘Evolution of Saturn’s mid-sized moons’, *Nature Astronomy*, 3(6), pp. 543–552. doi: 10.1038/s41550-019-0726-y.

Newman, S. F., Buratti, B. J., Jaumann, R., et al. (2007) ‘Hydrogen peroxide on Enceladus’, *The Astrophysical Journal*, 670(2), pp. L143–L146. doi: 10.1086/524403.

Nishimura, Y., Ino, T. and Iizuka, H. (1988) ‘*Acinetobacter radioresistens* sp. nov. isolated from cotton and soil’, *International Journal of Systematic Bacteriology*, 38(2), pp. 209–211. doi: 10.1099/00207713-38-2-209.

Noll, K. S., Johnson, R. E., Lane, A. L., et al. (1996) ‘Detection of ozone on Ganymede’, *Science*, 273(5273), pp. 341–343. doi: 10.1126/science.273.5273.341.

Noll, K. S., Johnson, R. E., McGrath, M. A., et al. (1997) ‘Detection of SO_2 on Callisto with the Hubble Space Telescope’, *Geophysical Research Letters*, 24(9), pp. 1139–1142. doi: 10.1029/97GL00876.

Nordheim, T. A., Hand, K. P. and Paranicas, C. (2018) ‘Preservation of potential biosignatures in the shallow subsurface of Europa’, *Nature Astronomy*, 2(8), pp. 673–679. doi: 10.1038/s41550-018-0499-8.

Nozais, C., Vincent, W. F., Belzile, C., et al. (2021) ‘The Great Whale River ecosystem: ecology of a subarctic river and its receiving waters in coastal Hudson Bay, Canada’, *Écoscience*, 28(3-4), pp. 1–20. doi: 10.1080/11956860.2021.1926137.

O’Malley-James, J. T. and Kaltenegger, L. (2018) ‘The vegetation red edge biosignature through time on Earth and exoplanets’, *Astrobiology*, 18(9), pp. 1123–1136. doi: 10.1089/ast.2017.1798.

O’Malley-James, J. T. and Kaltenegger, L. (2019) ‘Expanding the timeline for Earth’s photosynthetic red edge biosignature’, *The Astrophysical Journal*, 879(2), p. L20. doi: 10.3847/2041-8213/ab2769.

Oksanen, J., Blanchet, F. G., Friendly, M., et al. (2020) ‘vegan: Community Ecology Package Version 2.5-7’.

Oktavia, L., Mulyani, I. and Suendo, V. (2021) ‘Investigation of chlorophyl-*a* derived compounds as photosensitizer for photodynamic inactivation’, *Bulletin of Chemical Reaction Engineering & Catalysis*, 16(1), pp. 161–169. doi: 10.9767/BCREC.16.1.10314.161-169.

Olsson-Francis, K. and Cockell, C. S. (2010) 'Experimental methods for studying microbial survival in extra-terrestrial environments', *Journal of Microbiological Methods*, 80(1), pp. 1–13. doi: 10.1016/j.mimet.2009.10.004.

Onofri, S., Barreca, D., Selbmann, L., et al. (2008) 'Resistance of Antarctic black fungi and cryptoendolithic communities to simulated space and Martian conditions', *Studies in Mycology*, 61(1), p. 99. doi: 10.3114/SIM.2008.61.10.

Onofri, S., Selbmann, L., Pacelli, C., et al. (2018) 'Integrity of the DNA and cellular ultrastructure of Cryptoendolithic Fungi in space or Mars conditions: A 1.5-Year study at the International Space Station', *Life*, 8(2), p.23. doi: 10.3390/LIFE8020023.

Oren, A. and Rodriguez-Valera, F. (2001) 'The contribution of halophilic Bacteria to the red coloration of saltern crystallizer ponds', *FEMS Microbiology Ecology*, 36(2–3), pp. 123–130. doi: 10.1111/j.1574-6941.2001.tb00832.x.

Ortega-Retuerta, E., Joux, F., Jeffrey, W. H., et al. (2013) 'Spatial variability of particle-attached and free-living bacterial diversity in surface waters from the Mackenzie River to the Beaufort Sea (Canadian Arctic)', *Biogeosciences*, 10(4), pp. 2747–2759. doi: 10.5194/bg-10-2747-2013.

Painter, T. H., Duval, B., Thomas, W. H., et al. (2001) 'Detection and quantification of snow algae with an airborne imaging spectrometer', *Applied and Environmental Microbiology*, 67(3–12), pp. 5267–5272. doi: 10.1128/aem.67.11.5267-5272.2001.

Parada, A. E., Needham, D. M. and Fuhrman, J. A. (2016) 'Every base matters: assessing small subunit rRNA primers for marine microbiomes with mock communities, time series and global field samples', *Environmental Microbiology*, 18(5), pp. 1403–1414. doi: 10.1111/1462-2920.13023.

Pascoal, F., Costa, R., Assmy, P., et al. (2021) 'Exploration of the types of rarity in the arctic ocean from the perspective of multiple methodologies.', *Microbial ecology*. doi: 10.1007/s00248-021-01821-9.

Penru, Y., Raaijmakers, M. J. T., Guastalli, A. R., et al. (2012) 'Influence of high salinity on the degradation of humic acid by UV_{254} and H_2O_2/UV_{254}', *Ozone: Science & Engineering*, 34(2), pp. 101–108. doi: 10.1080/01919512.2012.649998.

Perovich, D. K. (2002) 'Ultraviolet radiation and the optical properties of sea ice and snow', in *UV Radiation and Arctic Ecosystems. Springer, Berlin, Heidelberg*, pp. 73–89. doi: 10.1007/978-3-642-56075-0_4.

Phillips, C. B. and Pappalardo, R. T. (2014) 'Europa Clipper Mission Concept: exploring Jupiter's ocean moon', *Eos, Transactions American Geophysical Union*, 95(20), pp. 165–167. doi: 10.1002/2014EO200002.

Pizzetti, I., Fuchs, B. M., Gerdts, G., et al. (2011) 'Temporal variability of coastal *Planctomycetes* clades at Kabeltonne station, North Sea', *Applied and Environmental Microbiology*, 77(14), pp. 5009–5017. doi: 10.1128/AEM.02931-10.

Popova, A. (2017) 'Spectral characteristics and solubility of beta-carotene and zeaxanthin in different solvents', *Comptes rendus de l'Académie bulgare des Sciences*, 70(1).

Porco, C. C., Helfenstein, P., Thomas, P. C., et al. (2006) 'Cassini observes the active south pole of Enceladus', *Science*, 311(5766), pp. 1393–1401. doi: 10.1126/science.1123013.

Postberg, F., Kempf, S., Schmidt, J., et al. (2009) 'Sodium salts in E-ring ice grains from an ocean below the surface of Enceladus', *Nature*, 459(7250), pp. 1098–1101. doi: 10.1038/nature08046.

Postberg, F., Schmidt, J., Hillier, J., et al. (2011) 'A salt-water reservoir as the source of a compositionally stratified plume on Enceladus', *Nature*, 474(7353), pp. 620–622. doi: 10.1038/nature10175.

Postberg, F., Khawaja, N., Abel, B., et al. (2018) 'Macromolecular organic compounds from the depths of Enceladus', *Nature*, 558(7711), pp. 564–568. doi: 10.1038/s41586-018-0246-4.

Price, P. B. (2007) 'Microbial life in glacial ice and implications for a cold origin of life', *FEMS Microbiology Ecology*, 59(2), pp. 217–231. doi: 10.1111/j.1574-6941.2006.00234.x.

Przytulska, A., Comte, J., Crevecoeur, S., et al. (2016) 'Phototrophic pigment diversity and picophytoplankton in permafrost thaw lakes', *Biogeosciences*, 13(1), pp. 13–26. doi: 10.5194/BG-13-13-2016.

Ramirez, R. M. and Kaltenegger, L. (2018) 'A methane extension to the classical habitable zone', *The Astrophysical Journal*, 858(2), p. 72. doi: 10.3847/1538-4357/AAB8FA.

Rapp, J. Z., Fernández-Méndez, M., Bienhold, C., et al. (2018) 'Effects of ice-algal aggregate export on the connectivity of bacterial communities in the central arctic ocean', *Frontiers in Microbiology*, 9(MAY), p. 1035. doi: 10.3389/fmicb.2018.01035.

Raulin, F., Hand, K. P., McKay, C. P., et al. (2010) 'Exobiology and planetary protection of icy moons', *Space Science Reviews*, 153(1–4), pp. 511–535. doi: 10.1007/s11214-009-9610-x.

Reddy, G. S. N., Matsumoto, G. I., Schumann, P., et al. (2004) 'Psychrophilic pseudomonads from Antarctica: *Pseudomonas antarctica* sp. nov., *Pseudomonas meridiana* sp. nov. and *Pseudomonas proteolytica* sp. nov.', *International Journal of Systematic and Evolutionary Microbiology*, 54(3), pp. 713–719. doi: 10.1099/ijs.0.02827-0.

Regberg, A., Burton, A., McCubbin, F., et al. (2018) 'Microbial ecology of NASA curation clean rooms', in *43rd COSPAR Scientific Assembly*. Held 28 January-4 February 43, p. PPP.3-18-18. (Accessed: 13 January 2022).

Regberg, A. B., Castro, C. L., Connolly, H. C., et al. (2019) 'Microbial ecology of the OSIRIS-REx assembly test and launch environment', in *50th Lunar and Planetary Science Conference.*

Reh, K., Spilker, L., Lunine, J. I., et al. (2016) 'Enceladus Life Finder: the search for life in a habitable moon', in *2016 IEEE Aerospace Conference. IEEE*, pp. 1–8. doi: 10.1109/AERO.2016.7500813.

Rettberg, P., Antunes, A., Brucato, J., et al. (2019) 'Biological contamination prevention for outer solar system moons of astrobiological interest: what do we need to know?', *Astrobiology*, 19(8), pp. 951–974. doi: 10.1089/ast.2018.1996.

Rezzonico, F. (2014) 'Nanopore-Based instruments as biosensors for future planetary missions', *Astrobiology*, 14(4), pp. 344–351. doi: 10.1089/ast.2013.1120.

Riedel, A., Michel, C., Gosselin, M., et al. (2008) 'Winter–spring dynamics in sea-ice carbon cycling in the coastal Arctic Ocean', *Journal of Marine Systems*, 74(3–4), pp. 918–932. doi: 10.1016/j.jmarsys.2008.01.003.

Van Riel, M., Hammans, J. K., Van De Ven, M., et al. (1983) 'Fluorescence excitation profiles of beta-carotene in solution and in lipid/water mixtures', *Biochemical and Biophysical Research Communications*, 113(1), pp. 102–107. doi: 10.1016/0006-291X(83)90437-0.

Roff, J. C. and Legendre, L. (1986) 'Physico-chemical and biological oceanography of Hudson Bay', *Elsevier Oceanography Series*, 44(C), pp. 265–292. doi: 10.1016/S0422-9894(08)70907-3.

Rogers, S. O., Theraisnathan, V., Ma, L. J., et al. (2004) 'Comparisons of protocols for decontamination of environmental ice samples for biological and molecular examinations', *Applied and Environmental Microbiology*, 70(4), pp. 2540–2544. doi: 10.1128/AEM.70.4.2540-2544.2004.

Roos, J. C. and Vincent, W. F. (1998) 'Temperature dependence of UV radiation effects on antarctic cyanobacteria', *Journal of Phycology*, 34(1), pp. 118–125. doi: 10.1046/j.1529-8817.1998.340118.x.

Rothschild, L. J. and Mancinelli, R. L. (2001) 'Life in extreme environments', *Nature*, 409(6823), pp. 1092–1101. doi: 10.1038/35059215.

Russell, M. J., Murray, A. E. and Hand, K. P. (2017) 'The possible emergence of life and differentiation of a shallow biosphere on irradiated icy worlds: the example of Europa', *Astrobiology*, 17(12), pp. 1265–1273. doi: 10.1089/ast.2016.1600.

Sagan, C., Thompson, W. R., Carlson, R., et al. (1993) 'A search for life on Earth from the Galileo spacecraft', *Nature*, 365(6448), pp. 715–721. doi: 10.1038/365715a0.

Salter, S. J., Cox, M. J., Turek, E. M., et al. (2014) 'Reagent and laboratory contamination can critically impact sequence-based microbiome analyses', *BMC Biology*, 12(1), p. 87. doi: 10.1186/s12915-014-0087-z.

Sangwan, P., Chen, X., Hugenholtz, P., et al. (2004) '*Chthoniobacter flavus* gen. nov., sp. nov., the first pure-culture representative of subdivision two, *Spartobacteria* classis nov., of the phylum *Verrucomicrobia*', *Applied and Environmental Microbiology*, 70(10), p. 5875. doi: 10.1128/AEM.70.10.5875-5881.2004.

dos Santos, R., Patel, M., Cuadros, J., et al. (2016) 'Influence of mineralogy on the preservation of amino acids under simulated Mars conditions', *Icarus*, 277, pp. 342–353. doi: 10.1016/j.icarus.2016.05.029.

Satomi, M., La Duc, M. T. and Venkateswaran, K. (2006) '*Bacillus safensis* sp.nov., isolated from spacecraft and assembly-facility surfaces', *International Journal of Systematic and Evolutionary Microbiology*, 56(8), pp. 1735–1740. doi: 10.1099/ijs.0.64189-0.

Saur, J., Duling, S., Roth, L., et al. (2015) 'The search for a subsurface ocean in Ganymede with Hubble Space Telescope observations of its auroral ovals', *Journal of Geophysical Research: Space Physics*, 120(3), pp. 1715–1737. doi: 10.1002/2014JA020778.

Scalo, J., Kaltenegger, L., Segura, A. G., et al. (2007) 'M Stars as targets for terrestrial exoplanet searches and biosignature detection', *AsBio*, 7(1), pp. 85–166. doi: 10.1089/AST.2006.0125.

SCAR (2017) ‘SCAR’s Code of Conduct for the Exploration and Research of Subglacial Aquatic Environments Background’. (Accessed: 5 March 2022).

Schmidt, B. E., Blankenship, D. D., Patterson, G. W., et al. (2011) ‘Active formation of “chaos terrain” over shallow subsurface water on Europa’, *Nature*, 479(7374), pp. 502–505. doi: 10.1038/nature10608.

Schwendner, P., Riedo, A., Melton, D. J., et al. (2022) ‘Microbial metabolism of amino acids—biologically induced removal of glycine and the resulting fingerprint as a potential biosignature’, *Frontiers in Astronomy and Space Sciences*, 9, p. 52. doi: 10.3389/FSPAS.2022.781542.

Schwieterman, E. W., Cockell, C. S. and Meadows, V. S. (2015) ‘Nonphotosynthetic pigments as potential biosignatures’, *Astrobiology*, 15(5), pp. 341–361. doi: 10.1089/ast.2014.1178.

Seager, S., Turner, E. L., Schafer, J., et al. (2005) ‘Vegetation’s red edge: a possible spectroscopic biosignature of extra-terrestrial plants’, *Astrobiology*, 5(3), pp. 372–390. doi: 10.1089/ast.2005.5.372.

Seel, W., Baust, D., Sons, D., et al. (2020) ‘Carotenoids are used as regulators for membrane fluidity by *Staphylococcus xylosus’*, *Scientific Reports*, 10(1), p. 330. doi: 10.1038/s41598-019-57006-5.

Segura, A., Walkowicz, L. M., Meadows, V., et al. (2010) ‘The effect of a strong stellar flare on the atmospheric chemistry of an Earth-like planet orbiting an M dwarf’, *Astrobiology*, 10(7), pp. 751–771. doi: 10.1089/ast.2009.0376.

Serindag, D. B. and Snellen, I. A. G. (2019) ‘Testing the detectability of extra-terrestrial O_2 with the extremely large telescopes using real data with real noise’, *The Astrophysical Journal*, 871(1), p. L7. doi: 10.3847/2041-8213/aafa1f.

Serrano, L., Peñuelas, J. and Ustin, S. L. (2002) ‘Remote sensing of nitrogen and lignin in Mediterranean vegetation from AVIRIS data’, *Remote Sensing of Environment*, 81(2–3), pp. 355–364. doi: 10.1016/S0034-4257(02)00011-1.

Shen, L., Liu, Y., Wang, N., et al. (2018) ‘Variation with depth of the abundance, diversity and pigmentation of culturable bacteria in a deep ice core from the Yuzhufeng Glacier, Tibetan Plateau’, *Extremophiles*, 22(1), pp. 29–38. doi: 10.1007/s00792-017-0973-8.

Sheridan, P. P., Miteva, V. I. and Brenchley, J. E. (2003) ‘Phylogenetic analysis of anaerobic psychrophilic enrichment cultures obtained from a Greenland glacier ice core’, *Applied and Environmental Microbiology*, 69(4), pp. 2153–2160. doi: 10.1128/AEM.69.4.2153-2160.2003.

Sherpa, M. T., Najar, I. N., Das, S., et al. (2018) ‘Bacterial diversity in an alpine debris-free and debris-cover accumulation zone glacier ice, North Sikkim, India’, *Indian Journal of Microbiology*, 58(4), pp. 470–478. doi: 10.1007/s12088-018-0747-8.

Sherwood, B. (2016) ‘Strategic map for exploring the ocean-world Enceladus’, *Acta Astronautica*, 126, pp. 52–58. doi: 10.1016/J.ACTAASTRO.2016.04.013.

Shields, A. L., Ballard, S., Johnson, J. A., et al. (2016) ‘The habitability of planets orbiting M-dwarf stars’, *Physics Report*, 663, p. 1-38. doi: 10.1016/J.PHYSREP.2016.10.003.

Shivaji, S., Begum, Z., Rao, S. S. S. N., et al. (2013) 'Antarctic ice core samples: culturable bacterial diversity', *Research in Microbiology*, 164, pp. 70–82. doi: http://dx.doi.org/10.1016/j.resmic.2012.09.001.

Shock, E. L. and McKinnon, W. B. (1993) 'Hydrothermal processing of cometary volatiles—applications to Triton', *Icarus*, 106(2), pp. 464–477. doi: 10.1006/icar.1993.1185.

Shtarkman, Y. M., Koçer, Z. A., Edgar, R., et al. (2013) 'Subglacial Lake Vostok (Antarctica) accretion ice contains a diverse set of sequences from aquatic, marine and sediment-inhabiting bacteria and Eukarya', *PLOS ONE*, 8(7), p. e67221. doi: 10.1371/journal.pone.0067221.

Smith, C. L., Russell, S. S., Hutzler, A., et al. (2021) 'A roadmap for a European extra-terrestrial sample curation facility – the EUROCARES project', *Sample Return Missions*, pp. 249–268. doi: 10.1016/B978-0-12-818330-4.00013-6.

Soderlund, K. M., Kalousová, K., Buffo, J. J., et al. (2020) 'Ice-ocean exchange processes in the Jovian and Saturnian satellites', *Space Science Reviews*, 216(5), pp. 1–57. doi: 10.1007/S11214-020-00706-6.

Sommerstein, R., Führer, U., Lo Priore, E., et al. (2017) '*Burkholderia stabilis* outbreak associated with contaminated commercially-available washing gloves, Switzerland, May 2015 to August 2016', *Eurosurveillance*, 22(49). doi: 10.2807/1560-7917.ES.2017.22.49.17-00213.

Spry, J. A., Siegel, B., Kminek, G., et al. (2021) 'Planetary protection knowledge gaps and enabling science for human Mars missions', *Bulletin of the AAS*, 53(4), p. 205. doi: 10.3847/25c2cfeb.4a582a02.

Squyres, S. W., Reynolds, R. T., Cassen, P. M., et al. (1983) 'Liquid water and active resurfacing on Europa', *Nature*, 301(5897), pp. 225–226. doi: 10.1038/301225a0.

Stelzer, B., Marino, A., Micela, G., et al. (2013) 'The UV and X-ray activity of the M dwarfs within 10 pc of the Sun', *Monthly Notices of the Royal Astronomical Society*, 431(3), pp. 2063–2079. doi: 10.1093/MNRAS/STT225.

Stevenson, J., Lunine, J. and Clancy, P. (2015) 'Membrane alternatives in worlds without oxygen: creation of an azotosome', *Science Advances*, 1(1), p. e1400067. doi: 10.1126/sciadv.1400067.

Strain, H. H., Thomas, M. R. and Katz, J. J. (1963) 'Spectral absorption properties of ordinary and fully deuteriated chlorophylls *a* and *b*', *BBA - Biochimica et Biophysica Acta*, 75(C), pp. 306–311. doi: 10.1016/0006-3002(63)90617-6.

Sundholm, D. (1999) 'Density functional theory calculations of the visible spectrum of chlorophyll *a*', *Chemical Physics Letters*, 302(5–6), pp. 480–484. doi: 10.1016/S0009-2614(99)00194-3.

Szalay, L., Tombácz, E. and Singhal, G. S. (1974) 'Effect of solvent on the absorption spectra and Stokes' shift of absorption and fluorescence of chlorophylls', *Acta Physica Academiae Scientiarum Hungaricae*, 35(1), pp. 29–36. doi: 10.1007/BF03159738.

Taniguchi, M. and Lindsey, J. S. (2021) 'Absorption and fluorescence spectral database of chlorophylls and analogues', *Photochemistry and Photobiology*, 97(1), pp. 136–165. doi: 10.1111/PHP.13319.

Tarter, J. C., Backus, P. R., Mancinelli, R. L., et al. (2007) ‘A reappraisal of the habitability of planets around M Dwarf stars’, *Astrobiology*, 7(1), pp. 30–65. doi: 10.1089/AST.2006.0124.

Tian, J. and Philpot, W. (2018) ‘Spectral transmittance of a translucent sand sample with directional illumination’, *IEEE Transactions on Geoscience and Remote Sensing*, 56(8), pp. 4307–4317. doi: 10.1109/TGRS.2018.2810815.

Tilley, M. A., Segura, A., Meadows, V., et al. (2019) ‘Modeling repeated M Dwarf flaring at an Earth-like planet in the habitable zone: atmospheric effects for an unmagnetized planet’, *Astrobiology*, 19(1), pp. 64–86. doi: 10.1089/ast.2017.1794.

Tinetti, G., Drossart, P., Eccleston, P., et al. (2018) ‘A chemical survey of exoplanets with ARIEL’, *Experimental Astronomy*, 46(1), pp. 135–209. doi: 10.1007/S10686-018-9598-X.

Trumbo, S. K., Brown, M. E. and Hand, K. P. (2019a) ‘H_2O_2 within Chaos Terrain on Europa’s Leading Hemisphere’, *The Astronomical Journal*, 158(3), p. 127. doi: 10.3847/1538-3881/ab380c.

Trumbo, S. K., Brown, M. E. and Hand, K. P. (2019b) ‘Sodium chloride on the surface of Europa’, *Science Advances*, 5(6), pp. 2–6. doi: 10.1126/sciadv.aaw7123.

Tsou, P., Brownlee, D. E., McKay, C. P., et al. (2012) ‘LIFE: Life Investigation For Enceladus a sample return mission concept in search for evidence of life.’, *Astrobiology*, 12(8), pp. 730–742. doi: 10.1089/ast.2011.0813.

Ustin, S. L., Gitelson, A. A., Jacquemoud, S., et al. (2009) ‘Retrieval of foliar information about plant pigment systems from high resolution spectroscopy’, *Remote Sensing of Environment*, 113, pp. S67–S77. doi: 10.1016/J.RSE.2008.10.019.

Vance, S., Harnmeijer, J., Kimura, J., et al. (2007) ‘Hydrothermal systems in small ocean planets’, *Astrobiology*, 7(6), pp. 987–1005. doi: 10.1089/ast.2007.0075.

Vance, S. D., Hand, K. P. and Pappalardo, R. T. (2016) ‘Geophysical controls of chemical disequilibria in Europa’, *Geophysical Research Letters*, 43(10), pp. 4871–4879. doi: 10.1002/2016GL068547.

Vavilin, D. V., Ermakova-Gerdes, S. Y., Keilty, A. T., et al. (1999) ‘Tryptophan at position 181 of the D2 protein of photosystem II confers quenching of variable fluorescence of chlorophyll: implications for the mechanism of energy-dependent quenching’, *Biochemistry*, 38(44), pp. 14690–14696. doi: 10.1021/BI9915622.

Vigneron, A., Cruaud, P., Mohit, V., et al. (2018) ‘Multiple strategies for light-harvesting, photoprotection, and carbon flow in high latitude microbial mats’, *Frontiers in Microbiology*, 9, p. 2881. doi: 10.3389/fmicb.2018.02881.

Vincent, W. F., Downes, M., Castenholz, R., et al. (1993) ‘Community structure and pigment organisation of cyanobacteria-dominated microbial mats in Antarctica’, *European Journal of Phycology*, 28(4), pp. 213–221. doi: 10.1080/09670269300650321.

Vincent, W. F., Mueller, D. R. and Bonilla, S. (2004) ‘Ecosystems on ice: the microbial ecology of Markham Ice Shelf in the high Arctic’, *Cryobiology*, 48(2), pp. 103–112. doi: 10.1016/j.cryobiol.2004.01.006.

Vincent, W. F. and Quesada, A. (2012) ‘Cyanobacteria in high latitude lakes, rivers and seas’, in *Ecology of Cyanobacteria II. Dordrecht: Springer Netherlands*, pp. 371–385. doi: 10.1007/978-94-007-3855-3_13.

Vincent, W. F. and Roy, S. (1993b) ‘Solar ultraviolet-B radiation and aquatic primary production: damage, protection, and recovery’, Environmental Reviews, 1(1), pp. 1–12. doi: 10.1139/a93-001.

Vítek, P., Ascaso, C., Artieda, O., et al. (2017) ‘Discovery of carotenoid red-shift in endolithic cyanobacteria from the Atacama Desert’, *Scientific Reports*, 7(1). doi: 10.1038/s41598-017-11581-7.

Waite, J. H., Combi, M. R., Ip, W. H., et al. (2006) ‘Cassini ion and neutral mass spectrometer: Enceladus plume composition and structure’, *Science*, 311(5766), pp. 1419–1422. doi: 10.1126/science.1121290.

Waite, J. H., Lewis, W. S., Magee, B. A., et al. (2009) ‘Liquid water on Enceladus from observations of ammonia and ^{40}Ar in the plume’, *Nature*, 460(7254), pp. 487–490. doi: 10.1038/nature08153.

Waite, J. H., Glein, C. R., Perryman, R. S., et al. (2017) ‘Cassini finds molecular hydrogen in the Enceladus plume: evidence for hydrothermal processes’, *Science*, 356(6334), pp. 155–159. doi: 10.1126/science.aai8703.

Waleron, M., Waleron, K., Vincent, W. F., et al. (2007) ‘Allochthonous inputs of riverine picocyanobacteria to coastal waters in the Arctic Ocean’, *FEMS Microbiology Ecology*, 59(2), pp. 356–365. doi: 10.1111/j.1574-6941.2006.00236.x.

Walker, C. C. and Schmidt, B. E. (2015) ‘Ice collapse over trapped water bodies on Enceladus and Europa’, *Geophysical Research Letters*, 42(3), pp. 712–719. doi: 10.1002/2014GL062405.

Wang, C. L., Ng, T. B., Yuan, F., et al. (2007) ‘Induction of apoptosis in human leukemia K562 cells by cyclic lipopeptide from *Bacillus subtilis* natto T-2’, *Peptides*, 28(7), pp. 1344–1350. doi: 10.1016/j.peptides.2007.06.014.

Wang, L., Wang, M., Zhang, J., et al. (2015) ‘An outbreak of *Burkholderia stabilis* colonization in a nasal ward’, *International Journal of Infectious Diseases*, 33, pp. 71–74. doi: 10.1016/j.ijid.2014.12.046.

Wellburn, A. R. (1994) ‘The Spectral determination of chlorophylls *a* and *b*, as well as total carotenoids, using various solvents with spectrophotometers of different resolution’, *Journal of Plant Physiology*, 144(3), pp. 307–313. doi: 10.1016/S0176-1617(11)81192-2.

Westall, F. and Brack, A. (2018) ‘The importance of water for life’, *Space Science Reviews*, 214(2), pp. 1–23. doi: 10.1007/s11214-018-0476-7.

Westall, Francès, Loizeau, D, Foucher, F., et al. (2013) ‘on Mars from a microbial point of view’, *Astrobiology*, 13(9), pp. 887–897. doi: 10.1089/ast.2013.1000ï.

Williamson, C. J., Cook, J., Tedstone, A., et al. (2020) ‘Algal photophysiology drives darkening and melt of the Greenland ice sheet’, *Proceedings of the National Academy of Sciences of the United States of America*, 117(11), pp. 5694–5705. doi: 10.1073/pnas.1918412117.

Wolstencroft, R. D. and Raven, J. A. (2002) ‘Photosynthesis: likelihood of occurrence and possibility of detection on Earth-like planets’, *Icarus*, 157(2), pp. 535–548. doi: 10.1006/ICAR.2002.6854.

Wood, J. M., Singh, N. K., Guan, L., et al. (2021) 'Performance of multiple metagenomics pipelines in understanding microbial diversity of a low-biomass spacecraft assembly facility', *Frontiers in Microbiology*, 12, p. 2739. doi: 10.3389/FMICB.2021.685254.

Xing, T., Yao, T., Liu, Y., et al. (2016) '*Polaromonas eurypsychrophila* sp. nov., isolated from an ice core', *International Journal of Systematic and Evolutionary Microbiology*, 66(7), pp. 2497–2501. doi: 10.1099/ijsem.0.001079.

Yabuzaki, J. (2017) 'Carotenoids database: structures, chemical fingerprints and distribution among organisms', *Database*, 2017(1), pp. 1–11. doi: 10.1093/database/bax004.

Yergeau, E., Michel, C., Tremblay, J., et al. (2017) 'Metagenomic survey of the taxonomic and functional microbial communities of seawater and sea ice from the Canadian Arctic', *Scientific Reports*, 7(1), p. 42242. doi: 10.1038/srep42242.

Zang, L. Y., Sommerburg, O. and Van Kuijk, F. J. G. M. (1997) 'Absorbance changes of carotenoids in different solvents', *Free Radical Biology and Medicine*, 23(7), pp. 1086–1089. doi: 10.1016/S0891-5849(97)00138-X.

Zhong, Z.-P., Solonenko, N. E., Gazitúa, M. C., et al. (2018) 'Clean low-biomass procedures and their application to ancient ice core microorganisms', *Frontiers in Microbiology*, 9(MAY), p. 1094. doi: 10.3389/fmicb.2018.01094.

IX APPENDIX

IX.1 Evolution of techniques used for contamination control during the sampling, processing, or biological analysis of ice cores from the last 23 years (Supplementary material of Chapters I and II)

Origin	Type of ice	Control	Replicates	Decontamination procedures	Analysis performed	Reference
Ellesmere Island (Canadian Arctic)	Glacier ice	N.A.	N.A	Sterile materials, Heat, Ethanol (95%) used on equipment/material, the filtration assembly was sterilized between samples	Culture-dependent analysis	(Dancer, Shears and Platt, 1997)
Vostok 5G ice core (Antarctica)	Lake accretion ice	N.A.	One ice core, ten ice sections	Sterile materials, Heat	Culture-dependent analysis	(Abyzov *et al.*, 2001)
Deep ice core – GISP2 (Greenland)	Glacier ice	Artificial sterile water ice core	N.A.	Sterile materials, Superficial layer removal (2-3mm), Ethanol (95%), Superficial layer removal (1 cm), Heat	Culture-independent and culture-dependent analysis	(Sheridan *et al.*, 2003), (Miteva, Sheridan and Brenchley, 2004)
Tallasksenvarden Nunatak (Antarctica)	Glacier ice	N.A.	N.A.	Sterile materials, Superficial layer removal	Culture-dependent analysis	(Shivaji *et al.*, 2013)
Vostok 5G ice core (Antarctica)	Lake accretion ice	Sterile water, Lake ice core water sterilized	One ice core, four ice sections	Sterile materials, Sodium hypochlorite solution at 4ºC, Sterile water	Culture-independent analysis	(D'Elia, Veerapaneni and Rogers, 2008, Shtarkman *et al.*, 2013),
Ellesmere Island (Canadian Arctic)	Sea ice	N.A.	Two ice cores	Sterile materials, the filtration assembly was sterilized between samples	Culture-independent analysis	(Hatam *et al.*, 2014)
Muztagh Glacier (Tibetan Plateau, China)	Glacier ice	N.A.	N.A.	Sterile materials, Superficial layer removal, Ethanol (95%), Sterile water	Culture-dependent analysis	(Xing *et al.*, 2016)
Cornwallis Island (Canadian Arctic)	Sea ice	N.A.	Eight ice cores per location	Sterile materials	Culture-independent analysis	(Yergeau *et al.*, 2017)
Yuzhufen Glacier (Tibetan Plateau)	Glacier ice	N.A.	One ice core, 4 sections, 1253 sub-sections	Sterile materials, Superficial layer removal, Sterile water, Ethanol (75%)	Culture-dependent analysis	(Shen *et al.*, 2018)
Matanuska Glacier (Alaska)	Glacier ice	N.A.	N.A.	Sterile materials, Superficial layer removal (5 mm), Sterile water, Ethanol (95%)	Culture-independent analysis	(Kayani *et al.*, 2018)
Changme Khang and Changme Khangpu glaciers (India)	Glacier ice	N.A.	One ice core per glacier	Sterile materials, Superficial layer removal, Sterile water, Ethanol (95%)	Culture-dependent analysis	(Sherpa *et al.*, 2018)
Scarisoara Ice Cave (Romania)	Perennial cave ice	N.A.	One ice core, five ice sections	Sterile materials	Culture-independent analysis	(Itcus *et al.*, 2018)
Guliya ice cap (Tibet)	Glacier	Artificial sterile water ice core, Air control, DNA extraction control, Standard 16S rRNA gene amplicon sequencing of controls	One ice core, five sections	Superficial layer removal, Ethanol 95% and new layer removed, Sterile water	Culture-independent analysis	(Zhong *et al.*, 2021)

Table IX.1 - Artificial sterile ice cores, as "mock" ice cores, were made in the laboratory and used as controls. N.A. means "non-available". Culture-dependent analysis refers to analysis performed on cultured microorganisms (e.g., colonies or liquid cultures). Culture-independent analyses include molecular biology studies, microscopy, and flow cytometry. This table was based on Table 1 from Christner *et al.*, (2005) (Christner *et al.*, 2005), updated to the present. From Coelho *et al.*, 2022, under review in *Sci Rep.*

IX.2 Taxonomic composition of prokaryotic communities in environmental samples after in-silico decontamination process (Supplementary material of Chapter II)

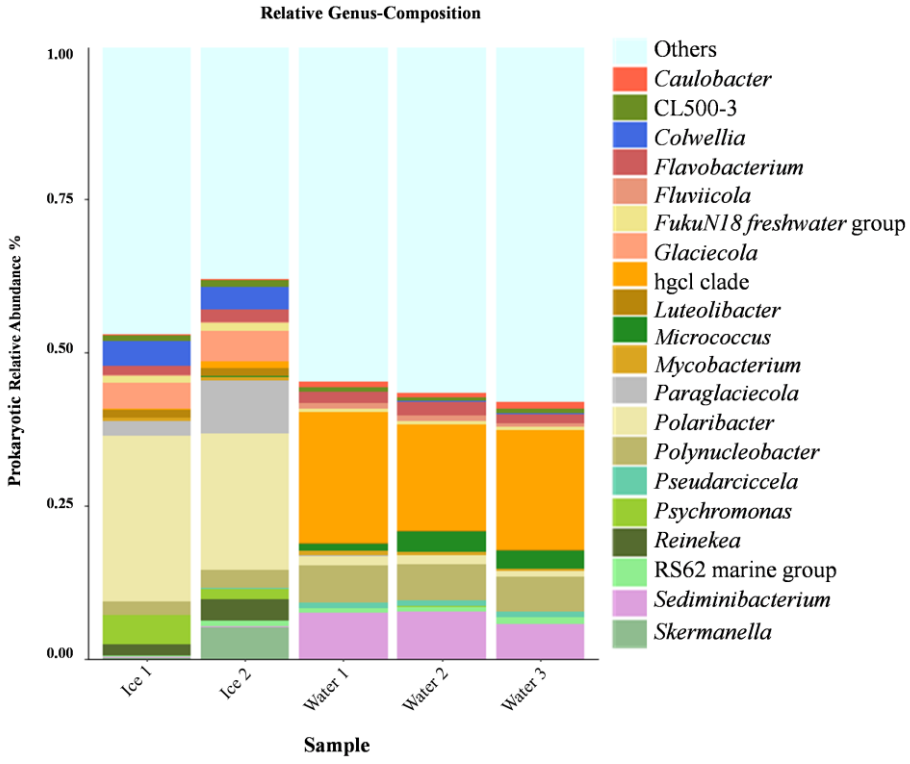

Figure IX.1 - Taxonomic composition of prokaryotic communities in environmental samples (ice and interface water, including replicates) after *in-silico* decontamination process where all OTUs present in the controls were removed. Results are based on the relative abundance of OTUs in the non-rarefied dataset. For improved readability, taxa below 0.5% of relative abundance were joined under the category "Others". Note that groups such as *Acinetobacter* and *Sulfurospirillum* are absent from the taxonomic profiles of these samples after removing contaminating OTUs. From Coelho *et al*., 2022, under review in *Sci Rep*.

IX.3 Rarefaction curves (Supplementary material of Chapter III)

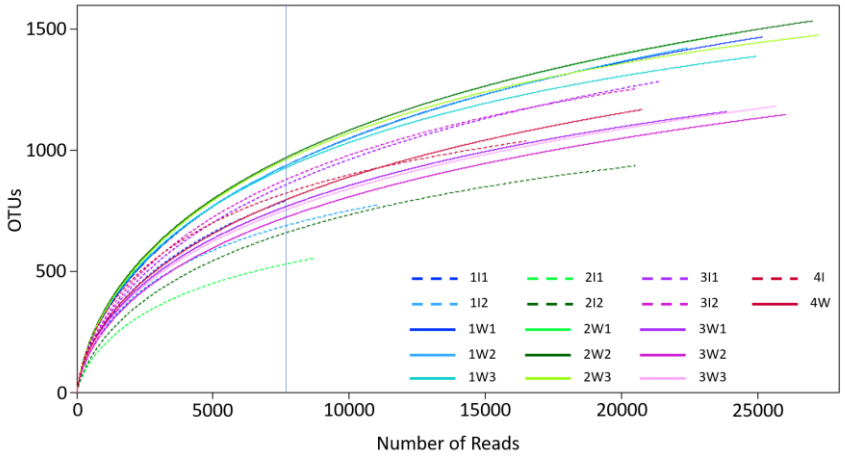

Rarefaction Curves
Rarefaction curves obtained for all the 17 samples, using function *rarecurve* (vegan package, R). The vertical line corresponds to the lowest number of reads (7634) which was determined for sample 1I1.

Figure IX.2 - Rarefaction curves projecting gain in OTU richness as a function of increasing sequencing depth. Shown are curves obtained for all sampling sites 1-4, using the function rarecurve (vegan package, R). The vertical line corresponds to the lowest number of 16S rRNA gene reads (7634) obtained for the characterization of a given sample, in this case, sample 1I1. This was used as a cut-off to compare alpha diversity metrics among samples **(Figure III.2)**. From Coelho *et al*., 2022, in *STOTEN*.

IX.4 Metadata (Supplementary material of Chapters III and IV)

Table IX.2 - Metadata collected for sampling sites 1 to 4. From Coelho *et al*., 2022, in *STOTEN*. Ice core size and ice cover depth were approximately 1 m for all sites.

Sampling site	**Coordinates**	**Snow depth (cm)**	**Chlorophylls µg/L**	**Sal PSU**	**BGA PC µg/L**	**Temp °C**	**fDOM QSU**
1	55.39°; -77.61°	20	0,86	10,4	1,49	0,4	35,9
2	55.38°; -77.62°	14	0,09	10,31	1,55	-0,4	35,4
3	55.30°; -77.76°	10	1,40	1,89	2,13	-0,1	30,1
4	55.27°; -77.81°	37	0,92	0,63	1,44	-0,02	41,5

IX.5 Phylum- and class-level prokaryotic community composition (Supplementary material of Chapter III)

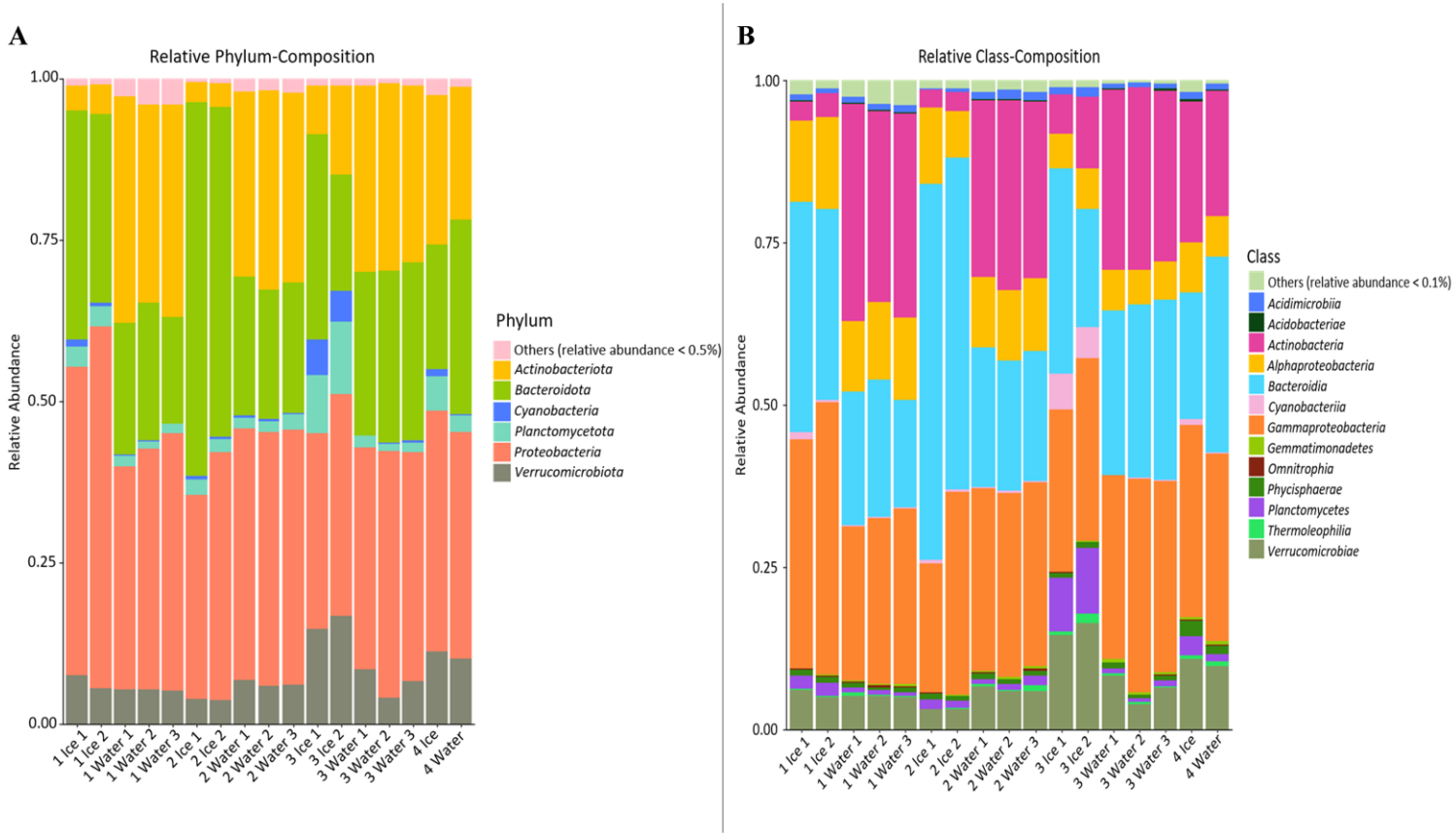

Figure IX.3 - Phylum- and class-level prokaryotic community composition based on the relative abundance of OTUs of the non-rarefied dataset. For improved readability, phyla below 0.5% and classes below 0.1% of relative abundance across the entire dataset were joined under the category "Others". From Coelho *et al*., 2022, in *STOTEN*.

IX.6 Taxonomic composition – with rarefied data. (Supplementary material of Chapter III)

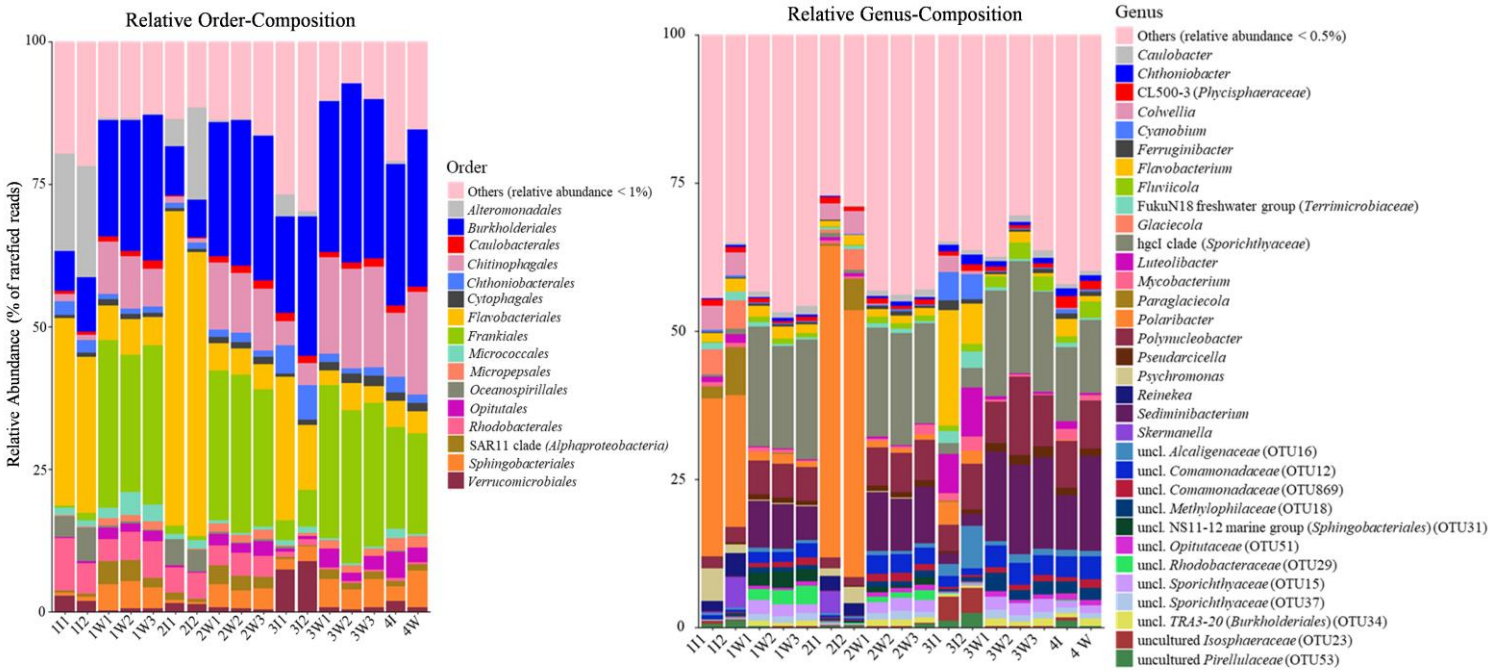

Figure IX.4 - Taxonomic composition of prokaryotic communities in ice and water. Left: order-level prokaryotic community composition based on the relative abundance of OTUs of the rarefied dataset. For improved readability, orders below 1% relative abundance across the entire dataset were joined under the category "Others". Right: genus-level prokaryotic community composition based on the relative abundance of OTUs of the rarefied dataset. For improved readability, genera below 0.5% relative abundance were joined under the category "Others". Diverse genera possessing low relative abundances (pink-labeled bars) are an integral part of both ice and water microbiomes. From Coelho *et al*., 2022, in *STOTEN*.

IX.7 Venn diagrams – with rarefied data (Supplementary material of Chapter III)

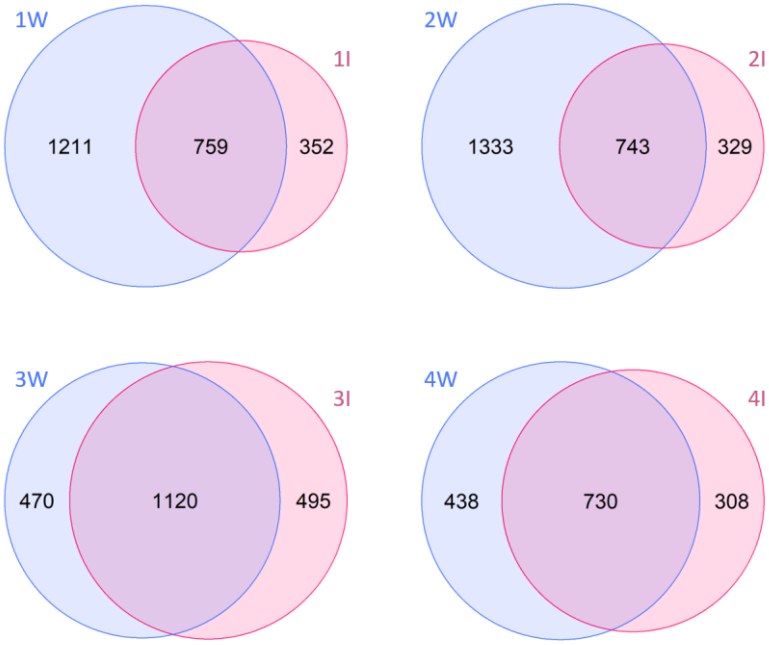

Figure IX.5 - Venn diagrams displaying OTUs shared by and unique to ice and interface water at each sampling site across the full, non-rarefied dataset. Replicates within each biotope (Ice *versus* Water) were pooled together for comparison between biotopes for each site (1 to 4). From Coelho *et al*., 2022, in *STOTEN*.

IX.8 Betadisper analysis results (Supplementary material of Chapter III)

Table IX.3 - Betadisper analysis results. From Coelho *et al*., 2022, in *STOTEN*.

	Ice	**Water**						
Betadisper	0.3587	0.1915						
The extent of variation (dispersion around Bray-Curtis similarity mean) in the OTU profiles of the ice communities (all sites) and water communities (all sites).								
	Site 1	**Site 2**	**Site 3**	**Site 4**				
Betadisper	0.3191	0.3201	0.2511	0.1664				
The extent of variation (dispersion around Bray-Curtis similarity mean) in the OTU profiles within each site, encompassing both water and ice samples.								
	1I	**1W**	**2I**	**2W**	**3I**	**3W**	**4I**	**4W**
Betadisper	0.2025	0.1220	0.2018	0.1200	0.1340	0.1111	-	-
The extent of variation (dispersion around Bray-Curtis similarity mean) in the OTU profiles of each biotope (I - Ice; W - Water) at each sample site.								

IX.9 Supplements from cultivation data (Chapter III)

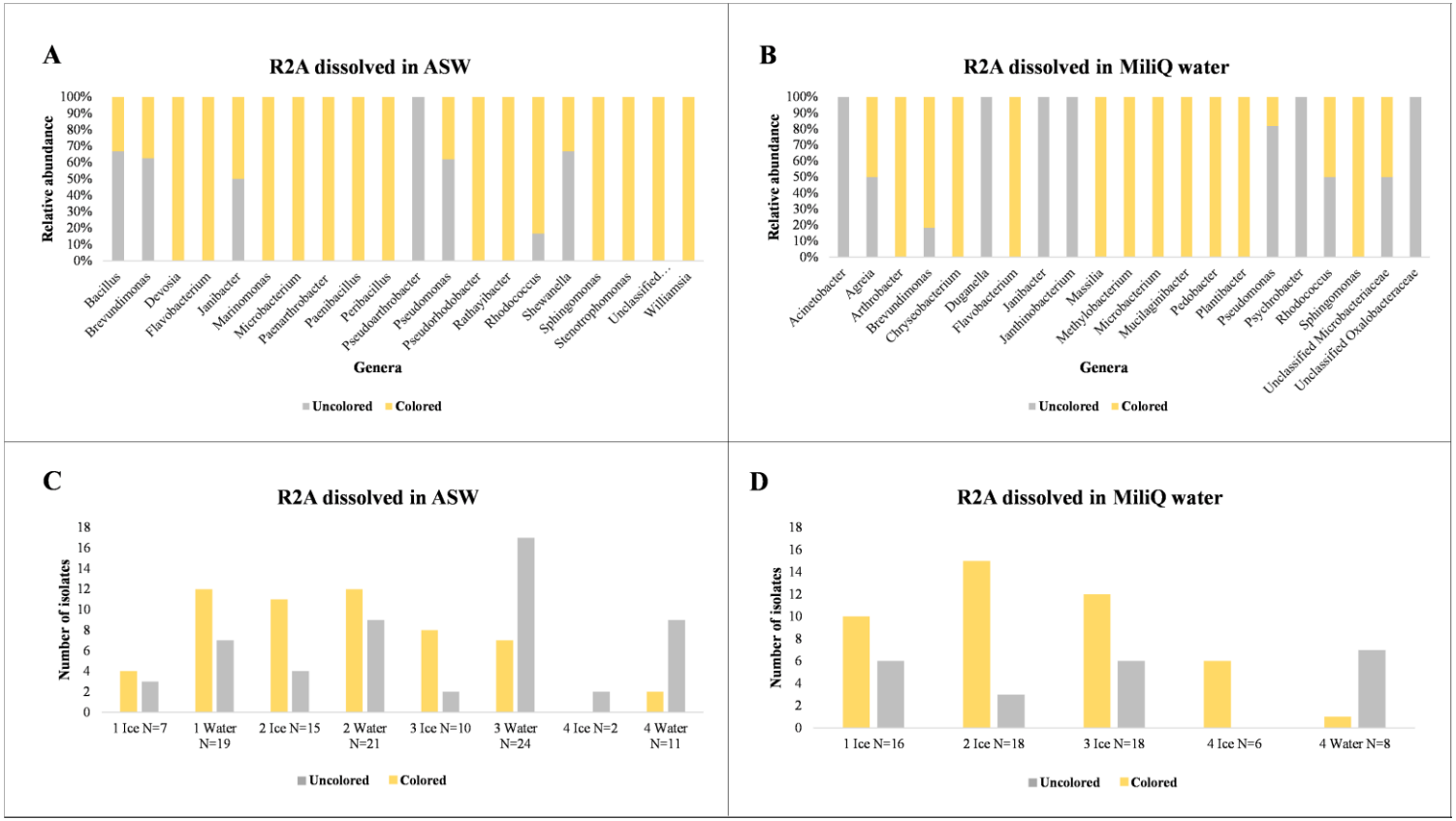

Figure IX.6 - Relative abundance of bacterial genera retrieved from ice and water on R2A medium dissolved in (A) sterile MiliQ water and (B) sterile Artificial Sea Water (ASW) from all sampling sites. From Coelho *et al.*, 2022, in *STOTEN*.

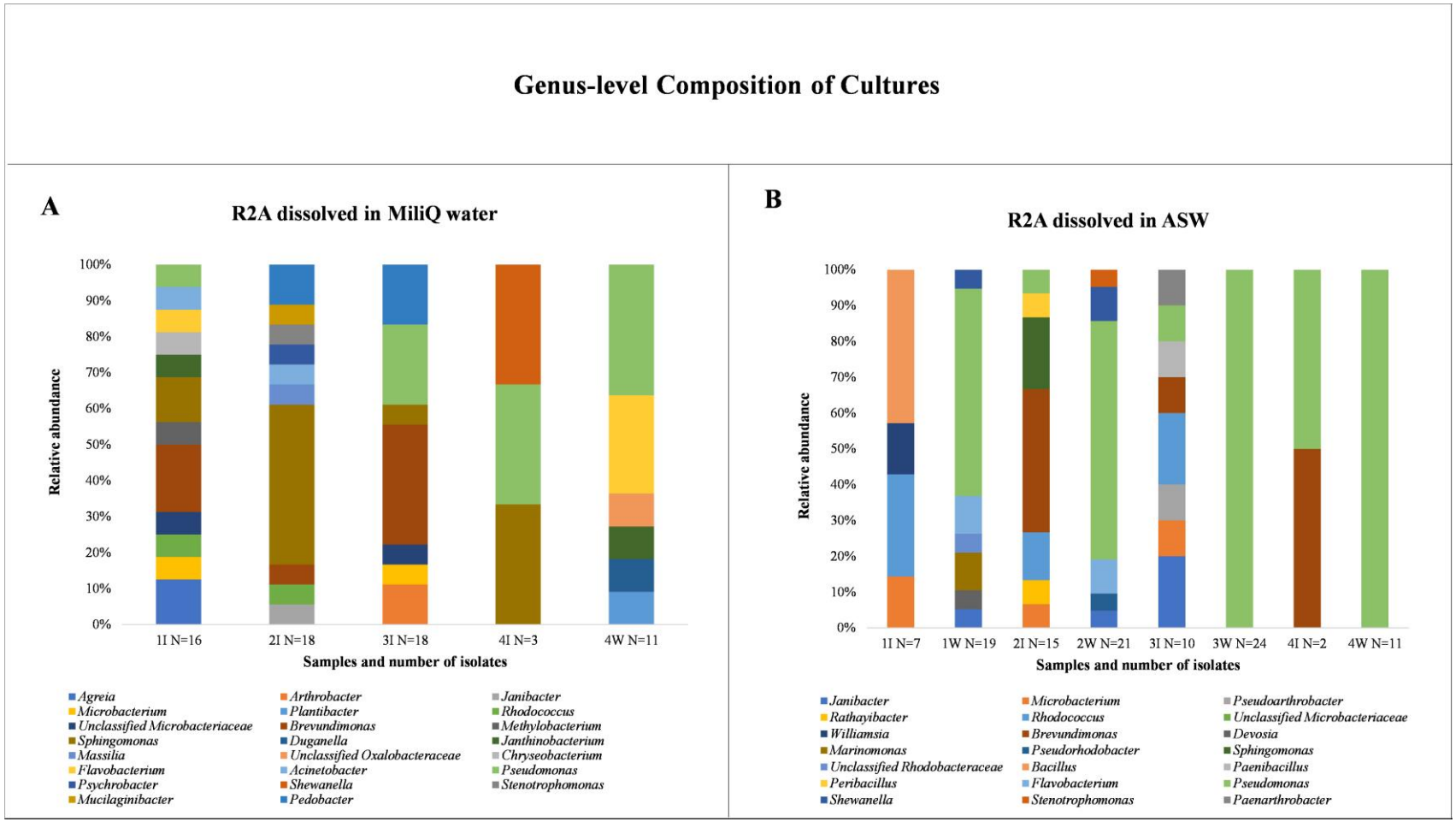

Figure IX.7 - Percentage of colored (yellow, pink, salmon, orange, violet) *versus* uncolored (translucent, white, cream, grey) colonies within genera isolated on R2A agar dissolved in (A) sterile Artificial Sea Water (ASW) and (B) sterile MiliQ water from all sampling sites. Comparison of numbers of colored and uncolored isolates cultured on R2A agar dissolved in (C) ASW and (D) in MiliQ water from different sampling sites. "N" represents the number of isolates from each sample. From Coelho *et al.*, 2022, in *STOTEN*.

IX.10 Data availability (Supplementary material of Chapters II and III)

16S rRNA gene Sanger sequences of bacterial isolates have been deposited at NCBI GenBank under the accession numbers [MZ067571 - MZ067720]. The Illumina sequencing dataset of this study was submitted to the European Nucleotide Archive (ENA) under the study accession number [PRJEB44116] with the sample accession numbers [SAMEA8547042–SAMEA8547060] and the run accession numbers [ERR5696667- ERR5696685].